Multi-user Receiver Structures for Direct Sequence Code Division Multiple Access

Ian W. Band

A thesis submitted for the degree of Doctor of Philosophy.

The University of Edinburgh

- May 1998 -

Abstract

This thesis reports on an investigation of various system architectures and receiver structures for cellular communications systems which discriminate users by direct sequence code division multiple access (DS-CDMA). Attention is focussed on the downlink of such a spread spectrum system and the influence of a number of design parameters is considered. The objective of the thesis is to investigate signal processing techniques which may be employed either at the receiver, or throughout the system to improve the overall capacity. The principles of spread spectrum communication are first outlined, including a discussion of the relative merits of spreading sequence sets, and a description of various signal processing techniques which are to be applied to the multi-user environment. The measure of system performance is introduced, and the conventional DS-CDMA system is analysed theoretically and through simulation to provide a reference performance level.

Adaptive algorithms, which iteratively approximate the minimum mean square error (Wiener) receiver filter, are then investigated, both in stationary additive white Gaussian noise (AWGN) and in a more realistic radio channel. The inter-dependence of the system chip-rate, maximum Doppler offset induced by the motion of the receiver and the tuning parameters of the adaptive algorithm is demonstrated. Aspects of forward error correction (FEC) coding are then investigated, with convolutional coding on the data used both as an alternative to and as a supplement of direct sequence spreading. The most efficient use of the available expansion in bandwidth is shown to be dependent on a balance between FEC coding power and the capacity of the spreading sequence set chosen.

Methods of combining mutiple access interference cancellation techniques with convolutional coding and Viterbi decoding are considered. New structures are proposed which incorporate FEC decoding at the intermediate stage of the canceller, and the performance of these receivers is analysed theoretically. Simulations confirm that significant capacity improvements may be achieved, at tolerable increases in computational complexity and processing delay. Receivers employing radial basis function (RBF) networks are shown to provide excellent capacity, but at the expense of exhorbitant computational demand. The architecture of these networks is investigated, with a comparison of the performance of networks constructed either at the chip or the bit level. Methods of reducing the complexity of such non-linear receivers are considered, and a new receiver, developed from the RBF network, but using the closest centre to estimate the data is described and shown to have similar performance to the conventional Gaussian kernel RBF network, but at considerably reduced complexity.

Finally, conclusions are drawn, and suggestions for future extensions of the work presented are proposed.

Declaration of originality

This thesis was composed entirely by myself. The work reported herein was conducted exclusively by myself in the Department of Electronics and Electrical Engineering at the University of Edinburgh. The software written to perform the simulations was written by myself with the following exceptions :-

- The routines used to allocate and de-allocate memory dynamically in C, which were supplied by D. Laurenson, and are given in Appendix C
- The routines used to generate Gaussian-distributed deviates, and to perform the matrix inversion used in the calculation of the Wiener filter, which were obtained from *Numerical Recipes in C*, reference [29]
- The routines used to generate the impulse response of the time-varying channel used in chapter 3, which were supplied by D. Laurenson, and are described in [28]
- The routines used to calculate the Voronoi diagram described in Chapter 6, which were obtained from the World Wide Web, URL `http://www.netlib.org/voronoi`, and are described in reference [94]

Ian W. Band

May 1998

Acknowledgements

There are many people to whom I owe a debt of thanks in the preparation of this thesis. Firstly, the academic staff of the Signals and Systems group at the Electrical Engineering department of Edinburgh University, in particular my supervisors Dr D. G. M. Cruickshank and Prof. P.M. Grant, for their guidance and assistance over the course of my time in the department. Secondly, the Research staff and post-graduate students, past and present, of the Signals and Systems group for continuous support and stimulation. At the risk of forgetting someone, the people I would like to thank include (but is not limited to) Richard, Candy, Gunther, Thomas, Iain S., John T., Sascha, Cathy, Rudy, Iain M., Paul, Justin, Jon A., Bill, Stevie, Emma, Marcus, Warren and Yoo-Sok. Finally, I would like to thank my family and friends, for being there.

I would also like to acknowledge the financial support of the *UK Engineering and Physical Sciences Research Council*, through Grants GR/J46401 and GR/K85360.

To Carol, for everything.

Contents

Abbreviations

AWGN	additive white Gaussian noise
AMPS	Advanced mobile phone system
BPSK	binary phase shift keying
BS	base station
CCI	co-channel interference
CDMA	code division multiple access
CM	constant modulus
COST	European Union commission on co-operation in science and technology
CTDMA	code and time division multiple access
CTIA	cellular telecommunication industry authority
DD	decision direction
DS-CDMA	direct sequence CDMA
ETSI	European Telecommunications Standards Institute
FDMA	frequency division multiple access
FEC	forward error correction
FH-CDMA	frequency hopping CDMA
FIR	finite impulse response
FPLMTS	future public land mobile telecommunication system
GSM	global system for mobiles (formerly *groupe speciale mobile*)
i.i.d.	independent, identically distributed
IC	interference cancellation
ICI	inter-chip interference
IIR	infinite impulse response
ISI	inter-symbol interference
LMS	least mean square

MAHO mobile assisted hand-over

MAI multiple access interference

MAP maximum *a priori*

MF matched filter

MFC matched filter cancellation

MFC+V matched filter cancellation with Viterbi algorithm

MLP multi-layer perceptron

MLSE maximum likelihood sequence sstimation

MMSE miniumum mean square error

MS mobile station

MSC mobile switching centre

MSE mean square error

MSRG modular shift register generator

MUD multi-user detection

MVC+V matched filter cancellation with intermediate data estimation using the Viterbi algorithm

NO-MMSE non-optimal miniumum mean square error

PCF post channel-matched filter

PCS personal communication system

PMF post matched filter

PN pseudo-noise

PPGC preferentially-phased Gold codes

PTN public telephone network

RBF radial basis function

RF radio frequency

RLS recursive least squares

SDMA space division multiple access

SNR signal to noise ratio

SSMA spread spectrum multiple access

SSRG simple shift register generator

TACS total access communication system

TDD time division duplexing

TDMA time divison multiple access

UMTS universal mobile telecommunication system

VA Viterbi algorithm

WDMA wavelength division multiple access

WFC Wiener filter cancellation

WFC+V Wiener filter cancellation with Viterbi algorithm

WVC+V Wiener filter cancellation with intermediate data estimation using the Viterbi algorithm

List of principal symbols

Symbol	Description
$(\mathcal{A}, \oplus)$	group of data alphabet set $\{0, 1\}$ with modulo 2 addition
$(\mathcal{B}, \times)$	group of binary phase shift keying (BPSK) alphabet set $\{1, -1\}$ with multiplication
b	number of digits input to the convolutional encoder
C	number of digits output from the convolutional encoder
C_d	minimum distance between cells which broadcast on the same frequency
$\underline{c_i}$	M-dimensional spreading sequence for user i
$\{\underline{c_i} : 1 \leq i \leq U\}$	set of U spreading sequences
D	dimension of input vector to the RBF network
$d(\cdot, \cdot)$	RBF metric, usually the Euclidean l_2 metric
d	data bit for required user, $d \in \mathcal{A}$
d_{free}	free distance of the convolutional code
E_b	Energy per data bit
E_b/N_0	signal to Gaussian noise ratio
$e(n)$	error between the soft approximation $\tilde{x}(n)$ and the original data bit $x(n)$
f_{bit}	data bit frequency
f_{chip}	chip frequency
$f_{Pen}(\cdot)$	penalty function for the adaptive algorithm
$\underline{g}$	Kalman gain vector in RLS algorithm
g_P	processing gain (linear version) $= W_{SS}/W_D = N_s$
G_P	processing gain (decibel version) $= 10 \log_{10} g_P$
$H(z)$	Chip-sampled impulse response of the channel, $H(z) = \sum_{j=0}^{j=n_h} h_j z^{-j}$

K	constraint length of the convolutional encoder
L	survivor path length in the decoding trellis for the Viterbi algorithm
M	length (in chips) of the spreading sequence
$\mathcal{M}$	misadjustment (ensemble averaged error after a sufficient number of training data) of the adaptive algorithm
N_0	single-sided Gaussian noise power spectral density
N_c	number of centres in the RBF network
N_m	number of m-sequences that may be generated by appropriate connections of a shift register configuration
N_r	number of digits (chips) read at one time by the receiver ($N_r = N_s$ for the AWGN channel, but N_r may be chosen $\geq N_s$ for multipath channels to capture the total energy from one data bit)
N_s	number of output digits per data bit
N_{test}	number of test (unknown) data bits
N_{train}	number of training (known) data bits
n_h	number of chips spanned by the impulse response of the multipath channel
P/N	signal to noise power ratio
$\mathcal{P}$	$\subseteq \mathbb{R}^D$, set of centres in the RBF network
$\mathcal{P}'$	reduced set of centres
$\underline{q}_i(n)$	C-dimensional convolutional code for user i at time T_n
R	rate of the convolutional encoder $R = b/C$
$S_D(f)$	power spectral density of data signal
$S_{SS}(f)$	power spectral density of spread spectrum signal
$\underline{s}(n)$	N_s-dimensional vector of baseband transmitted signal at time step n
T	time
$T(d)$	transfer function, defining the weight spectra of the convolutional code
T_{bit}	period of one data bit
T_{chip}	period of one data chip
U	number of simultaneously active users

$\mathcal{V}(p_i)$	Voronoi polygon associated with point p_i
$\mathcal{V}(\mathcal{P})$	Voronoi diagram associated with set of centres $\mathcal{P}$
W	bandwidth
W_D	bandwidth of data signal
W_{SS}	bandwidth of spread spectrum signal
$\underline{w}$	N_r-dimensional vector of receiver tap weights
$\underline{w}_{zero}$	zero-forcing tap weight vector
$\underline{w}_{Wiener}$	Wiener filter tap weight vector
w_i	weight associated with centre $p_i \in \mathcal{P}$
x	image of d under χ, $x \in \mathcal{B}$
$x_1(n)$	(also denoted $x(n)$), the desired data bit for user 1 at $T = T_n = nT_{bit}, n \in \mathbb{N}$
$x_i(n)$	data bit for user i at time T_n, $1 \leq i \leq U$
$\underline{x}(n)$	$= (x_1(n), x_2(n), \ldots, x_U(n))^T$, the U-dimensional vector of desired data bits for all active users
$\tilde{x}(n)$	approximation (soft decision) to original data bit $x(n)$
$\hat{x}(n)$	approximation (hard decision) to original data bit $x(n)$
$\underline{y}(n)$	N_r-dimensional vector of received signal corresponding to data bit $x(n)$
$\underline{z}(n)$	N_s-dimensional vector of iid additive white Gaussian noise samples at time $T = T_n$
z^{-1}	unit chip delay
${z_{bit}}^{-1}$	unit bit delay
δ	initialisation value for RLS algorithm
λ	forgetting factor for RLS algorithm, $0 < \lambda \leq 1$
μ	step size for LMS algorithm
Φ_{yy}	autocorrelation matrix of the signal vector
$\underline{\phi}_{yx}$	cross-correlation vector between the received signal $\underline{y}$ and the original data symbol x
$\psi(\cdot)$	radially symmetric kernel
$\psi_G(\cdot)$	Gaussian kernel, defined by $\psi_G(\zeta) = \exp(-\zeta^2/2\sigma^2)$
$\rho(n)$	approximation to autocorrelation matrix in RLS algorithm

σ^2	variance of additive white Gaussian noise samples ($= N_0/2$)
$\tau(N)$	Euler totient function = number of integers less than N which are relatively prime to N

List of Figures

List of Tables

Chapter 1

Introduction

Personal communication systems (PCS) aim to provide [1] "communication services in any form from any person to any other person in any place at any time through any medium and without any delay by using one pocket-sized unit at minimum cost with acceptable quality and security through the use of a single personal telecommunication reference number". The demand on communication services is now no longer limited to voice traffic, but encompasses a swathe of other media from electronic mail to fax data and even video. The increased quality and security of digital data is also becoming increasingly attractive to a seemingly ever expanding consumer market. Additionally, this heightened expectation is developing as the shift away from fixed telecommunication sites to truly portable mobile units appears relentless. Clearly, present-day PCS [2] fall some way short of this lofty goal in many if not all of the above criteria, and, although the rapid evolution thus far of digital wireless technology [3] indicates the pace of development, the fulfilment of all of these requirements is not yet attainable.

This thesis is concerned with investigating the application of various signal processing techniques to improve future PCS. Specifically, the improvement sought is in increasing the capacity, which may be expressed in terms of the number of subscribers able to communicate at an acceptable error rate for a given bandwidth, of digital PCS which employ direct sequence code division multiple access (DS-CDMA).

This chapter will first discuss the technical reasons for the adoption of a cellular structure for PCS, and indicate the scale of the international marketplace. The various techniques which allow multiple access to the system resources will then be briefly described in section 1.2, before the main objectives of the work are outlined in section 1.3. Finally, the layout of the subsequent chapters will be defined in section 1.4.

1.1 Cellular communications background

In this section, the cellular approach to wireless communication systems will be described. The reasons for adopting a cellular structure for the radio coverage areas will be outlined in section 1.1.1, which also describes some common terms often used in the cellular environment. An outline of the commercial aspects of PCS is then detailed in section 1.1.2, which also indicates the present status of some cellular systems. Conclusions are then drawn in section 1.1.3.

1.1.1 Why cellular ?

The importance of available radio frequency (RF) bandwidth may be judged from the famous "Shannon equation" [4]

$$C_c = W \log_2 \left(1 + \frac{P}{N}\right) \tag{1.1}$$

where C_c is the capacity of a communications channel, measured in bits / s, W is the bandwidth in Hz and P/N is the signal to noise power ratio. This direct relationship between capacity and bandwidth has led to an increased demand, and hence an increased scarcity of this resource.

The more efficient use of RF bandwidth [5], together with improved service capability and overall performance prompted the adoption of a cellular structure for wireless communication systems. The main advantage of this technique, outlined in Figure 1.1, is that a subset of the allocated frequency range may be used in each cell. A network of such cells may then be constructed over the total region of interest, allowing the frequency range in *e.g.* Cell 1 to be re-used in Cell A, thus more efficiently using the overall bandwidth assigned to the entire network for communications.

The disadvantage in taking a cellular approach is that the frequency range employed in one cell (*e.g.* cell 1 in Figure 1.1) cannot be re-used in any of its neighbouring cells. In this example, the tessellation is shown via hexagons, so that each cell has six neighbours and therefore the frequency re-use factor is $1/7$. In practice however, the cell coverage areas will be less regular, with the boundaries between cells being less well-defined, so that the precise re-use factor will vary depending on the exact network topology and required signal to noise ratio (SNR). The other important parameter for cellular systems is the minimum distance separating two base-stations broadcasting at the same frequency (shown as C_d in the figure) expressed as a ratio of some measure of the cell size (such as its radius r_c, as shown in the figure).

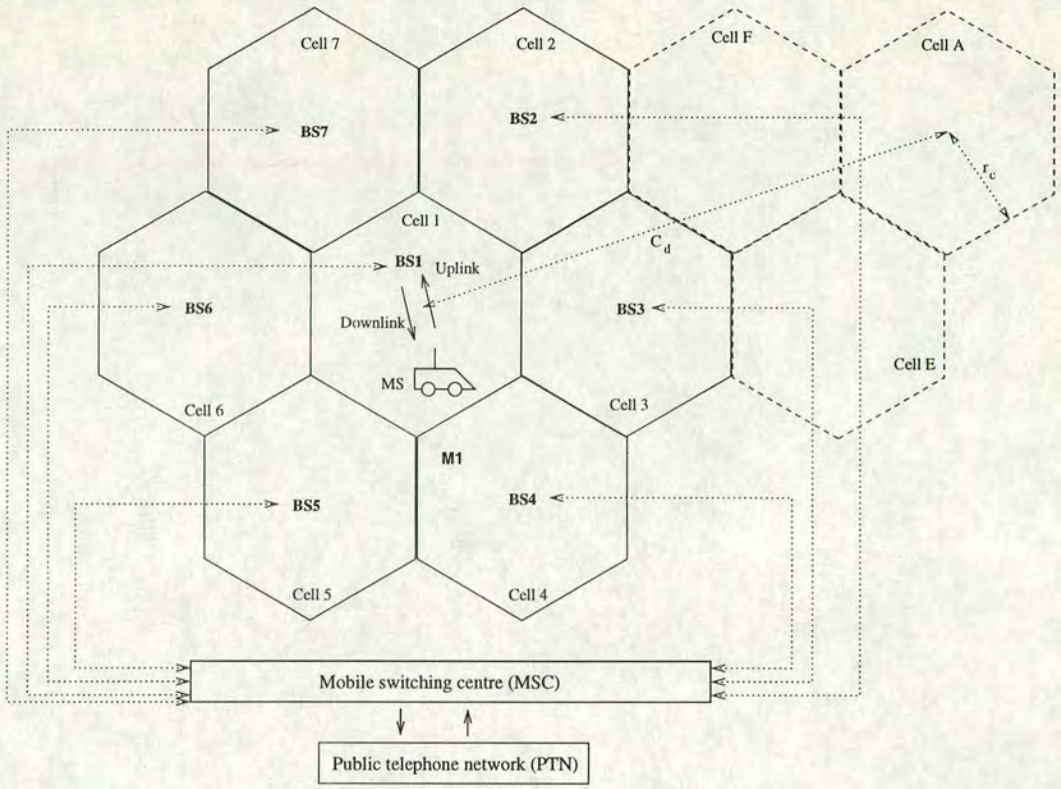

Figure 1.1: The cellular principle and some defining terms

The base stations (BS) are normally located at the centre of each cell, using omni-directional antennas[1] and the interface between the cellular network and the public telephone network (PTN) is via the mobile switching centre (MSC), which controls the individual base station currently in charge of the call. The process of changing the allocated base station is known as handover, which may be further categorised as soft, in which case a new BS is allocated before communication with the active BS is terminated, or hard, in which the communication is suspended completely before the new BS establishes contact [2]. Recently, mobile assisted handover (MAHO) schemes have been proposed [6], in which the decision to change base stations is influenced by the mobile, thus placing less demand on the base station.

MAHO schemes are more suited to schemes using very small (pico) cells, such as those in offices. The size of the cells used, which depends on the type of terrain and the number of users expected within each cell, is shown in Table 1.1, with typical applications.

[1] Increased capacity may be achieved by sectorizing the cell using antennae divided so that they cover equal sectors of the coverage area. Typically, sectors of angular width of 120° are used, but problems may occur for mobiles at the boundary between sectors, leading to the "ping-pong" effect, in which control is rapidly alternated between adjacent sectors

[2] In addition, inter-system handoff, or roaming, may occur when a mobile moves between cells controlled by different mobile switching centres

Application	Average cell diameter	Name
Sub-urban	1 - 10 km	macro-cell
Urban	1 km	mini-cell
Street	100 m	micro-cell
Office	< 10 m	pico-cell

Table 1.1: Sizes of cells and associated uses

The RF path from the base station to the mobile is termed the downlink, or forward channel, and is synchronous (all the users' individual signals are aligned), whilst the complementary path from the mobile to the base station is known as the up-link, or reverse channel, and consists of signals which are (in general) unaligned. Further complications on the uplink include the fact that the signals travel through different paths to reach the base station, so each signal will experience different fading and delay statistics, and the possibility of step changes in the signal as users either begin or cease transmission. In this study, only the downlink will be considered.

The passage of mobiles between cells leads to another problem, since arriving/departing mobiles will invariably be located at the edge of a cell (or sector, if sectorisation is employed), whilst existing users may be closer to the base station. This situation is not specifically a problem in handover, but will occur in general when the mobiles are at different (RF) distances from the base station. This "near-far problem" requires careful power control throughout the system to avoid swamping of the signal received by the base station by one particular mobile close to the base station, or insufficient power being received by a mobile far from the base station to enable communication.

1.1.2 Commercial exploitation: recent history and projections for the future

The commercial exploitation of cellular wireless networks has seen dramatic growth in the past few decades [7]. Figure 1.2 presents the number of subscribers, and the revenue obtained, of wireless communications systems in the USA alone since the mid-1980's.

The data was obtained from the World-Wide Web homepage of the Cellular Telecommunications Industry Authority (CTIA), (URL `http://www.wow-com.com/consumer/`). Predictions for turn of the century subscriber numbers are in the region of 50 million in the USA and 200 million world-wide, although recent reports from the CTIA suggest that there may already be more than 50 million users in the USA, and a recent prediction [8] places the total number of

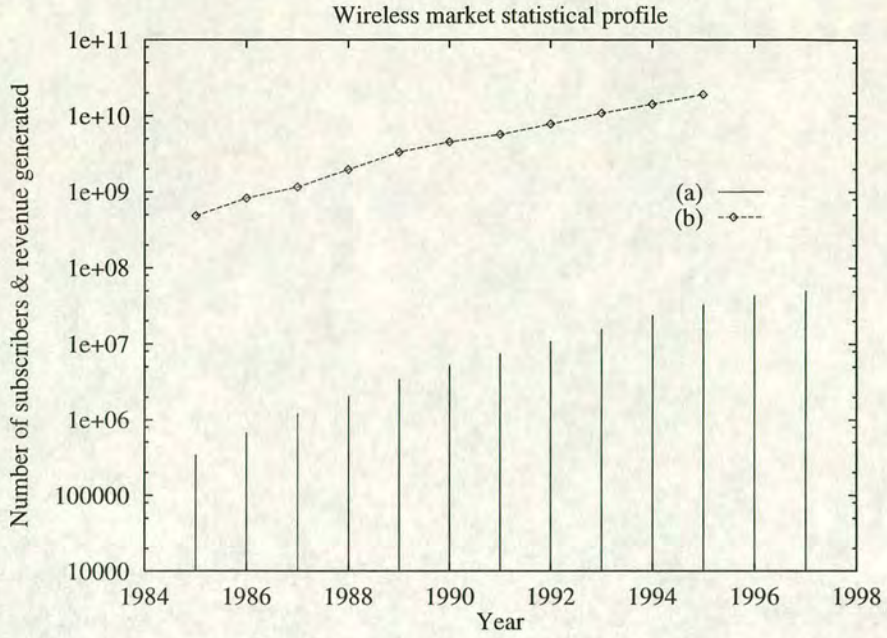

Figure 1.2: *Number of subscribers of wireless phones and the revenue generated (US $) in the USA; (a) number of subscribers; (b) revenue*

subscribers by the end of the century close to 600 million.

The application of CDMA technology (which will be described later) for cellular PCS has been pioneered by the North American company Qualcomm Inc., and digital cellular systems using CDMA are in competition with the European digital global system for mobiles (GSM) for the worldwide mobile communications marketplace. The following is a selection of the CDMA cellular PCS systems which are currently being, or are soon expected to be established (the information is courtesy of the CDMA Development Group World-Wide Web homepage, URL `http://www.cdg.org/`).

In Africa, Telecel International in The Congo and in Zambia have recently announced the deployment of CDMA based systems for digital cellular telephone networks, with the Zambian system aiming to provide service to over 10 000 subscribers. In South America, a Peruvian company, Telefonica, has recently ordered 25 000 CDMA handsets for its digital cellular PCS network. Most of the other South American countries are also actively conducting trials of CDMA systems for cellular mobile telecommunications. Asia has also seen a huge growth in demand for personal mobile communication systems. In South Korea, there are presently over 2 million subscribers to SK Telecom's CDMA mobile service, while five test areas have been designated in China. In Shanghai, a cellular network is planned to be operational in early 1998, with a capacity of 60 000 subscribers, while in Hong Kong, 150 000 subscribers to Hutchison Telecom's system are expected in the near future. With projections for the end of the century at

around 2 million mobile phone users in Shanghai alone, the opportunities for CDMA networks in Asia are clearly extensive. In Europe, much research effort has been concentrated on pursuing a universal mobile telecommunications system (UMTS), which may combine elements of the already established GSM and CDMA technologies [9]. Trials of the integration of CDMA systems with existing GSM digital networks have recently been announced in Germany and the United Kingdom, with the results expected to be unveiled in the near future.

1.1.3 Conclusions

The key point is that demand for mobile phone services of sufficient quality to provide additional services as well as simply voice data is expected to exceed the capability offered by present technologies. Consequently, there exists a requirement for improving the quality and capacity of existing and proposed digital cellular networks, through the use of more sophisticated signal processing techniques. Before proceeding to a description of the various signal processing techniques considered, the different methods of achieving a multiple access capability are first reviewed.

1.2 Multiple access background

The main task for the communication system designer is to make the best use of available system resources. In the past, the limitations have been mainly due to technology (*e.g.* the difficulty of construction of sufficiently fast or complex processors or the excessive power requirements which limit portability), however now the challenge is to make the most efficient use of the radio frequency bandwidth to maximise both the quality and quantity of possible calls.

There are three principal methods of providing a multiple access capability within the cellular radio environment [3] , which may be differentiated by the resource which is to be shared, or divided between the subscribing users.

[3]Outwith cellular radio, PDMA, in which radio beam polarisation is the discriminant, SDMA, employing directional antennae to provide isolation in space and WDMA in optical communications, where individual users are assigned specific wavelengths are also used [10]

1.2.1 Frequency division multiple access (FDMA)

This technique separates the active signals by assigning a different subrange of the cell's total allocated frequency range to each user. [4] This method is used in both the US advanced mobile phone system (AMPS) and the UK total access communications system (TACS). Both these systems are analogue and are often referred to as first generation systems. An obvious disadvantage of this technique is that it limits the total number of mobiles that may be simultaneously active. Further disadvantages include the fact that when a new site is to be added in to the network, problems can arise due to insufficient availability of bandwidth to accomodate the new base station. Additionally, hardware problems may arise, due to the demands of filtering the signal, and since this is a narrowband system, there is no inherent diversity to combat the effects of a multipath channel. Perhaps most importantly, since FDMA is an analogue system, it is potentially susceptible to interception, or jamming of a call.

1.2.2 Time division multiple access (TDMA)

In this technique, the time allowed for each user to communicate with the base station is restricted to be within one of a set of slots within one time frame. Suitably fast and powerful processing units have only in the past few decades been available to make this approach feasible. This multiple access method is used in the global system for mobiles (GSM) [5] European system, which was the first digital cellular standard for voice communications and low-rate data transmission and is therefore termed a second generation system. GSM uses blocks of 200 kHz, split into 8 time slots and uses a bit rate of 270.8 kbit/s, which means that intersymbol interference (ISI) occurs. To combat this, a 26-bit training sequence is inserted into the data stream and an interleaver with a delay of 80ms is used to provide time diversity. This system also uses slow frequency hopping to improve the efficiency of the interleaver. TDMA systems, although they still require frequency re-use, have the advantage of being able to use the diversity from multipath channels to improve performance, and do not suffer from quite the same limitations on filtering as FDMA systems, although considerable resources must be expended in maintaining the timing and synchronisation of the signals.

[4] this simplification ignores the requirement for guard bands to prevent leakage or cross-talk between users [11]
[5] originally the *groupe speciale mobile*

1.2.3 Spread spectrum multiple access (SSMA)

The third alternative is to allocate each user a specific signature, or spreading sequence and to use this sequence to expand the bandwidth, or "spread the spectrum" of the signal to be transmitted. At the receiver, estimation of the original data is performed by the inverse process, given knowledge of the required user's spreading sequence. While this may seem a needless increase in both complexity and bandwidth requirement, the key to the claimed increases in system-wide capacity [12] is that spread spectrum systems can tolerate a frequency re-use factor of one, *i.e.* the same frequency in adjoining cells, since the distinction between users is achieved via the spreading sequences. The allocation of different sequences, or codes, to different users has given rise to the term code division multiple access (CDMA). Although this is strictly a misnomer since any individual code is not a resource to be divided up and shared amongst the users, but rather distinct complete codes are allocated to each user, this term will also be used here.

There are two[6] main strategies within spread spectrum; direct sequence (DS-CDMA) [13] in which the data bit modulates the spreading sequence to produce the signal to be transmitted, and frequency hopping (FH-CDMA) [14], in which the signature sequence defines the "hopping pattern" of the signal. This designates the instantaneous frequency at which the communication is to take place. FH-CDMA, with its roots in military applications, is principally concerned with evading eavesdropping of a signal, and interception of the original data. This technique is inherently resistant to jamming of the signal by a third party, since, without knowledge of the hopping pattern, such an approach would involve expending a finite jamming power over a wide range of possible frequencies. For the mobile environment however, which is the focus of this study, frequency hopping is less practical, since the hopping would have to be performed at a high rate to achieve a reasonable processing gain.

The recent commercial implementation of DS-CDMA communications systems with the second generation cellular standard IS-95 [15], together with a large body of ongoing research work at both industrial and academic levels, has made this technique a strong candidate for third generation systems [16, 17] which will be required to supply high rate data communications as well as digital voice traffic, and will form the main subject of this study. Here, attention will be focussed on signal processing techniques to improve the downlink capacity of a system

[6] Strictly, a further two strategies exist; time-hopping (TH), in which the spreading sequence controls the allocation of the timeslot of a data bit, potentially leading to increased security, and chirp systems, in which the frequency is continuously (usually linearly) either increased or decreased, and is mainly used in radar applications

employing direct sequence CDMA.

1.2.4 Hybrid methods

Additionally, there exist hybrid techniques, combining elements of some or all of the above multiple access methods. Most notable amongst these are the incorporation of DS-CDMA techniques into the GSM environment to produce code and time division (CTDMA) [18] as a potential candidate for UMTS [19]. Significant research effort has also been invested into systems employing orthogonal frequency division multiplexing (OFDM) [20], which is particularly suited to digital broadcasting of radio and television [21]. Although novel combinations of OFDM with CDMA [22, 23] have been investigated, the European Telecommunications Standards Institute (ETSI) recently decided [24] to adopt an approach based mainly on DS-CDMA, and so this will form the main area of study of this work.

1.3 Objectives of the work

The objective of the work presented is to investigate signal processing methods which may be employed either throughout the DS-CDMA system, or only at the mobile receiver to either decrease the probability of error of a data estimate, or increase the capacity of the communication system as a whole. In addition, these improvements to system performance must not be at the expense of too great an increase in system complexity, or overall delay, since practical implementation of these methods is an important consideration.

1.4 Thesis structure

The layout of the thesis is as shown in Figure 1.3.

A description of the various facets of a DS-CDMA signal is first given in Chapter 2, which also introduces some of the signal processing techniques to be used in later chapters. This is followed in Chapter 3 by an investigation into the applicability of adaptive algorithms at the mobile receiver, whether used in a stationary additive white Gaussian noise (AWGN) channel,

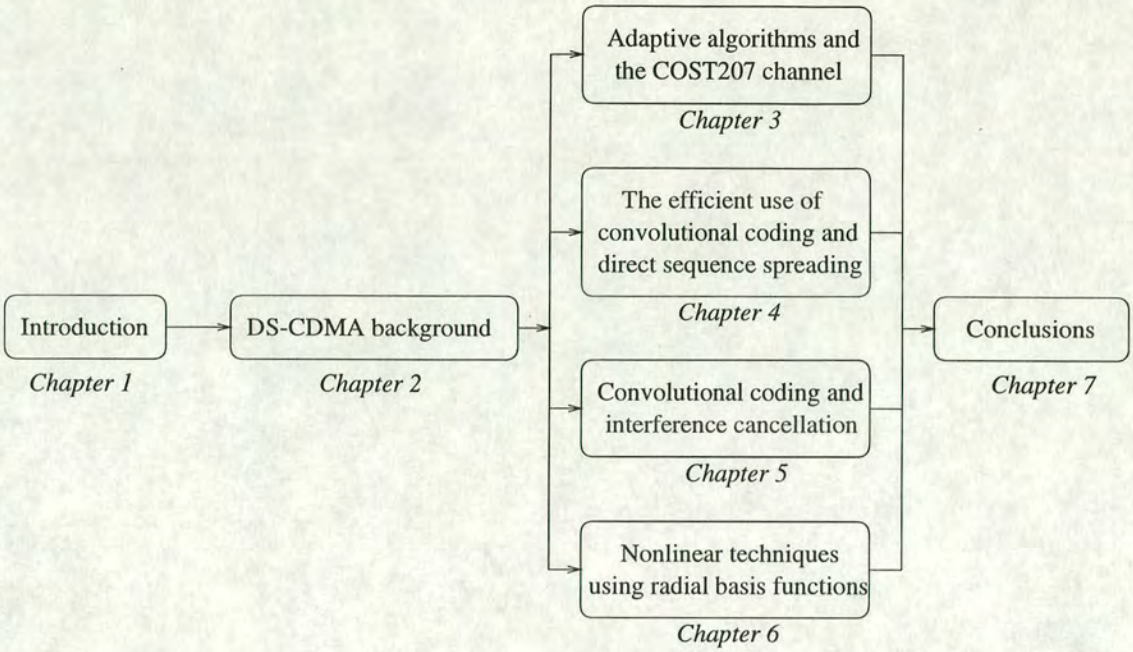

Figure 1.3: The subjects considered in the appropriate parts of this Thesis

or in a time-varying channel, which more closely models the behaviour of a mobile radio environment. The application of forward error correction to the DS-CDMA signal is considered in Chapter 4, which considers convolutional coding both as a replacement for, and in conjunction with direct sequence spreading. Chapter 5 details the use of interference cancellation schemes when the data is both convolutionally encoded and modulated by a spreading sequence. The use of non-linear receivers, specifically employing radial basis functions, is outlined in Chapter 6. Here, a new non-linear receiver structure, which employs the nearest neighbour algorithm to obtain its data estimate, is introduced and investigated. Finally, a summary of the main achievements of the work, together with an indication of possible future developments, is presented in Chapter 7.

Chapter 2

DS-CDMA background

In this chapter, the use of direct sequence spread spectrum techniques to provide a multiple access communications capability is reviewed. The principle of spread spectrum is first outlined in section 2.1, and the application of this technique to produce a multiple access system is then described in section 2.2. Various aspects of the system design are then considered in section 2.3, which also introduces some of the signal processing techniques which will be studied in the context of the DS-CDMA environment in later chapters. Finally, the main ideas discussed in the chapter are summarised in section 2.4.

2.1 Spread spectrum communication principles

To illustrate the concept of spread spectrum communication more fully, it is useful to consider the profiles of the original and spread signals in both the time and frequency domains. As discussed in section 1.2.3, a simple expansion of bandwidth is not by itself sufficient for a system to be termed spread spectrum. Rather, the bandwidth expansion must be accomplished by means of a separate signature, or spreading sequence, which is known to both co-operating parties, and is independent of the data bits [25], which are themselves assumed to be both independent and randomly distributed. The spread signal is then formed by modulating this spreading sequence by the data bit to be communicated. The modulation scheme chosen here for the data is binary phase shift keying (BPSK), so that if the data bit of interest at time index [1] n is $d(n) \in \mathcal{A} = \{0, 1\}$, then this may be transformed to give $x(n) \in \mathcal{B} = \{1, -1\}$, via the isomorphism χ, where $\chi : \mathcal{A} \rightarrow \mathcal{B}$ is chosen[2] to be $x = \chi(d) = 1 - 2d$, where, when required,

[1] Time discrete data will be assumed in the following, so that a continuous analogue signal $x(t); 0 \leq t < \infty$ will be represented by the corresponding sampled sequence, which will be denoted $\{x(n) : 0 \leq n < \infty\}$

[2] to preserve the group structure

x may be written for $x(n)$ and d for $d(n)$ for brevity without ambiguity. Let this transformed sequence of data bits $x(n)$ have period T_{bit}, and let the spreading sequence of length M (whose elements are designated chips to distinguish them from the data bits) have frequency f_{chip} (normally $\gg (1/T_{bit})$ but shown shorter here for illustrative purposes) as depicted in the upper part of Figure 2.1, which shows the case for $M = 7$. Note that in the lower part of the figure, it is assumed that $f_{chip} \gg f_{bit}$, or equivalently that $T_{chip} \ll T_{bit}$.

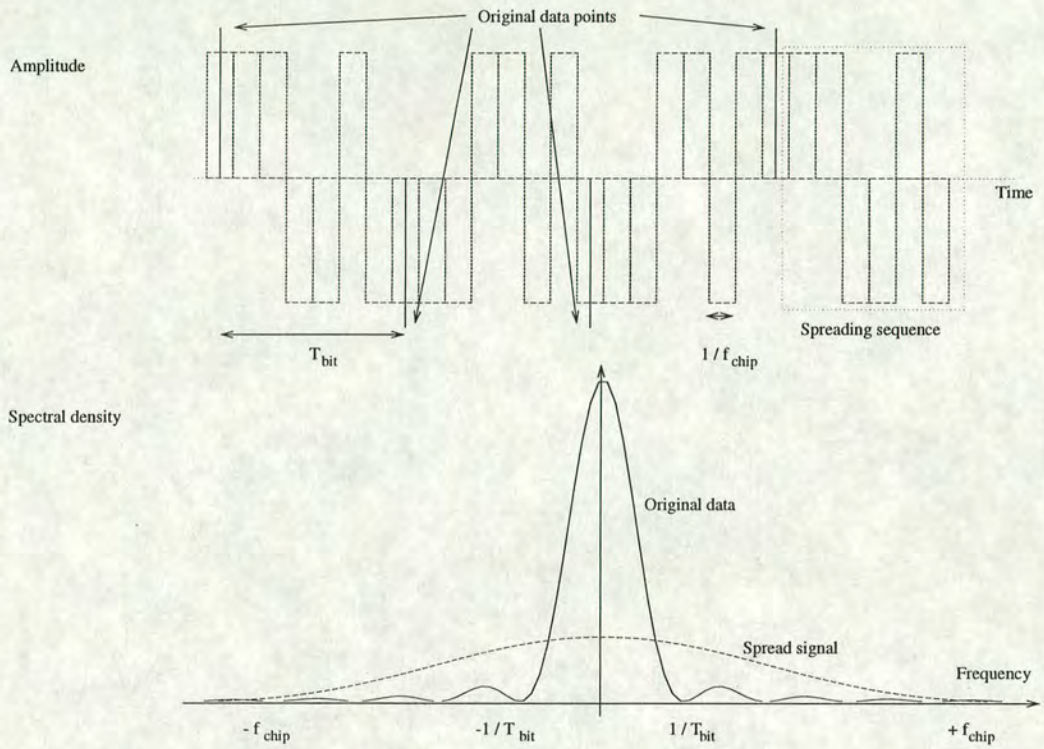

Figure 2.1: Spread spectrum concept in time and frequency domains

With the above assumption that the data is random and independent, the power spectral density of the original (i.e. unspread) signal is then given by [26]

$$S_D(f) = T_{bit}\left(\frac{sin\pi fT_{bit}}{\pi fT_{bit}}\right)^2 \tag{2.1}$$

while, assuming the spreading sequence itself is long and pseudo-random, that of the spread signal (i.e. the modulation of the spreading sequence by the data) is

$$S_{SS}(f) = \frac{1}{f_{chip}}\left(\frac{sin\pi f/f_{chip}}{\pi f/f_{chip}}\right)^2 \tag{2.2}$$

The relationship between these spectral densities is sketched in the lower part of Figure 2.1. It may be seen that the effects of any tone-like noise (*e.g.* as a result of single, or discrete multiple frequency jamming [27]), narrow-band interference (*e.g.* from other existing communication

systems [28–30]) or white noise (finite power over a wide range of frequencies *e.g.* thermal noise) which then interferes with the signal between transmission and reception may be reduced at the receiver when the inverse despreading and filtering operation is performed.

The enhancement in performance due to the bandwidth expansion and contraction process is termed the processing gain g_P, and defining W_{SS} to be the bandwidth associated with the spread signal and W_D to be that for the data signal, the processing gain may [3] be taken to be

$$g_P = \frac{W_{SS}}{W_D} = \frac{T_{bit}}{T_{chip}} \tag{2.3}$$

Thus in the simplified scenario outlined above, the processing gain is simply M, the length of the spreading sequence. The processing gain is normally quoted in its decibel form as

$$G_P = 10\log_{10}(g_P) \tag{2.4}$$

While this processing gain affords the spread spectrum system some degree of immunity to external interference from other communication systems, it is clear that, as the power of interference increases in the entire frequency range of operation, the system will begin to degrade. Thus, while the spread spectrum system is largely tolerant of external interfering factors, there will be a degradation in performance as the number of spread spectrum signals in the same cell increases. [4] The sources of this interference are the other users in the cell of interest (inter-cell) and leakage from adjoining cells (intra-cell). The work presented here will focus solely on inter-cell interference, with intra-cell interference being modelled generally by encompasing its effects into the overall background noise level.

To enable a fair comparison of systems, the background noise will be expressed in terms of a modified form of the signal to noise ratio, which takes into account the processing gain described above. As a convention, this will be termed the signal to Gaussian noise ratio, denoted by E_b/N_0 in the following. The decibel form of this processing-gain compensated noise ratio is given by Equation 2.5, which is derived in Appendix B, in which the linear processing gain g_P is given by N_s.

$$\frac{E_b}{N_0} = 10\log_{10}(\frac{g_P}{2\sigma^2}) \tag{2.5}$$

The quantity σ^2 is the variance of the Gaussian noise.

[3] Strictly, the processing gain is defined in terms of the improvement in performance at a certain probability of error between the original and spread signals, but the definition adopted here is consistent with many other texts, *e.g.* [31]

[4] The use of orthogonal spreading sequences avoids this degradation until capacity is reached at which point the system collapses. However, the presence of a dispersive channel will destroy this orthogonality.

2.2 Basic principles of DS-CDMA systems

As outlined in the previous section, the spread spectrum signal is obtained from the current data bit and the spreading sequence. The transition from this single user system to one affording multiple access is then achieved by allocating each user a unique spreading sequence. In addition to direct sequence spreading the general baseband description of a DS-CDMA communications system consists of many elements, a selection of which are shown in Figure 2.2.

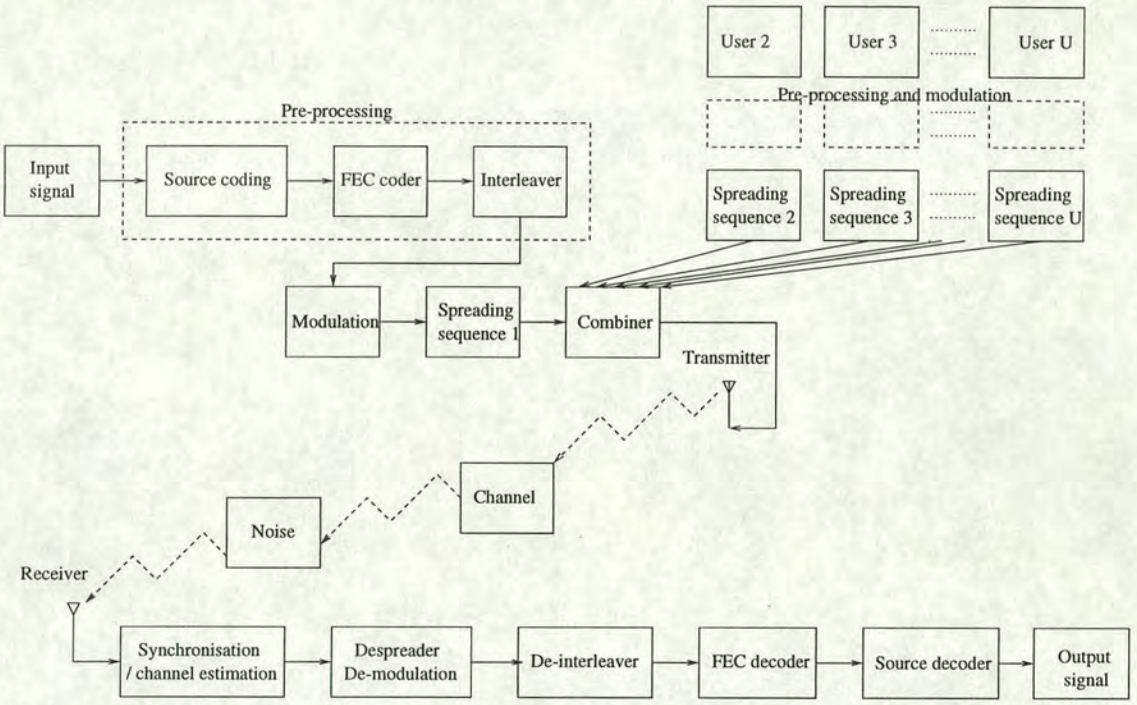

Figure 2.2: Block diagram for general DS-CDMA communications system

The input signal is first pre-processed by incorporating source coding and forward error correction (FEC), before the interleaver stage is applied to separate adjacent bits in an effort to afford some protection from a fading channel producing a block of errors. Modulation (in this case binary phase shift keying, or BPSK) is then performed before bandwidth expansion by the user-specific spreading sequence. The other users' encoded and spread signals are then combined to form the transmitted signal. At the mobile, the received signal must be synchronised (for instance by estimating the channel) before the despreading and demodulation operations are performed. The required data may then be estimated by decoding the resultant signal.

The allocation of resources to each of these elements to maximise either the quality of calls, or the number of simultaneous calls which may be handled by the network is an important consideration for the system designer, and some of these elements will be discussed more fully

in later Chapters.

The principal measure of performance of a system will be the number of data bits which are estimated incorrectly, as a fraction of the total number of unknown data bits sent, in a statistically significant number of trials. This will then form the main performance statistic denoted P_e. The independent variable in these Monte Carlo simulations will be either the signal to Gaussian noise ratio (E_b/N_0) for a fixed number of users, or the number of users (loading) for a fixed background noise level. Thus, in the following, the important quantities that must be assessed are the capacity of a system to cope with more users for a given background noise level, and the susceptibility of a system to data errors for various noise levels with a given number of users.

The next section details the construction of a simplified form of the baseband signal to be transmitted, while section 2.2.2 considers the influence of a multipath channel on this signal. Then, in section 2.2.3, various processing techniques which may be applied at the receiver are described. An example system, showing the performance in additive white Gaussian noise is considered in section 2.2.4, which demonstrates how the performance of a DS-CDMA system degrades as the interference is increased. This section concludes with a discussion of the principles described.

2.2.1 Transmitter principles

A simplified form of the transmitter for the downlink of a DS-CDMA system is shown in Figure 2.3. The transmitted signal, $\underline{s}(n)$, at time $t = nT_{bit}$ is constructed by coherently summing the modulation of the spreading sequence of each user, $\underline{c}_u$, by that user's BPSK data bit $x_u(n)$ over all active users, to give

$$\underline{s}(n) = \sum_{u=1}^{u=U} \underline{c}_u x_u(n) \tag{2.6}$$

In the uplink, the process is essentially the same, with the important difference that the users are no longer synchronised, which may be modelled by inserting user-specific time-delays on the resulting spread signal. These delays are normally uniformly distributed on the semi-open interval $[0, T_{bit}\ )$. The principal effect of this is to destroy any specially constructed correlation properties of the spreading sequences, so that it may be equivalently modelled using random sequences.

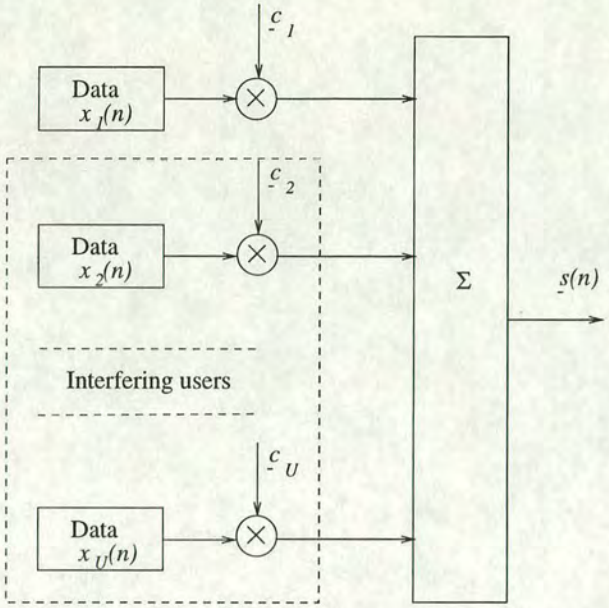

Figure 2.3: Simplified synchronous DS-CDMA downlink transmitter for U active users

2.2.2 The communication channel

In this section, the communications channel is described and some of the terms often encountered in this area are defined. Then, in section 2.2.2.3, the modelling of a specific channel model, which will be used later, is outlined.

2.2.2.1 Multipath channel background

The received signal does not, in general, consist solely of the direct line of sight (LOS) signal transmitted from the base station. Rather, in addition to general background noise, the received signal comprises a combination of individual signals which have been reflected off obstacles, such as buildings, between the base station and mobile receiver, and thus arrive at various delays, corresponding to the length of each of the associated RF paths [32]. This situation, termed a multipath channel, is illustrated in Figure 2.4, and is also, in general time-varying, due to motion of the receiver, or of the intervening obstructions.

If the number of scatterers is large and evenly distributed with no dominant signal path, the received signal is said to be subject to Rayleigh fading, while if one path (usually the direct one) dominates, the fading is termed Rician [32]. In general, the up and downlink frequencies are different, so that the channel effects, which are frequency-specific, are not the same. If the same frequency is to be used on the up and downlink, then time division duplexing (TDD) must

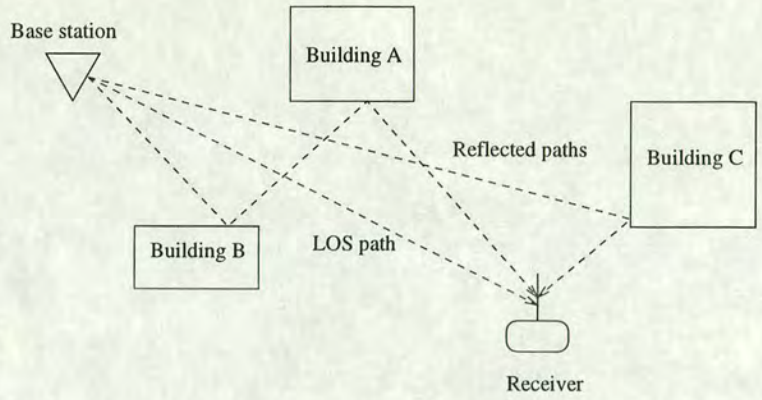

Figure 2.4: *Principle of multipath: the received signal consists of many reflections and/or diffractions of delayed versions of the transmitted signal*

be incorporated in the system to ensure sufficient separation. This RF round trip delay time limits the size of cells, which may be an important consideration in large rural areas, with a small widely distributed population.

The presence of a dispersive channel (whether time-varying or not) means that individual chips in the transmitted signal affect, and are affected by, a number of their immediate neighbours. This inter-chip interference (ICI) also effectively destroys any special correlation properties of the spreading sequences, so that, even on the downlink, where individual users' spread signals are synchronously aligned, any special properties of the spreading sequence set will be lost. A RAKE receiver could be employed to attempt to counter this effect, but in the work discussed here, other means of processing the received signal will be considered.

2.2.2.2 Channel effects

There are two main parameters of a channel which are of interest; namely the range of frequencies for which the channel effects are essentially the same, termed the coherence bandwidth and denoted f_0, and the time duration over which the channel response is essentially invariant, which is termed the coherence time and denoted T_0. These may be calculated [32] from the two dual functions $S(\tau)$, the multipath intensity profile, and $S(\nu)$, the Doppler power spectral density, which are measures of the received signal power as functions of delay time τ and Doppler shift ν respectively, for a transmitted impulse in the appropriate domain. The functions have characteristic shapes, which are sketched in Figure 2.5.

From $S(\tau)$, the largest time delay T_m, equal to the maximum delay for which a significant

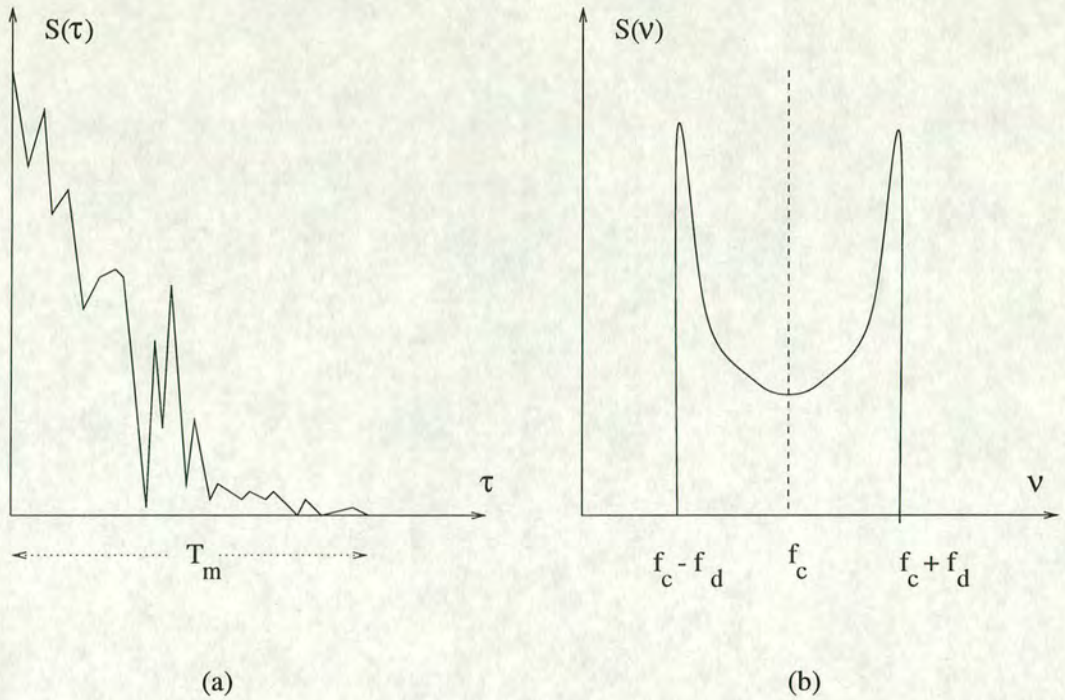

Figure 2.5: *Received power as a function of two independent variables: (a) multipath intensity profile $S(\tau)$; (b) Doppler power spectral density $S(\nu)$*

power is received could be used to define the channel coherence bandwidth. However, it is more useful to measure the distribution of the delays, and a valuable parameter is the standard deviation, or root mean squared (RMS) value, which is termed the delay spread σ_τ,

$$\sigma_\tau = \sqrt{(\bar{\tau^2}) - (\bar{\tau})^2} \tag{2.7}$$

The coherence bandwith f_0 is then inversely proportional to this quantity, with the exact constant of proportionality varying depending on the correlation value required (0.5 is commonly used). This sets an upper limit on the transmission rate that may be used without causing inteference beteween adjacent chips, and may also be obtained from the frequency correlation function, which is the Fourier transform of the multipath intensity profile $S(\tau)$.

Similarly, the channel coherence time T_0 may be obtained from the Doppler power spectral density $S(\nu)$, by defining the spectral broadening, or Doppler spread f_d, as indicated on the figure. The maximum of this quantity occurs for motions directly to and from the base station, and is then given by

$$f_{d_{max}} = \frac{v}{c} f_c \tag{2.8}$$

where v is the mobile speed, c is the electro-magnetic propagation speed and f_c is the carrier

frequency. The channel coherence time T_0 is then inversely proportional to this value, with the constant of proportionality popularly given by 0.423, which arises from the geometric mean of two different characterisations [32]. The coherence time may also be obtained from the time correlation function, which is the Fourier transform of the Doppler power spectrum, and is therefore the dual of the frequency correlation function.

2.2.2.3 Modelling of the COST 207 radio channel

The effects of a multipath channel may be modelled by forming the convolution of the transmitted signal $\underline{s}(n)$ with the impulse response $H(z)$, of the channel, which may be characterised by

$$H(z;t) = \sum_{j=0}^{j=n_h} h_j(t) z^{-j} \tag{2.9}$$

where n_h is the number of chips spanned by the multipath delay. In the analyses considered here, n_h will be a fixed (small) number, although this parameter could also be time-varying. The individual tap weights $h_j(t)$, which may also be time varying, are usually obtained by sounding the channel using a pilot signal of known amplitude and phase, and must be estimated with sufficient accuracy to counter the effects produced by the channel. The calculation of these channel tap weights is now discussed.

Studies by the European co-operation in the field of scientific and technical research (COST) on the characteristics of mobile radio channels at 900 MHz [5] resulted in the adoption of many standard RF channel models, which are distinguished by the situation to which they are to be applied and the number of taps in the representative impulse response. The channel chosen here is the typical urban (TU) 6-tap channel model, which must be acknowledged as one of the least dispersive of the various scenarios. More dispersive channel models include the bad urban (BU) and hilly terrain (HT) situations. The calculation of the channel impulse response tap weights are performed by the C routines generously provided by D. Laurenson of the Department of Electronics and Electrical Engineering, and are described in more detail in [33]. Figure 2.6, which is adapted from that paper, shows the calculation in detail for the coefficient of one delay tap, h_1.

The Gaussian noise sample, which may be obtained by the process described in [34] is fed into

[5] This program was COST-207, whose successor, COST-231 has recently been superseded by COST-259. The latter programs are concerned with channel models near 2GHz, which is expected to be the frequency for the next generation of personal communication systems.

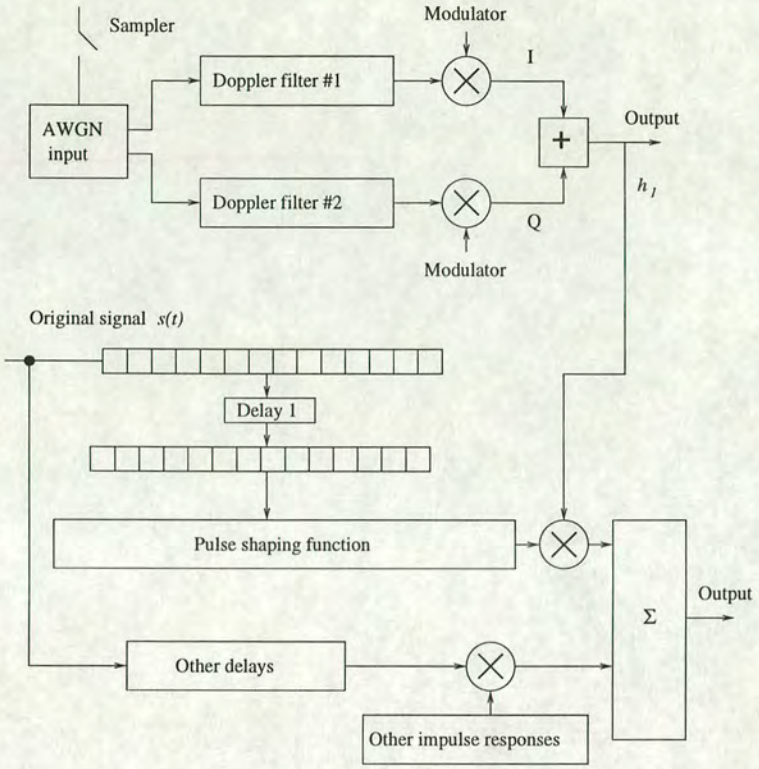

Figure 2.6: *Construction and use of the channel impulse response coefficients in the COST 207 model*

the two Doppler filters, corresponding to the real and imaginary components of the complex channel tap weight. These filters may be characterised as either classical, type 1 or type 2, depending on the desired filter characteristics, and are described more fully in [35]. The outputs from these are then used to construct a complex phasor and summed to give the final impulse response coefficient for the suitably delayed incoming signal. This process is then repeated over all the delay taps (6 in the case considered here) to give the final output as the convolution of the instantaneous impulse response, $H(z)$, of the channel with the shaped and delayed version of the transmitted signal $\underline{s}$. A more exact description of the channel modelling calculations employed in this study will be given in section 3.4.

2.2.3 Receiver principles

The task of the receiver is to recover the intended data $x(n)$ by collapsing the spectrum of the received signal vector $\underline{y}(n)$. This is performed by integrating the product of the received signal with a locally held replica of the required user's spreading sequence. Practically, this is achieved by the correlator receiver, shown in Figure 2.7. The received signal, consisting of N_r chips is passed to the block of delay elements, where z^{-1} represents a delay of one chip, until

the complete N_r-chip signal has been read in [6]. These values are then passed in parallel to the multiplier block, which forms the scalar product of $\underline{y}(n)$ and the tap weight vector $\underline{w} \in \mathbb{C}^{N_r}$, where N_r is the number of tap weights, which is set to 8 in the figure.

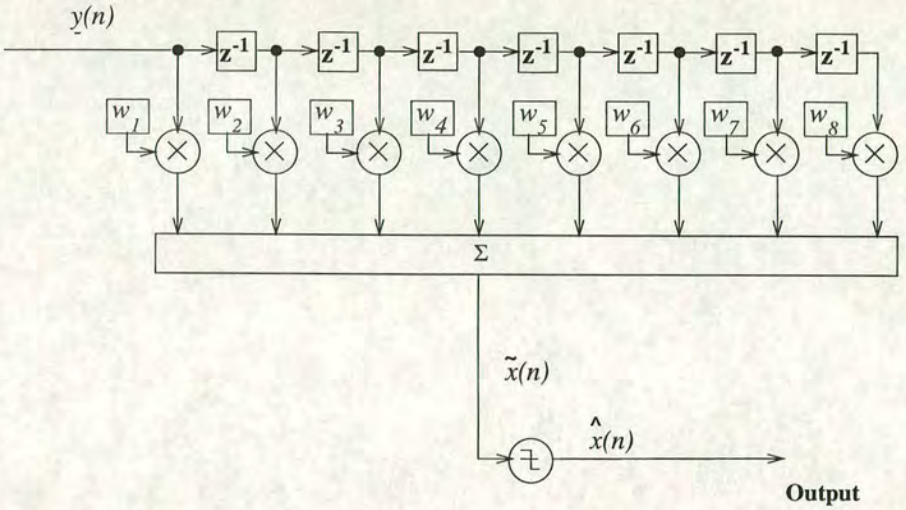

Figure 2.7: DS-CDMA correlator receiver with 8 tap weights

This finite impulse response (FIR) filter block [36] produces a soft output, $\tilde{x}(n)$, which is then passed to the sign-decision block to give a hard estimate, $\hat{x}(n)$, of the original data bit, $x(n)$ for the user of interest. The conceptually simplest receiver, the matched filter (MF) receiver, is simply the correlator receiver with M tap weights, $\{w_j : 1 \leq j \leq M\}$, matched to the complex conjugate time-reverse [7] of the original spreading sequence of the required user which, without loss of generality, we may take to be user 1. In practice, the acquisition and synchronisation of the chip-level signal is a highly non-trivial task [25]. Techniques to achieve synchronisation involve the use of a pilot signal, which may be modelled by one additional user, whose data is constant. Perfect timing will be assumed in the following, except where stated.

2.2.4 Example downlink system

Consider the reduced form of Figure 2.2, shown in Figure 2.8, in which $\underline{x}(n) = (x_1(n)x_2(n) \cdots x_U(n))^T$ represents the data vector of all users at time $t = nT_{bit}$, $\underline{s}(n)$ (of length M) is the resultant spread signal and $\underline{z}(n)$ represents the M-dimensional vector of Gaussian noise samples which, for the downlink, are iid and have a variance of σ^2.

[6] alternatively, it is possible to read successive chip samples in to the receiver at each clock count in a serial manner, or to use a hybrid serial-parallel correlator (SPC), by employing a number of sub-blocks, each corresponding to a specific portion of the spreading sequence which has the advantage of requiring less hardware

[7] since the received signal will be the time-reverse of the transmitted signal

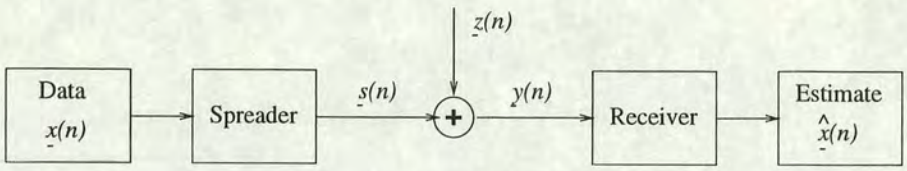

Figure 2.8: Communication principle in the additive white Gaussian noise channel

Under the assumptions of long randomly selected spreading sequences with no special cross-correlation properties, the theoretical analysis of this system [37] leads to the predicted probability of error for the matched filter ($P_e^{MF}(U, g_P)$) to be given by

$$P_e^{MF}(U, g_P) = Q\left(\sqrt{\frac{g_P}{\sigma^2 + (U-1)}}\right) \tag{2.10}$$

where U is the number of users, σ^2 is the variance of the noise and g_P is the linear processing gain, which is simply M in this case. The function $Q(\zeta)$ is the standard Gaussian upper cumulative distribution function as defined in [38] by

$$Q(\zeta) = \frac{1}{\sqrt{2\pi}} \int_{\zeta}^{\infty} e^{-\frac{z^2}{2}} dz \tag{2.11}$$

It is also possible, as shown in Appendix B, to express equation 2.10 in terms of the complementary error function, using the identity

$$Q(\zeta) = \frac{1}{2} \operatorname{erfc}\left(\frac{\zeta}{\sqrt{2}}\right) \tag{2.12}$$

The predictions of equation 2.10 may be compared against the results from Monte Carlo simulations of a system employing 31-chip random spreading sequences, shown in Figure 2.9. The perfomance statistic is the probability of error, P_e, as described in section 2.2, and is simulated for increasing numbers of users for a typical noise level of 7 dB [39], as well as a more noisy environment of 4 dB, and the limit as the background noise tends to zero ($E_b/N_0 \rightarrow \infty$).

The spreading sequences are periodically shuffled (using the efficient shuffling algorithm described in [40]) to avoid biasing of the results by particular cross-correlations due to individual pairs of sequences, and it may be seen that this technique results in simulations which are in close agreement with theoretical predictions. Importance sampling (IS, or variance reduction) techniques [41] have recently been applied to the DS-CDMA environment [42] to reduce the computation time required for probabilities of error below around 10^{-4} by biasing the noise samples to produce an artificially large number of errors. This technique is not employed here, since care must be taken to ensure that the results obtained by this process are statistically

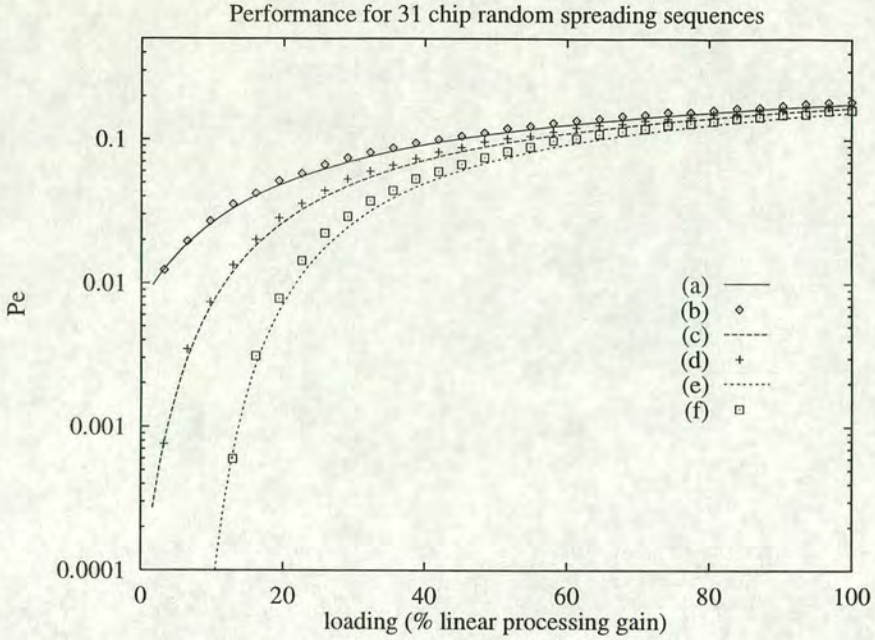

Figure 2.9: *Theoretical and simulated probability of error in the AWGN channel for the matched filter receiver with 31-chip random spreading sequences: (a) theoretical, $E_b/N_0 = 4$ dB; (b) simulation results, $E_b/N_0 = 4$ dB; (c) theoretical, $E_b/N_0 = 7$ dB; (d) simulation results, $E_b/N_0 = 7$ dB; (e) theoretical, $E_b/N_0 \to \infty$; (f) simulation results, $E_b/N_0 \to \infty$*

significant. As may be seen, the performance degrades smoothly as the number of active users increases. The performance also varies smoothly with background noise, so that each of these phenomena may be taken to constitute the interference in the system. The results for $E_b/N_0 \to \infty$ are also in very close agreement with those of [43], which are for an asynchronous system using Gold sequences, thus demonstrating that random sequences may be used to accurately model the effects of a loss of timing information on a specially constructed spreading sequence set.

2.2.5 Discussion

This section has demonstrated that the capacity of a DS-CDMA system is interference (whether from MAI or noise) limited. The performance (in terms of the probability of error P_e) has been shown to degrade gracefully as the number of simultaneous users increases. This means that improving the capacity of such spread spectrum systems may be achieved either by reducing the total interference by enhancing single user detection methods or by making use of the structured nature of the multiple access interference through improved interference cancellation (IC), joint detection (JD) or multi-user detection (MUD) techniques. Before considering the

relative benefits and costs of these approaches, some aspects of the system design will first be described.

2.3 Aspects of DS-CDMA system design

In this section, various aspects of DS-CDMA system design, the application of which will be discussed in greater detail in subsequent chapters, are introduced. In section 2.3.1, the use of various spreading sequences is discussed, while some alternatives to the simple matched filter receiver are described in section 2.3.2. Techniques of encoding the data to protect against errors are briefly outlined in section 2.3.3, with interference cancellation techniques described in section 2.3.4. Multi-user detectors, which make efficient use of the interference on all the users' signals simultaneously are introduced in section 2.3.5. Finally, an indication of some non-linear receiver structures is given in section 2.3.6.

2.3.1 Choice of spreading sequences

The choice of spreading, or signature sequences, is an important one for the system designer. Historically, this choice was motivated by the requirement for a low probability of inference of the spreading sequence, and hence interception of the transmitted data, since the over-riding requirement was security [44]. This prompted the desire for very long sequences which could be generated easily by co-operating parties but which at the same time, were difficult for interfering, or eavesdropping parties to infer. However, the advent of the implementation of spread spectrum techniques for multiple access communications has shifted the emphasis somewhat away from such security issues to maximising the number of subscribers who are able to access a system simultaneously [13], while maintaining a reasonable error performance. Because the spread signal is correlated against a target sequence in the receiver, the main characteristics of a set of sequences which determines its suitability for DS-CDMA, are its even and odd[8] auto- and cross-correlation properties.

[8] even correlation is when bits of the same sign are used with a spreading sequence, while odd correlation is when oppositely signed bits are used

2.3.1.1 Randomly selected sequences

Spreading sequences chosen purely at random would theoretically be ideal for single-user DS-SS communications systems, since the probability of inference of the sequence, and hence eavesdropping of the data signal is low. The disadvantage in using completely randomly-chosen sequences for multiple access systems is that spreading sequences selected at random have poor cross-correlation properties, since they must be reasonably short for a practical system and by definition, no attempt has been made to optimise their cross-correlation values[9].

2.3.1.2 Pseudo-random sequences: m-sequences

The earliest attempts [45–47] to produce long sequences, suitable for spread spectrum communications, made use of linear feedback shift registers (LFSR), an example of which is shown in Figure 2.10 for 5 taps.

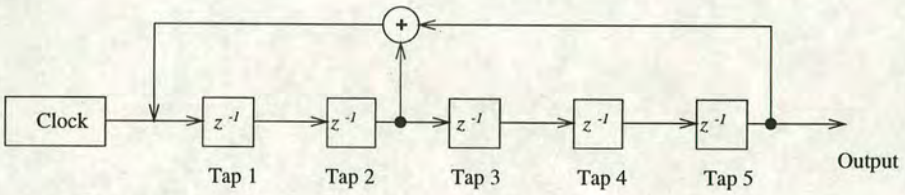

Figure 2.10: Example linear feedback shift register with 5 taps

The specific tap connections which are included in the feedback loop may either be specified directly as $[5, 2]_s$[10], or expressed via the characteristic polynomial as $x^5 + x^3 + 1$, or in octal format [48] as 51_o. The longest sequence which may be generated by such an arrangement is the maximal [49] or m-sequence, and has a length of $2^{n_t} - 1$ where n_t is the number of taps. Thus, in the example case shown here, the m-sequence has length 31. The autocorrelation of an m-sequence is two valued, with a peak when the phase offset is zero, while the cross-correlation between m-sequences is also well-defined. However, the total number of m-sequences which may be generated by an appropriate series of connections [50] of an n_t-stage register is limited to $N_m(n) = (1/n_t)\tau(2^{n_t} - 1)$ where τ is the Euler totient function[11], so that in the system considered here, there are only 6 m-sequences. Thus, although the correlation properties of m-sequences are more favourable for DS-CDMA than sequences selected at random, the relatively

[9] although it must be acknowledged that very long randomly selected sequences would have zero cross-correlation on average

[10] connections from tap 0 and tap 5 are assumed, so only the length of the register and the intermediate tap connection(s) are required

[11] $\tau(n)$ is given by the number of integers less than n which are relatively prime to n, e.g. $\tau(31) = 30$

small number of m-sequences compared to their length means that they are of only limited use for a multiple access spread spectrum system.

2.3.1.3 Pseudo-random sequences: Gold sequences

To gain increased capacity (at the expense of altering the correlation properties slightly), a pair of m-sequences may be used to construct a set of Gold sequences [51], which have the property that the cross-correlation is always -1 when the phase offset is zero. Non-zero phase offsets produce a correlation value from one of three possible values. The choice of preferred pairs of m-sequences is described in [48], while preferrentially phased Gold sequences (PPGS), which expand the region of low cross-correlation to include points closer to the zero phase offset, have also been proposed for a DS-CDMA system [52]. Since their synchronised correlation characteristics are good, while their unsynchronised characteristics are not excessive, Gold sequences offer a reasonable choice of spreading sequences for DS-CDMA systems, and will therefore be used in later chapters.

2.3.1.4 Orthogonal sequences: Walsh sequences

For multiple access, it is obviously optimum if the cross-correlation between spreading sequences is zero. This may be achieved by using Walsh sequences[12] [53], which, since they are mutually orthogonal, offer maximum capacity if synchronised, but, because of high cross-correlations for non-zero phase offsets, induce a greater amount of MAI than simply using random sequences if timing is not maintained.

In the investigations reported here, Gold sequences and random sequences will be used as the two main spreading sequences, since Gold sequences demonstrate situations which are synchronised and near orthogonal, while random sequences are able to mimic the use of other sequences when timing impairments are present or when the properties of the sequences have been corrupted due to inter-chip interference arising from the presence of a dispersive channel.

[12] sometimes denoted Rademacher-Walsh sequences

2.3.2 Linear and adaptive receiver structures

The matched filter receiver described in section 2.2.3 may be replaced by alternative structures, which are distinguished by the values of the receiver tap weights $\underline{w}$, with the intention of better estimating the required data. The architectures considered here are all FIR filters, while adaptive filters, described in section 2.3.2.3, may be made IIR by employing decision-direction, in which one or more of the previously estimated values are assumed correct, and then used as training data to update the tap weights. This can lead to stability problems if the initial decision proves to be incorrect, forcing the tap weights away from ideal values. In the following, it will be useful to define a penalty or cost function, $f_{Pen}(\cdot)$, of the difference e between the original data bit of the desired user $x(n)$ and its estimated value $\tilde{x}(n)$. Requirements on the nature of this function will be described in section 2.3.2.3.

2.3.2.1 The zero-forcing filter

The zero-forcing filter [54] is an FIR filter, whose tap weights are given by inverting the auto-correlation matrix, discussed in the next section, of the received signal. This filter completely removes the deterministic MAI, but suffers from the disadvantage that the non-deterministic background noise is amplified, and so will not be considered further here.

2.3.2.2 The Wiener filter

The Wiener [55], or minimum mean square error (MMSE [56]) filter is given by minimising the expectation of the square error penalty function

$$f_{Pen}(x(n), \tilde{x}(n)) = (e(n))^2 = (x(n) - \tilde{x}(n))^2 \tag{2.13}$$

For the DS-CDMA receiver, the tap weights are given by [57]

$$\underline{w}_{Wiener} = \Phi_{yy}^{-1} \underline{\phi}_{yx} \tag{2.14}$$

where Φ_{yy} is the autocorrelation matrix of the signal vector and $\underline{\phi}_{yx}$ is the cross-correlation vector between $\underline{y}$ and the original data symbol $x(n)$. The inversion of the matrix is the main drawback to this approach since the dimension of the square matrix is equal to the receiver filter length N_r. Even with specialised techniques such as Choleski decomposition, inversion

of the positive definite autocorrelation matrix requires $O(N_r^3)$ operations, where N_r is the number of receiver tap weights, which in this application is at least[13] the length of the spreading sequence, and so for long spreading sequences, this represents a significant overhead, reducing the practicality of this approach. Hpwever, it must be acknowledged that for shorter spreading sequences, such as considered in the next chapter, direct matrix inversion (DMI) may be computationally feasible, and could represent an alternative to the adaptive techniques which will now be considered. Here, the inversion is achieved using routines from [34]. As will be shown, the Wiener filter represents the target tap weights of an adaptive filter with Equation 2.13 as penalty function, and so will be used as a reference for the performance of such receievers.

2.3.2.3 The adaptive filter

An example adaptive filter is shown in Figure 2.11, in which the number of receiver tap weights N_r is set to 8.

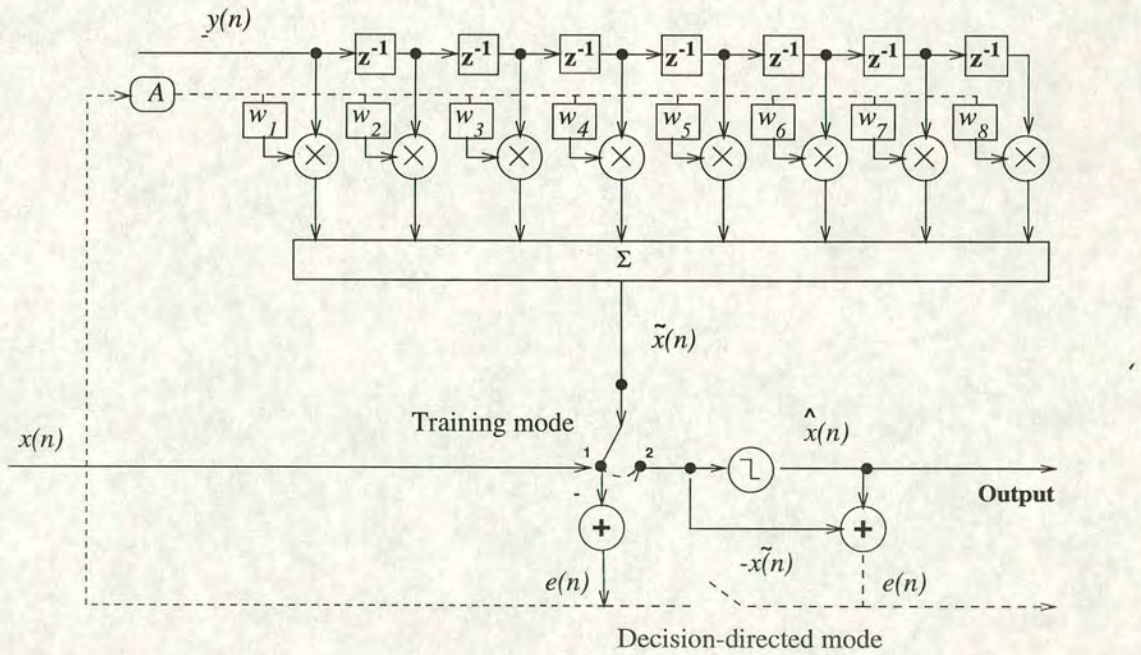

Figure 2.11: Example adaptive receiver filter with 8 tap weights

The motivation for the use of adaptive algorithms lies in the desire to change the individual taps of the receiver filter to respond to changes in the communication channel. The traditional implementation of adaptive receivers is that a sequence of *a priori* known training data is incorporated into the data stream at pre-arranged times. It is important to acknowledge that

[13] N_r could be set greater than N_s to capture energy from a dispersive channel

this effectively reduces the overall data rate of the system, which is the main drawback of this approach.

Algorithms for adapting the receiver without using training bits are termed blind and proceed by adapting the tap weights to optimise some function of the resulting soft decision. Examples include attempting to ensure that the intermediate soft decision has a constant modulus (CM), which for BPSK modulation would be unity, or maximisation of energy (MOE) of the soft decision. The disadvantages in using blind adaptation for the DS-CDMA radio environment are firstly the great length of time required to achieve practical results and secondly, that the receiver may lock on to the data stream of an interfering user, rather than the desired user. Recently, [58] a linearly constrained CM algorithm has been proposed for single user detection in DS-CDMA in which the constraints imposed essentially force the tap weights to have components aligned with and orthogonal to the desired user's signal. The work presented here will, however, focus only on trained algorithms, which are also termed reference directed.

The goal of any adaptive algorithm [59] is to use this training data to force the receiver tap weights to minimise some cost or penalty function, $f_{Pen}(\cdot)$, of the difference metric between the original data bit and its estimated value. The only requirement for this penalty function [60] is that it be a monotonic increasing function of the absolute value of its argument, with a global[14] minimum at zero. Here, the number of training bits is given by N_{train}, and the sequence of training data by $\{x(n) : 1 \leq n \leq N_{train}\}$.

In the following sections, we shall again consider the square error penalty function, given by equation 2.13 With this penalty function, the resulting target tap weights have been shown to be given by the Wiener filter, of Section 2.3.2.2 [57], so that these algorithms may be viewed as an iterative approximation to the Wiener filter. Two adaptive methods which employ this least square error penalty function are the least mean square (LMS) [61] and the more complex recursive least squares (RLS) [62] algorithms. These algorithms are depicted schematically in Figure 2.12, with an idea of the complexity of each method given in Table 2.1.

As may be seen, the order of operations of the algorithms are broadly similar, each performing a correlation with an FIR filter to obtain a (soft) estimate, $\tilde{x}(n)$ of the training data bit $x(n)$, as in the correlator receiver. The error $e(n)$ in this estimate is then used to update the tap weights of the FIR receiver filter.

[14] the presence of local minima in the penalty function is essentially why blind adaption via the constant modulus algorithm is prone to error

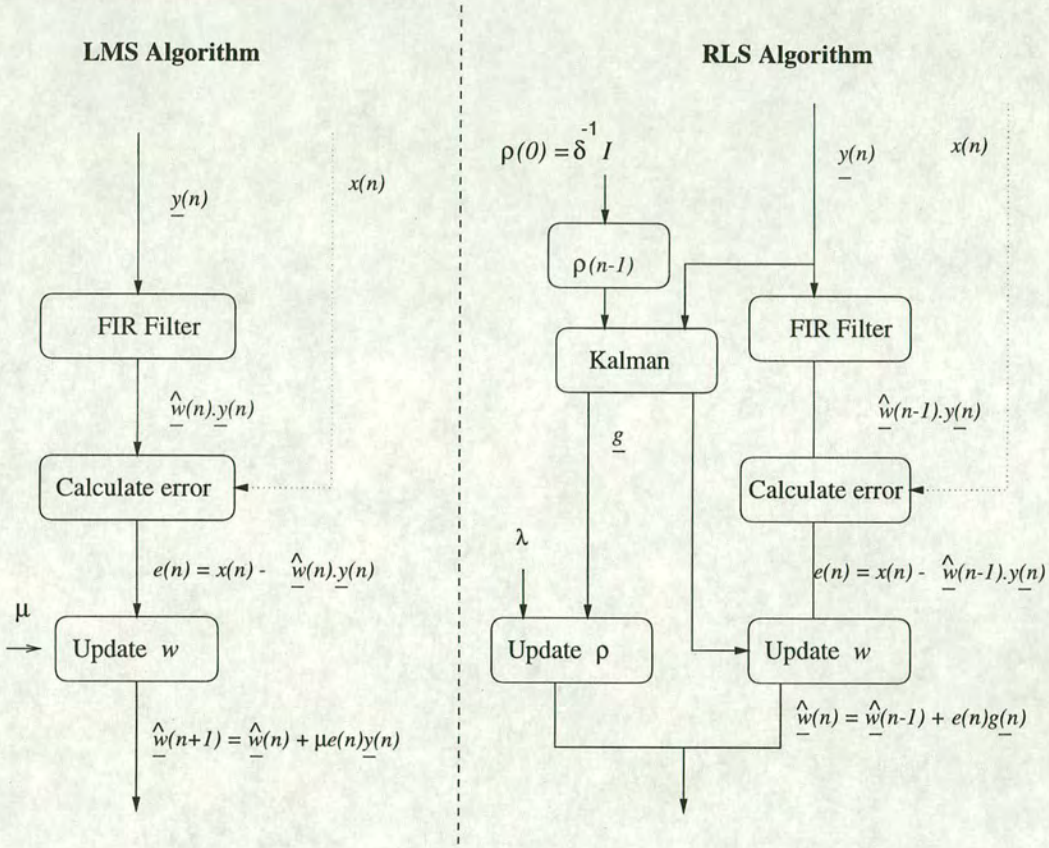

Figure 2.12: Comparison between LMS and RLS algorithms

Algorithm	Multiplications	Divisions	Additions/Subtractions
LMS	$2N_r$+1	0	$2N_r$
RLS	$2N_r^2$+7N_r+5	N_r^2+4N_r+3	$2N_r^2$+6N_r+4

Table 2.1: Complexity of LMS and RLS algorithms

In the LMS algorithm, this is performed by a simple weighting of the error by the *step size* μ, while in the RLS algorithm, the error is used to update the current estimate of the inverse of the autocorrelation matrix $\rho(n)$, and the tap weights are updated using the Kalman gain vector $\underline{g}$. The additional input to the RLS algorithm is the forgetting factor λ, which controls how influential previous received signals are in forming the current estimate of the optimal filter. Thus, strictly, the RLS algorithm does not minimise 2.13, but rather the modified form given by equation 2.15.

$$f_{Pen}(x(n), \tilde{x}(n)) = \sum_{i=1}^{n} \lambda^{n-i}(e(i))^2 \tag{2.15}$$

The exponential weighting factor λ means that the effective memory of the algorithm is given by $1/(1-\lambda)$ data bits. This parameter may be tuned to neglect the influence of older data bits which may lead the receiver to adapt the tap weights to incorrect values, as may for example be the case in a time-varying channel.

The application of these two adaptive algorithms to a DS-CDMA system in AWGN and of the RLS algorithm in a time-varying channel is discussed in more detail in Chapter 3, but the main criteria by which an adaptive algorithm may be judged are [62] the complexity of the algorithm, the speed of convergence, and the residual error, or misadjustment present once the algorithm has converged. As may be seen from Table 2.1, the LMS requires O(N_r) flops[15], while the RLS requires O($N_r{}^2$), making the latter a more complicated algorithm as the filter length is increased. The convergence properties of these algorithms will be investigated in the next chapter. Additional properties which may also be important are the robustness of the algorithm to cope with degenerate or ill-conditioned input values, the numerical properties of the algorithm in the presence of quantisation errors and the structure of the algorithm, which may affect its implementation in hardware.

2.3.3 Forward error correction

Forward error correction (FEC) [60] is frequently employed in communication systems where it is important that a message be received with as few errors as possible. Examples include space communications [63] and audio compact disc players [31]. FEC coding sacrifices resources,

[15] floating point operations

in terms of the data rate, to provide some extra information about a particular data bit. This information is then used to estimate the original data bit, with greater integrity than if the original data rate had been used.

FEC codes fall into two main categories; linear block codes, which append one or more code digits to the original data bit, and non-linear[16] convolutional codes, which use a number of input digits to calculate the code word, as shown schematically in Figure 2.13.

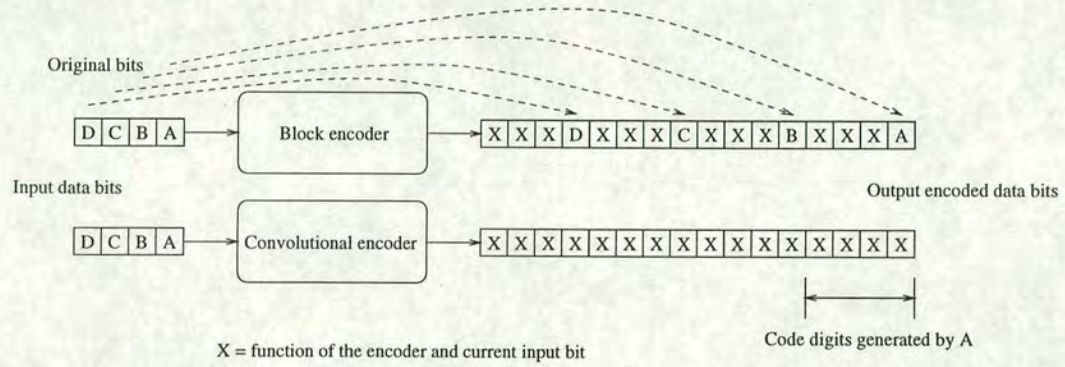

Figure 2.13: Forward error correction using block and convolutional encoders

In the following, only convolutional coding, and variants thereof, will be considered, since there exists a commonly agreed standard for their decoding which is readily available in hardware, and because block codes are less suited to the mobile wireless communications environment.

The specifics of convolutional coding are described in section 2.3.3.1, followed by an example in section 2.3.3.2. The error-correcting performance of this particular configuration is analysed in section 2.3.3.3, and the method adopted here to decode the received data stream is described in section 2.3.3.4.

2.3.3.1 Convolutional encoding

Convolutional encoding maps each original data bit onto a coded sequence of digits,a process which may alternatively be considered as a transition of a Markov process [36]. Because only certain coded sequences may precede and follow any given coded sequence, corresponding to allowable transitions, the receiver is able to detect when less than a given number of errors occur, and, depending on the coder configuration, correct one or more individual data bit errors.

[16] in the sense that the output is not simply a function of the current input, and they do not obey the superposition principle

There are a number of parameters which describe the specific implementation of convolutional coding; these are the rate of the encoder and the constraint length. The rate R of the encoder is defined as the ratio of input data bits (b) to the number of output digits (C), while the constraint length K is the number of input bits which the encoder uses to form this output. Convolutional codes may be generated by a set of shift registers, whose output is the result of modulo 2 addition[17] of up to K original data bits. The designation of the encoder is given by the octal form of the tap connections to the modulo-2 adder. The C-dimensional convolutionally encoded sequence for user u at time T_n, obtained from data bit $x_u(n)$ will be designated $\underline{q}_u(n) \in \mathcal{A}^C$ to distinguish this from the DS-CDMA spreading sequence $\underline{c}_u(n)$.

2.3.3.2 Example of convolutional encoder

To illustrate the above principles, Figure 2.14 shows a constraint length 3, rate $1/2$ encoder defined by $(7,5)_8$, where the octal subscript will be assumed in future. The time delay z_{bit}^{-1} in the shift register arrangement represents a delay of one data bit, in contrast to the z^{-1} used previously, which represents a delay of one chip. Knowledge of the encoder permits the

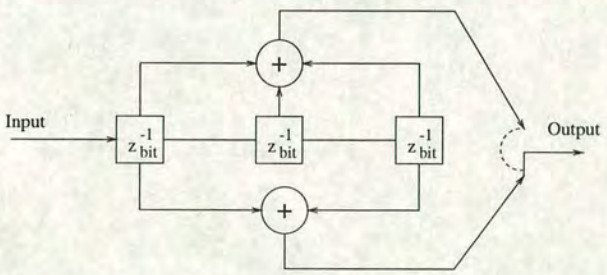

Figure 2.14: Rate $1/2$, constraint length 3 $(7,5)_8$ convolutional encoder

construction of a transition table, as shown in Table 2.2, in which there are four distinct states, corresponding to the values of the previous two[18] data bits.

An alternative representation of the transition table is the state diagram, shown in Figure 2.15, in which the nodes are labelled as in the transition table and the output code sequences are shown circled for the appropriate combination of current state and input data bit.

In the figure, the transitions produced by an input of 0 are shown as solid lines, while those corresponding to a 1 are shown as dashed lines. Thus, the state diagram may be used to calculate

[17] for input bits in the set $\mathcal{A}$

[18] in general, there are 2^{K-1} states, corresponding to the previous $K-1$ data bits

Previous two data bits	Current state	Input data bit	Output code word	New state
00	a	0	00	a
		1	11	b
01	b	0	10	c
		1	01	d
10	c	0	11	a
		1	00	b
11	d	0	01	c
		1	10	d

Table 2.2: *Transition table showing output code words for each input data bit at each state for the (7,5) convolutional encoder*

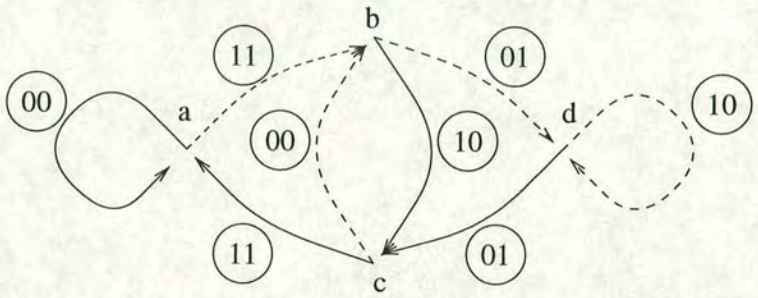

Figure 2.15: The state diagram for the $(7, 5)$ convolutional encoder

the output of the coder for a given stream of input data bits. It may also be employed to derive the theoretical performance, as described below.

2.3.3.3 Theoretical analysis of convolutional codes

The error correcting power of a particular code configuration depends on the ability to identify and correct individual bit errors. To analyse the theoretical performance of a convolutional coding structure, the distance (in terms of the Hamming metric) between code words will be considered. In this analysis, attention will be fixed on the all-zeros codeword (00 in this case where the rate $R = 1/2$).

From the state diagram in Figure 2.15, it is possible to calculate the transfer function $T(d)$, which provides the distance (or weight) spectrum of the code, denoted $\{a_k\}_{k=d_{free}}^{\infty}$, where d_{free} is the free distance of the code [31], which represents the minimum possible run of ones before the all-zeros codeword may again be output for an input of zero. Splitting node a into

two and denoting the new node (representing the output) as e, the transfer function is given by

$$T(d) = \frac{X_e}{X_a} \tag{2.16}$$

where X_i represents the distance measure in arriving at node i.

In this case, the transfer function is given by

$$T(d) = d^2\left(\frac{d}{1-d}\right)\left(\frac{d^2(1-d)}{1-2d}\right) = \frac{d^5}{1-2d} = \sum_{k=5}^{\infty} a_k d^k \tag{2.17}$$

so that $d_{free} = 5$ and the elements of the weight spectrum are given by $a_k = 2^{k-5}$.

This then provides a mechanism for calculating an upper bound on the error performance of the convolutional code, since if the probability of error in choosing between any two particular code-words [31] is given by

$$P_2 = Q\left(\sqrt{2\frac{E_b}{N_0}Rd}\right) \tag{2.18}$$

where R is the rate of the code and d is the distance, then the total error probability is bounded by

$$P_e \leq \sum_{d=d_{free}}^{\infty} a_d P_2(d) \tag{2.19}$$

$$= \sum_{d=d_{free}}^{\infty} a_d Q\left(\sqrt{2\frac{E_b}{N_0}Rd}\right) \tag{2.20}$$

$$\simeq \sum_{d=d_{free}}^{d=d_{upper}} a_d Q\left(\sqrt{2\frac{E_b}{N_0}Rd}\right) \tag{2.21}$$

where d_{upper} is chosen so that sufficiently accurate results may be obtained. Optimum connections for various rate and constraint length convolutional codes may be found in *e.g.* [64]. Catastrophic codes, for which there exists at least one path of zero Hamming distance from a non-zero state to itself, are rarely used due to instability problems, and will not be considered here.

2.3.3.4 Forward error correction decoding: The Viterbi algorithm

The exact details of how the receiver operates to decode the data stream, while maintaining a balance between performance, complexity and storage requirements is non-trivial [65], and algorithms to estimate the original data fall into two categories. The commonest is

maximum likelihood sequence estimation (MLSE), most popularly implemented using the Viterbi algorithm [66], while alternative approaches include sequential decoding, which is most commonly implemented using either the Fano algorithm [65] or the more storage-intensive [31] stack algorithm, or variants thereof, *e.g.* [67]. The latter non-optimal techniques essentially involve keeping track of a non-fixed number of possible values, and making a retrograde step if the initial tentative decisions are found to be in error. The decoding algorithm used here will be the Viterbi algorithm (VA) [68], implemented as described in [69]. This technique proceeds by using the state diagram of the encoder to construct a trellis, the surviving branches of which at each time step are determined by a comparison between the received signal and all possible transmitted signals[19].

If the Hamming metric is used in this comparison, the process is termed hard decision, while if the Euclidean metric is used, the decoder is operating in soft decision mode. The latter improves performance by around 2 dB for most values of E_b/N_0 [70], and is the scheme adopted here.

After an appropriate amount (corresponding to the survivor path length, L) of data has been received and analysed, the algorithm makes a decision on the optimal path back through the trellis and hence deduces the initial data bit. Thus, a decision is only made on a particular data bit after encoded digits arising from L data bits have been received, as shown in Figure 2.16, in which C, the number of output digits is set to 3 and L is set to 4, for illustrative purposes.

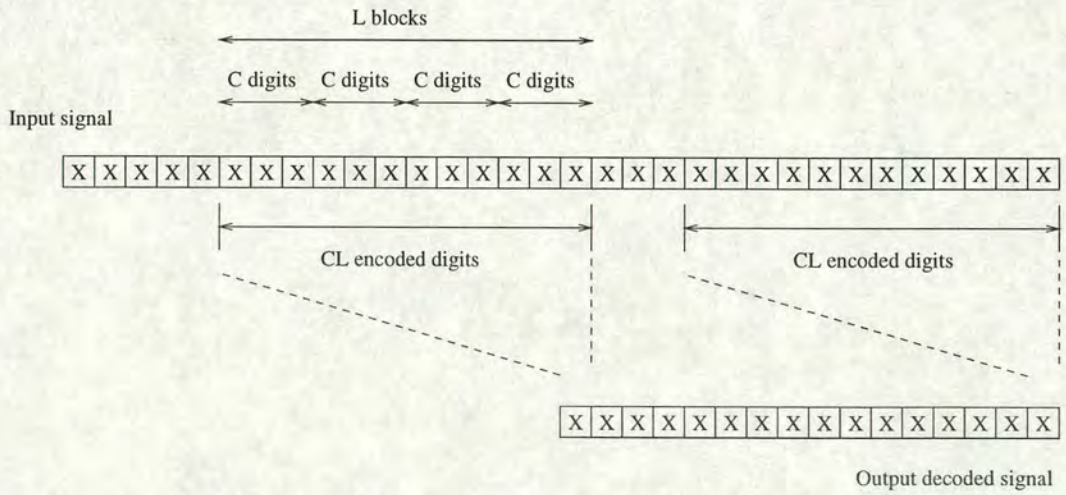

Figure 2.16: *The parts of the received signal involved in the decoding operation with* $C = 3$ *and* $L = 4$

This represents an additional processing delay which must be tolerated by the system as a whole. It has been shown [70] that provided the survivor path length, L, is greater than 4 or

[19] which is a subset of all possible *data* symbols by virtue of the encoding process

5 times the constraint length, K, then the performance is not greatly reduced from a much larger trellis. In many scenarios, a sequence of zeros of length $K-1$ is periodically inserted into the data stream to drive the trellis to a known state. This technique perhaps artificially improves the performance, since an error made in this block of flushing data, leading to an incorrect trellis state is then overridden when the next block of data is read in, because the decoder assumes a known starting state for each new block of data. However, it has been shown [70] that the performance is similar whether the data stream is flushed in this way or not. In this implementation, flushing zeros are used and the trellis is re-calculated for each data bit, beginning from the point corresponding to the previous L bits of data. This increases the computation time, but is equivalent to having an infinitely long trellis, which is periodically sampled. Thus the output decoded data bit always depends on all the next L data bit's worth of information, which is termed the memory of the algorithm.

The disadvantages in using FEC in any communication system are the sacrifice of resources (in terms of the data-rate) to accommodate the extra coding, the delay imposed by processing the signal at the receiver before data may be output, and the storage requirements of any decoding algorithm. With convolutional coding and Viterbi decoding, the delay is a linear function of K, while the storage is exponential in K. While a processing delay is tolerable in many situations, excessive delays (*e.g.* greater than 5ms for speech data) may not be appropriate in the wireless communications environment, in which the properties of the transmission channel may change rapidly over time, or for which the demands of the system require near real-time communication. The application of convolutional coding to the DS-CDMA environment is considered in more depth in Chapter 4, which also discusses the efficient allocation of resources to FEC coding and direct sequence spreading.

2.3.4 Interference cancellation

Single-user communications systems are typically mainly affected by unstructured background noise and structured interference from ISI arising from multipath channels. On the other hand, DS-CDMA systems are also affected by structured multiple access interference (MAI) from the encoded signals of other users. Of the many ways to combat this interference (*e.g.* [71]), the two which are considered in this work are interference cancellation, described in this section, and joint detection, or multi-user detection (MUD), described later. Interference cancellation (IC) [72] exploits knowledge of the other users' spreading sequences to attempt to remove

their contributions from the received signal. [20] This technique was successfully deployed for the DS-CDMA environment in [43], using a matched filter for the initial estimate, in an asynchronous system employing Gold spreading sequences. The theoretical analysis of the synchronous system with random spreading sequences has been developed in [37], in which a Wiener filter was used for the intermediate data estimate. In [73], a Wiener filter was employed both for the initial estimate and for the final data extraction, and it was demonstrated there that the performance afforded by this arrangement surpassed any other single-stage cancellation structure.

The successive [74], or serial interference cancellation principle [75] is shown in Figure 2.17, while that for parallel cancellation is shown in Figure 2.18

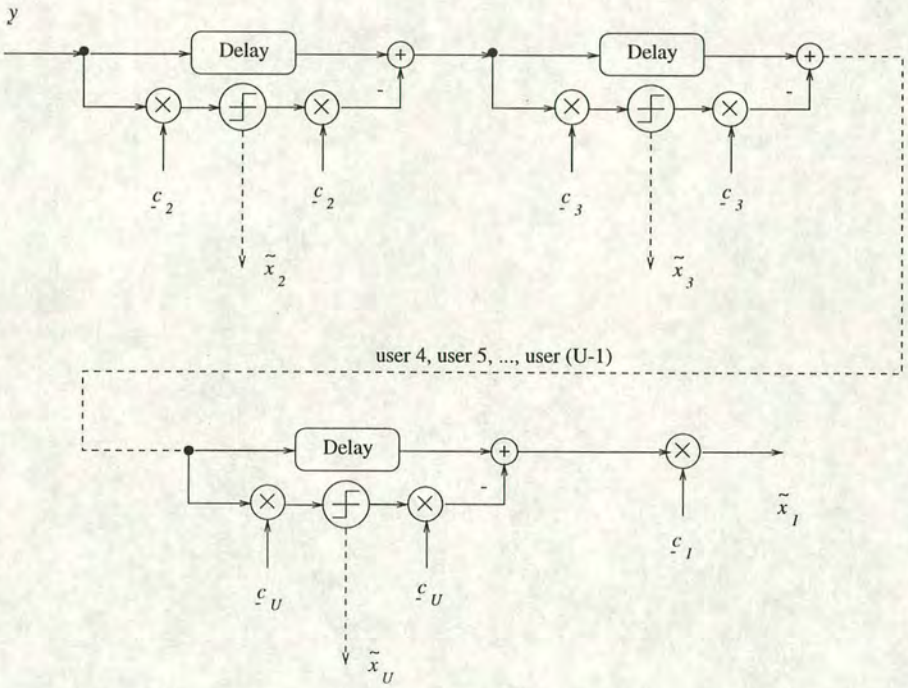

Figure 2.17: Successive interference cancellation technique for U active users

The delay incurred by interference cancellation is fixed for the parallel implementation, but variable for the serial approach, since this depends on the number of users whose contributions have to be estimated and cancelled. On the uplink, it may be beneficial to use the serial approach, and only cancel users whose data may be estimated with a reasonable degree of accuracy, since, as will be shown, incorrect estimation and cancellation reduces the final performance. This approach may also be useful if no power control is available, since the strongest contributions may be estimated and cancelled first, before a decision is made whether to proceed with cancelling the contributions from the remaining users. Serial cancellation

[20] The security implications of allowing users access to other users' signals may also be an important consideration.

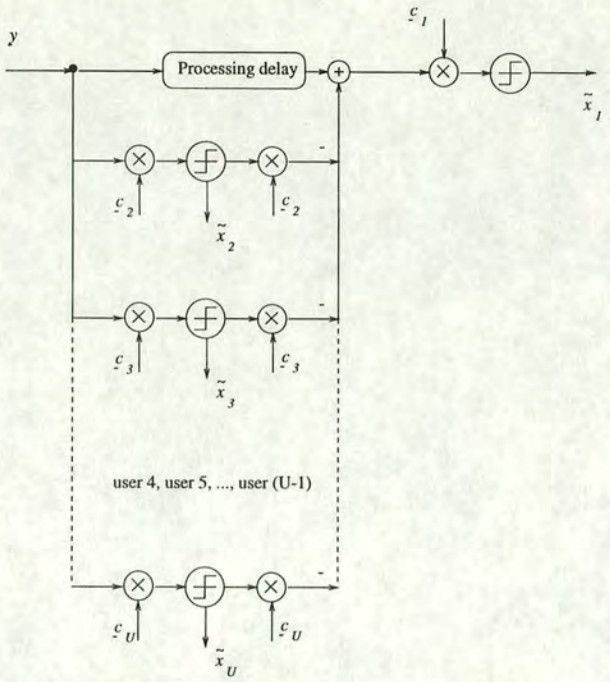

Figure 2.18: Parallel interference cancellation technique for U active users

suffers poor performance when all users have the same power, which is the case considered here, so the cancellation schemes proposed here will all be implemented in a parallel fashion. The application of interference cancellation to the DS-CDMA system will be considered in more depth in Chapter 5, which investigates the combination of forward error correction using convolutional coding with parallel interference cancellation.

2.3.5 Multi-user detection techniques

Rather than attempting to cancel the interference from the other users in the system, the principle of multi-user detection (MUD, or joint detection) [76] operates by treating the multiple access interference as additional information, which may be used to obtain a better estimate of the intended data. An overview of MUD techniques is given in [77], but the general principle, illustrated in Figure 2.19 is to calculate a set of soft decisions (obtained here using a bank of matched filters) which, taken together, form a sufficient statistic for $x_1(n)$, even though the individual soft decision $\tilde{x}_1(n)$ may not be. MUD detectors are near-far resistant [78], however the disadvantage of using an MUD approach is that the complexity of the receiver increases in a non-linear (usually exponential [79]) manner, so that the most useful place to carry out this operation is at the base station [80], where sufficient resources are likely to be more readily available.

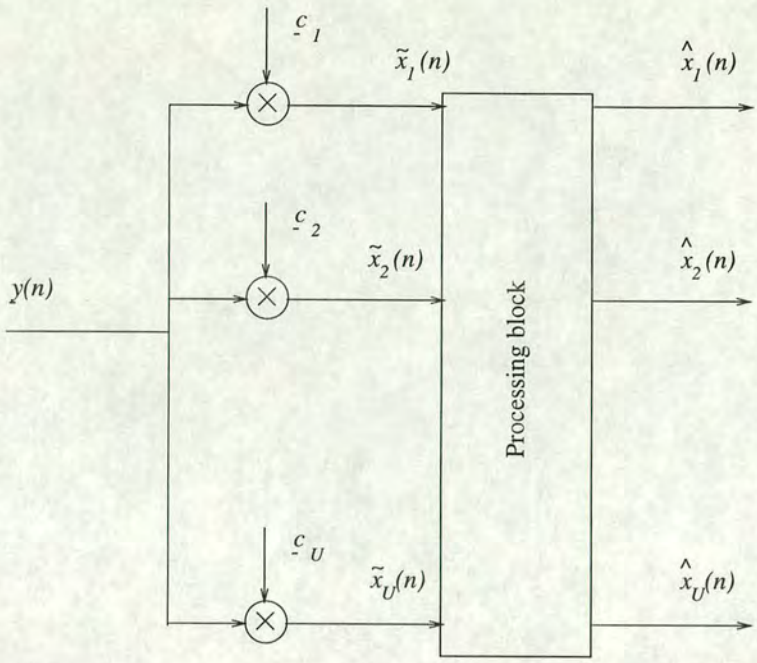

Figure 2.19: Principle of multi-user detection (MUD)

2.3.6 Non-linear receiver structures

Effects due to the communication channel, together with undesired cross-correlations if non-orthogonal spreading sequences are used, can cause the problem of estimating the original data from the received signal to be non-linear[21]. If this occurs, the performance of conventional linear receivers can become severly limited, so that the only way to correctly infer the required data is by non-linear methods. Such an approach, involving the multilayer perceptron (MLP), has been shown to provide a promising structure for an equaliser for a single user communications system subject to a dispersive channel and is described in [81], while an approach involving Volterra series polynomials for CDMA was successfully taken in [82].

The optimal non-linear symbol-based decision equaliser is the Bayesian receiver, which was shown in [83] and [84] to be realisable by a radial basis function (RBF) network. This network defines a mapping $f_{RBF} : \mathbb{R}^D \rightarrow \mathbb{R}$, where D is the dimension of the input vector. The technique, which is a limited-time maximum likelihood sequence estimator, proceeds by evaluating the distance[22] of the input test point from a set of known points, or centres $\underline{p}_i \in \mathcal{P} \subseteq \mathbb{R}^D$ and then calculating a series of non-linear functions of these distances. The output from the network is then given by a weighted sum of these values, as illustrated in Figure 2.20 for a simple case of a network with 3 centres whose input is formed by taking succesively

[21] *i.e.* the decision surface may not be separated by a hyperplane
[22] under a suitable metric defined on $\mathbb{R}^D$

delayed samples of the signal $\underline{y}$.

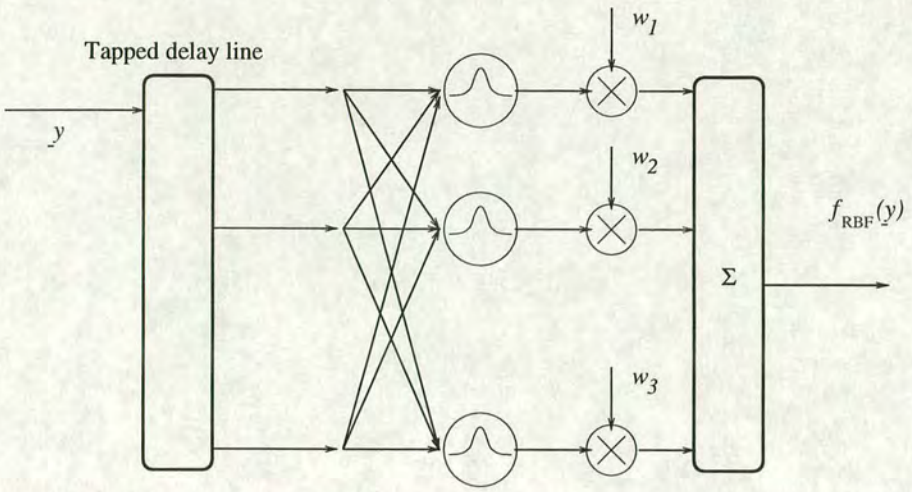

Figure 2.20: Radial basis function network with 3 centres

In general, with N_c centres in the network, the output is given by

$$f_{RBF}(\underline{y}) = \sum_{i=1}^{N_c} w_i \psi \left[d(\underline{y}, \underline{p}_i) \right] \tag{2.22}$$

where w_i is the weight associated with the centre $\underline{p}_i$, the distance $d(\cdot, \cdot)$ from each centre to the input test point is usually evaluated using the Euclidean l_2 metric and $\psi(\cdot)$ is a radially symmetric function, which is monotonic in the sign of its argument. Although recent results suggest that it may be of merit in some circumstances to use different radial functions, or kernels, for each centre [85], the approach adopted here is to use the same kernel shape for each centre. Of the many available [86], the most commonly used is the Gaussian kernel, defined by

$$\psi_G(\zeta) = \exp\left(-\frac{\zeta^2}{2\sigma^2} \right) \tag{2.23}$$

where σ controls the width of the individual RBF kernels. This is similar to a neural network, with the hidden layer represented by the non-linear basis functions. The incorporation of an RBF network into a DS-CDMA receiver for a system exhibiting non-linearities will be considered in more detail in Chapter 6. This chapter will also illustrate the performance advantage gained by this approach, which implements the optimal Bayesian receiver, compared to a simple matched filter and investigate some methods for reducing the complexity of these receiver structures, to make their practical implementation more attractive.

2.3.7 Discussion

This section has outlined various facets of the system design of a DS-CDMA system. The various sequences which may be used to spread the data, and the resulting error performance, have been described. Alternatives to straightforward matched filtering of the received signal have been outlined, and various adaptive strategies to enhance the desired part of the received signal, whilst reducing the multiple access interference, have been outlined. The use of forward error correction has been investigated with regard to a single user communication system. Two methods of cancelling the multiple access interference have been indicated, along with the principles of multi-user detection. Finally the application of non-linear techniques incorporating radial basis functions at the receiver has been introduced.

2.4 Summary

This chapter has reviewed the basic principles of spread spectrum communications and described the implementation of direct sequence code division multiple access. The transmitter structure has been defined, the model for the communication channel introduced and various receiver structures have been described. The performance of a simple benchmark system, using only direct sequence spreading in Gaussian noise, has been detailed, and shown by analysis and simulation to be interference-limited. Various signal processing techniques which may be incorporated into the system have been described. The next chapters will explore these topics in more detail, emphasising the compromises which must be made to achieve increases in overall system capacity, and will investigate whether this performance increase may be achieved at tolerable increased demands on the receiver complexity.

Chapter 3

Adaptive algorithms

In this chapter, the adaptive approximation of the minimum mean square error receiver for the downlink of a DS-CDMA system is investigated. The scenario considered here is first outlined in section 3.1, which also discusses the influence of the tuning parameters of two of the more popular adaptive algorithms; the LMS and RLS algorithms. This section also briefly discusses the effects of MAI on the LMS algorithm, demonstrating the data-dependence of this algorithm. The convergence in Gaussian noise only of these two algorithms is considered in section 3.2, while the performance after convergence is described in section 3.3. The details of the time-varying multipath channel considered are then described in section 3.4. Section 3.5 focusses on the RLS algorithm when used in this channel and considers the factors which influence convergence. The corresponding error performance for the 7-chip random spreading sequence set is then discussed in section 3.6. Some alternative strategies are outlined in section 3.7, and this chapter concludes with a summary in section 3.8 of the main results obtained and their implications for future work.

3.1 Scenario considered

The aim of the work presented here is to adaptively approximate receiver tap weights which will enhance the signal from the desired user, whilst reducing the effects of the multiple access interference. The simulations discussed in this chapter are all performed with respect to the scenario indicated in Figure 3.1, with the proviso that the channel effects may be bypassed if required, to investigate convergence and performance measures in stationary AWGN alone. Additionally, the Gaussian noise may also be bypassed to gauge the convergence performance of the algorithms in MAI alone.

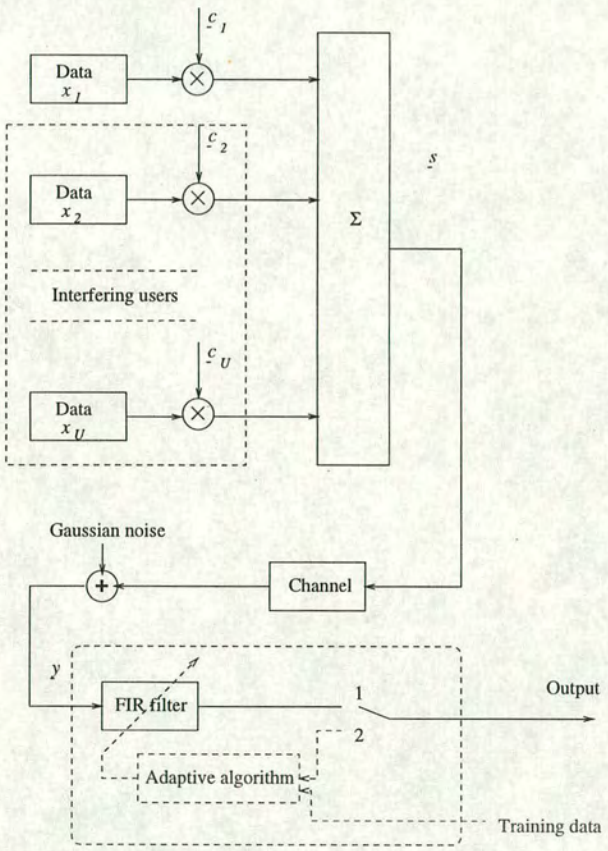

Figure 3.1: Block diagram showing data flow

The adaptive FIR receiver filter, discussed in section 2.3.2.3 is chosen to have the same number of tap weights as the length of the spreading sequence, so that no extra allowance is made for the dispersion effects of the channel. To incorporate these effects, the receiver filter could be extended by a number of chips to capture all the energy from one transmitted data bit. In the stationary AWGN case, N_{train} training data bits are transmitted, after which the tap weights are held fixed and the N_{data} test data are then used to calculate the simulated probability of error, P_e. In the case of the time-varying channel, a number of data cycles are employed, each consisting of a block of N_{train} training data, followed by N_{data} test data bits. The tap weights in the receiver are then reset and a fresh cycle of training followed by testing is performed. The performance statistic is then calculated based on the total number of test data bits. The number of active users is held fixed throughout the simulations, so that effects due to the birth and death of new signals are not modelled. In practice, this could be achieved by constraining users to only begin or cease transmission at the beginning of a new data cycle, since the target tap weights will be shown to depend on the number of simultaneous users.

The channel considered is the reduced typical urban 6-tap channel model as defined in the COST 207 study [35]. The time-varying impulse response of the channel is calculated using the method originally developed in [33], and previously discussed in section 2.2.2.3. The shaping function used is the raised cosine model with 100 % excess bandwidth [31], given by

$$f_{rc}(t) = \left[\frac{\sin\left(\frac{\pi t}{T_c}\right)}{\frac{\pi t}{T_c}}\right]\left[\frac{\cos\left(\frac{\pi\beta t}{T_c}\right)}{1-4\beta^2\left(\frac{t^2}{T_c^2}\right)}\right] \tag{3.1}$$

where β, the roll-off factor, is set to 1. This pulse is shown in Figure 3.2 (a), and has a spectrum of

$$F_{rc}(f) = \begin{cases} T_c & , \quad 0 \leq |f| \leq \frac{1-\beta}{2T_c} \\ \frac{T_c}{2}\{1+\cos\left[\frac{\pi T_c}{\beta}\left(|f|-\frac{1-\beta}{2T_c}\right)\right]\} & , \quad \frac{1-\beta}{2T_c} \leq |f| \leq \frac{1+\beta}{2T_c} \\ 0 & , \quad |f| > \frac{1+\beta}{2T_c} \end{cases} \tag{3.2}$$

which is also depicted in Figure 3.2 (b). This shaping function avoids interchip interference if the delays imposed on the signal are integer multiples of the chip period. Although it must be acknowledged that exact chip delays are unlikely to occur in practice, the advantage of this pulse shape is that the ICI is zero if the channel is not dispersive.

The transmitted signal $\underline{s}$ is first convolved with the chip-sampled instantaneous impulse response

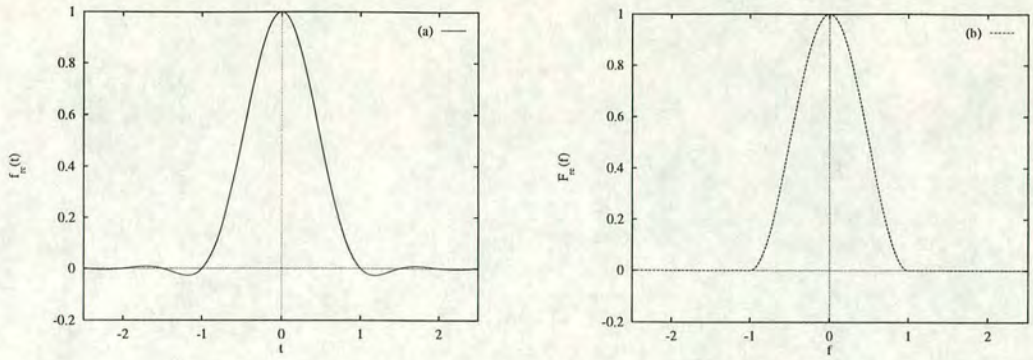

Figure 3.2: *The profile of the raised cosine pulse with 100 % excess bandwidth: (a) $f_{rc}(t)$; (b) $F_{rc}(f)$*

of the channel $H(z;t)$, given by

$$H(z;t) = \sum_{j=0}^{j=n_h} h_j(t) z^{-j} \tag{3.3}$$

where n_h is the number of taps in the channel, which is 6 in the case considered here. The calculation of the individual complex tap weights of the channel model is described in more detail in section 2.2.2.3. The samples of the noise are taken to be iid Gaussian random variables with variance σ^2, which is related to the signal to Gaussian noise ratio by equation 2.5, and the spreading sequences are of length M.

The receiver employs either the LMS or RLS algorithm, both of which are described briefly in section 2.3.2.3 and derived more fully in *e.g.* [62] or [60]. There are a number of details relating to these algorithms which are now discussed to aid clarity. The version of the LMS algorithm chosen is the one derived in [62], *i.e.* the weighting factor is given by μ, rather than 2μ, as in [60]. There are a number of parameters which are important with regard to the RLS algorithm, namely

- The forgetting factor λ, or equivalently the memory of the algorithm, given approximately [62] by $1/(1-\lambda)$
- The small positive constant δ in the RLS algorithm [1], used in the initialisation of the estimate of the inverse of the autocorrelation matrix $\rho^{-1}(0) = (1/\delta)I$, where I is the identity matrix
- The version of the RLS algorithm used, as defined in [62]. Throughout, version II will be employed, which does not make the assumption that ρ^{-1} is Hermitian (i.e. $\rho^{*-T} = \rho^{-1}$).

[1] δ is an estimate of the final mean square error, but its exact value is irrelevant to the convergence characteristics of the algorithm [87]

Before proceeding to the results in Gaussian noise only, it is useful to briefly consider the effect of the step size parameter μ and the number of active users on the convergence of an adaptive algorithm in the presence only of MAI. For this investigation, the LMS algorithm will be used for illustrative purposes.

3.1.1 LMS convergence in the absence of Gaussian noise

To judge the convergence capabilities of an adaptive algorithm, it is sufficient to consider the mean square error (MSE) between training data bit $x(n)$ and its approximation $\tilde{x}(n)$, produced after each training data bit. Here, the MSE of equation 2.13 is ensemble averaged over 100 independent trials using equation 3.4.

$$MSE_{new}(n) = \frac{(ensemble - 1)MSE_{old}(n) + e(n)}{ensemble} \tag{3.4}$$

For illustration, convergence graphs for the LMS algorithm are presented in Figure 3.3 for a DS-CDMA system using 31-chip Gold spreading sequences, with 7 active users. The simulations are performed for values of $\mu = 0.0003, 0.0007, 0.007$ and 0.009, where μ is the step-size.

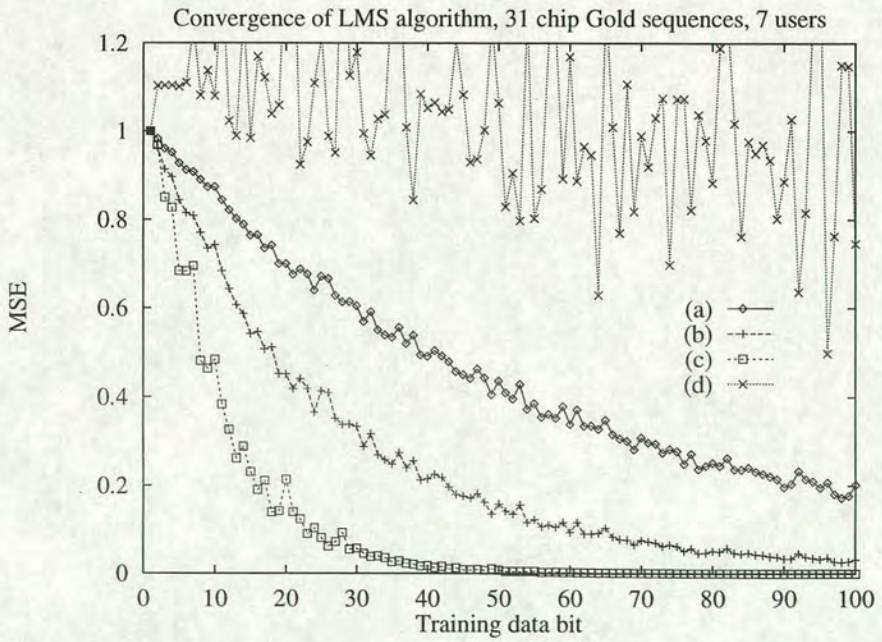

Figure 3.3: *Convergence of the LMS algorithm averaged over 100 ensembles for 31-chip Gold sequences without Gaussian noise: (a) $\mu = 0.0003$; (b) $\mu = 0.0007$; (c) $\mu = 0.007$; (d) $\mu = 0.009$*

The results indicate the general idea that smaller values of μ require a longer training time to converge to the noise floor. This time may be decreased by increasing μ, but if this parameter is increased beyond a certain value, the algorithm diverges. The dependence of LMS convergence on the number of active users may be judged from Figure 3.4, which shows the final value of the MSE again averaged over 100 ensembles, after 200 training data bits, for various values of μ for the full range of active users.

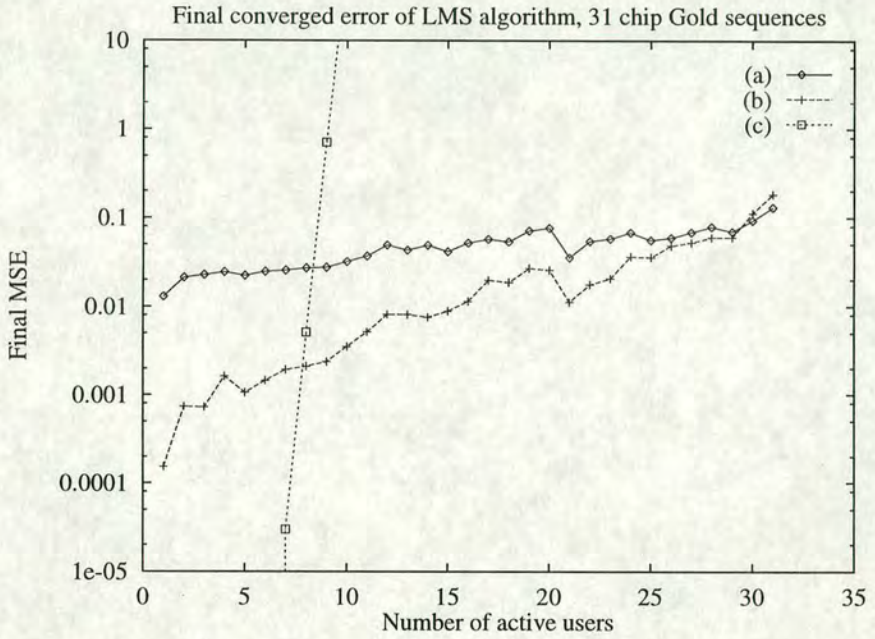

Figure 3.4: *Final converged error (100 ensembles) after 200 training data of the LMS algorithm for 31-chip Gold spreading sequences without Gaussian noise: (a) $\mu = 0.0007$; (b) $\mu = 0.0014$; (c) $\mu = 0.007$*

It is obvious that the step-size which appeared optimal for 7 users causes the algorithm to diverge beyond 9 users, and also that there is a trade-off between the speed of adaption and the value of the final error. As a compromise, the value of μ will be set to 0.0014 for the systems using 31-chip Gold spreading sequences to ensure convergence (at least in the absence of Gaussian noise) for all users.

In conclusion, even without Gaussian noise, the convergence of the LMS algorithm is strongly dependent on the number of users, so that the value of the step-size μ must be chosen to suit the worst-case scenario (which in this case means the maximum number of possible users since the system is interference-limited). This requirement could lead to inefficient use of resources if individual users abruptly begin or cease transmission.

3.2 LMS and RLS convergence in Gaussian noise

The effects of adding Gaussian noise into the system are now considered. Here, the signal to Gaussian noise ratio, E_b/N_0, is set at values of 3, 10 and 25 dB, and 100 ensembles of mean square error against iteration are averaged for a system with 31 users. The LMS is implemented with $\mu = 0.0014$, as discussed above. The results, shown in Figure 3.5 indicate that the LMS algorithm fails to converge when the noise is significant, performs poorly in moderate noise situations since it reaches an irreducible MSE, and only converges slowly under low noise conditions.

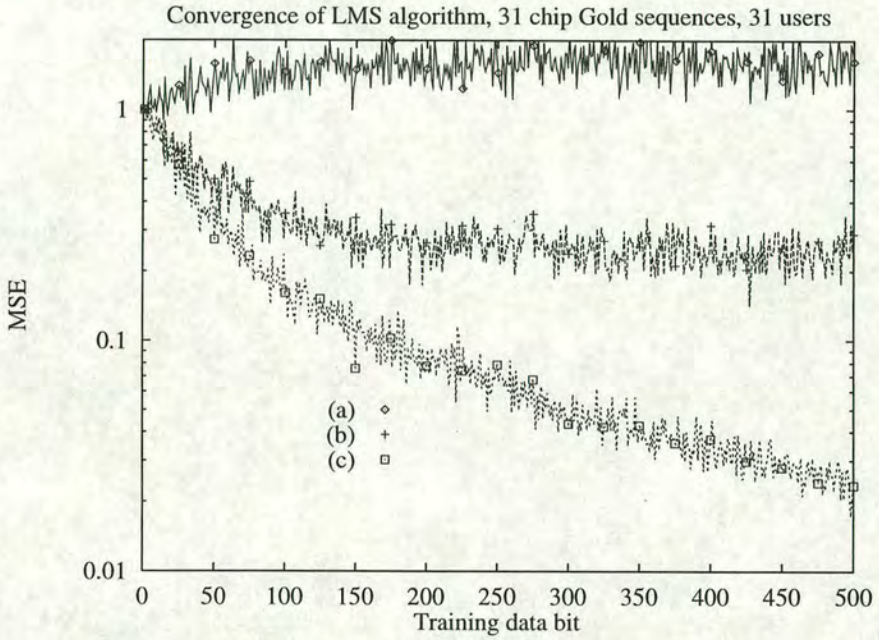

Figure 3.5: *Convergence of the LMS algorithm over 100 ensembles with $\mu = 0.0014$ for 31 users in a 31-chip Gold sequence system in Gaussian noise: (a) 3 dB; (b) 10 dB; (c) 25 dB*

Turning now to the RLS algorithm, Figure 3.6 shows convergence curves for both LMS and RLS algorithms for 31 users in a 31-chip Gold sequence system where $E_b/N_0 = 25$ dB, while Figure 3.7 shows the equivalent results for 7 users using 7-chip spreading sequences. In these cases, 1000 ensembles have been averaged to obtain significant estimates for the convergence profiles, and the initial value δ in the RLS algorithm is set to 0.001. The forgetting factor, λ, is set to 0.99.

As may be seen, the RLS algorithm converges much more rapidly, (theoretically, within $2M$ iterations [62]) and to a lower mean square error than even the fastest converging value of the LMS adaptation parameter. Figure 3.6 also demonstrates another facet of the LMS

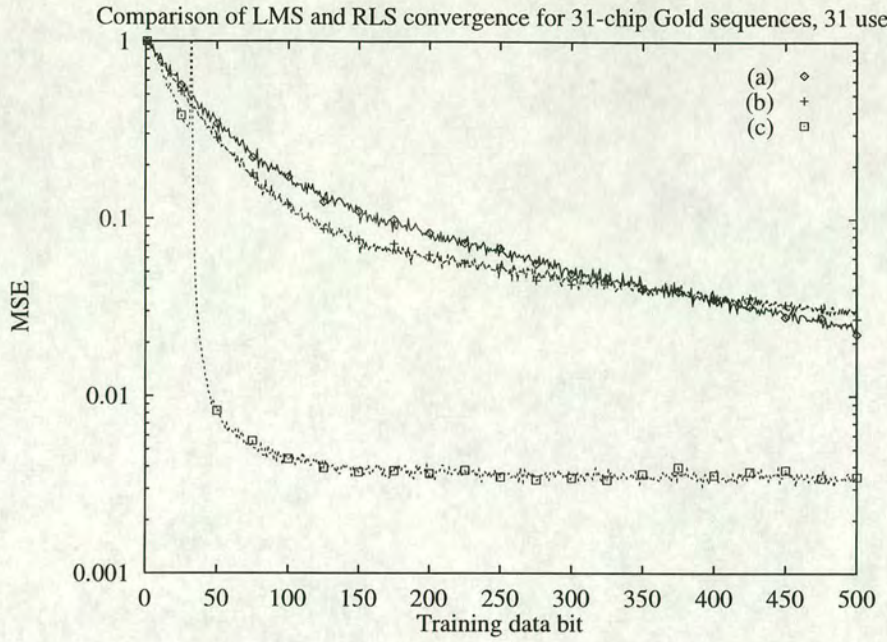

Figure 3.6: *LMS and RLS convergence curves averaged over 1000 ensembles for 31 users in a 31-chip Gold sequence system with $E_b/N_0 = 25$ dB: (a) LMS, $\mu = 0.0007$; (b) LMS, $\mu = 0.0014$; (c) RLS, $\lambda = 0.99$*

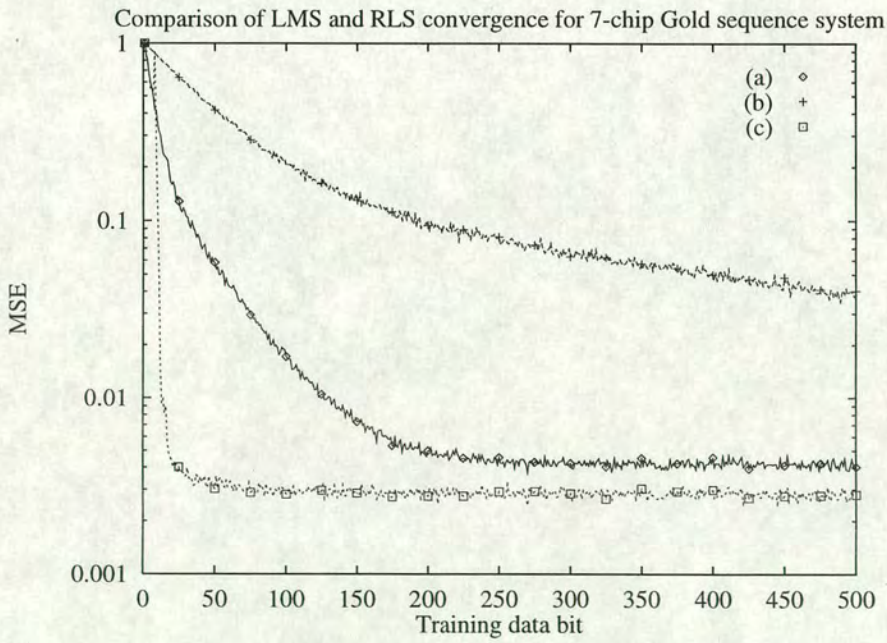

Figure 3.7: *LMS and RLS convergence curves averaged over 1000 ensembles for 7 users in a 7-chip Gold sequence system with $E_b/N_0 = 25$ dB: (a) LMS, $\mu = 0.014$; (b) LMS, $\mu = 0.0014$; (c) RLS, $\lambda = 0.99$*

algorithm; namely that the value for μ which provides faster convergence also leads to a higher misadjustment, or converged error, so that some compromise must be made between speed and accuracy if this algorithm is employed. The initial divergence of the RLS algorithm is characteristic of this method [62], with a peak in the MSE at exactly M iterations.

3.3 LMS and RLS error performance in Gaussian noise

To reduce the computation time, and also to enable comparison with [57], the error performance simulations are carried out using the 7-chip Gold spreading sequence system only. The performance in terms of probability of error (P_e) for given E_b/N_0 values for this case may be simulated by considering the ratio of data bit errors to number of test data sent. The results are shown in Figure 3.8, together with the theoretical BPSK performance curve, obtained from Equation B.13, and the simulated performance of a matched filter receiver.

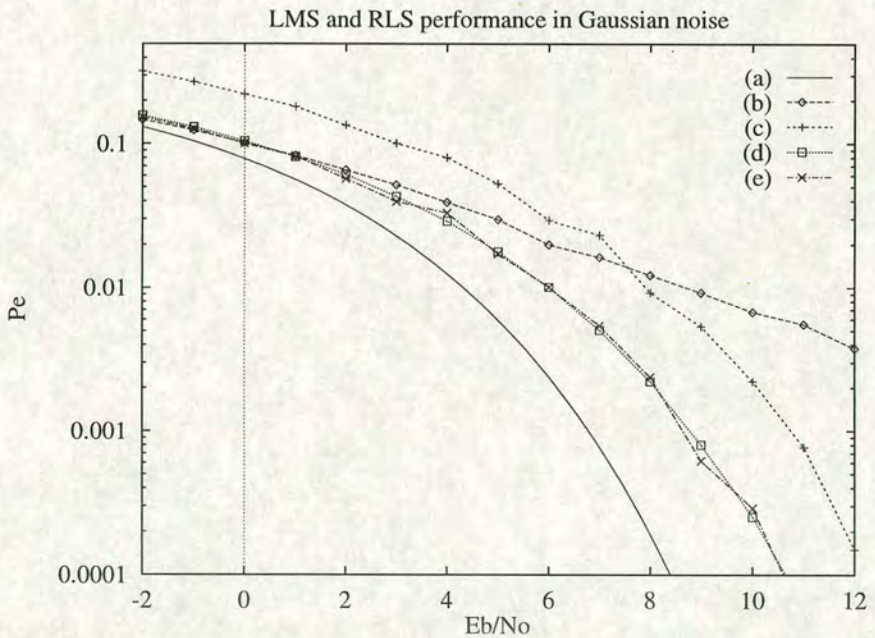

Figure 3.8: *LMS and RLS algorithm performance in Gaussian noise using 7-chip Gold sequences for 7 equal power users: (a) theoretical BPSK; (b) matched filter, 7 users; (c) LMS, $\mu = 0.014$; (d) LMS, $\mu = 0.0014$; (e) RLS $\lambda = 0.99$*

Because the channel is stationary, the receiver filter is trained for 1000 data bits, and then the tap weights are held fixed, while the test data is sent. Thus, decision-directed training [88] is not employed. In practical terms, this is an unrealistic amount of training data, but the principle is clear; the LMS with the smaller value of μ has almost as good performance as the RLS, but requires a significantly larger amount of training data to achieve this. The LMS with the larger

$\mu = 0.014$, which converges more rapidly as has been demonstrated in section 3.2 is more susceptible to data errors than the RLS algorithm. As the noise decreases, the advantage of using adaptive algorithms over straightforward matched filtering becomes greater. This result is consistent with previous studies [57] of these adaptive algorithms.

Thus it is clear that to adaptively approximate the Wiener filter in a reasonably short training time, the RLS algorithm offers a better method than the LMS. The disadvantage in using the RLS is its greater computational requirement. The next development is to consider this algorithm in a time-varying channel, which has also recently been investigated in [89]. This evaluation is once again split into two parts; the convergence of the algorithm, and its subsequent error performance. Before discussing the results, the details of the evaluation of the time-varying multipath channel are first outlined.

3.4 Channel details

The system chip-rate selected is 1 228 800 chip/s, as used in the IS-95 standard [15]. As described in section 3.1, the channel used in this study is the typical urban (TU) model, with 6 channel taps in the impulse response. Since the largest delay of this model is 5 μs, an approximation for $f_0 T_{chip}$ is therefore 0.16, so that inter-chip interference will occur. The maximum Doppler shift present is arbitrarily chosen to be 30 Hz, which is equivalent to a vehicle speed of 36 km/hr at a transmission rate of 900 MHz. The Doppler spread, which has the characteristic profile as sketched in Figure 2.5 (b) is then determined by the type of filter for the relevant tap, as described in [35]. Given this Doppler spread, the channel may be described as slow fading, so that the channel tap weights may be approximated by linear interpolation between samples of the channel impulse response which are calculated as in section 2.2.2.3.

The software used to generate the channel impulse response coefficients is described in [33] and, because of the preceding remarks, the computation time may be reduced by periodically generating samples of the impulse response, and then linearly interpolating between these to obtain the instantaneous values. In the case considered, where the maximum Doppler shift is 30 Hz, a sampling rate of around 1000 Hz is used, so that there are around 30 sampled points per cycle, corresponding to obtaining a new channel impulse response approximately every 1000 chips.

An important difference between the model used here and conventional fading channel models (*e.g.* [32]) is that since the main interest here is in the effect of inter-chip interference, the individual tap powers are normalised by the overall power of the channel filter taps, so that the signal power before and after the channel effects are incorporated is the same. This effectively ignores any flat fading effects, and so the noise variable labelled E_b/N_0 may be interpreted as the instantaneous signal to Gaussian noise ratio.

3.5 RLS convergence in time-varying multipath

This section investigates the convergence of the RLS algorithm in the channel described above. The convergence properties of the algorithm for systems with various length spreading sequences are first described in section 3.5.1. The misadjustment, or final converged error, with respect to background noise is then considered in section 3.5.2.

3.5.1 Channel equalisation: effect of code length

To investigate the effect of code length on the convergence properties of the algorithm, the MSE, again averaged over 1000 ensembles, is calculated for systems employing 7, 31 and 63-chip Gold spreading sequences for both the stationary AWGN channel and for the time-varying multipath channel. Convergence curves are presented in Figure 3.9 for the respective systems for one active user with $E_b/N_0 = 7$ dB.

The RLS algorithm is implemented for the stationary case with $\lambda = 1$, so that it has infinite memory, while for the time-varying case, $\lambda = 0.99$, so that the effective memory, given approximately [62] by $1/(1-\lambda)$ bits, is 100 data bits. It may be seen that the overall behaviour for the AWGN channel and for the multipath channel is similar, with the same characteristic peak in the error at the Mth training data bit, and convergence being achieved at around the $2M$th training data bit[2], so that training may be stopped at this point to send the (unknown) test data and form the performance statistic. The increase in final MSE with increasing spreading code length is also evident, and is accentuated with the extra influence of the time-varying channel.

[2]this is a feature of the RLS algorithm, since the tap weights are only adapted after information corresponding to one data bit is gathered

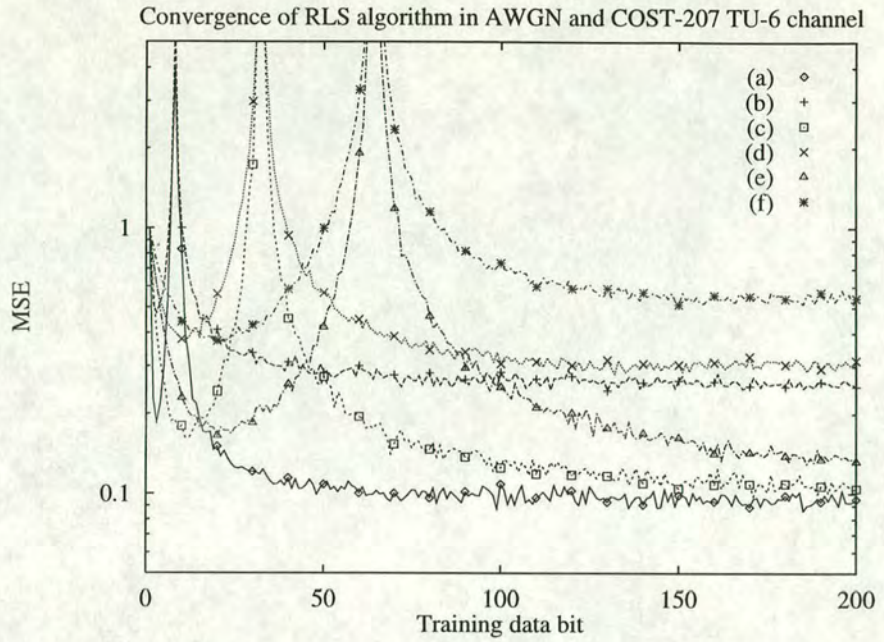

Figure 3.9: *Convergence of RLS algorithm in COST-207 6-tap TU channel, 1 active user, $E_b/N_0 = 7$ dB: (a) 7-chip, AWGN; (b) 7-chip, TU; (c) 31-chip, AWGN; (d) 31-chip, TU; (e) 63-chip, AWGN; (f) 63-chip, TU*

This final MSE is due to two effects; firstly the misadjustment, $\mathcal{M}$, present in the stationary environment, and given approximately [62,90] as

$$\mathcal{M} \simeq \frac{1}{M}\left(1+\frac{M}{N_{train}}\right)\sigma^2 + M\left(\frac{1-\lambda}{1+\lambda}\right) \tag{3.5}$$

where N_{train} is 200 in this case. The second effect is the additional corruption of the received signal by ICI, as a result of the multipath channel, as described in section 2.2.2.2. This could be compensated for by making an estimate of the channel impulse response, and using an equaliser to attempt to combat the effects of the channel, as described in [91].

These results also indicate another trade-off which must be made between lower MAI interference, which may be achieved by using longer spreading sequences, and the performance restrictions which this imposes. The drawback to using longer sequences, aside from the obvious increase in computation time, is that the channel is more likely to change over the period required to transmit sufficient data to train the receiver tap weights completely. The impact of this on the IS-95 system [15], which uses 64 chip Walsh spreading sequences [53], is likely to make an adaptive approach less practical.

3.5.2 Channel equalisation: effect of background noise

The effect of signal to Gaussian noise ratio (E_b/N_0) on the convergence of the RLS algorithm is now investigated. Here, both 7-chip and 31-chip spreading sequence systems are considered, and the final value of the MSE after 200 bits of training data, ensemble averaged over 1000 independent trials, is calculated for one active user. The results are shown in Figure 3.10 for both the stationary Gaussian noise channel, in which case infinite memory is employed, and the 6-tap typical urban channel model, for which the value of the forgetting factor, λ is set to 0.99. The figure also presents the theoretical values for the stationary case obtained from equation 3.5 with λ set to 1.

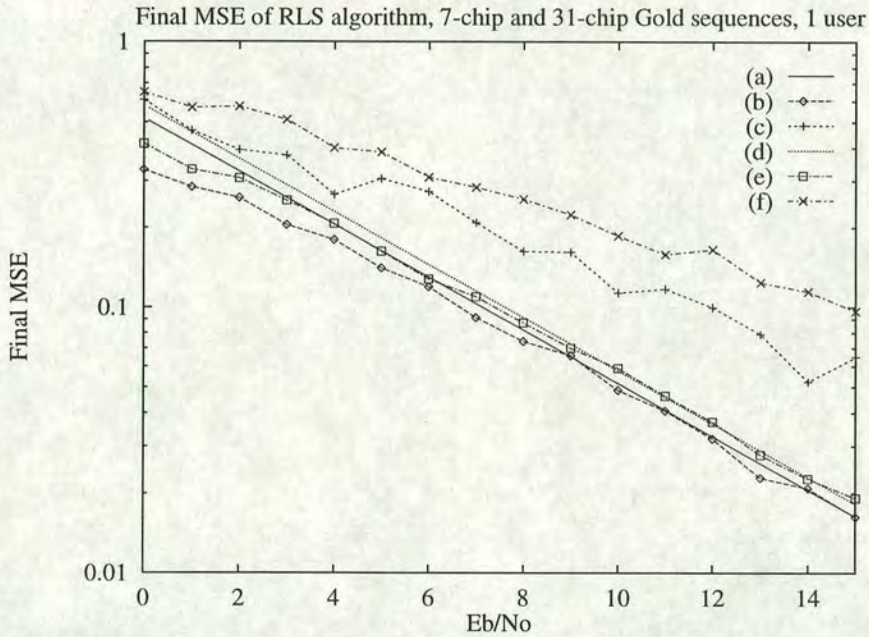

Figure 3.10: *Effect of channel on final mean square error for various values of E_b/N_0: (a) Equation 3.5 ($\lambda = 1.0$, $M = 7$); (b) AWGN (7-chip); (c) COST 207 TU channel ($\lambda = 0.99$, $M = 7$); (d) Equation 3.5 ($\lambda = 1.0$, $M = 31$); (e) AWGN (31-chip); (f) COST 207 TU channel ($\lambda = 0.99$, $M = 31$)*

The results show an asymptotic tendency toward the theoretical predictions for larger E_b/N_0 values in the stationary cases. As expected, there is a deviation in the final MSE when the channel is included, due to the additional corruption of the signal by ICI. The minor fluctuations in the results for the multipath case are likely due to insufficient averaging of the full range of fading induced by the model. However, the results are encouraging, although longer spreading sequences will not be able to produce as low a final MSE for the reasons cited in section 3.5.1.

3.6 RLS performance in time-varying multipath

The MSE produced by the RLS algorithm, while a reasonable pointer to its capability, offers only a limited indication of its ability to separate the spreading sequences and thus recover the original data correctly. To investigate this, the error performance, again measured as simulated probability of error (P_e), estimated over a suitably large number of independent trials, is now investigated. To reduce the computation time, the simulations are only performed for the 7-chip sequence set. Since section 3.5.1 demonstrated that convergence is broadly achieved after $2M$ training data bits, and it is important to utilise the full memory of the algorithm, which with $\lambda = 0.99$, is around 100 data bits, N_{train} is set to 14 ($2M$) and N_{data} is set to 77 ($11M$), so that each data cycle lasts 91 bits. The receiver tap weights are then reset, and a new data cycle is transmitted. The performance as the number of simultaneous users and the background noise level is varied, is shown in Figure 3.11.

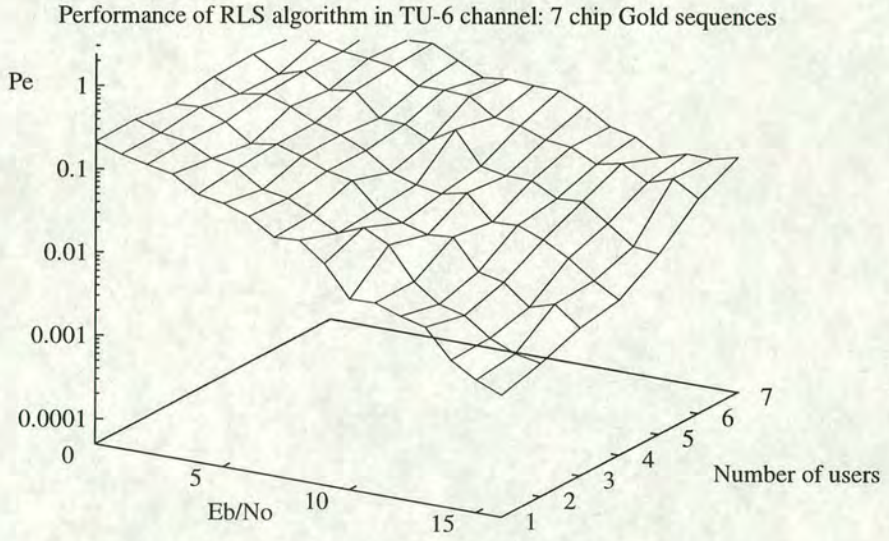

Figure 3.11: *Probability of error against E_b/N_0 and number of active users for the RLS algorithm ($\lambda = 0.99$) in the TU channel for 7-chip Gold sequences*

Although this configuration clearly suffers reduced performance for more than about 5 users, the equivalent system, when used in the stationary Gaussian noise channel, experiences similar degradation in performance. An alternative view of the same information is presented in Figure 3.12, which shows the number of users which may be supported against the required E_b/N_0 for a given probability of error. The results have been obtained from linearly interpolating the previous results, and show the characteristic increase in required E_b/N_0 as the target probability of error is reduced.

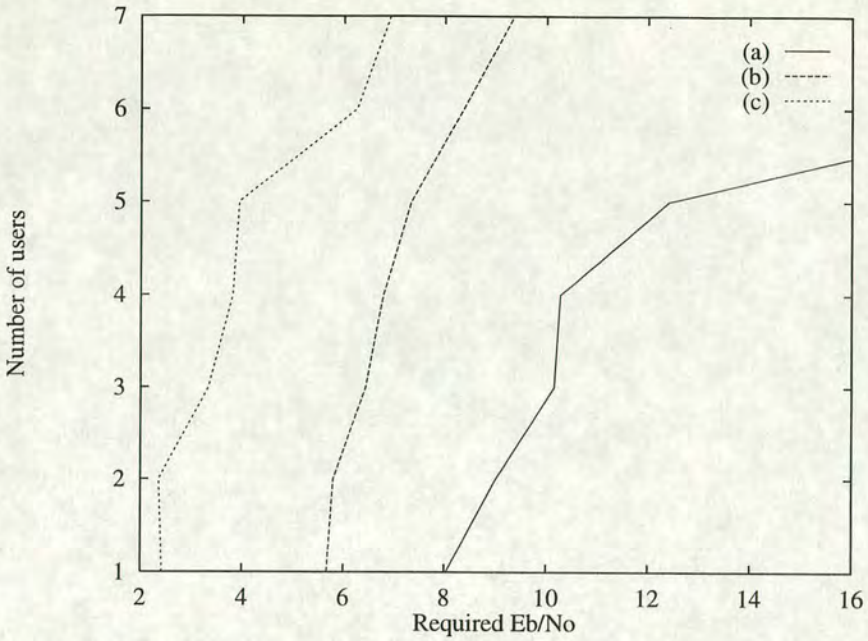

Figure 3.12: *Number of users which may be supported against required E_b/N_0 for a given probability of error for the RLS algorithm ($\lambda = 0.99$) in the TU channel for 7-chip Gold sequences: (a) P_e=0.01; (b) P_e=0.05; (c) P_e=0.1*

Thus, the RLS algorithm appears to be able to compensate for the effects of the channel without introducing significant further degradation, and so could be employed as an alternative to a RAKE receiver [92]; the traditional method for combatting unknown multipath interference. The RAKE operates by combining soft decisions arising from filtering a number of delayed replicas of the received signal by a number of copies of the required de-spreading sequence (termed fingers). While this could be used to combine non-adjacent parts of the received signal, the MMSE receiver combines any time or space diversity present in an optimal way, and therefore would be expected to have the best performance.

In the stationary case, reduced interference may be obtained by employing longer spreading sequences, with relatively lower cross-correlation values [50]. However, as has already been shown, the channel effects become more detrimental for longer sequences, so that some compromise must be reached between system capacity and performance.

3.7 Various adaption strategies

In this section, various alternative strategies to the system used previously are analysed. The first, in section 3.7.1 considers the effects of other data chip rates. The second alternative is to

modify the cycles of training, testing and resetting so that the tap weight values from the old configuration are retained as the starting point for the next update period. Thirdly, the effect of the value of the forgetting factor, λ is considered in section 3.7.3.

3.7.1 Alternative chip rates

Although the chip rate prescribed by the IS-95 standard [15] is 1228800 chip/s, other systems have different chip rates, and so it is of interest to investigate the effects previously discussed when different chip rates are used. The chip rate selected here is 1×10^5 chip/s, again with the single user case. An immediate problem with using a lower chip rate is that the effects of the channel will be more pronounced, unless the value of λ is reduced to prevent the algorithm from remembering outdated channel estimates. For the lower chip rate, λ is set to 0.95 so that the effective memory is reduced to around 20 data bits. This is chosen to ensure that the 7-chip Gold sequence system has sufficient time to converge, although other (larger) values of λ would have to be used for systems employing longer spreading sequences, since they would require longer training times.

The results are shown in Figure 3.13, which also shows the equivalent performance statistics for the IS-95 system and the theoretical BPSK performance curve from equation B.13.

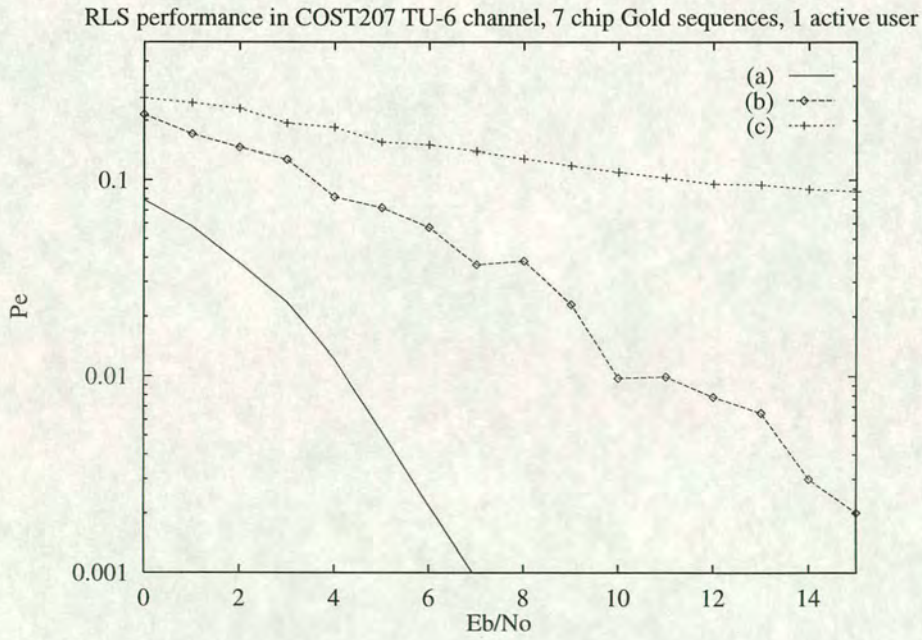

Figure 3.13: *RLS performance against E_b/N_0 for 7-chip Gold sequences, 1 active user: (a) theoretical BPSK in AWGN, (b) IS-95 chip rate, (c) 1×10^5 chip/s, $\lambda = 0.95$*

As may be seen, the slower chip-rate system has significantly poorer performance, likely to be due to the channel changing after the algorithm has converged. The consequences for longer chip spreading sequences, and higher values of Doppler shift are even more acute, so that future systems will require high chip rates to remain feasible. This places further increased demands on the resolution and capability of the hardware deployed.

3.7.2 Tap weight resetting

The fact that the channel is time-varying may lead one to attempt to use "old" information in the form of the previous receiver tap weights, rather than resetting them after the end of each data cycle. To investigate this, the IS-95 chip rate is again employed, and the performance with and without resetting is considered. The results are presented in Figure 3.14 for two values of the forgetting factor λ equal to 0.95 and 0.99.

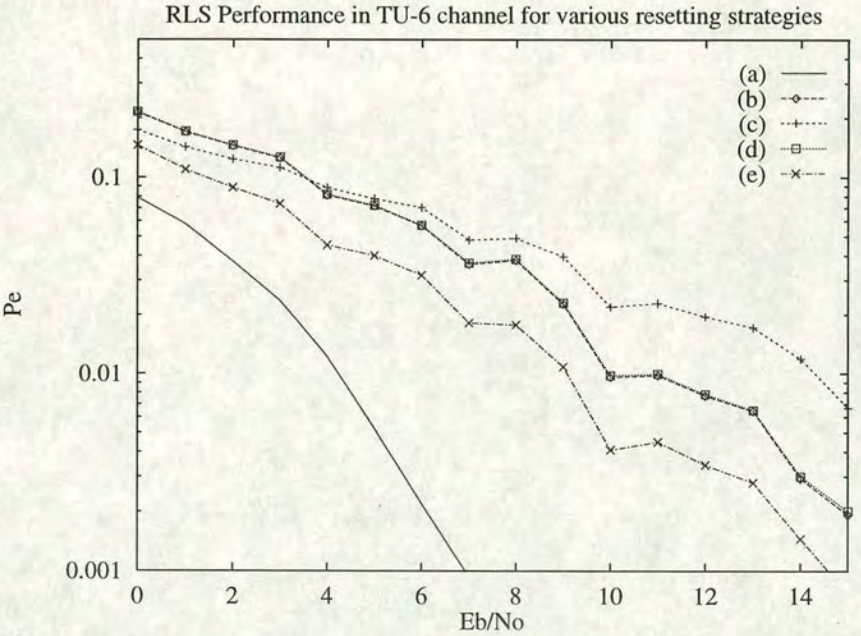

Figure 3.14: *Probability of error against E_b/N_0 with and without tap weight resetting: (a) theoretical BPSK, (b) $\lambda = 0.99$, with resetting; (c) $\lambda = 0.99$, without resetting; (d) $\lambda = 0.95$, with resetting, (e) $\lambda = 0.95$, without resetting*

With resetting, the performance appears almost identical for the two values of λ, however the results without resetting show a more pronounced dependence on λ. With $\lambda = 0.99$, the memory appears to be too great, so that incorrect adjustments are being made to the RLS tap values, leading to a higher proportion of data bit errors. Not resetting with $\lambda = 0.95$ gives better performance than resetting, and appears to be the optimum strategy in this case. However,

the problem with not resetting the RLS algorithm is that any step change in the signal, for example caused by the abrupt switching on or off of a particular user, even at a pre-arranged admissable instant, could cause the RLS algorithm to become unstable. In addition, all the calculations discussed here have been performed with double precision arithmetic, and the use of lower precision arithmetic, as may be required to reduce complexity in the receiver, has been shown [93] to increase the chance of instability and error propagation of this algorithm.

Thus, although it appears optimal to not reset the weights, in practical situations, where the characteristics of the signal are not known *a priori* and lower precision arithmetic may be imposed, it may be better to reset the receiver tap weights between data cycles, even though this strategy has slightly worse performance. Further investigations, perhaps using other combinations of training and data lengths, may provide some more insight into this phenomenon and may form an area of future study.

3.7.3 Varying forgetting factor

As described in section 2.3.2.3, the main parameter of the RLS algorithm is the forgetting factor λ, which controls the memory of the algorithm. In the stationary case, it is normally sufficient to use infinite memory ($\lambda = 1$), however, in the case of a time-varying channel, this parameter may be tuned to provide a compromise between remembering enough data to train effectively while avoiding converging to old (and probably incorrect due to changes in the channel) values of the receiver tap weights. Again, the investigation of this parameter will be based on the two criteria of convergence and error performance.

3.7.3.1 Channel equalisation

Figure 3.15 shows the effect of varying both the forgetting factor and the number of active users, on the final mean square error (MSE), over 500 ensembles of 200 data bits, for E_b/N_0 equal to 10 dB for the 7-chip spreading sequence set.

The previous chip rate (1×10^5 chip/s) has been used here, where it may be seen that the final value is largely independent of the number of users. The variation, predominantly due to varying λ, arises because the time required to transmit 200 data bits is comparable to the timescale over which the channel is changing, and thus the algorithm is prone to converge to

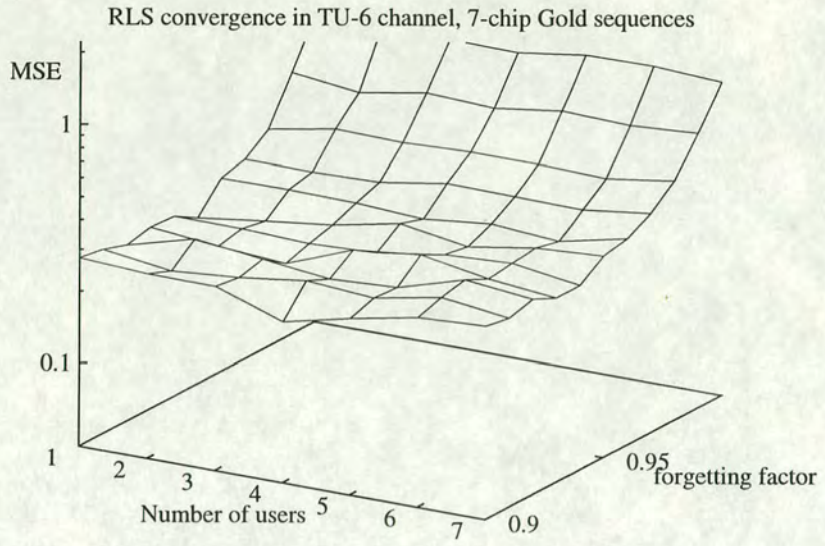

Figure 3.15: *Variation in final convergence value with λ and number of active users for $E_b/N_0 = 10$ dB*

previous incorrect values.

3.7.3.2 Error performance

To investigate the effect of λ on the error performance, the IS-95 chip rate is again used, with one user, and with resetting. The performance for a range of values of E_b/N_0 is shown in Figure 3.16, which shows only slight variation with λ, in agreement with the results in section 3.7.2.

One may expect the performance for $\lambda = 1$ to not be as good as indicated, since this corresponds to remembering every previous data bit. However, the improved performance is attributable to the resetting operation which effectively prevents the algorithm from using data values older than the training and testing data cycle length of 91 data bits. Since this is a short enough timescale compared to the changes in the channel (at this chip-rate), the performance is reasonable even for apparently unlikely values of λ. Thus, computational savings may be made by simply setting λ to 1 and resetting the tap weights after each cycle. If resetting is not employed, as may be seen from Figure 3.17, the performance does indeed deteriorate as λ approaches 1.

The figure also demonstrates the large variation in performance with comparatively small changes in λ as $\lambda \rightarrow 1$, so that for a practical system, close monitoring and fine tuning of this parameter would be required.

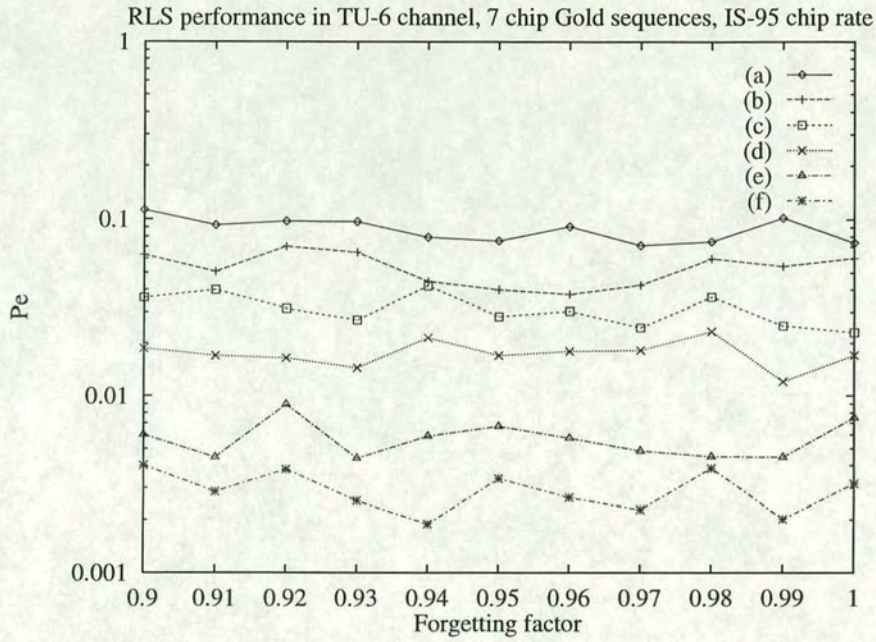

Figure 3.16: *Probability of error against λ for various values of E_b/N_0 for the IS-95 chip rate with resetting: (a) 4 dB; (b) 6 dB; (c) 8 dB; (d) 10 dB; (e) 12 dB; (f) 14 dB*

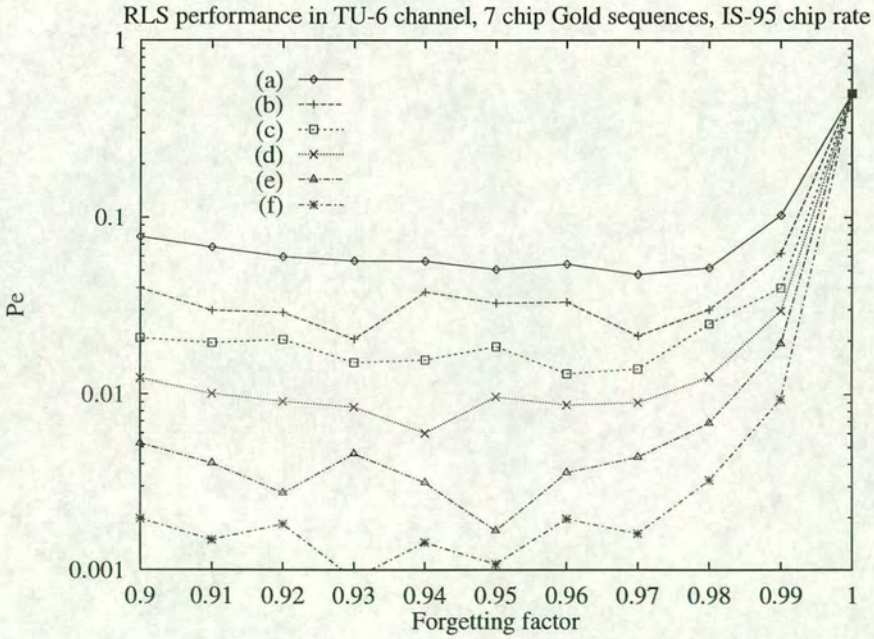

Figure 3.17: *Probability of error against λ for various values of E_b/N_0 for the IS-95 chip rate without resetting: (a) 4 dB; (b) 6 dB; (c) 8 dB; (d) 10 dB; (e) 12 dB; (f) 14 dB*

3.8 Discussion

In this chapter, the application of two adaptive algorithms to the DS-CDMA environment has been described and analysed. It has been shown that the LMS algorithm is dependent on both the number of participating users and the level of signal to Gaussian noise. In the stationary AWGN channel, the final mean square error achievable by the LMS has been shown to be greater than that due to the RLS algorithm. The LMS also requires variable training times to converge, while the RLS converges within a time only dependent on the length of the spreading sequence set used. The performance of the LMS in AWGN has been shown to be only at best as good as the RLS, with this performance level only achieved after significant amounts of training. The convergence and performance of the RLS algorithm in a particular non-stationary environment has been investigated. The effects of sequence length and background noise level on the convergence properties of the algorithm have been discussed, and the influence of various parameters on convergence and system performance has been examined.

Other channel models, such as the less typical rural or hilly scenarios could also be investigated, as could higher vehicle speeds, which, with the attendant increase in maximum possible Doppler shift, will likely lead to degradation in performance. However, it is expected that the channel model and the parameters reported here provide a reasonably general model for many situations. Traditional anti-multipath techniques, involving RAKE receivers, either require a pilot channel or a sufficiently high signal-to-noise ratio to enable estimation of the number and strength of the multipath components. The adaptive techniques examined here require only a reasonable signal to noise ratio and sufficient time to converge. More elaborate receiver structures, employing multiple access interference (MAI) cancellation or data-encoding to provide some forward error protection will be investigated in the following chapters, which will also discuss the suitability of these more computationally-intensive receivers to a nonstationary environment.

The crucial point is whether there is sufficient time for the adaptive algorithm to drive the tap weights to the correct values, and this depends on the time required to transmit the required number of data bits compared to the time over which the channel changes. One possibility to ensure that there is sufficient time is to perhaps use short sequences to equalise the channel, combined with longer ones to actually encode the data. In summary, it has been shown that it is feasible to use an adaptive algorithm to compensate for the detrimental effects of a non-stationary channel, provided training can be performed in an appropriate time-scale.

Chapter 4

Convolutional coding in a DS-CDMA system

In this chapter, the use of convolutional coding as a means of forward error correction (FEC) for the DS-CDMA environment is investigated. The basic principles of convolutional coding in the context of a DS-CDMA system are first described in section 4.1, which builds on the ideas previously described in section 2.3.3.1. The first system, in which various methods of convolutional coding are used as an alternative to direct sequence spreading, is described in section 4.2. Results from some simulations to investigate this structure are then presented in section 4.3, and the implications of these results are discussed in section 4.4. A more conventional system, employing a combination of coding and spreading, is then considered in section 4.5, which explores the balance between devoting resources to coding or spreading, while maintaining a fixed processing gain. Results obtained from systems employing both Gold and random spreading sequences are described in section 4.6 and discussed in section 4.7. Finally, the main ideas discussed in the chapter are summarised and implications for future work are outlined in section 4.8.

4.1 Principles of convolutional coding applied to the DS-CDMA environment

The principles of forward error correction for a single user communication system have previously been briefly outlined in section 2.3.3. In this study, attention is focussed on convolutional codes, which are distinguished by two parameters; the rate and the constraint length. The rate, R, of a convolutional encoder is defined as the ratio of the number of input to output

digits, while the constraint length, K, is the number of input digits that the encoder uses to construct the encoded sequence. To accomodate multiple access, different code configurations may be allocated for each user and the resulting encoded sequence may be used in place of the spreading sequences, as discussed in the first system, or the digits of these encoded sequences may themselves be used to modulate the user's spreading sequence, which is the technique described in the second system.

Before proceeding to a detailed description of the systems considered, it is important to specify some parameters of the particular decoding mechanism employed. As described in section 2.3.3.4, the Viterbi algorithm (VA) is used to decode the received vector, with soft decision decoding employed throughout, using double precision arithmetic. The use of lower precision does not significantly decrease the performance [70], but is not implemented here so as to obtain as accurate results as possible.

An important parameter in the radio communications environment is the delay incurred by any additional processing, since this may ultimately degrade the quality of service (QOS) of a system. The maximum delay considered here for the convolutional code decoding portion of the receiver is arbitrarily set to 32 data bits, so that constraint lengths of up to $K = 6$ may be considered. The use of longer constraint lengths requires a greater processing delay to maintain the increased coding power, and this may prove intolerable for practical systems, which require additional processing delays for other portions of the receiver.

4.2 System 1 description

The first system considered is mainly concerned with a variant of convolutional coding [94] which has recently been applied to the DS-CDMA environment [95] and which provides coding and spreading in one step. Before detailing the operation of this encoder, the model for the communications system to be considered is defined. The flow of data in this scenario is shown in Figure 4.1, in which each user's data bit is first processed by the relevant encoder unit, before combining at the summer.

Multiple access is achieved in this system by assigning different code generators to each user. Optionally, the encoded data stream may be further randomised by a chip-by-chip multiplication of the output code sequence by the appropriate randomiser sequence. The motivation for this

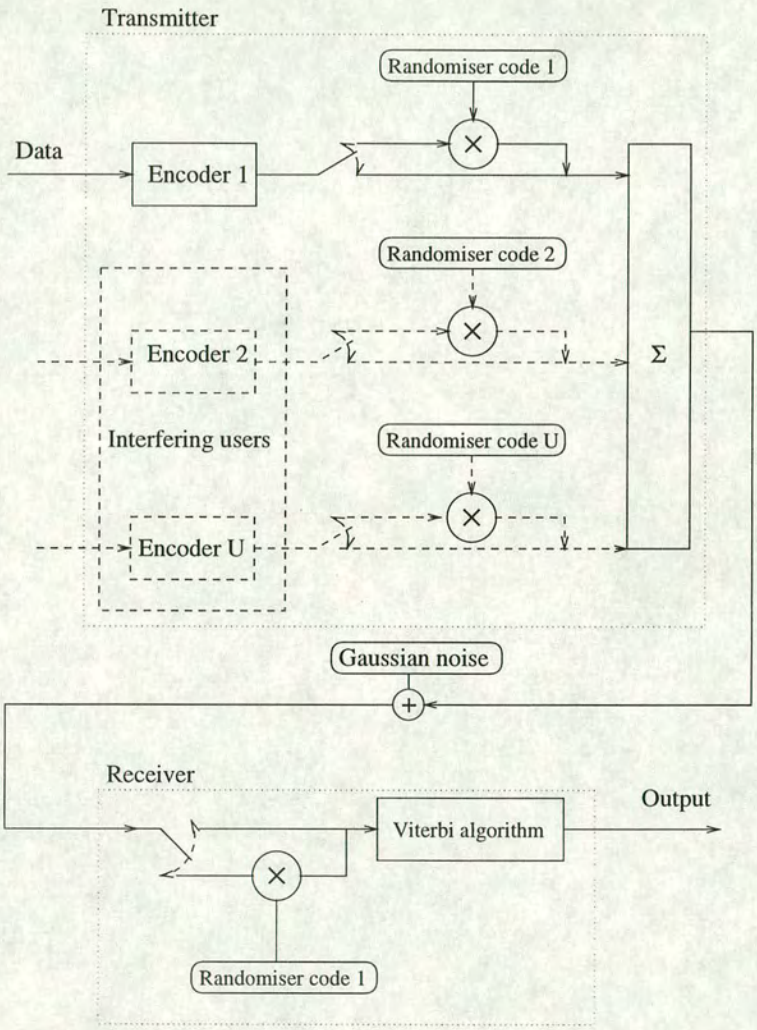

Figure 4.1: System 1 considered to compare methods of convolutional coding performance

will be discussed later. This use of convolutional coding may be viewed as an alternative to direct sequence spreading, in which the mapping from input data bit to output code word replaces the operation of direct sequence spreading [1]. Additive white Gaussian noise is then added to this transmitted signal, to form the received signal which is to be processed by the receiver to produce the estimate of the original data bit.

The performance of the encoded systems is compared to that of a system employing only direct sequence spreading with random sequences and a receiver consisting of either the conventional matched filter of section 2.2.3, or the minimum mean square error (Wiener) filter as described in section 2.3.2.2. Although a direct implementation of the latter receiver requires knowledge which may not be readily available, it has previously been shown in Chapter 3 that the Wiener filter may be adequately approximated by an appropriately tuned adaptive algorithm, and thus is useful as a benchmark, representing an upper performance bound on such an adaptive strategy. The matched filter represents the corresponding lower bound, since it would clearly be inefficient to employ a system with poorer performance than this.

4.2.1 Orthogonal convolutional coding

The orthogonal (or Hadamard [53]) convolutional encoder [94] represents an alternative to the standard convolutional encoding process as detailed in section 2.3.3.1. This encoder incorporates a second set of shift registers connected in parallel with the conventional unit data bit delay blocks, again represented by z_{bit}^{-1}. An example of this arrangement is shown in Figure 4.2, which demonstrates the case for a rate $1/8$ constraint length 3 system. The switches at the output of this secondary set are toggled at rates 1, 2, 4, (*etc* for higher K) times the chip rate so that for each data bit input to the top register-set, a unique 2^K-digit Walsh sequence, $\underline{q} = (q_1, q_2, \cdots, q_{2^K})^T$ [53] is output, as demonstrated for the $K = 3$ system in Table 4.1.

Multiple access is achieved by assigning each user a unique 1-1 mapping between the two sets of shift registers [96], so that each input is connected to one and only one output. The particular Walsh sequence output for a given input data bit thus depends on three quantities; the incoming data bit itself, the present state of the upper register system, and the arrangement of connections between the two set of registers. Note that this now reduces the effective number of degrees of freedom of the code, since the output code rate is now determined completely by the constraint

[1] It must be acknowledged that this technique is not strictly spread spectrum communication as defined previously, since that requires that the spreading sequences be independent of the data [25]

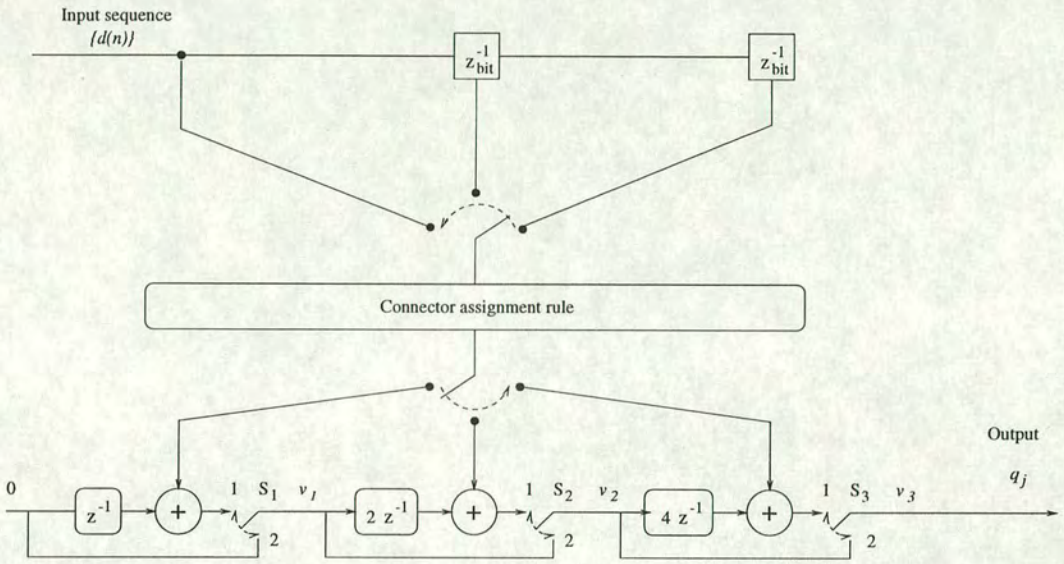

Figure 4.2: Rate $1/8$ orthogonal convolutional encoder

Time step j	S_1	S_2	S_3	Output q_j
1	1	1	1	v_3
2	2	1	1	v_3
3	1	2	1	v_3
4	2	2	1	v_3
5	1	1	2	v_2
6	2	1	2	v_2
7	1	2	2	v_1
8	2	2	2	v_1

Table 4.1: *States of the switches S_i and corresponding output code chips q_j from the orthogonal convolutional encoder for the range of time steps $1 \leq j \leq 2^K$*

length to be 2^K, rather than in the conventional convolutional case, where these two parameters are independent.

This method of assigning connections means that the system is theoretically capable of supporting $K!$ users, although practically, the number of users which can be supported is more limited, as will be discussed later.

It must also be acknowledged that in Gaussian noise, simple direct sequence spreading using Walsh sequences offers 2^K users the potential to communicate with no multiple access interference, as described in section 2.3.1.4. The use of Walsh sequences in this context may not provide such immunity since it is possible for the same Walsh sequence to be generated by different users, thus causing a clash of output encoded sequences. If the processing gain is not to be increased further, the method now discussed may be used to counter this problem.

4.2.2 Orthogonal coding with randomiser

The use of additional randomising sequences has been proposed by Ormondroyd and Maxey [96] to improve the spectral characteristics of the Walsh codes, thus increasing the ability of this scheme to separate users. No additional spreading of the transmitted signal spectrum is produced by this stage, in which competing users are assigned different random sequences, and the output from each orthogonal convolutional encoder is simply multiplied chip-by-chip by the appropriate random sequence. These random sequences are selected to be the same as those used in the system employing only direct-sequence spreading, so that no artificial bias is introduced due to particular cross-correlation effects. This randomising process is similar to that which occurs in the IS-95 system [15], in which the derived code sequence is combined with a mask, consisting of a portion of a long user-specific m-sequence, to form the transmitted signal.

4.3 System 1 results

The ratio of the number of errors to the total number of transmitted data values (typically one million trials are performed) forms the main output statistic (P_e), which may be calculated as a function either of number of users for a fixed background noise level, as in the first cases, or of background noise level for a fixed number of users, considered in the subsequent sections.

4.3.1 Performance for fixed E_b/N_0

The performance as the number of users is varied is considered for two constraint-length systems, $K = 3$ and $K = 6$, for background noise values of $E_b/N_0 = 5$ dB and 7 dB. This is to simulate systems with a variety of processing gains, since the $K = 3$ orthogonal coder will have a linear processing gain g_P equal to 8, a value typical for many hybrid systems [2], while the $K = 6$ orthogonal systems will have $g_P = 64$ which is closer to the processing gain of the IS-95 standard.

The results for the orthogonal coder for $K = 3$ are naturally only simulated for up to 6 active users, while for $K = 6$, theoretically 720 connections are possible. In practice, only a subset of up to 64 connections are in use at any one time, although the particular configurations used are periodically re-selected at random from the complete set of possible combinations.

4.3.1.1 Constraint length 3 systems

Figure 4.3 shows the performance of the various techniques for $E_b/N_0 = 5$ dB. As may be seen, none of the proposed schemes approach the performance of the Wiener filter for 2 or more users. When only a single user is present, all the coded schemes have lower average error probability than a direct spreading only architecture, as expected, although orthogonal coding is worse than devoting all resources to FEC coding.

The performance of the convolutional-only system rapidly deteriorates with increasing users. This result is probably due to the inadequacies of the short constraint length connections used, since the error-correcting capabilities of the codes are being compromised by the interference from the additional users. Thus, this technique is impractical at providing a reliable multiple access method. The orthogonal-only coded system performs slightly better as the loading is increased, although beyond 2 users, this approach is worse than conventional matched filtering of a direct spreading only system. The additional randomising stage produces a further improvement in performance, although still not as good as the direct spreading system with the Wiener receiver filter.

Figure 4.4 shows the performance of the systems for $E_b/N_0 = 7$ dB.

[2] *e.g.* such as proposals for extending the GSM system using code and time division multiple access (CTDMA) [18]

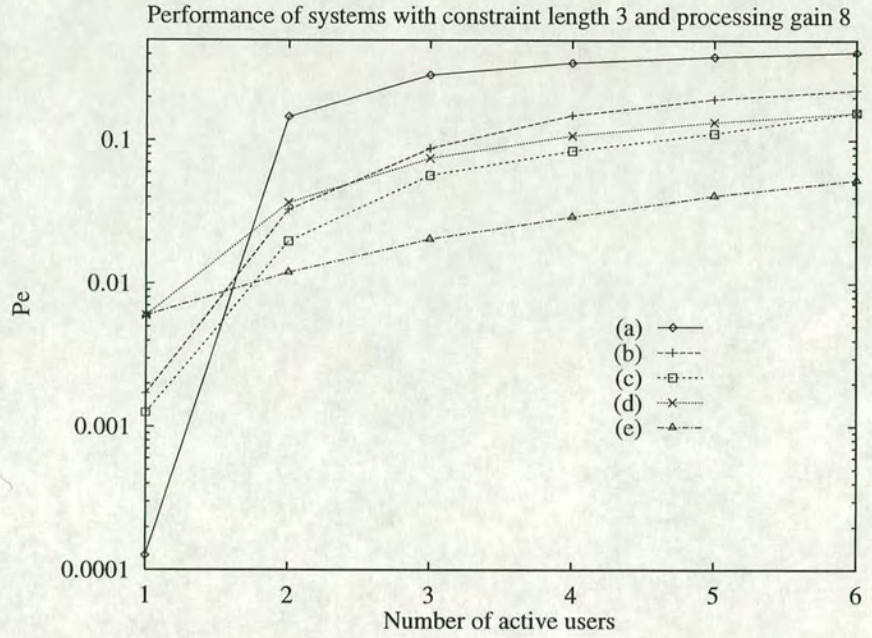

Figure 4.3: *Probability of error vs number of active users for systems with $K = 3$ and $g_P = 8$ with E_b/N_0 = 5 dB: (a) convolutional only; (b) orthogonal only; (c) orthogonal with randomiser (d) matched filter; (e) Wiener filter*

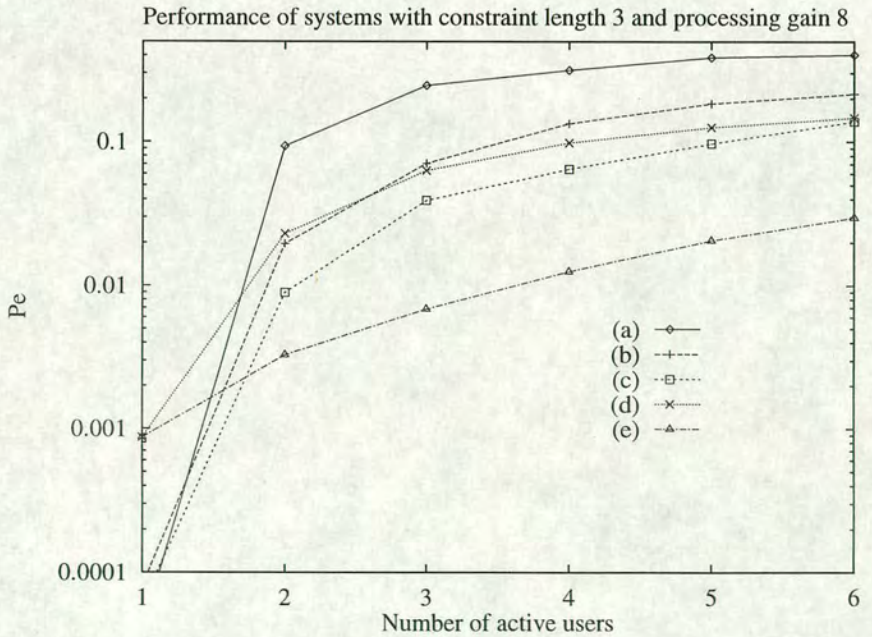

Figure 4.4: *Probability of error vs number of active users for systems with $K = 3$ and $g_P = 8$ with E_b/N_0 = 7 dB: (a) convolutional only; (b) orthogonal only; (c) orthogonal with randomiser (d) matched filter; (e) Wiener filter*

Again, the additional randomiser improves the performance of the orthogonal convolutional coder, but still not to as good as that of the Wiener filter for more than one user. The convolutional only system again has very poor peformance, and so will not be considered for the longer constraint length investigation.

4.3.1.2 Constraint length 6 systems

For more practical systems with $K = 6$ and a processing gain of 64, only four systems will be considered; the orthogonal coders with and without randomisation, together with uncoded systems with a matched filter and a Wiener filter receiver structure.

The results for $E_b/N_0 = 5$ dB are shown in Figure 4.5 from which it may be seen that although the orthogonal convolutional coder with the additional randomiser stage has the best performance for less than around 15 users, as the number of users is increased, this system's performance degrades rapidly, and the uncoded system with the Wiener filter receiver offers the better performance. Indeed, for more than about 30 users, the orthogonal coder with the randomiser is actually poorer than simply using a matched filter receiver on an uncoded system, even with random spreading sequences. Without the randomiser, the ill-effects of the clashes of outputs, in which the same Walsh code is produced for different input conditions, may be seen in the poor performance of the orthogonal only system.

Figure 4.6 shows the corresponding performance of the systems if the signal to Gaussian noise ratio is increased to 7 dB.

The orthogonal coder with the randomiser is again clearly superior for very low numbers of users, however, for 15 users, which was the previous important loading, the Wiener filter now has the best performance. Thus, reducing the background noise for 15 users reverses the relative performance of the systems using the Wiener filter with an uncoded signal and that using the orthogonal convolutional encoder with the additional randomiser. This result may be explained by conjecturing that the Wiener filter is better able to make use of the reduction in background noise, and thus has increased performance. As in the previous case, there occurs another critical loading point, this time around 32 users, for which the orthogonal coder with randomiser is poorer than simply using a matched filter receiver on an uncoded system with random spreading sequences. The orthogonal only encoder again performs poorly for all loading values, as in the lower constraint length case.

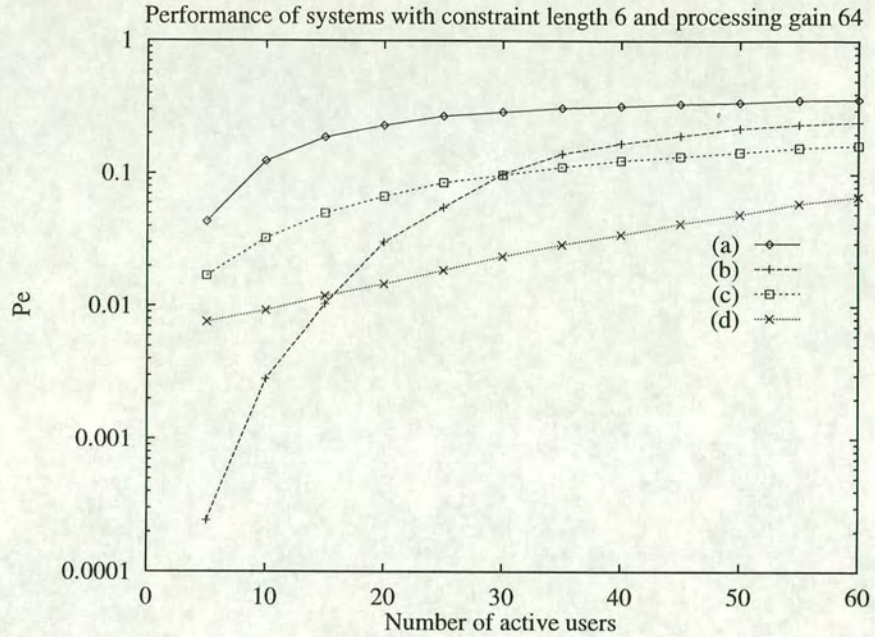

Figure 4.5: *Probability of error vs number of active users for systems with $K = 6$ and $g_P = 64$ with $E_b/N_0 = 5$ dB: (a) orthogonal only; (b) orthogonal with randomiser; (c) matched filter; (d) Wiener filter*

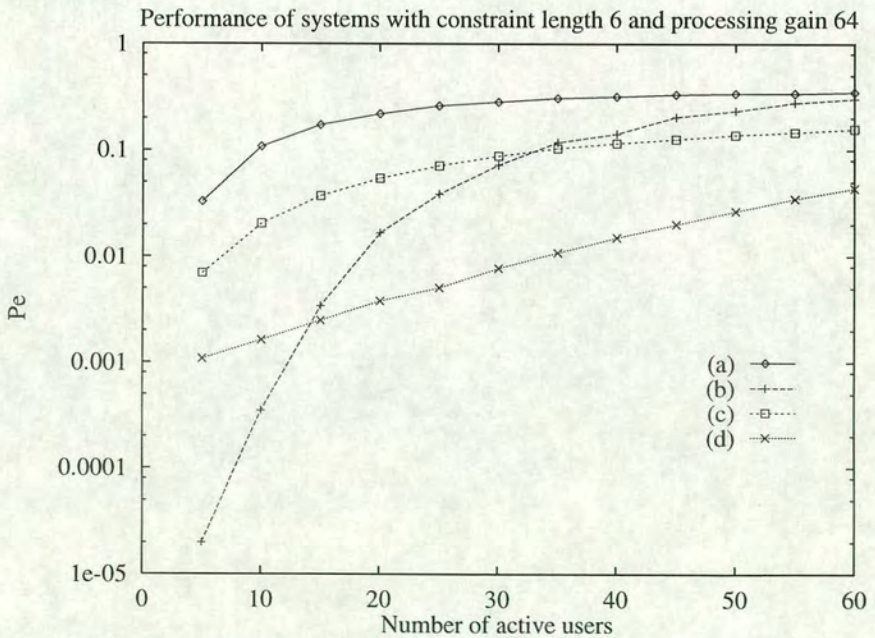

Figure 4.6: *Probability of error vs number of active users for systems with $K = 6$ and $g_P = 64$ with $E_b/N_0 = 7$ dB: (a) orthogonal only; (b) orthogonal with randomiser; (c) matched filter; (d) Wiener filter*

4.3.2 Performance for fixed number of active users

Since interference arises from both multiple access demands and background noise, it is important to also consider the relative performance of the schemes as the background noise is varied, for fixed number of active users. For this investigation, attention is focussed on the shorter processing gain ($g_P = 8$) systems.

4.3.2.1 Performance for 2 users

A more detailed analysis of the $K = 3$ system for the 2-user case is shown in Figure 4.7 which shows the performance over a range of noise values.

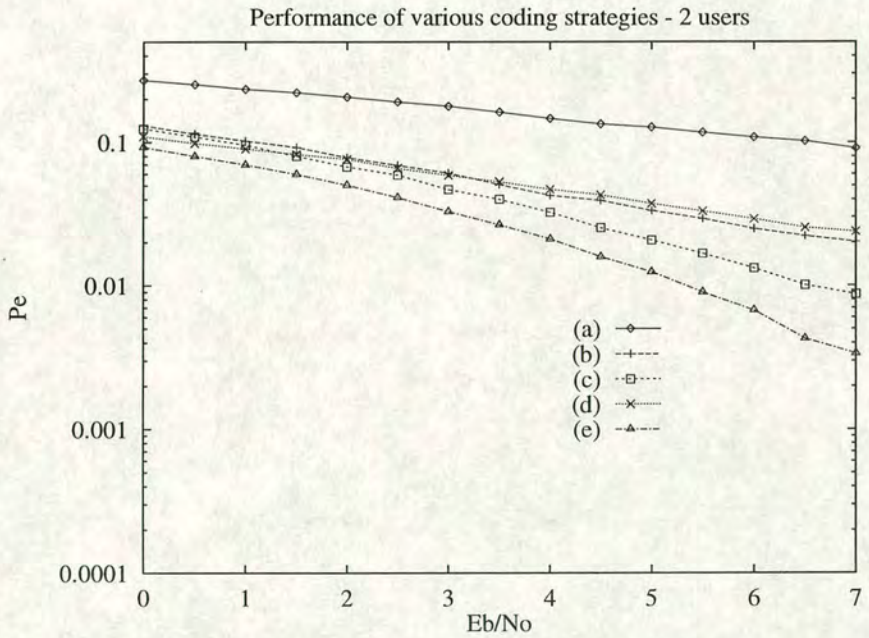

Figure 4.7: *Probability of error vs E_b/N_0 for $K = 3$ systems with 2 users: (a) convolutional only; (b) orthogonal only; (c) orthogonal with randomiser; (d) matched filter; (e) Wiener filter*

It may be seen that the incorporation of the randomiser improves the performance of the orthogonal system to a level better than straightforward matched filtering, and approaching that of the MMSE receiver. The use of orthogonal only, or conventional convolutional coding schemes leads to much poorer results. This is probably due to clashes where the same output sequence is generated simultaneously by different users, causing the Viterbi algorithm to lock on to the wrong path. This situation cannot be resolved by any receiving methodology, but it may be expected that fewer such instances would occur for longer constraint-length systems.

4.3.2.2 Performance for 3 users

The 3-user performance curves in Gaussian noise are shown in Figure 4.8.

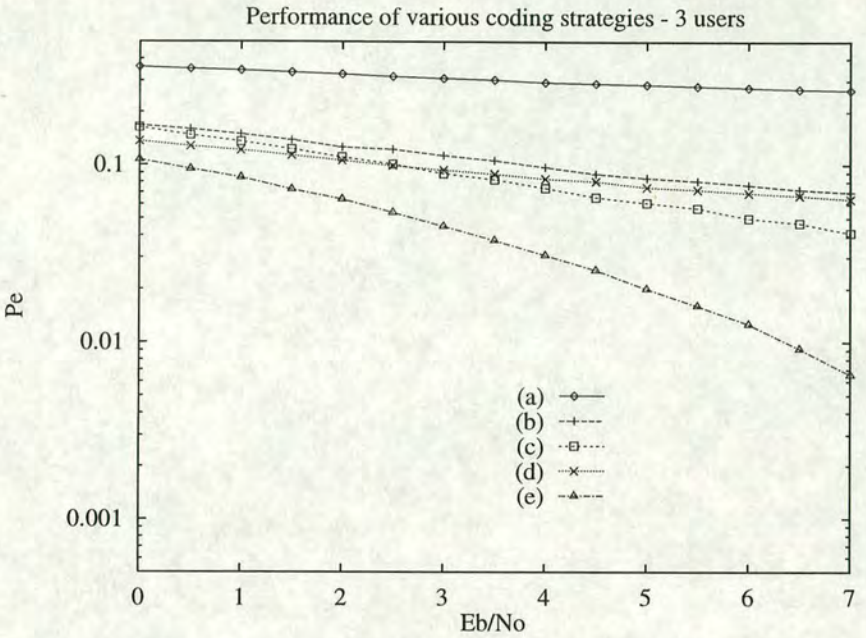

Figure 4.8: *Probability of error vs E_b/N_0 for $K = 3$ systems with 3 users: (a) convolutional only; (b) orthogonal only; (c) orthogonal with randomiser; (d) matched filter; (e) Wiener filter*

While, as expected, the performance of both the convolutional only and pure orthogonal systems is increasingly unreliable, the performance of the orthogonal convolutional coder with the additional randomising stage may approach being acceptable for sufficient signal to Gaussian noise ratio values. However, this system's performance is only marginally better than that of the unencoded system with a conventional matched filter and it is apparent that direct sequence spreading only, combined with the Wiener receiver filter remains the best approach over the complete range of noise levels.

4.3.3 Performance in a stationary multipath channel

The performance of the orthogonal systems with and without the additional randomisation stage is also considered in a stationary multipath channel, defined by the impulse response $H(z) = 1.0 + 0.5z^{-1}$, which is suitably normalised to avoid affecting the overall signal to Gaussian noise ratio. In this implementation, perfect channel knowledge is assumed, and the received signal $\underline{y}$ is first passed through the inverse (IIR) channel filter to give the compensated

received signal, denoted $\underline{y'}$, and given by

$$y'[i] = (\frac{1}{h_0})(y[i] - h_1 y'[i-1]) \tag{4.1}$$

It is this compensated signal, $\underline{y'}$, which is then analysed by the Viterbi decoder in the receiver. The performance results of the orthogonal systems with and without randomisation for both AWGN and in the multipath channel are shown in Figure 4.9 for $E_b/N_0 = 5$ dB and in Figure 4.10 for $E_b/N_0 = 7$ dB.

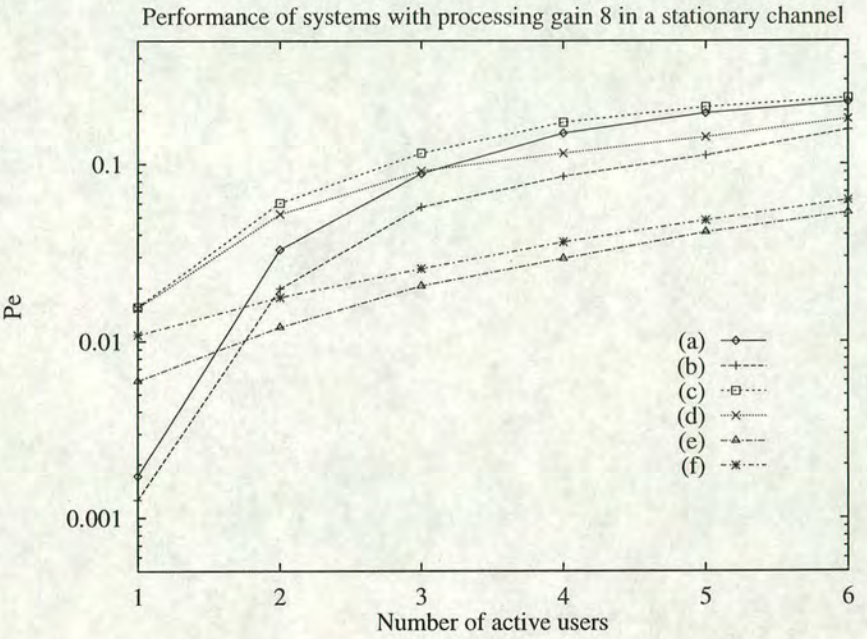

Figure 4.9: *Probability of error vs number of users in a stationary channel for $K = 3$ systems with $E_b/N_0 = 5$ dB : (a) orthogonal only in AWGN; (b) orthogonal with randomiser in AWGN; (c) orthogonal only in multipath channel; (d) orthogonal with randomiser in multipath channel; (e) Wiener in AWGN; (f) Wiener in multipath channel*

To enable a fair comparison, the Wiener receiver has been extended to capture all the energy emanating from one data bit. It may be seen that the effect of the channel is to generally worsen the performance of all the systems, with the orthogonal systems in particular suffering markedly reduced performance. This is probably due to loss of orthogonality of the Walsh sequences after passing through the channel.

Thus, even using perfect channel knowledge and a possibly unstable pre-processing IIR filter stage, the orthogonal coder with additional randomisation does not appear to offer better performance than a system with equal processing gain and the Wiener receiver filter, which could be approximated by an adaptive algorithm.

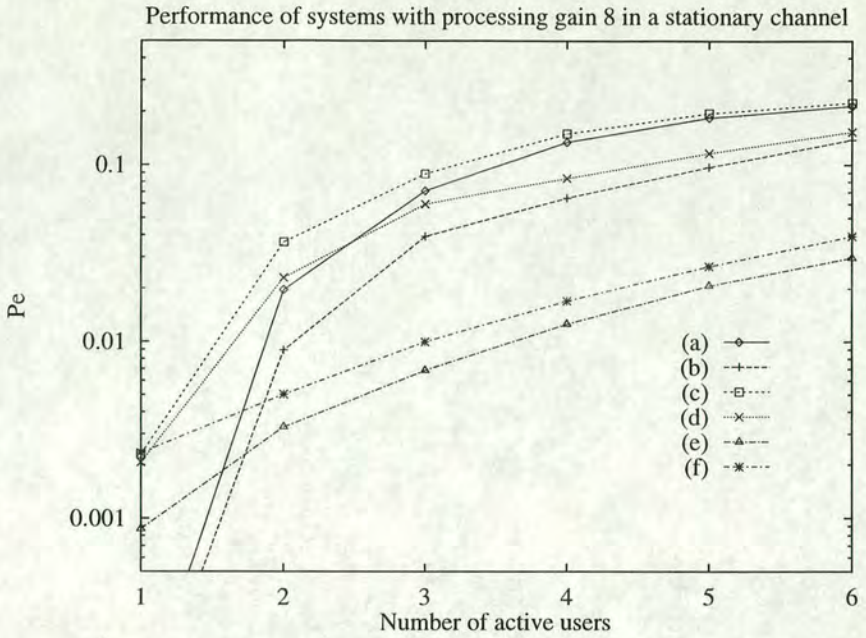

Figure 4.10: *Probability of error vs number of users in a stationary channel for $K = 3$ systems with E_b/N_0 = 7 dB: (a) orthogonal only in AWGN; (b) orthogonal with randomiser in AWGN; (c) orthogonal only in multipath channel; (d) orthogonal with randomiser in multipath channel; (e) Wiener in AWGN; (f) Wiener in multipath channel*

4.4 System 1 discussion

It has been demonstrated that attempting to construct a multiple access scheme via convolutional coding alone is an unsuccessful strategy, due to the sensitivity of the decoding schemes to what amounts to significant MAI. The use of the orthogonal convolutional encoder, together with additional randomising sequences to improve the spectral characteristics of the output Walsh codes, rather than produce any further spreading of the signal spectrum, has been shown to produce performance characteristics comparable to those of conventional convolutional coding for single user scenarios, while permitting reasonable performance for low numbers of competing users. However, the performance as the number of users increases is reduced compared to that of the Wiener filter, principally because of the effect discussed previously; namely that the same Walsh sequence may be produced by more than one user, and the likelihood of such clashes increases with the number of active users.

Thus, it may be concluded that it is inefficient to attempt a multiple access technique based only on a convolutional coding strategy, so that incorporation of forward error correction into the DS-CDMA environment may be better achieved by a combination of coding and spreading. In addition, the storage requirements of the orthogonal convolutional encoder are much greater

than conventional high rate convolutional coding, combined with direct sequence spreading. This technique is designated system 2, and is now discussed.

4.5 System 2 description

In the second system considered, the more conventional technique of combining convolutional coding with direct sequence spreading is investigated. The allocation of resources to the respective parts of the transmitter (whether FEC coding or direct sequence spreading) is of primary concern in practical cellular communications applications and so it is useful to consider the performance of various systems comprising different proportions of convolutional encoding and direct sequence spreading, whilst maintaining a given overall bandwidth expansion.

Boudreau [97] has calculated the theoretical performance (in terms of Chernoff upper bounds) of systems employing convolutional coding and trellis coding combined with spreading. The performance of actual systems, however, may be significantly superior (as much as 1.5 dB in some cases); this improvement being a non-linear function of E_b/N_0. The limited amount of simulations in [97] means that it is instructive to consider the simulated performance of such systems.

4.5.1 Allocation of resources

For the investigations considered here, the values for the code rate R and corresponding direct sequence spreading sequence length M for the various systems are shown in Table 4.2. (The symbols correspond to those which will be used in the presentation of the results.) Also shown is the resulting linear processing gain, g_P, for each system and the octal format of the tap connections used for the convolutional codes.

It may be seen that the rates of the codes and the lengths of the corresponding spreading sequences have been selected to maintain an overall linear processing gain g_P of around 500 (equivalent to a G_P of around 27 dB). Also, the tap connections in the coder are the same for each user, so that discrimination is solely provided by the direct sequence spreading portion. An obvious development would be to allocate different connections for each user, combined with different spreading sequences, although this would require a dedicated Viterbi decoder for

K	$R=\frac{1}{2}$ $M=255$ + $g_P=510$	$R=\frac{1}{4}$ $M=127$ □ $g_P=508$	$R=\frac{1}{8}$ $M=63$ × $g_P=504$	$R=\frac{1}{16}$ $M=31$ △ $g_P=496$
3	(5,7)	(5,7,7,7)	(7,7,7,5,5,5,7,7)	(7,7,7,5,5,5,7,7, 7,7,7,7,5,5,7,7)
4	(17,15)	(13,15,15,17)	(17,17,13,13,13,15,15,17)	(17,17,13,13,13,15, 15,17, 17,17,13,13,13,1 5,15,17)
5	(23,35)	(25,27,33,37)	(37,33,25,25,35,33,27,37)	(37,33,25,25,35,33,2 7,37, 37,33,25,25,35,3 3,27,37)
6	(53,75)	(53,67,71,75)	(53,67,71,75,53,67,71,75)	(53,67,71,75,53,67, 71,75, 53,67,71,75,53,6 7,71,75)

Table 4.2: Convolutional codes used in the various simulations for system 2

each user. The method implemented here means that the same decoder unit could be used for any user, given their spreading sequence, which may be easier to implement practically.

The choice of tap connections for rates $1/2$ ($M = 255$) [3] and $1/8$ ($M = 63$) mirror those in [97] for constraint lengths 3,4 and 5 whilst those for $R = 1/4$ are motivated by the results of Larsen [64]. While it is acknowledged that the repetition of the rate $1/8$ code to form the rate $1/16$ code may be sub-optimal, especially for the larger constraint-length systems, this configuration is liable to have similar properties to any optimal arrangement, and is thus employed here.

The complexity and storage requirements for the various systems are shown in Table 4.3, assuming $L \simeq 5K$,

K	Delay (bits)	Add compare & select (ACS)	Path storage
3	15	4	60
4	20	8	160
5	25	16	400
6	30	32	960

Table 4.3: Complexity and storage requirements for the various simulations for system 2

The number of add, compare and select (ACS) operations is given by $2^{(K-1)}$, while the path storage calculations require $L \times 2^{(K-1)}$ memory locations [31]. These estimates exclude the

[3] Strictly, Gold codes of length 255 do not exist [48], however "Gold-like" sequences may be constructed with the required cross-correlation of -1 at the synchronous point. Those used here are obtained from the m-sequences $[8,2,3,4]_s$ and $[8,3,5,6]_s$

requirements for the branch metric calculations, described in section 2.3.3.4, and which are in general a non-trivial function of the constraint length.

4.6 System 2 results

As discussed previously, the interference in a DS-CDMA system in Gaussian noise has two main sources, the background noise level and the multiple access interference from other users. Therefore, the performance of the systems must be considered for various values of both these quantities. In the first four sections, both Gold and random sequences are used as the spreading sequences and there are 20 active users present, while in the next two, random sequences have been chosen to spread the convolutionally-encoded data, and the values of E_b/N_0 are held fixed at 2.0 dB and 4.0 dB respectively. The choice of random spreading sequences is motivated by the fact that in a multipath environment such as those defined in the COST207 study [35], the presence of intersymbol interference will corrupt the near-orthogonal qualities of Gold codes. Note that in this case, the percentage loading is calculated from the number of active users and the overall linear processing gain (g_P), taking the code rate into account, rather than simply the length of the appropriate spreading sequence.

4.6.1 Performance for various constraint lengths

In the figures, the performance of each system is compared with the theoretical binary phase shift keying (BPSK) bound from Equation B.13 and the performance of an uncoded DS-CDMA system with 511-chip spreading sequences.

4.6.1.1 Constraint length 3

The first case considered here is for constraint length 3 and the results using Gold spreading sequences are shown in Figure 4.11.

It is apparent that in this case, the rate $1/2$ system performs better than the other configurations, with the rate $1/8$ system also performing well. The relatively poor performance of the rate $1/16$ system is probably due to the reduced capacity of the Gold sequences (20 users with 31-

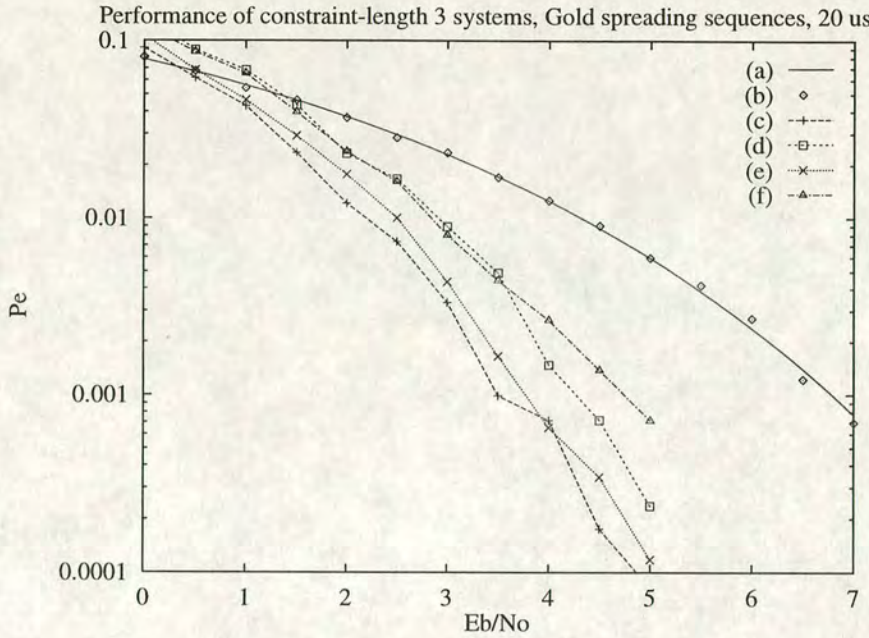

Figure 4.11: *Performance of convolutionally coded DS-CDMA systems with constraint length 3 for 20 users employing Gold spreading sequences: (a) theoretical BPSK; (b) uncoded,* $M = 511$*; (c) rate* $1/2$*,* $M = 255$*; (d) rate* $1/4$*,* $M = 127$*; (e) rate* $1/8$*,* $M = 63$*; (f) rate* $1/16$*,* $M = 31$

chip spreading means that the multiple access interference is more significant than the longer spreading systems), combined with the possible sub-optimality of the convolutional codes. The reason for the anomalously poor performance of the rate $1/4$ system is less clear, although this may simply be an unfortunate combination of rate and constraint length. Further investigations may provide some insight about this behaviour.

Notwithstanding these comments, even the poorest performing convolutional code is still significantly better than the 20-user uncoded DS-CDMA system for values of E_b/N_0 greater than about 1 dB.

For random spreading sequences, shown in Figure 4.12, the relative performance of the convolutionally encoded systems is broadly similar, although the absolute error probabilities are not.

The major differences are that, because of the higher cross-correlations due to random spreading sequences, the performance of all the systems are generally worse, with the rate $1/16$ and $1/8$ systems having inferior performance to uncoded CDMA for most of the values of E_b/N_0 considered. As in the previous case, the rate $1/2$ system performs best, while the rate $1/4$ is the second best, in contrast to the results obtained using Gold sequences.

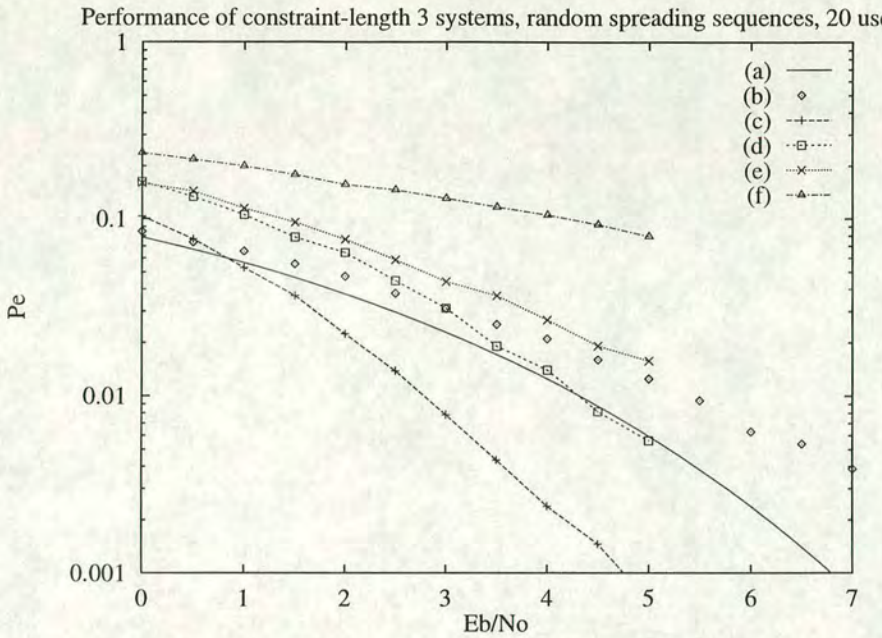

Figure 4.12: *Performance of convolutionally coded DS-CDMA systems with constraint length 3 for 20 users employing random spreading sequences: (a) theoretical BPSK; (b) uncoded,* $M = 511$*; (c) rate* $1/2$*,* $M = 255$*; (d) rate* $1/4$*,* $M = 127$*; (e) rate* $1/8$*,* $M = 63$*; (f) rate* $1/16$*,* $M = 31$

4.6.1.2 Constraint length 4

The results for constraint length 4 systems are presented in Figure 4.13, from which it may be seen that the rate $1/4$ and $1/8$ systems, which are now very similar, are slightly better than the rate $1/2$ system, while the rate $1/16$ system is still suffering from the increased MAI of the 31-chip Gold sequences in a similar way to the $K = 3$ case.

The improved performance of the rate $1/4$ system is probably due to the increased error correcting power of this combination. Where a greater variety of tap connections is available (*i.e. longer constraint length*), it is prudent to make as full use of them as possible, thus increasing the power of the code and permitting more resources (bandwidth) to be invested in the direct spreading part, to allow greater capacity.

Thus, while the choice of rate and constraint length are notionally independent, the use of appropriate rate codes, which make use of the full range of available connections for a given constraint length can lead to marked improvements in performance.

The results using random spreading sequences are shown in Figure 4.14. Again, the rate $1/16$ system is worse than the uncoded one, while now the rate $1/2$ and $1/4$ systems have comparable

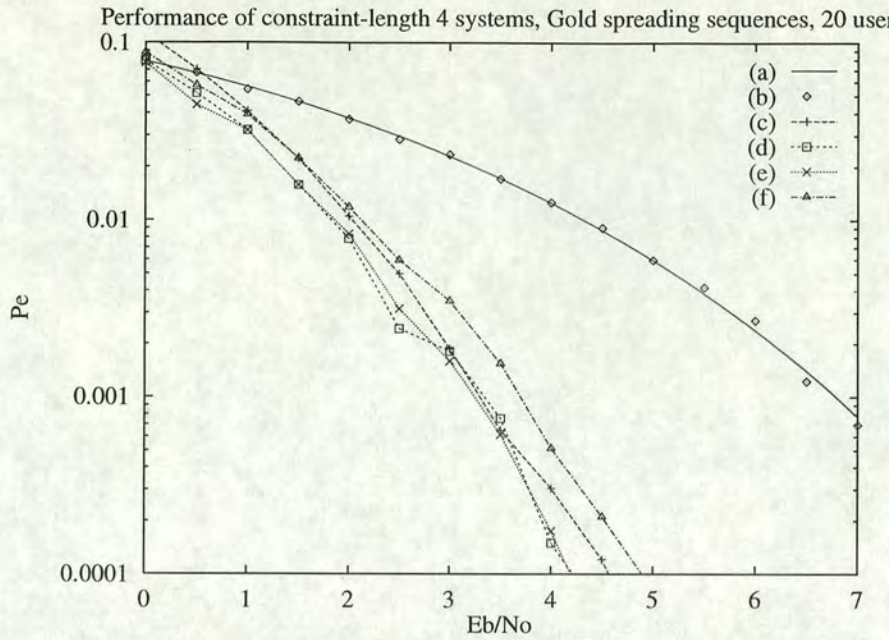

Figure 4.13: *Performance of convolutionally coded DS-CDMA systems with constraint length 4 for 20 users employing Gold spreading sequences: (a) theoretical BPSK; (b) uncoded,* $M = 511$*; (c) rate* $1/2$*,* $M = 255$*; (d) rate* $1/4$*,* $M = 127$*; (e) rate* $1/8$*,* $M = 63$*; (f) rate* $1/16$*,* $M = 31$

performance.

4.6.1.3 Constraint length 5

Figure 4.15 shows the results obtained using systems with a constraint length of 5.

This appears to confirm the trend noted previously, namely that the systems with rates $1/2$ and $1/16$ are inferior to those with convolutional code rates of $1/4$ and $1/8$, which make more efficient use of the increased power, by virtue of their larger constraint lengths, of the convolutional codes. A point of interest is that now the performance of the rate $1/16$ system is better than the rate $1/2$ system. This is again due to the greater number of available connections, which is beginning to compensate for the relatively larger MAI of the 31-chip spreading module, in contrast with the first two cases with their shorter constraint lengths.

The performance of the rate $1/2$ system at E_b/N_0 values lower than around 1 dB is also worthy of note, since it is now inferior to direct sequence spreading alone. This is probably also due to the increased power of the convolutional codes, since more errors are introduced from the Viterbi algorithm losing track of the correct path through the trellis. Thus it is not always

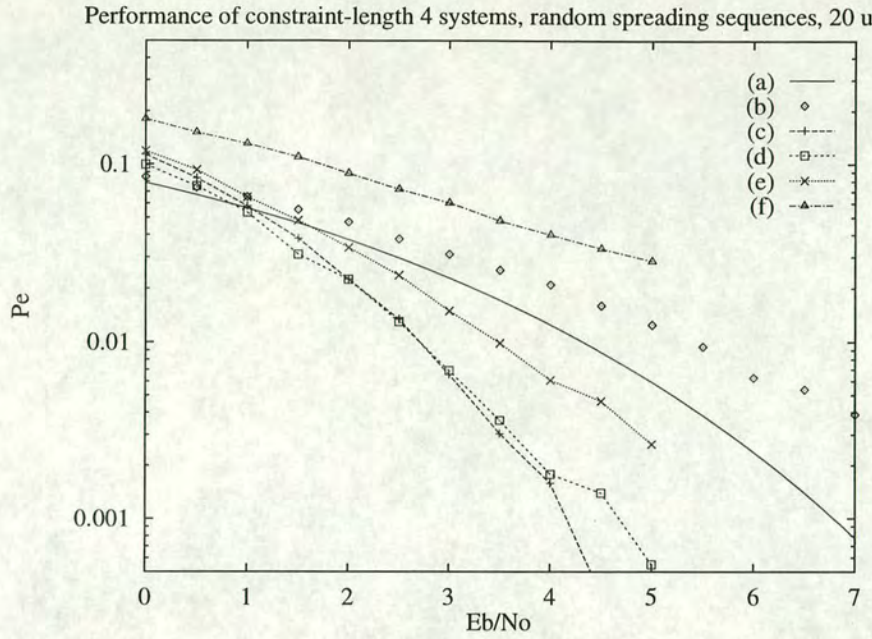

Figure 4.14: *Performance of convolutionally coded DS-CDMA systems with constraint length 4 for 20 users employing random spreading sequences: (a) theoretical BPSK; (b) uncoded, $M = 511$; (c) rate $1/2$, $M = 255$; (d) rate $1/4$, $M = 127$; (e) rate $1/8$, $M = 63$; (f) rate $1/16$, $M = 31$*

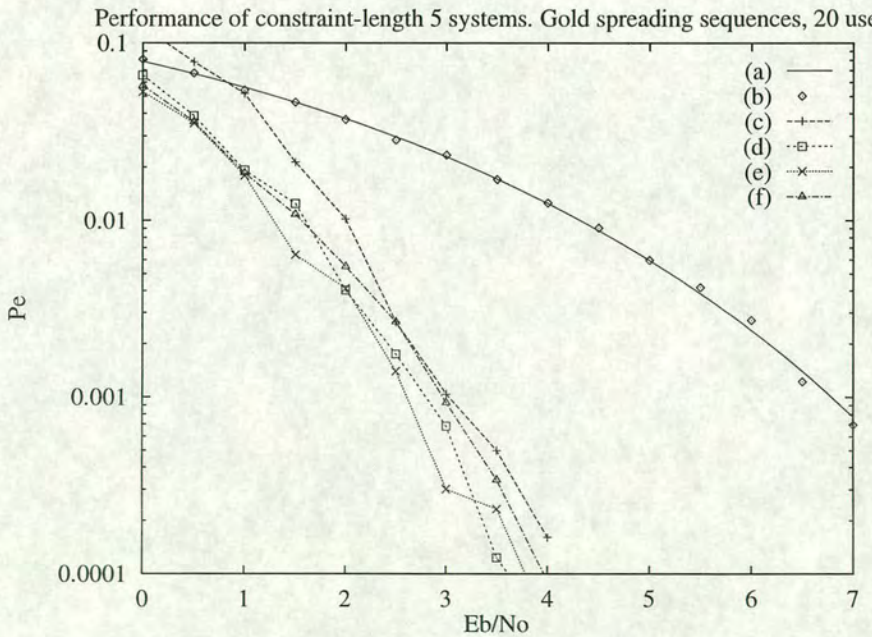

Figure 4.15: *Performance of convolutionally coded DS-CDMA systems with constraint length 5 for 20 users employing Gold spreading sequences: (a) theoretical BPSK; (b) uncoded, $M = 511$; (c) rate $1/2$, $M = 255$; (d) rate $1/4$, $M = 127$; (e) rate $1/8$, $M = 63$; (f) rate $1/16$, $M = 31$*

beneficial simply to increase the constraint length independently, since more errors may be introduced in high noise environments. This effect will be examined in more detail later, in which the additional noise will be due to increasing numbers of users.

Figure 4.16 shows the performance of the corresponding constraint length 5 systems, using random spreading sequences.

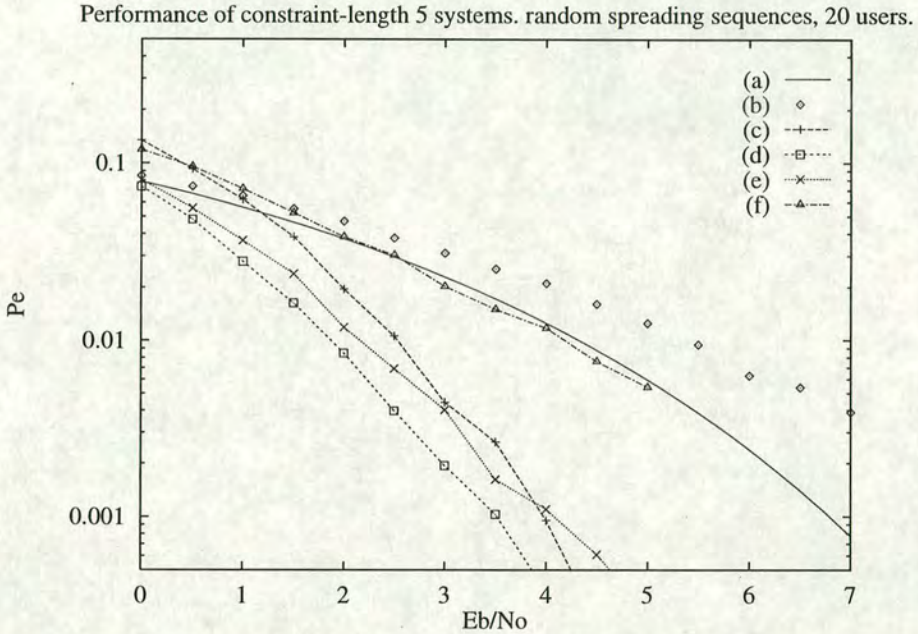

Figure 4.16: *Performance of convolutionally coded DS-CDMA systems with constraint length 5 for 20 users employing random spreading sequences: (a) theoretical BPSK; (b) uncoded,* $M = 511$*; (c) rate* $1/2$*,* $M = 255$*; (d) rate* $1/4$*,* $M = 127$*; (e) rate* $1/8$*,* $M = 63$*; (f) rate* $1/16$*,* $M = 31$

This also confirms the trend outlined, with the rate $1/4$ system having the best performance. The rate $1/2$ and $1/8$ systems now have similar performance, while the rate $1/16$ is now slightly better. The performance of the rate $1/2$ system for low E_b/N_0 mirrors that using Gold sequences, which provides further evidence for the phenomenon of the Viterbi algorithm being unable to locate the correct path through the trellis under high noise conditions, and thus producing more errors than an uncoded system.

4.6.1.4 Constraint length 6

For constraint length 6, shown in Figure 4.17, the trend outlined previously is reinforced, with the rate $1/8$ and rate $1/4$ systems better than the rate $1/16$ and $1/2$ systems, respectively.

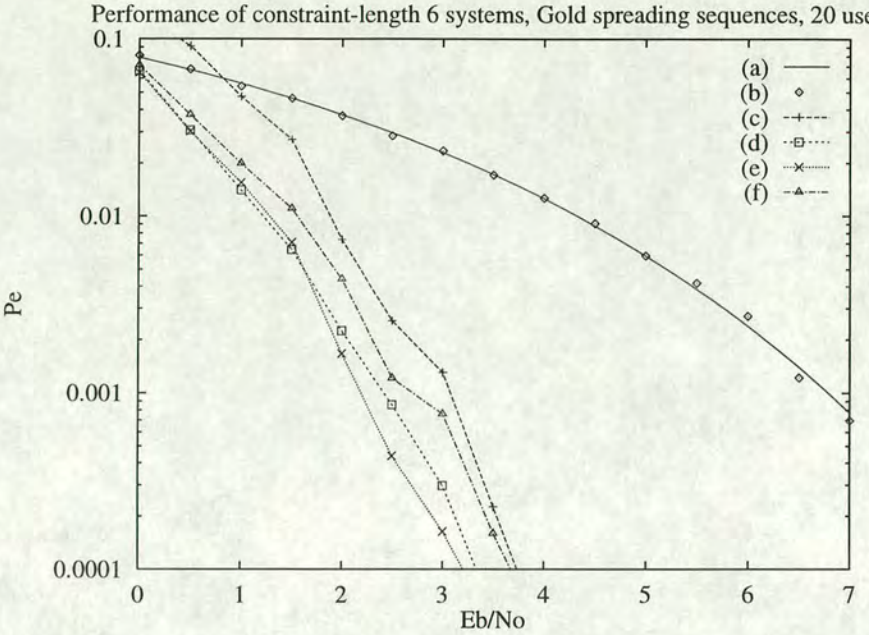

Figure 4.17: *Performance of convolutionally coded DS-CDMA systems with constraint length 6 for 20 users employing Gold spreading sequences: (a) theoretical BPSK; (b) uncoded,* $M = 511$*; (c) rate* $1/2$*,* $M = 255$*; (d) rate* $1/4$*,* $M = 127$*; (e) rate* $1/8$*,* $M = 63$*; (f) rate* $1/16$*,* $M = 31$

The rate $1/16$ system has better performance than in the previous Gold sequence systems since again, more efficient use is made of the available tap connections. As with constraint length 5, the rate $1/2$ system performs significantly poorer than the conventional case for E_b/N_0 values below around 1 dB. This is again due to the Viterbi algorithm producing a higher number of errors when an incorrect path through the trellis is selected. Thus, care needs to be exercised when employing a long constraint length, high rate convolutional code under conditions of high noise.

The performance of the systems when using random spreading sequences is shown in Figure 4.18. Again the rate $1/4$ and $1/8$ systems have the best performance, with that of the rate $1/16$ system only slightly poorer. The increased constraint length of the rate $1/2$ system again causes problems for E_b/N_0 values below around 1 dB. Thus simply increasing the constraint length does not always increase the power of a convolutional code uniformly, and in high noise situations, may lower the overall system performance.

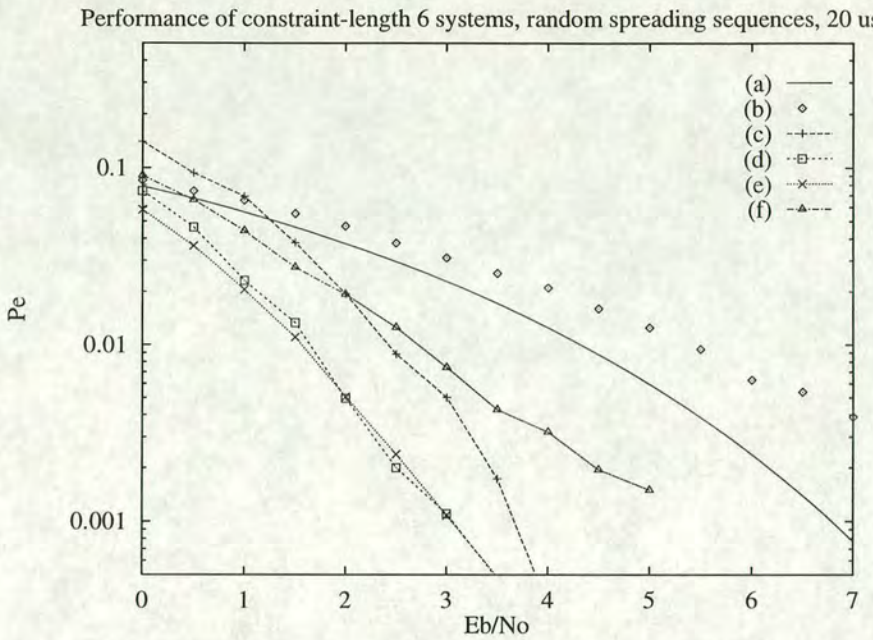

Figure 4.18: *Performance of convolutionally coded DS-CDMA systems with constraint length 6 for 20 users employing random spreading sequences: (a) theoretical BPSK; (b) uncoded,* $M = 511$*; (c) rate* $1/2$*,* $M = 255$*; (d) rate* $1/4$*,* $M = 127$*; (e) rate* $1/8$*,* $M = 63$*; (f) rate* $1/16$*,* $M = 31$

4.6.2 Performance for varying capacity

The simulations in this section are only performed with random spreading sequences, as a first approximation at modelling effects due to an unknown dispersive channel. The performance of these systems with varying numbers of active users may be judged from figure 4.19, for which the background noise level E_b/N_0 is set at 2.0 dB.

For very low loading (around 2 %), the systems behave much as discussed previously, with the $K = 3$, rate $1/16$ system performing even worse than uncoded DS-CDMA, and the $K = 3$ rate $1/4$ system only marginally better. In general, the $K = 6$ systems have better performance, due to the increased power of the FEC codes, however it is interesting that even for very low numbers of users, the rate $1/2$ $K = 3$ and $K = 6$ systems are very similar.

As the loading is increased, various effects may be seen. In particular, the only systems which continue to outperform uncoded DS-CDMA are the $K = 6$ rate $1/4$ and $K = 3$ rate $1/2$ configurations. These systems represent the most efficient use of the combination of rate, constraint length (and hence power) and spreading capacity, and thus have superior performance.

Significantly, the $K = 6$ rate $1/8$ combination, which appeared to be the best for the previous

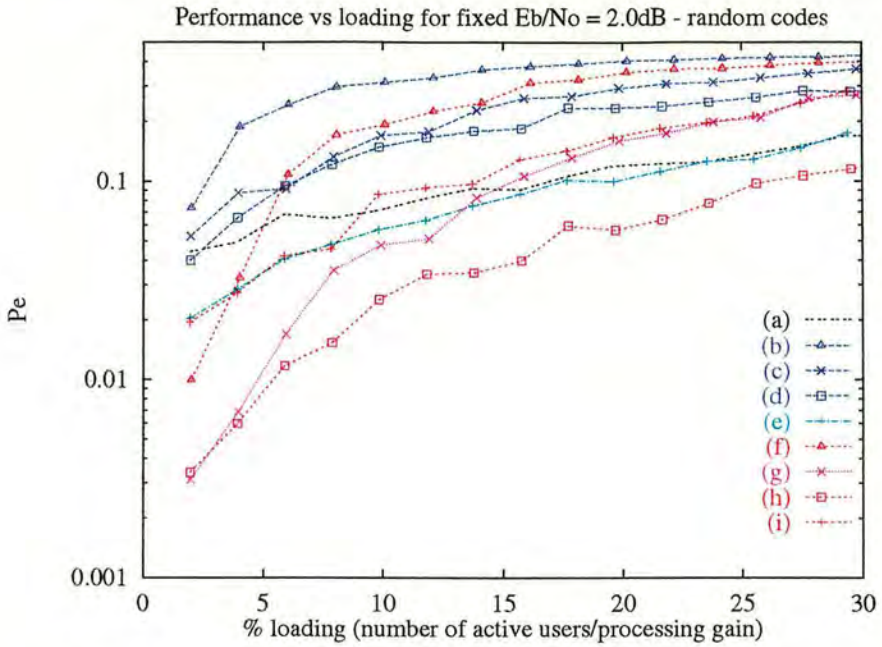

Figure 4.19: *Performance of convolutionally coded DS-CDMA systems with constraint lengths 3 and 6 for $E_b/N_0 = 2.0$ dB, with random spreading sequences; (a) uncoded, $M = 511$; (b) $K = 3$, rate $1/16$; (c) $K = 3$, rate $1/8$; (d) $K = 3$, rate $1/4$; (e) $K = 3$, rate $1/2$; (f) $K = 6$, rate $1/16$; (g) $K = 6$, rate $1/8$; (h) $K = 6$, rate $1/4$; (i) $K = 6$, rate $1/2$*

cases with 20 users using either Gold or random spreading sequences, does not have such good performance (at least when using random spreading sequences) as the number of users is increased. In addition, the $K = 6$ rate $1/2$ combination has poorer performance than the equivalent $K = 3$ system. Although this may at first appear counter-intuitive, the reason is due to the increased overall noise causing the Viterbi algorithm to lock on to the wrong path through the trellis, and hence produce more errors, as discussed previously.

The equivalent results for $E_b/N_0 = 4.0$ dB are shown in Figure 4.20.

This confirms some of the results in the previous case; specifically, that although the $K = 6$ rate $1/2$ system is better for low loading, as the loading is increased its performance becomes worse than the same rate $K = 3$ system, and that the beneficial effects of most convolutional coding systems are lost as the loading increases. As in the previous case, the optimal system as the number of users is increased is that using $K = 6$ rate $1/4$ convolutional codes, with 127-chip spreading sequences.

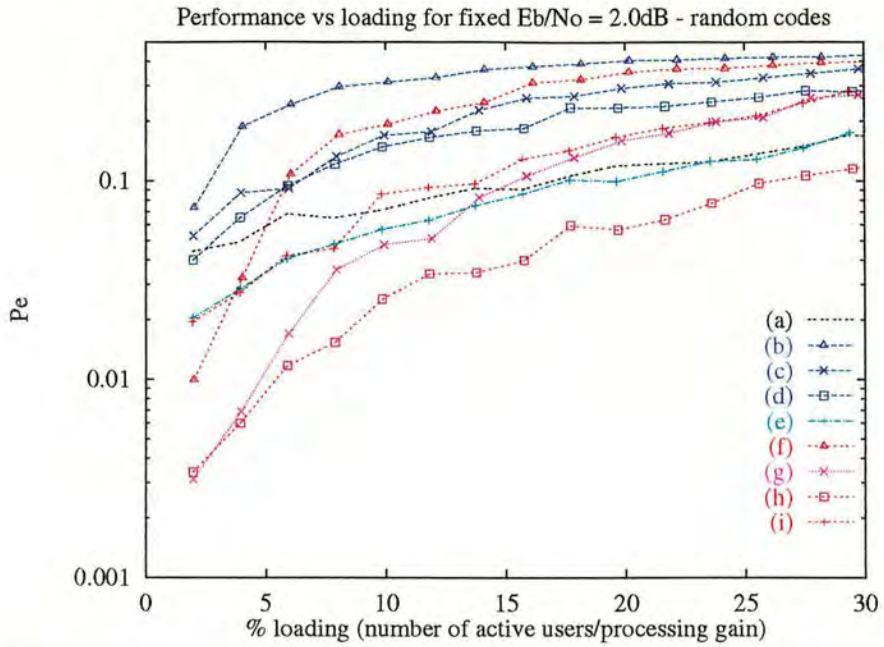

Figure 4.20: *Performance of convolutionally coded DS-CDMA systems with constraint lengths 3 and 6 for $E_b/N_0 = 4.0$ dB, with random spreading sequences; (a) uncoded, $M = 511$; (b) $K = 3$, rate $1/16$; (c) $K = 3$, rate $1/8$; (d) $K = 3$, rate $1/4$; (e) $K = 3$, rate $1/2$; (f) $K = 6$, rate $1/16$; (g) $K = 6$, rate $1/8$; (h) $K = 6$, rate $1/4$; (i) $K = 6$, rate $1/2$*

4.7 System 2 discussion

This section has compared the simulated performance of a number of strategies utilising non-linear convolutional codes combined with direct sequence spreading for use in a processing-gain limited DS-CDMA cellular communication system. Convolutional codes with constraint lengths up to $K = 6$ have been considered, with rates of $1/2$, $1/4$, $1/8$ and $1/16$, together with appropriate length spreading sequences.

With an overall processing gain of approximately 27 dB and 20 active users employing Gold spreading sequences, the optimal strategy seems to be the combination of a constraint length 6, rate $1/8$ convolutional code and 63-chip spreading sequences, although increasing the constraint length beyond the values considered here may cause a different combination of spreading sequence length and coding rate to be optimal. Significantly, this result is again obtained if random sequences are used to spread the convolutional encoded sequence.

Increasing the number of users and employing random spreading sequences means that this arrangement is no longer optimal, and that convolutional codes of the same constraint length but rate $1/4$ should be used instead. The ill-effects of simply increasing the constraint length

without a corresponding adjustment of the convolutional code rate are also demonstrated. These observations serve to exhibit the fine balance that exists between the power of the convolutional code (obtained from a combination of both its rate and constraint length), the capacity of the spreading sequences and the noise level, whether from the background noise, or from MAI produced by other subscribers on the system.

4.8 Summary

This Chapter has discussed the use of convolutional coding as applied to the multi-user DS-CDMA environment. The basic principles of implementing forward error correction using convolutional codes in a multiple access scenario were first described, following which two systems were considered. The first system described simply replaces the direct sequence spreading by the encoded sequence produced by the FEC unit, while the second combines coding and spreading to produce the overall processing gain.

In the context of a limited processing-gain system, two encoding structures have also been discussed, the conventional convolutional encoder and the orthogonal convolutional coder. The orthogonal convolutional coder was shown to have poor performance, unless augmented with an additional randomising stage to avoid the number of occasions on which the output Walsh sequence is the same for different users with different input conditions. It was also shown that for greater than very light loading, the performance of the orthogonal convolutional coder with the randomiser is not as good as that of an uncoded system with the same bandwidth expansion and using random spreading sequences, provided the receiver is able to calculate the Wiener filter. This was shown in the previous chapter to be possible by implementing an adaptive algorithm. In addition, the training overhead imposed by such a technique is no worse than the additional bandwidth requirements for an FEC encoder. A possible application of such short processing-gain systems could be in the extension of existing technology, as used for example in the GSM system, by incorporating a short spreading sequence DS-CDMA system into each time frame of the GSM system. This code and time division multiple access system has been proposed [98] as a possible contender for the future European UMTS standard.

For systems with a greater available processing gain, the efficient utilisation of bandwidth between convolutional coding and direct sequence spreading has been discussed. The requirement for a balance of resources has been demonstrated, as has the reduction in performance if the

constraint length is simply increased without a corresponding adjustment in the convolutional coding rate. It has also been demonstrated that the use of FEC in a multiple access environment, while clearly advantageous if the signal is sufficiently clean, may prove deliterious if the interference (whether arising from background noise or MAI) is more significant.

This chapter has also stressed the differences between single user communications, where the interference is generally unstructured Gaussian noise and multiple access systems where, unless the systems use purely random (and very long) spreading sequences, the interference is structured. This structured interference affects the performance of the Viterbi decoder, possibly causing it to perform worse than if no FEC coding were employed. The following chapter will consider methods of cancellation of this structured interference before attempting to recover the desired signal. As a future development of the work presented here, other FEC coding schemes, such as turbo-coding or super-orthogonal coding could be investigated, but it may be anticipated that the above conclusions will be broadly upheld, namely that FEC encoding is of benefit when the signal can be processed to reduce the interference, but will produce more errors than an uncoded strategy otherwise. The increased processing delay associated with such increased complexity FEC coding schemes may hinder the application of these techniques for a rapidly varying channel. In addition, the simulations have been carried out with random spreading sequences, as a first attempt at modelling a dispersive channel. A further future development would be to investigate the effects of a more realistic channel model, as considered for adaptive algorithms in the previous chapter.

Chapter 5

Combined Viterbi decoding and interference cancellation in a DS-CDMA System

In this chapter, the application of multiple access interference (MAI) cancellation methods to the downlink of a DS-CDMA system will be investigated. Specifically, the focus will be on combining parallel MAI cancellation, introduced in section 2.3.4, with forward error correction (FEC) using convolutional coding, as discussed in the previous chapter. The motivation for an approach of this nature will first be outlined in Section 5.1, which compares the theoretical and simulated performance of a single stage cancellation receiver applied to a DS-CDMA system without FEC coding, before briefly describing the extension of this principle to FEC encoded systems. The various proposed receiver architectures to be considered in more detail are described in Section 5.2. A theoretical analysis of these receiver structures is then developed in Section 5.3, followed by the results of some Monte Carlo simulations in Section 5.4. Possible improvements to the receivers considered here are then proposed in Section 5.5, with a summary of the main results of the chapter in Section 5.6.

5.1 Motivation

The important point about the interference in a DS-CDMA system is that, for non-orthogonal spreading sequences in Gaussian noise, it may be considered as consisting of two parts[1].

[1] For orthogonal spreading sequences there is no MAI on the transmitted signal, and hence only non-deterministic background noise is present.

The first is a non-deterministic portion, arising from the background noise, and the second is a deterministic portion, produced by multiple access interference (MAI) resulting from the coherent addition of the other users' spread signals at the transmitter. The reason for using non-orthogonal spreading sequences is that under practical conditions, the transmitted signal will also be subject to the effects of a multipath channel, so that the properties of any special spreading sequence set will likely be destroyed.

The most efficient receivers, therefore, will use this knowledge by estimating and cancelling the interfering users' contributions from a suitably delayed version of the received signal, with the intention of increasing the probability of correctly de-correlating this new signal, and thus inferring the desired user's data. This principle, which is here implemented as parallel MAI cancellation, is demonstrated in Figure 5.1 for a system with U active users, in which, as usual, the desired user is number 1.

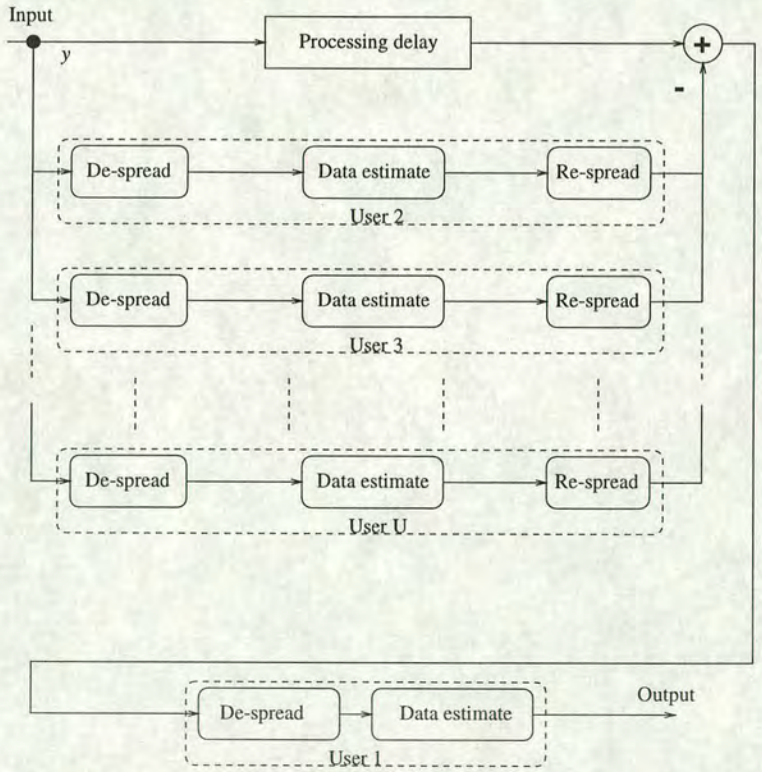

Figure 5.1: *Parallel mulitple access interference cancellation principle in a DS-CDMA system with U active users*

It may be seen that this structure, when used on the uplink, relies on accurate timing and power information to be available at the base station, since the delay and strength of each user's signal must be specified to correctly align and scale each signal to be cancelled. If this arrangement is to be incorporated into the receiver on the downlink, for which all the users' signals are synchronised, only the initial signal acquisition information is required. With U active users,

and a linear processing gain of M, this structure requires $(2U-1)M$ multiplications, and the same number of additions and subtractions, which is the main disadvantage to this technique. Of lesser importance is that all of the interfering users' spreading sequences must be available to the mobile. In either case, the processing delay imposed must not be too exhorbitant, since there will likely be other delays in the system as a whole (*e.g.* that imposed by any FEC decoding or interleaving of the data).

Before considering the extension of this principle to signals with forward error correction, it is useful to compare the theoretical and simulated performance of the single stage MAI canceller receiver when used in a DS-CDMA system which does not employ FEC coding.

5.1.1 Theoretical analysis of single stage matched filter canceller

It may be shown [37] that the probability of a bit error for a single-stage canceller employing matched filters (P_e^{MFC}) on a DS-CDMA system with no FEC coding on the data and random spreading sequences applied to independent data may be approximated by

$$P_e^{MFC}(U, g_P) = Q\left(\sqrt{\frac{g_P}{\sigma^2 + 4(U-1)P_e^{MF}(U, g_P)}}\right) \tag{5.1}$$

where, as previously, U is the number of users, g_P is the linear processing gain and $P_e^{MF}(U, g_P)$ is the error performance of a standard matched filter receiver with the relevant parameters as specified in equation 2.10. Again, σ^2 is the variance of the Gaussian noise, and $Q(\cdot)$ is the standard Gaussian upper cumulative distribution function defined in equation 2.11. The factor 4 arises because if an error is made, the power of the resulting (incorrect) intermediate spread signal for that user is quadrupled, since the amplitude is doubled for BPSK modulation.

5.1.2 Simulated performance of single stage matched filter canceller

The results of Monte Carlo simulations using 31 chip random spreading sequences are shown in Figure 5.2 for the matched filter canceller (MFC) receiver along with the predictions using equation 5.1.

Comparing the simulated results with those presented in Figure 2.9, it may be seen that incorporation of the canceller increases the number of supported users for a given probability

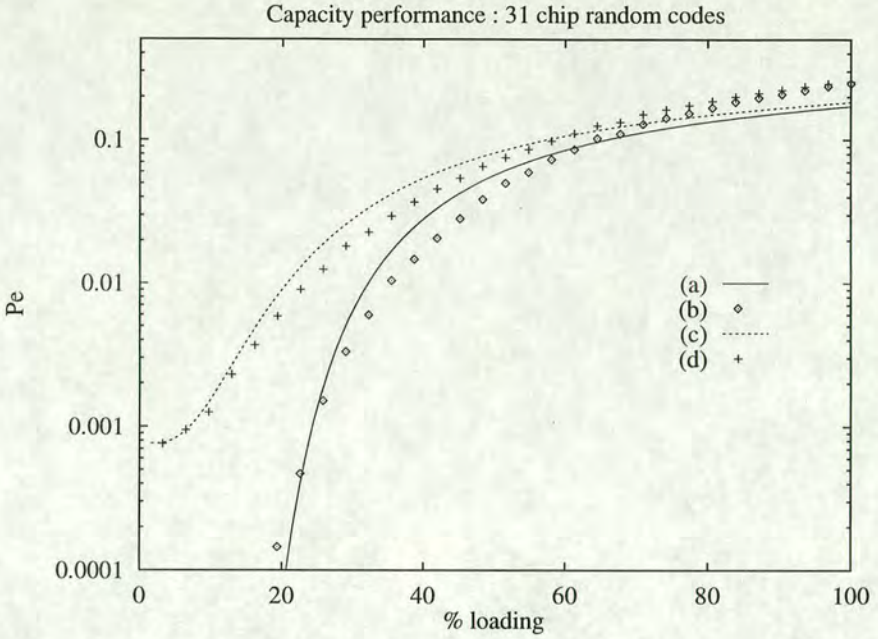

Figure 5.2: *Theoretical and simulated probability of error for matched filter cancellation (MFC): (a) theoretical, MAI only; (b) simulated, MAI only; (c) theoretical, $E_b/N_0 = 7$ dB; (d) simulated, $E_b/N_0 = 7$ dB*

of error. In particular, for $P_e = 0.01$, 8 users (25 % capacity) may be supported, compared to less than half that number if a receiver based only on a matched filter is employed.

The existence of a critical capacity level, beyond which the use of MAI cancellation leads to a reduction in performance compared to straightforward matched filtering is a consequence of the remark above, that incorrect intermediate decisions will cause the reconstructed signal for that user to have four times its original power, and hence degrade the performance in a similar manner to additional background noise.

The variation in predicted and simulated performance is due to two main reasons; firstly, the noise on the signal at the input to each correlator is not independent, as is assumed in the analysis, and secondly, the Gaussian approximation is not completely valid since for low numbers of interferers, the combined noise will not closely approximate that distribution. A technique to provide a closer approximation is discussed in [6].

It must be acknowledged that interference cancellation, unlike FEC coding, does not improve the perfomance beyond that of the matched filter with a single user, however the use of additional stages in the canceller iteratively reduces the MAI so that for low numbers of users, the performance is simlar to the single user case, until the critical level is reached, at which point the performance abruptly collapses [43]. Unfortunately, an error in this paper over-estimates

this critical loading point, which simulations over a range of spreading sequence length have demonstrated is close to 70 % of g_P.

To ease the computational overhead in the simulations, only single stage cancellers will be considered here. Future developments of this receiver architecture could consider the trade-offs between the increased performance afforded by further stages of cancellation and the subsequent additional processing delay which this requires.

Thus, interference cancellation increases the capacity of spread spectrum multiple access systems which do not employ FEC coding, so the focus of the remainder of this Chapter is to investigate whether a similar performance increase is possible with FEC-encoded DS-CDMA signals. The transmitter structure considered is as specified in system 2 of Chapter 4, *i.e.* the data is first convolutionally encoded and then the resulting encoded digits are spread by the user's signature sequence. The convolutional coding element has a constraint length K and code rate R, so that, as before, the overall (linear) processing gain (g_P) is given by M/R, where M is the length of the spreading sequence.

5.1.3 Extension to FEC-encoded DS-CDMA

The extension of the concept of MAI estimation and cancellation to the FEC-encoded DS-CDMA environment requires increased sophistication in the receiver, since the initial estimation stage must now consist of the conventional correlator receiver to collapse the spectrum of the interfering users' signals, together with some method for estimating the FEC-encoded data, as shown in Figure 5.3.

The interference from the other users must then be re-generated before being subtracted from a delayed version of the original received signal. Finally, an additional correlation of this derived signal against the desired user's signature sequence must be made before the FEC decoder is used for the second time to obtain the final estimate of the original data sequence. The overall delay incurred is thus twice that of a conventional FEC decoding system, while the increase in storage requirements is O($(U-1)M$), since intermediate signals from $U-1$ interferers must be calculated and stored.

In addition, to properly reconstruct the encoded data, prior to spreading, the cancellation-based receiver requires the additional knowledge of the FEC encoder structure for each of

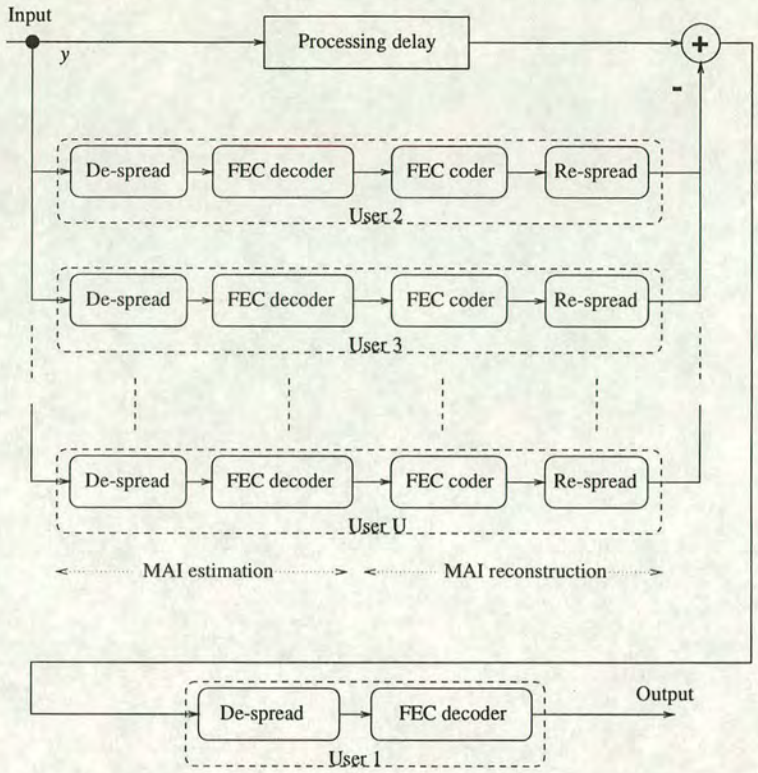

Figure 5.3: Extension of MAI cancellation technique to an FEC-encoded DS-CDMA system

the interfering users, as well as each of their spreading sequences. This again may have an impact if security is important. In practice, a different encoder could be assigned to each user, in which case the receiver would then require extra storage of the appropriate tap connections for each user, but here the same encoder is used, partially to reduce the complexity, but also to demonstrate the effectiveness of this approach, even under what may be sub-optimal constraints [2]. This simplification also means that the receiver for a specific user could also be adapted easily for other users. The various methods by which the intermediate signal is constructed will now be described.

5.2 Structures considered

The relative benefits of four receiver structures incorporating MAI cancellation with FEC coding will be considered, compared to a standard matched filter (MF), or matched filter canceller (MFC) receiver, with equivalent overall processing gains.

[2]The number of available efficient tap connections for a given constraint length could pose a limiting factor on this approach, so that, for example, groups of users would have to share the same convolutional encoding structure, as is implemented here.

The four receivers considered share a common structure; the incoming signal is split into as many parallel paths as required and each replica is correlated with an appropriate de-spreading sequence. An estimate is then made of the original data bit and the deduced interference is reconstructed and cancelled from a delayed copy of the received signal. A final correlation is then performed with respect to the desired user, and the final data extraction is performed by a Viterbi algorithm to give an estimate of the original data sequence. The distinguishing features of the receivers to be considered are the tap weights of the initial and final despreading filter, and the method used to estimate the intermediate data.

Receiver A, shown in Figure 5.4 and designated MFC+V, uses a matched filter to despread the received signal, followed by a sign decision block to estimate the individual digits of the convolutional code sequence.

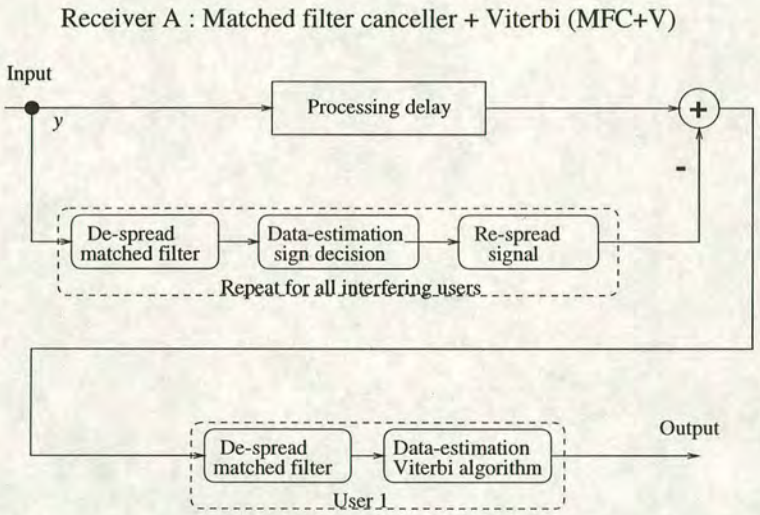

Figure 5.4: *Receiver A: MAI cancellation using matched filter and sign decision before final data extraction using the Viterbi algorithm (MFC+V)*

Use of the simple hard limiter is acknowledged to be a non-optimal strategy, since no account is taken of the fact that the individual digits constitute the encoded sequence and hence are no longer independent. However, this simpler strategy reflects the application of conventional MAI cancellation techniques to the DS-CDMA environment, and so is useful for comparison purposes. In addition, using a sign decision block to estimate the digits of the code sequence overcomes the requirement for this receiver to possess the FEC-encoding parameters of the other users, so that although complete code sequences may be inferred, the underlying data bits which produced the corresponding state transitions are not deduced by this receiver, which may be an attractive option from a security viewpoint.

Receiver B, shown in Figure 5.5, again only uses a sign decision to estimate the encoded

sequences, but in this receiver, the initial and final de-correlation is performed by a Wiener filter.

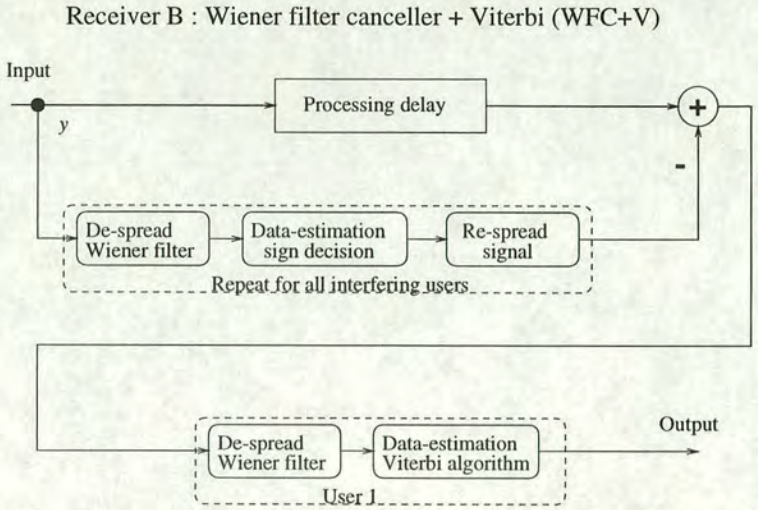

Figure 5.5: *Receiver B: MAI cancellation using Wiener filter and sign decision before final data extraction using the Viterbi algorithm (WFC+V)*

This MMSE filter could either be approximated using some adaptive algorithm, as in Chapter 3, or even calculated directly, since the receiver must have all the interfering users' spreading sequences available to reconstruct the interference, and the only additional quantities required to calculate the coefficients of this filter are estimates of the multipath channel and the background noise level. These estimates could be obtained for instance by employing a pilot signal on the data stream.

The new receiver architecture, illustrated in Figure 5.6, is given by including a Viterbi decoder for each user to make the initial data estimate, rather than the conventional sign decision estimator, used in the previous two receivers.

The motivation for using this structure is that the initial MAI estimation is now performed in terms of the most likely sequence, rather than simply the component digits, as in the previous receivers. Thus, in this approach, complete encoded sequences are estimated, before their digits are re-spread and the resulting contribution cancelled from the original signal. The obvious disadvantage in this approach is the increase in complexity since the Viterbi algorithm must be applied for each interfering user, thus requiring $O((U-1)M2^{K-1})$ storage and $O((U-1)LM2^{K-1})$ calculations. Thus, to limit this increase to manageable levels, only short constraint-length (K=3) FEC portions will be considered.

Finally, the fourth receiver structure considered here is as shown in Figure 5.7, which differs

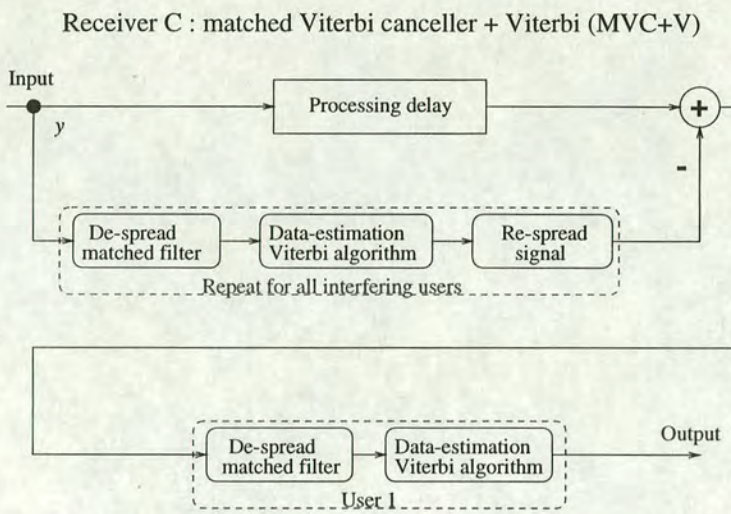

Figure 5.6: *Receiver C: MAI cancellation using matched filter and Viterbi algorithm before final data extraction using the Viterbi algorithm (MVC+V)*

from receiver C only in the despreading vector used at each stage, which is now a Wiener filter.

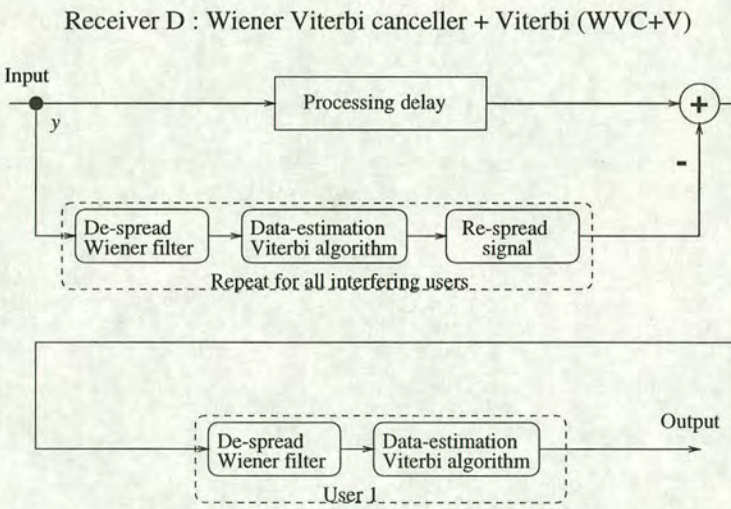

Figure 5.7: *Receiver D: MAI cancellation using Wiener filter and Viterbi algorithm before final data extraction using the Viterbi algorithm (WVC+V)*

As before, the construction of the Wiener filter is not an insurmountable task for the receiver, since most of the knowledge required is already available to perform the cancellation.

Although these new structures introduce an extra processing delay since a number of extra passes of the data with the Viterbi algorithm are required, the extra delay is linear in the memory of the Viterbi decoder and so is not considered exhorbitant in view of the performance increases which may be anticipated. Before proceeding to the results from some Monte Carlo simulations, however, it is instructive to consider an analysis of the expected perfomance of these receivers.

5.3 Theoretical analysis

Because this analysis is based on the Gaussian assumption, extended using the central limit theorem, the predictions may not be quantitatively accurate, since the errors may not be independent and, for low loading, the multiple access interference is evidently non-Gaussian. In addition, the theoretical analysis of the performance of convolutional decoding algorithms becomes increasingly unreliable as the interference increases. However, the qualitative behaviour should be representative of the relative merits of the receivers, and so is of more interest here.

The theoretical analysis [99] of Viterbi decoding of convolutional codes for a single user communication system, as outlined in section 2.3.3.4 leads to the following approximation for $P_e^V(E_b/N_0)$, the probability of error for the Viterbi decoder as a function of the signal to Gaussian noise ratio,

$$P_e^V(\frac{E_b}{N_0}) \leq \sum_{d=d_{free}}^{\infty} a_d \phi(d; R, \frac{E_b}{N_0}) \simeq \sum_{d=d_{free}}^{d=d_{upper}} a_d \phi(d; R, \frac{E_b}{N_0}) \tag{5.2}$$

where

$$\phi(d) = Q\left(\sqrt{dR\frac{E_b}{N_0}}\right) \tag{5.3}$$

and the set of coefficients $\{a_d\}$ for particular convolutional code configurations may be determined (*e.g.* [99]) by considering the expected departure of the Viterbi decoder from a known path through the trellis.

Invoking the Gaussian assumption means that the multiple access interference may be regarded simply as additional noise, so that equations 5.1 and 5.2 may be combined to give the expected probability of error for receiver structure A, $P_e^{MFC+V}(U, g_P)$, as

$$P_e^{MFC+V}(U, g_P) \leq P_e^V\left(\sqrt{\frac{g_P}{\sigma^2 + 4(U-1)P_e^{MF}(U, g_P)}}\right) \tag{5.4}$$

Receiver B has a similar structure to A, except that the initial and final de-spreading is achieved by correlation with a Wiener filter, which, as demonstrated in Chapter 3, upper bounds the performance of a least mean square adaptive algorithm, given sufficient training. By analogy with the analysis for receiver A, the expected probability of error P_e^{WFC+V} for this receiver may be estimated as

$$P_e^{WFC+V}(U, g_P) \leq P_e^V \left(\sqrt{\frac{g_P}{\sigma^2 + 4(U-1)P_e^{WF}(U, g_P)}} \right) \tag{5.5}$$

where $P_e^{WF}(U, N)$ is as defined in [37].

The initial data estimate formed by the proposed new receiver C is obtained from the application of a Viterbi decoder, so that by a similar argument to the above, the expected performance for this arrangement is given by

$$P_e^{MVC+V}(U, g_P) \leq P_e^V \left(\sqrt{\frac{g_P}{\sigma^2 + 4(U-1)P_e^{V}(U, g_P)}} \right) \tag{5.6}$$

Finally, receiver D also has a Viterbi decoder as the initial estimator, but uses a Wiener filter for the de-spreading processes, so will again form an upper bound on the performance of an adaptive algorithm which uses equation 2.13 as its penalty function.

The predicted performance of these receivers may be compared by reference to Figure 5.8, which shows the above expressions evaluated as a function of capacity (*i.e.* percentage of the overall processing gain) for $g_P = 126$ and a signal to Gaussian noise level of $E_b/N_0 = 5$ dB.

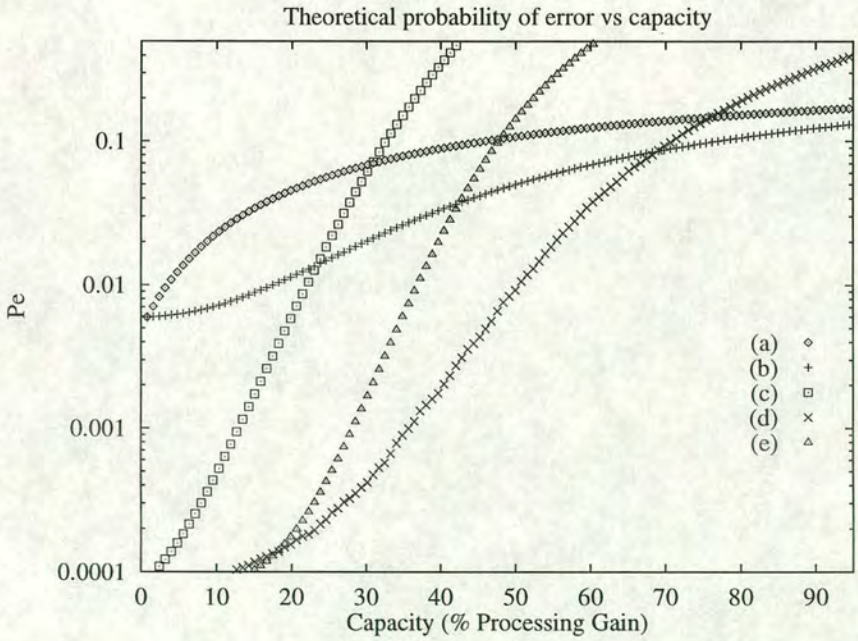

Figure 5.8: *Theoretical probability of error vs capacity for the various schemes for $g_P = 126$ and $E_b/N_0 = 5$ dB : (a) matched filter; (b) matched filter canceller; (c) matched filter canceller with Viterbi; (d) Wiener filter canceller with Viterbi; (e) matched Viterbi canceller with Viterbi*

Predictions of probabilities of error in excess of 0.5 are due to the divergence of the truncated sums in the predicted probability of error for the Viterbi algorithm.

It may be seen that the inclusion of the Viterbi decoder prior to cancellation leads to a predicted increase in capacity of approximately 15 %, or 19 users, as compared to the sign-decision approach at a probability of error of around 1.0×10^{-3}. This increase in performance is most likely due to the fact that decisions leading to the wrong code sequence, or even an impossible code sequence (since the corresponding transition in the state diagram is impossible), are avoided when the interference is manageable.

If the interference becomes too great however, the Viterbi algorithm used in the initial estimation stage is more likely to follow the wrong path in the decoding trellis, and thus the attempt at correction actually degrades performance. Re-encoding and spreading of this incorrectly deduced data bit leads to an increase in the overall interference at the subsequent cancellation stage. This has two effects on the final decoding stage. The first is analogous to the power increase of a factor of four in the interference for the equivalent system without FEC coding, since some, or all of the digits in the inferred encoded sequence will be incorrect, while the second is the attendant reduction in performance of the Viterbi algorithm as discussed in the previous Chapter, where the performance degrades rapidly under significant noise conditions, because the algorithm selects the wrong path through the trellis.

5.4 Simulations

The simulations considered are also all conducted for systems with an overall processing gain (g_P) of 126, so that comparison may be made with the predicted performance, shown in Figure 5.8. This bandwidth expansion is also similar to that employed in the IS-95 system [15].

The Viterbi algorithm employed by all the FEC-encoded systems uses soft decision decoding and a survivor path length (memory) of 32 data bits. Rate $\frac{1}{2}$, constraint length 3 convolutional coding is used on the data stream with all the users having the same tap connections. As discussed in the previous chapter, the use of more powerful coding may be expected to give suitably enhanced results, provided that a balance is maintained between FEC coding power and the corresponding amount of spreading invested.

For the systems employing FEC-coding, randomly selected signature sequences of length 63

chips are used to further spread the convolutional code sequence. Rnadom sequences are used because any multipath channel will likely reduce any special correlation properties of other spreading sequence sets. Typically 10^5 data bits are transmitted before the performance statistic P_e is formed, so that probabilities of error in excess of 1.0×10^{-3} may be considered statistically significant [41]. The uncoded systems employ random spreading sequences of length 126, so that a fair comparison may be made, based on equivalent overall bandwidth expansion.

5.4.1 Performance for fixed E_b/N_0

As previously, the simulations are performed with respect to capacity for a fixed background noise, and with respect to E_b/N_0 for a fixed capacity. In this section, the levels of E_b/N_0 are set to 5 dB and 7 dB.

5.4.1.1 Performance for $E_b/N_0 = 5$ dB

The results obtained for the various architectures for $E_b/N_0 = 5$ dB are shown in Figure 5.9. Comparison with the theoretical predictions in Figure 5.8 shows the general trend that the absolute error probabilities are higher, but that the relative performance between the receivers is broadly similar to prediction.

As predicted, for low numbers of users, the convolutional coding systems have much better performance than those without, with receiver A supporting 25 users at the same probability of error (10^{-2}) as the single user scenario with the conventional canceller. Use of the Wiener filter (receiver B) as the internal and external de-spreading filter increases this figure to around 38 users.

The Viterbi cancellers (C and D) show very good performance, with the matched filter Viterbi canceller (C) surpassing the performance of the standard matched filter canceller (B) for up to around 25 % capacity with an expected P_e of around 10^{-2}. At this level, the Wiener Viterbi canceller (D) is able to support 60 users, demonstrating that the combination of this structure with an adaptive algorithm could give promising results.

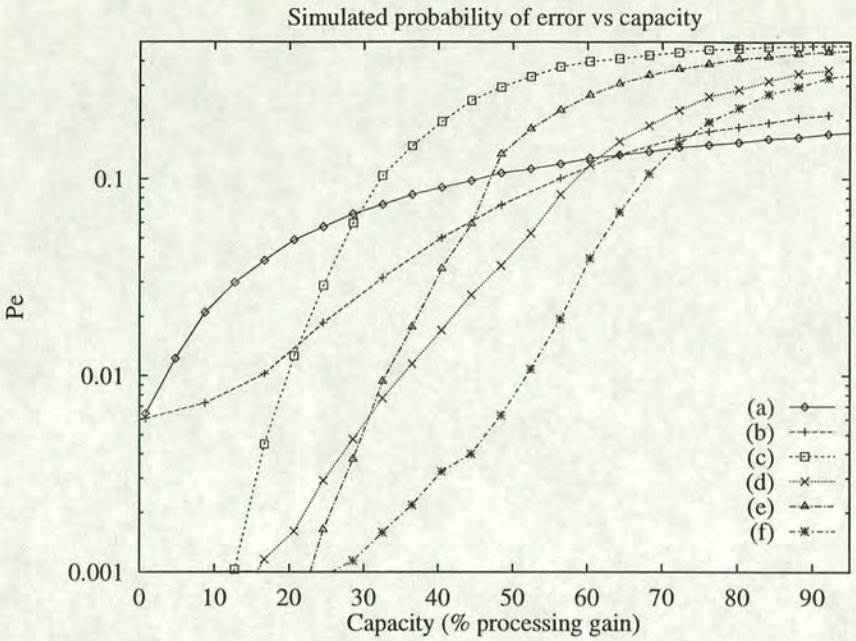

Figure 5.9: *Simulated probability of error vs percentage capacity for the various schemes for* $g_P = 126$ *and* $E_b/N_0 = 5$ *dB : (a) matched filter; (b) matched filter canceller; (c) matched filter canceller with Viterbi; (d) Wiener filter canceller with Viterbi; (e) matched Viterbi canceller with Viterbi; (f) Wiener Viterbi canceller with Viterbi*

5.4.1.2 Performance for $E_b/N_0 = 7$ dB

The situation for $E_b/N_0 = 7$ dB, shown in Figure 5.10 is similar to the above, with again very good performance achieved by using the Wiener filter together with the Viterbi canceller.

Receiver D again offers the best capacity, supporting 60 users at a probability of error around 10^{-3}, which is the same as that for the single user with conventional cancelling structures without forward error correction. The performance of receiver A is also worthy of note, since for under around 30 users, its performance surpasses that of the equivalent processing gain single stage matched filter canceller. The reason the performance of the Wiener Viterbi canceller (receiver D) appears to saturate for low capacity is likely due to insufficient simulation time.

It must also be acknowledged that the new structures do suffer from poorer performance as the loading is increased beyond a certain level, but this is in the area where very little can be done to alleviate the effects of large multiple access interference, so that no communication is possible anyway.

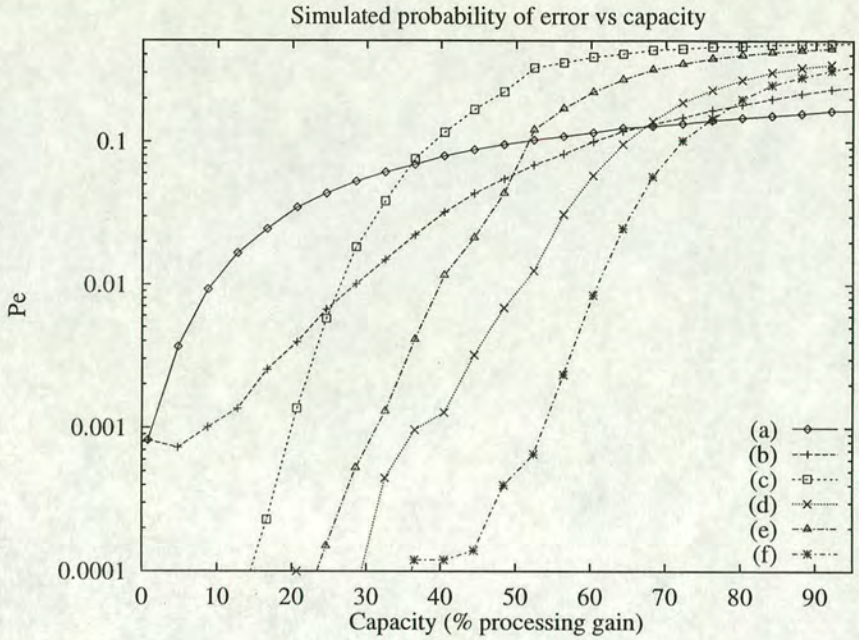

Figure 5.10: *Simulated probability of error vs percentage capacity for the various schemes for $g_P = 126$ and $E_b/N_0 = 7\,dB$: (a) matched filter; (b) matched filter canceller; (c) matched filter canceller with Viterbi; (d) Wiener filter canceller with Viterbi; (e) matched Viterbi canceller with Viterbi; (f) Wiener Viterbi canceller with Viterbi*

5.4.2 Performance for fixed capacity

To gauge the performance of the various receivers as the background noise is varied, the loading is held fixed for the next two simulations.

5.4.2.1 Performance for 25 % capacity

The performance of the systems considered with 31 active users ($\simeq$ 25% capacity) is presented in Figure 5.11.

For this loading, receiver C is approaching the performance of receiver D, indicating that for reasonably low numbers of users, a matched filter could be employed successfully, without recourse to using an adaptive algorithm to approximate the Wiener filter.

5.4.2.2 Performance for 40 % capacity

The results for 50 users or 40 % are shown in Figure 5.12.

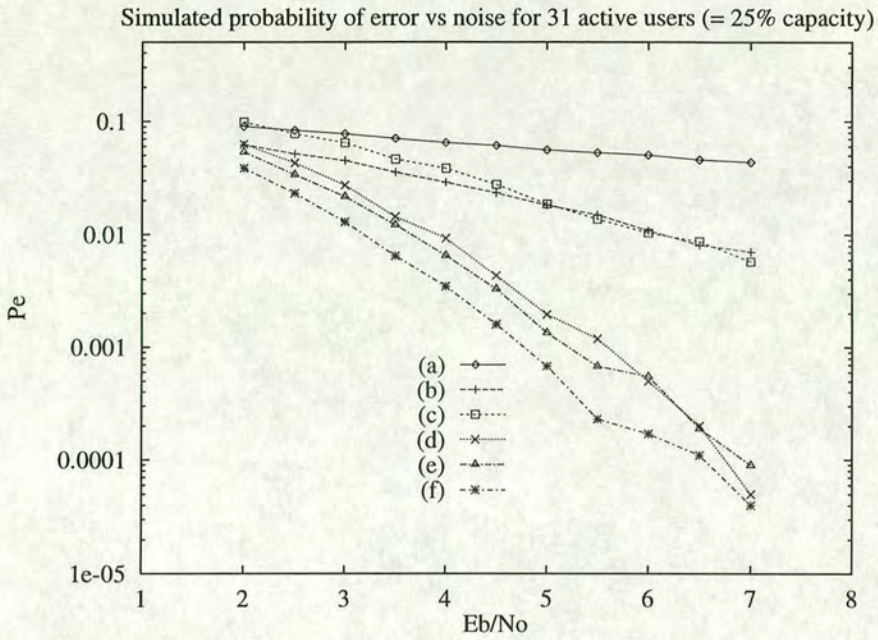

Figure 5.11: *Simulated probability of error vs E_b/N_0 for 25 % capacity for the various schemes with $g_P = 126$: (a) matched filter; (b) matched filter canceller; (c) matched filter canceller with Viterbi; (d) Wiener filter canceller with Viterbi; (e) matched Viterbi canceller with Viterbi; (f) Wiener Viterbi canceller with Viterbi*

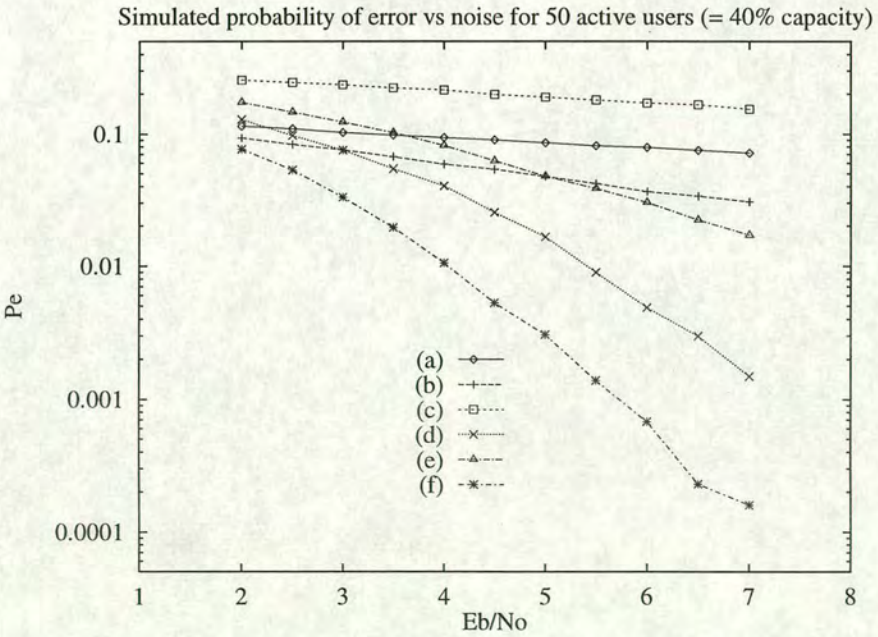

Figure 5.12: *Simulated probability of error vs E_b/N_0 for 40 % capacity for the various schemes with $g_P = 126$: (a) matched filter; (b) matched filter canceller; (c) matched filter canceller with Viterbi; (d) Wiener filter canceller with Viterbi; (e) matched Viterbi canceller with Viterbi; (f) Wiener Viterbi canceller with Viterbi*

For the higher levels of MAI experienced by the system at this loading, it may be seen that the systems employing Wiener filters have better performance, as may be expected, but that the inclusion of the proposed new structure still leads to increased performance. Indeed, even at this loading, receiver D is still able to achieve an estimated P_e of around 1.0×10^{-3} at $E_b/N_0 = 6$ dB, an improvement of 1 dB over even the conventional single user system. It is also clear that the level of MAI present at this loading means that many of the intermediate decisions made by receiver A are incorrect, leading to poorer performance than a simple matched filter, irrespective of E_b/N_0. Although for low E_b/N_0, receiver C also makes many incorrect decisions, leading to similarly poor performance, as the background noise is reduced, the symbol based cancellation scheme is able to improve the performance of this receiver, so that the performance becomes better than an equivalent processing gain matched filter canceller.

5.5 Improvements

The results presented here clearly only provide an indication of the benefits available by an approach combining interference cancellation and FEC coding on a DS-CDMA system. A number of modifications could be considered to improve the performance of these receivers further.

The most immediate improvement would be to investigate additional stages of cancellation, although any gains achieved would necessarily have to be weighed against the increase in complexity and delay associated with this approach. These impositions may mean that such a computationally-intensive technique could only be practically implemented at the base station, which means that each user's delay must be estimated, since the intermediate signals must be aligned properly to avoid producing more interference.

The use of soft-output devices at the intermediate stage prior to cancellation [100] may be expected to improve the overall performance since this approach weighs less heavily those decisions which have been judged less reliable, thus reducing error-propagation. This could also be combined with some thresholding technique, in which cancellation of a particular user's derived signal is only performed if a sufficient level of confidence can be associated with the intermediate decision.

The calculation of the Wiener filter in receivers B and D requires an accurate estimate of the

background noise, which may not readily be available. A possible alternative to this could be the zero-forcing filter of section 2.3.2.1, the calculation of which only requires the various spreading sequences, or the non-optimal minimum mean square error (NO-MMSE) filter [101], which replaces the estimate of σ in the calculation of the Wiener filter in Equation 2.14 by an upper bound on this parameter.

Additionally, the use of sub-optimal convolutional decoding techniques, such as the Fano or stack algorithm may reduce the computational overhead or processing delay involved, although the sub-optimal performance of these algorithms may lead to more intermediate estimation errors, and thus reduced overall performance.

5.6 Discussion

In this Chapter, a new receiver structure for convolutionally-encoded DS-CDMA communications systems has been proposed. The new structure, employing parallel MAI cancellation, obtains its intermediate data estimate using a Viterbi decoder, rather than the straightforward sign decision used by conventional interference cancellation receivers. The disadvantage of this approach is the increase in receiver complexity, which may be judged by combining the complexity requirements of the interference canceller portion, an O(UM) process, with those of the intermediate data estimation stage and those for the final Viterbi algorithm, discussed in the previous chapter. For the sign-decision estimators, the additional complexity is simply determined by the receiver filter (either a matched filter or Wiener filter). For those receivers whose intermediate estimation is given by the Viterbi algorithm, a pass must be made through the data for each user present. Since each pass requires $L2^{(K-1)}$ storage locations, a choice must be made whether to attempt a truly parallel approach, or to recycle storage and decode each user in a serial fashion. For reasonably short constraint lengths, such as those considered here, this increase in complexity is likely to be tolerable.

The error performance of this receiver has been derived analytically and simulated using both matched filters and Wiener filters to provide the initial and final direct sequence despreading. These structures have also been compared to conventional cancellation techniques, and equivalent processing-gain systems using matched filters and matched filter cancellers.

Significant performance improvements have been achieved, with the new system, when employing

a Wiener filter to collapse the encoded signal spectrum, able to support 60 users ($\simeq$ 50% of the processing gain) at the same probability of error as the single user conventional case for a range of background noise values. In moderate capacity regimes, the use of a matched filter in the proposed system approaches the performance of a Wiener filter combined with conventional cancellation.

In conclusion, this technique, which is practically feasible in hardware, is a promising one for the reduction of multiple access interference in a convolutionally-coded DS-CDMA system.

Chapter 6

Radial basis function network receiver structures for DS-CDMA

In this chapter, non-linear signal processing techniques, using radial basis function (RBF) networks, will be considered as receiver structures for the DS-CDMA communications environment. The motivation for using RBF networks in a spread spectrum communication system will first be outlined in section 6.1. The details of the construction of the received signal and the receiver network for two systems, which are distinguished by their respective input, will then be described in section 6.2. The input to the first system is obtained by correlating the received signal using either a filter matched to the original spreading sequence, or one obtained by convolving the spreading sequence with an estimate of the impulse response of the channel, while the second system is based on the incoming chip-level signal. The results from this investigation are then presented in section 6.3. As will be demonstrated, the main disadvantage of an RBF-based approach is the high computational overhead involved, due to the large number of centres which are required as the number of inputs to the network increases. To counter this, section 6.4 will examine schemes for reducing the complexity of the RBF-based receiver, without unduly reducing this technique's performance. A new non-linear receiver, with comparable performance to one using an RBF network, will be proposed, and a graphical interpretation of this, based on the Voronoi diagram [102], will be used to provide a scheme for reducing the number of centres in the network. Finally, the main results of the chapter will be summarised in section 6.5.

6.1 Motivation

As discussed previously, there are three main sources of interference in a DS-CDMA system; multiple access interference which occurs from cross-correlations if non-orthogonal sequences are used to spread the data, corruption of the transmitted signal by the communication channel, and background noise.

The traditional method of collapsing the spectrum is for the mobile to use a RAKE receiver, with a bank of correlators, whose weights are either matched to the original spreading codes, or obtained via convolution with the impulse response of the channel. The soft decisions thus obtained may optionally be further processed (e.g. by a minimum mean square error filter) before being thresholded to provide the final estimate of the data. However, the presence of a multipath channel can cause the space spanned by these intermediate soft decisions to no longer be linearly separable, so that estimation of the original signal by linear techniques may be prone to a significant number of errors, regardless of the signal to noise ratio.

This situation is analogous to the exclusive OR problem[1], which was solved adaptively by employing the use of a non-linear radial basis function (RBF) network in [103], or the problem of equalisation of an unknown channel, for which RBF functions have also been shown to provide good performance [84]. A review of the theoretical basis of functional approximation via RBF networks is given in [104]. Although this approach has been applied to many problems for which linear techniques are unsuitable [86], only a relatively small number of authors (*e.g.* [105], [106]) have considered RBF network based receiver structures for DS-CDMA, since the excellent performance obtained is only achieved at the expense of increased computational complexity, which will be discussed in section 6.2.2.

As indicated in section 2.3.6, for a given input vector $\underline{y}$ and a set $\mathcal{P}$ of N_c reference points, or centres, the (soft) output of the RBF network is given by

$$f_{RBF}(\underline{y}) = \sum_{i=1}^{N_c} w_i \psi \left[d(\underline{y}, \underline{p}_i) \right] \tag{6.1}$$

where w_i is the weight associated with each centre $\underline{p}_i \in \mathcal{P}$. A sign decision is then made on this output to provide an estimate of the data. The distance of the input point to each centre is calculated using the metric $d(\cdot, \cdot)$, which is normally taken to be the Euclidean l_2 metric

[1] This essentially consists of separating some decision space using a non-linear boundary

and $\psi(\cdot)$ represents a non-linear basis function, or kernel. There are various choices for kernel functions, which will be investigated further in section 6.4.3, but for the initial investigations, the Gaussian kernel, defined by

$$\psi(\zeta) = \psi_G(\zeta) = \exp\left(-\frac{\zeta^2}{2\sigma^2}\right) \tag{6.2}$$

where σ^2 controls the width of each kernel and is the noise power, will be used. The centres are located by calculating the noise-free response of the system to all possible combinations of inputs, so that this approach, as applied to a DS-CDMA system, requires knowledge of all the active users' spreading sequences as well as information about the channel to locate the centres and an estimate of the signal to noise ratio to specify the kernel widths.

6.2 The RBF network receiver in a DS-CDMA system

The application of an RBF network receiver to the downlink of a DS-CDMA communications system is now discussed. The model used for the received signal is first discussed in section 6.2.1, while the details of the formation of the various networks considered are described in section 6.2.2.

6.2.1 The received signal

To simplify the calculations, forward error correction will not be included on the data signal, so that construction of the received vector $\underline{y}$ may be modelled by the process shown in Figure 6.1.

The BPSK data bits $\{x_u, 1 \leq u \leq U\}$ are used to modulate the user-specific spreading sequences $\{\underline{c}_u, 1 \leq u \leq U\}$. These are of length M chips, and the resultant signals are then synchronously combined to form the transmitted signal vector $\underline{s}$, given by

$$\underline{s} = \sum_{u=1}^{u=U} \underline{c}_u x_u \tag{6.3}$$

This signal then passes through a multipath channel, which is again modelled at baseband by a linear transversal filter with impulse response $H(z) = \sum_{j=0}^{j=n_h} h_j z^{-j}$, where z^{-1} represents a

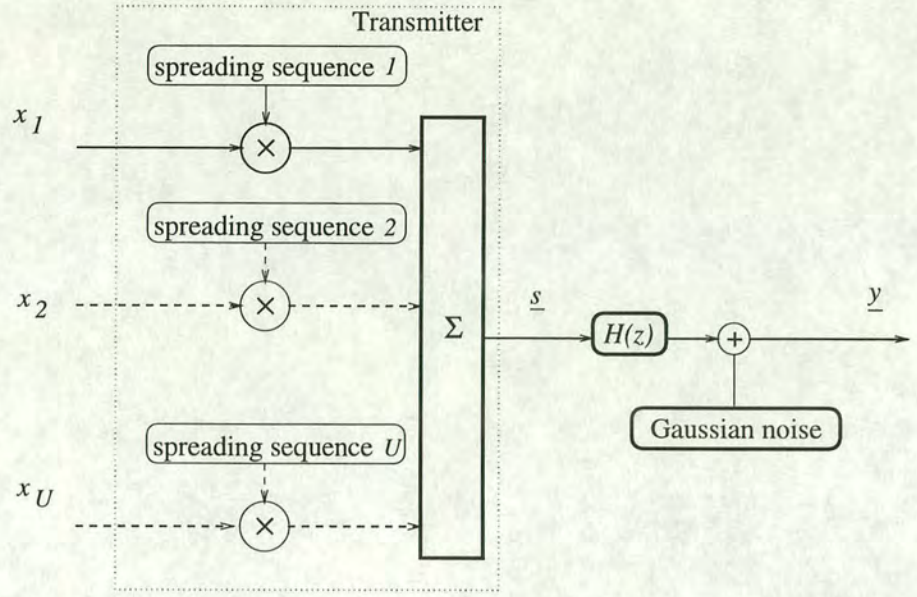

Figure 6.1: Construction of the received signal

delay of one chip and n_h is the number of chips spanned by the impulse response of the channel. The channel is assumed stationary in the investigations, although an adaptive technique [107] has also been shown to provide excellent performance, and could be employed when the channel is time-varying. The subsequent vector components are then added to iid samples of additive white Gaussian noise (AWGN) of zero mean and variance σ^2, where the signal to Gaussian noise ratio, E_b/N_0, is again given by

$$\frac{E_b}{N_0} = \frac{M}{2\sigma^2} \tag{6.4}$$

to give the signal, $\underline{y}$, received by the mobile.

6.2.2 Construction of the network

As with many neural network type approaches, the performance of the RBF network receiver is heavily dependent on the pre-processing applied to the data, before it is input to the network. The investigations reported here will consider the use of two distinct receiver structures. The input to the first of these structures consists of the result of pre-filtering the received signal, either by a matched filter, designated the post matched filter (PMF) approach and shown in Figure 6.2 or by the matched filter convolved with the impulse response of the channel, designated the post channel-matched filter (PCF), and shown in Figure 6.3.

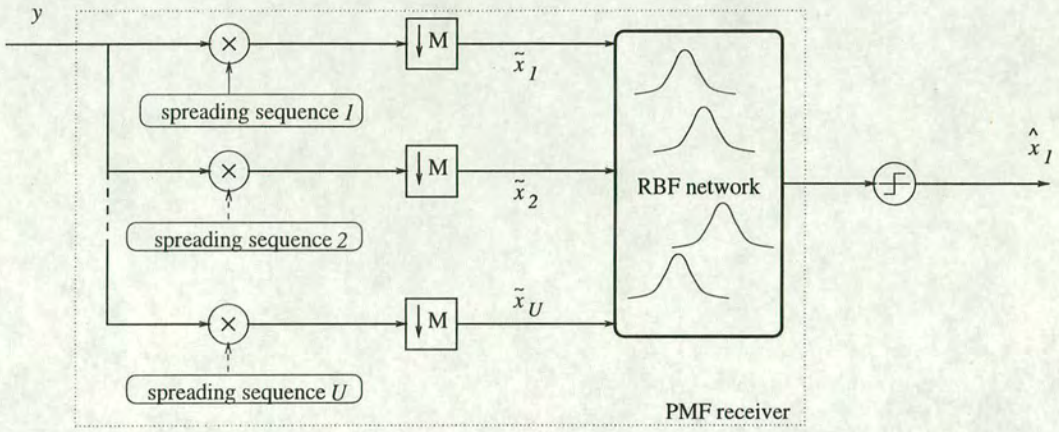

Figure 6.2: The RBF network implemented as a post matched filter (PMF) processor block

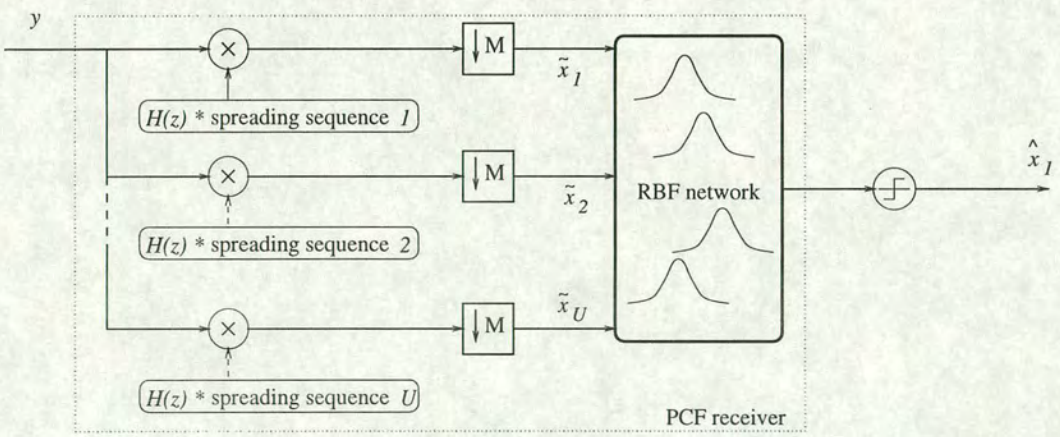

Figure 6.3: *The RBF network implemented as a post channel-matched filter (PCF) processor block*

The downsampling is performed with respect to the processing gain, which in this case is simply M, the length of the spreading sequence. Thus, this approach is effectively a multi-user detector, which may be tuned to the user of interest by the network.

The input to the second type of receiver structure is the received chip-level sequence, as used in [105] and [106], and so this method is designated the direct (DRBF) approach, outlined in Figure 6.4.

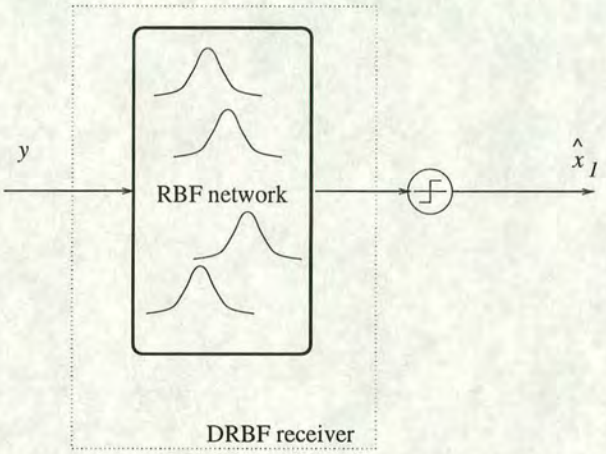

Figure 6.4: The direct RBF network (DRBF) receiver

The inputs to the first two structures are therefore at the bit rate, whilst those for the DRBF are at the chip rate.

The number of centres in the network N_c is a function of the number of users, while each centre's dimension D depends on the number of input digits to the network. The situation is summarised in Table 6.1, in which the total number of active users is U, and the spreading code length is M.

Channel	Method	Number of centres N_c	Dimension of each centre D
AWGN	PMF	2^U	U
AWGN	DRBF	2^U	M
multipath	PMF	2^{2U}	U
multipath	PCF	2^{3U}	U
multipath	DRBF	2^{3U}	(M) or $(M + n_h - 1)$

Table 6.1: Relative complexity of the various RBF network receiver implementations

In AWGN, both the PMF and DRBF require 2^U centres, but the dimension of the input signal, and hence of each centre, is the number of users, and length of the spreading sequence respectively. In a multipath channel (in which it is assumed that the multipath delay does not extend over

more than M chips), the PCF and DRBF use all possible combinations of previous, current and next data bit, and thus require 2^{3U} centres, while the PMF approach only considers the ICI arising from the previous and current data bits, so only requires 2^{2U} centres. As in the AWGN case, the dimension of the centres in each network is different, since the dimension of the input vector will be different, unless $U = M$.

With the above values for N_c and D, the number of calculations required for the Gaussian kernel RBF network is $(3D+2)N_c$ multiplications, $3N_c - 1$ additions, and N_c square root and exponential evaluations. Even assuming that each of these operations may be performed in one floating point operation (flop), the evaluation therefore requires $(3D + 7)N_c - 1$ flops, which grows exponentially with the number of active users.

It is important to acknowledge a significant change in the assumptions made at this point, since for the multipath channel implementations of the RBF network receivers, it is assumed that perfect channel knowledge is available to construct the RAKE and locate the RBF centres respectively. This is in contrast to the receivers described earlier, which in some cases had no such information available. Indeed, had this been available, there would be no need to train an adaptive algorithm. In addition, the DRBF may be extended by specifying a number of chips over which to extend the filter, to capture the complete energy originating from one data bit, as in [105]. In this case, the input vector to the RBF network is taken to have length $M + n_h - 1$, where n_h is, as before, the number of chips which span the impulse response of the multipath channel, as indicated in the table.

In the following, it will be useful to define $\mathcal{P}^+$ as the set $\{\underline{p}_i \in \mathcal{P} : \text{Original data bit from the desired user was a } +1\}$, and $\mathcal{P}^-$ as the set $\{\underline{p}_i \in \mathcal{P} : \text{Original data bit from the desired user was a } -1\}$. Clearly, to satisfy linear independence and uniqeness conditions, it is required that $\mathcal{P} = \mathcal{P}^+ \cup \mathcal{P}^-$ and $\mathcal{P}^+ \cap \mathcal{P}^- = \emptyset$.

6.3 Results

The performance of the structures described above will now be considered in both additive white Gaussian noise in sections 6.3.1 and 6.3.2, and in a stationary multipath channel with impulse response $H(z) = 0.3482 + 0.8704z^{-1} + 0.3482z^{-2}$, in sections 6.3.3 and 6.3.4. Random spreading sequences will again be used, and the performance criteria will be P_e, as previously

defined in section 2.2. The performance of the proposed receivers will be compared against that of the linear minimum mean square error (Wiener filter) receiver, as defined in Equation 2.14. To enable a fair comparison, the Wiener filter will be implemented with the same information as the RBF network, *i.e.* at the bit-level to compare with the PMF and PCF, and at the chip-level to compare with the DRBF.

6.3.1 Performance in AWGN for varying E_b/N_0

The results for 2, 4 and 7 users for the chip-level receiver structures are shown in Figure 6.5, and those for the bit-level receivers are shown in Figure 6.6.

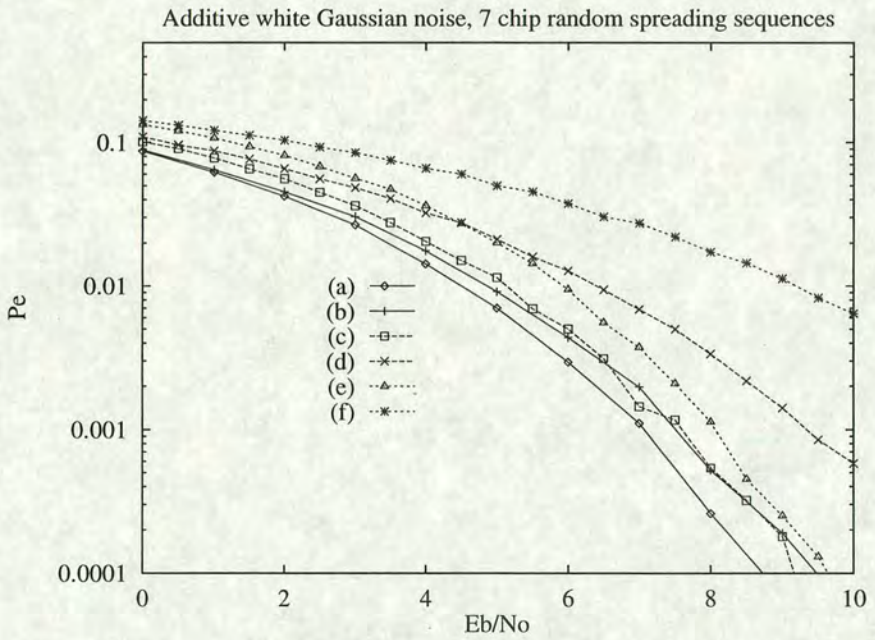

Figure 6.5: *Performance of chip-level receivers in AWGN, 7-chip random spreading sequences, varying E_b/N_0 : (a) 2 users, DRBF; (b) 2 users, Wiener; (c) 4 users, DRBF; (d) 4 users, Wiener; (e) 7 users, DRBF; (f) 7 users, Wiener*

For the chip-level receivers, the DRBF network outperforms the Wiener filter for the loadings considered for all background noise values. Indeed, the advantage of the DRBF over the Wiener increases as the number of users increases. For the bit-level receivers, the difference between the two approaches is less significant, although the PMF is still better than the Wiener filter, for 2 and 4 users. For 7 users, the PMF has much better performance as the background noise is reduced. This is probably because, in this regime, the interference is predominantly MAI, and so the non-linear PMF is better able to separate users. The behaviour of the receivers for low E_b/N_0 values, where it must be acknowledged that performance is poor for both strategies, is

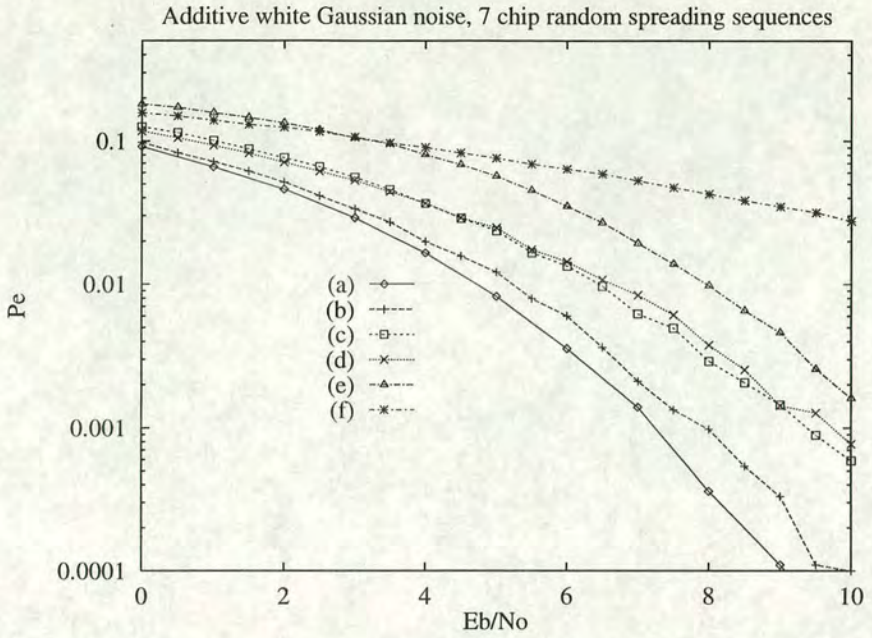

Figure 6.6: *Performance of bit-level receivers in AWGN, 7-chip random spreading sequences, varying E_b/N_0 : (a) 2 users, PMF; (b) 2 users, Wiener; (c) 4 users, PMF; (d) 4 users, Wiener; (e) 7 users, PMF; (f) 7 users, Wiener*

probably due to the fact that the noise on the output from the matched filter bank is correlated, since the spreading sequences are non-orthogonal. In this case, the Mahalanobis metric [108] should strictly be used in place of the Euclidean distance metric in Equation 6.1, however the Euclidean metric will be retained in the simulations discussed here, to reduce the computational effort.

6.3.2 Performance in AWGN for varying loading

Figures 6.7 and 6.8 show the performance as the loading is varied for fixed E_b/N_0 of the chip-level and bit-level receivers respectively.

Again, the RBF network receivers generally perform better than the linear Wiener filters constructed using the same information. For the chip-level structures, the DRBF has clearly better performance than the Wiener filter, with again the improvement increasing with increasing signal to Gaussian noise ratio, while the performance of the bit-level structures are closer, only diverging for larger numbers of users. This is again probably due to the PMF being better able to cope when the interference is predominantly MAI. Thus, when the interference is Gaussian noise-dominated, the performance of the two systems is similar, while if the interference

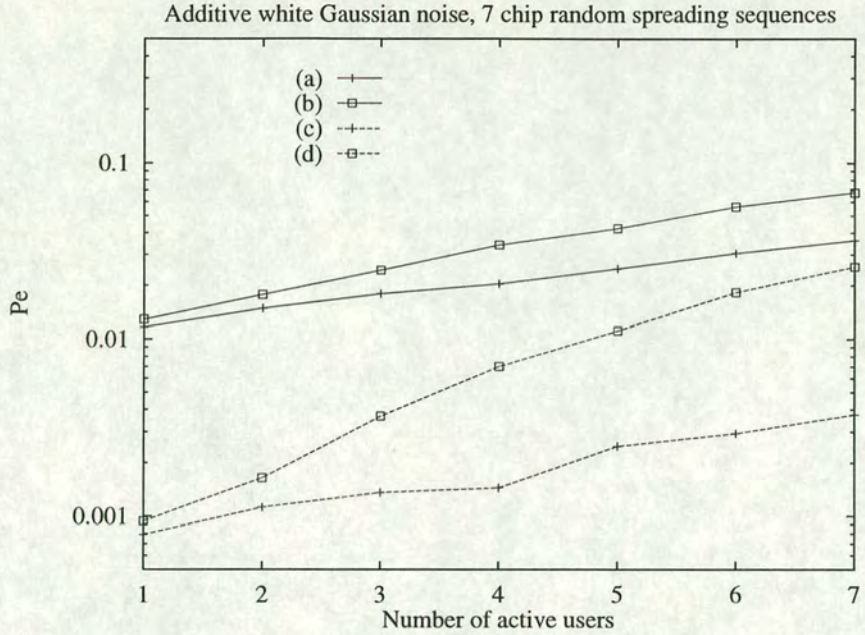

Figure 6.7: *Performance of chip level receivers in AWGN, 7-chip random spreading sequences, varying loading at two values of E_b/N_0: (a) DRBF, 4 dB; (b) Wiener, 4 dB; (c) DRBF, 7 dB; (d) Wiener, 7 dB*

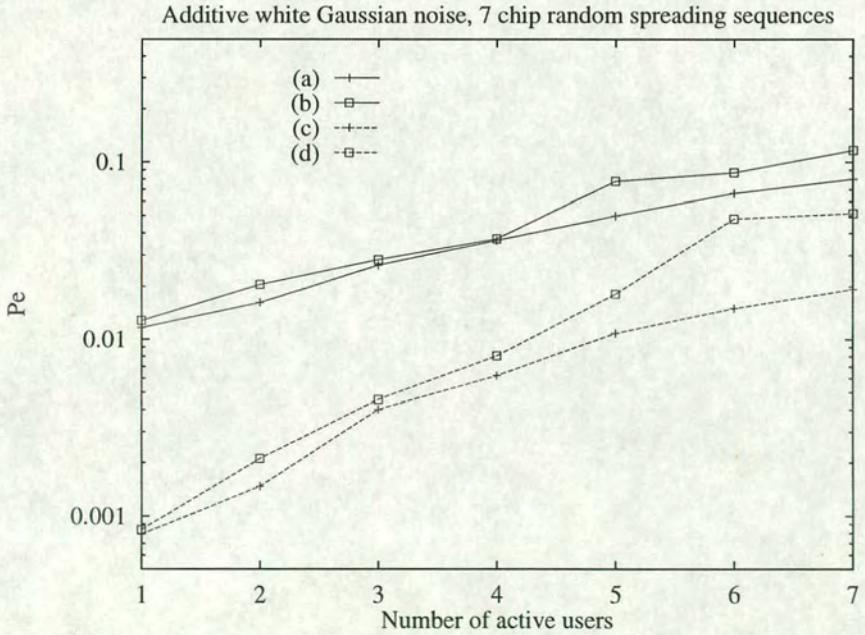

Figure 6.8: *Performance of bit level receivers in AWGN, 7-chip random spreading sequences, varying loading at two values of E_b/N_0: (a) PMF, 4 dB; (b) Wiener, 4 dB; (c) PMF, 7 dB; (d) Wiener, 7 dB*

becomes dominated by MAI, the RBF network structures have a performance advantage of around 1.5 dB.

6.3.3 Performance in multipath channel for varying E_b/N_0

For the stationary multipath case, the chip-level receivers will be extended in time to capture the total energy from one data bit[2], while the inputs to the processing blocks for the bit-level receivers will be calculated by match filtering the received signal with a sequence obtained by convolving the channel impulse response with the appropriate spreading code. To reduce the computation time, only the results for 2 active users, shown in Figure 6.9 will be considered.

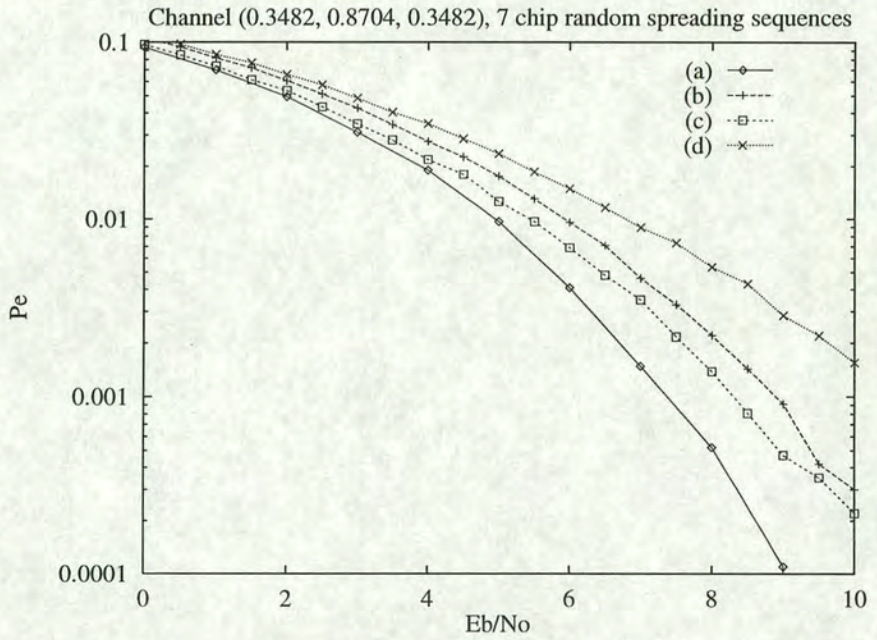

Figure 6.9: *Performance of chip-level receivers in multipath channel, 7-chip random spreading sequences, varying E_b/N_0: (a) extended DRBF; (b) extended chip-level Wiener; (c) PCF RBF network; (d) bit-level Wiener*

Again, the non-linear RBF network structures have better performance than their linear counterparts. The performance of the DRBF is again optimal, while the PCF RBF receiver is worthy of further investigation, since it has better performance than not only the Wiener filter implemented with the same information, but also than the chip-level Wiener filter receiver. The receivers based on the outputs of the matched filter bank are in general not as good as those implemented directly, however the possibility of incorporating a noise-whitening filter to counter the correlated nature of the inputs to these receivers may be worthy of future investigation.

[2] so that the dimension of the input vector is 9 chips in this case

6.3.4 Performance in multipath channel for varying loading

Figure 6.10 shows the performance of the various receiver structures as the loading is varied for $E_b/N_0 = 7$ dB. The simulations for the DRBF receiver are terminated at 5 users to avoid excessively large numbers of calculations[3].

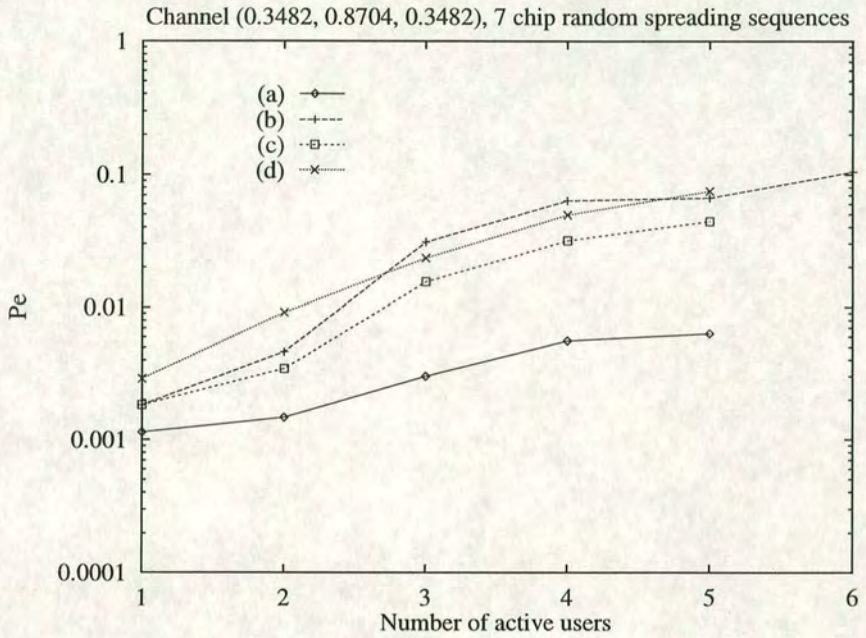

Figure 6.10: *Performance of RBF receivers in multipath channel for $E_b/N_0 = 7$ dB, 7-chip random spreading sequences, varying loading: (a) DRBF; (b) extended chip-level Wiener; (c) PCF RBF network; (d) bit-level Wiener*

From the figure, it may be seen that the reasonable performance of the PCF RBF receiver outlined above is maintained as the number of users increases, although the DRBF has clearly better performance. The disadvantage of the DRBF receiver, however, is that the number of centres which must be calculated and stored increases exponentially with the number of users, so that methods must be investigated to reduce the complexity of this approach.

6.4 Complexity reduction methods

In this section, a variety of methods for reducing the inherent complexity of RBF-based receivers will be proposed. This complexity arises from two distinct sources which will be treated separately in the analysis. The first contribution is from the number of centres involved in

[3] 6 users would require 2^{18} centres for each data bit

the calculation of the output from the network, while the second is the computational effort associated with each centre. Clearly a reduction in either of these components will reduce the overall computational requirement, and thus may provide motivation for the practical application of this technique.

The most natural method of reducing the number of centres is to assume that the hard estimates obtained are correct, and to use the receiver in a decision directed mode. This approach halves the number of centres which contribute to the evaluation of the decision statistic, and is described in section 6.4.1. In section 6.4.2, a specific spreading sequence set and channel are defined to allow a more detailed investigation of the role of the centres of the network. This scenario is then employed to consider complexity reduction through replacing the transcendental function in equation 6.1 by an algebraic one, which requires fewer calculations. The effect of this approach will be described in section 6.4.3, which considers two such kernels. Then in section 6.4.4, a new approach will be described, which proceeds by selecting the nearest neighbour centre to the input test statistic. An interpretation of this procedure, which leads to considering the appropriate decision boundary in terms of a subset of the Voronoi diagram [102] will then be proposed in section 6.4.4.1. This approach provides a mechanism for centre reduction, by identifying those centres which do not contribute to the decision, and may thus be discarded from the network without adversely affecting the performance. Possible methods to extend this technique to time-varying multipath channels will then be considered in section 6.4.4.2.

6.4.1 The decision directed approach

In this approach, the previous decision is assumed to be correct, and the information resulting from this is used to discard exactly half[4] of the total number of centres, since they correspond to the previous data bit being of opposite sign. This decision direction (DD) approach is popular in adaptive techniques such as those described in Chapter 3.

6.4.1.1 Results

The direct (DRBF) structure is used to investigate the performance of decision direction. The results for the 7 chip random spreading sequence set in the channel defined previously are

[4] since each centre is equally likely

shown in Figure 6.11.

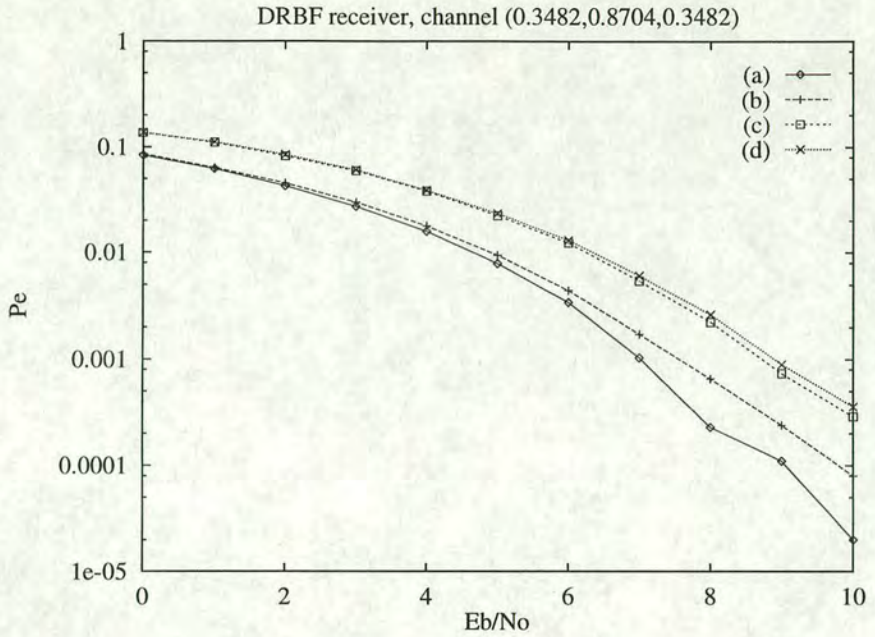

Figure 6.11: *Performance of the decision directed DRBF receiver in multipath channel, 7-chip random spreading sequences, varying E_b/N_0: (a) 1 user without DD; (b) 1 user with DD; (c) 4 users without DD; (d) 4 users with DD*

The implementation here uses the first of each block of 32 data bits as a known training bit, such as would be required in a time varying channel, to prevent error propagation. The results show that decision direction, with its lower computational demand, only slightly reduces the performance compared to the complete network receiver, and so may be worthy of future investigation. A possible future development would be to threshold the soft decisions so that decision direction is only applied if a certain level of confidence in the result is attained.

6.4.2 Example situation

Before proceeding to investigate methods of reducing the computation associated with each centre, it is useful to define a set of spreading sequences and a particular channel, which will have certain characteristics. Since RBF functions appear most useful when the interference is non-linear, and in order to make a graphical interpretation possible, this section will return to the post matched filter (PMF) implementation, with a spreading sequence set consisting of a two-user "broken" 4-chip code set, given by $c_1 = (+1, +1, -1, -0.7)^T$, $c_2 = (+1, -1, +1, -1)^T$, and the particular multipath channel defined by $H(z) = 0.25 + z^{-1}$. Note that the power of the noise has not been adjusted to compensate for the inefficient code employed by user 1, which

has been artificially created to make a simple nonlinearly separable problem. To enable a fair comparison, the Wiener filter will also operate at the output of the matched filter bank, and so will be at the bit-level.

The number of centres in the (PMF) RBF network is thus $2^{2(U)} = 2^4 = 16$, and the location of these centres from the point of view of user 1 is shown in Figure 6.12. From the diagram, it is apparent that the output space spanned by the centres from user 1 is non-linearly separable, *i.e.* it is not possible to draw a straight line which correctly partitions the output space to separate centres produced from opposite data bits. Although the locations are the same as for user 1, the centres from user 2's point of view are linearly separable, since the associated weights are different. This may be seen in the figure which also shows the decision boundaries[5] for both users for the bit-level Wiener filter and the Gaussian kernel RBF network for $E_b/N_0 = 15$ dB.

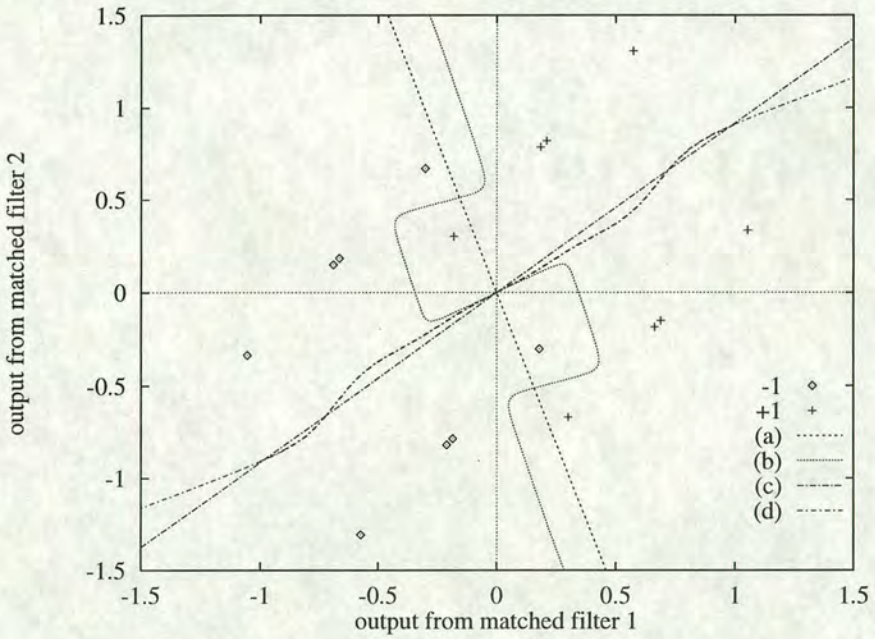

Figure 6.12: *Location of centres and decision boundaries of receivers for $E_b/N_0 = 15$ dB: (-1) centres produced from a -1 from user 1; (+1) centres produced from a $+1$ from user 1; (a) Bit level Wiener filter decision boundary (user 1); (b) RBF network decision boundary (user 1); (c) Bit level Wiener filter decision boundary (user 2); (d) RBF network decision boundary (user 2)*

At this noise level, the Gaussian kernel RBF network correctly partitions the output space, and thus a reasonable error performance may be expected. However, the linear decision boundary obtained using the bit-level Wiener filter for user 1 is not able to correctly separate the centres as required for the reasons outlined above. Indeed, it may be expected that this filter will cause 2 out of every 16 data points to be in error for user 1, leading to a predicted $P_e \simeq 0.125$. These

[5] where the value of the RBF function in equation 6.1 is identically zero

predictions may be verified by considering Figure 6.13, which shows the error performance of the RBF and bit-level Wiener filters for a range of noise values.

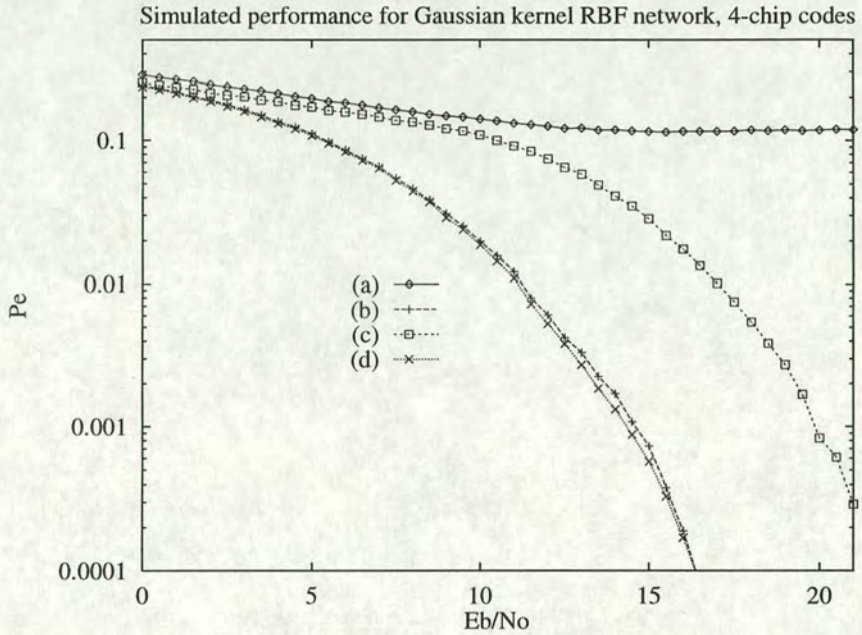

Figure 6.13: *Performance of RBF network and Wiener filter receivers : (a) Wiener, user 1; (b) Wiener, user 2; (c) RBF, user 1; (d) RBF, user 2*

As predicted, the Wiener filter for user 1 reaches an irreducible P_e of around 0.125 for high values of E_b/N_0, while the performance of the bit-level RBF processor increases with the signal to Gaussian noise ratio. Since user 2 is linearly separable, the performance of the linear Wiener and non-linear RBF network receivers are very similar.

The variation of the performance of the RBF network receiver with E_b/N_0 for user 1 may be predicted from Figure 6.14 , which shows the activation function, *i.e.* the surface generated by the RBF network from equation 6.1 for three values of E_b/N_0.

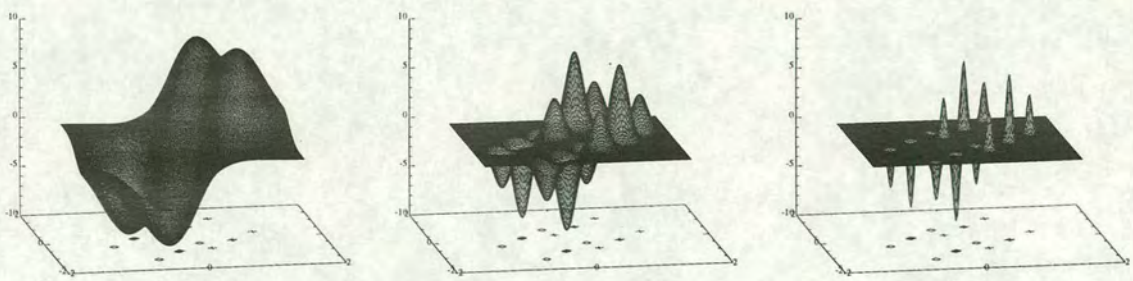

5dB *15dB* *25dB*

Figure 6.14: *Centres and generated surfaces for the Gaussian kernel RBF network for $E_b/N_0 =$ 5, 15 and 25 dB*

Clearly, for low values of E_b/N_0, the spread of the basis functions leads to a loss in distinction,

so that contributions from individual centres are aggregated together in the activation function, and thus the performance is relatively poor. As the signal to Gaussian noise ratio increases, more definition is achieved, so that individual centres now contribute separately, leading to increased performance.

6.4.3 Kernel simplification

The first method of complexity reduction is to employ alternative kernels in equation 6.1, which are designed to reduce the number of calculations required per centre. It must be acknowledged that only the speed of calculation will be improved since the dominant requirement is that of storage. The Gaussian kernel defined in equation 6.2 requires a series of exponential calculations, which may impose too great a computational load on the receiver, so the first alternative considered is the inverse multi-quadratic kernel [86], defined by

$$\psi(\zeta) = \psi_{a_1}(\zeta) = \frac{1}{\sqrt{\zeta^2 + \sigma^2}} \tag{6.5}$$

and the modified inverse multi-quadratic, defined by

$$\psi(\zeta) = \psi_{a_2}(\zeta) = \frac{1}{1 + v\frac{\zeta^2}{2\sigma^2}} \tag{6.6}$$

both of which are avoid the necessity for the exponential evaluation used in Equation 6.1.

The decision boundaries for these algebraic kernels, again for user 1, compared to that for the Gaussian kernel of the previous section, are shown in Figure 6.15 for $E_b/N_0 = 15$ dB.

The algebraic kernels are clearly able to separate the centres arising from different data bits, although the reduced decay rate of the algebraic kernels causes their decision boundaries to always be interior to the Gaussian kernel decision boundary, so that their performance may be expected to be slightly worse.

The error performance of these algebraic kernels is shown in Figure 6.16.

As may be seen, the modified kernel has slightly better performance than the traditional inverse multi-quadratic kernel, and both algebraic kernels have only slightly poorer performance than the full Gaussian kernel.

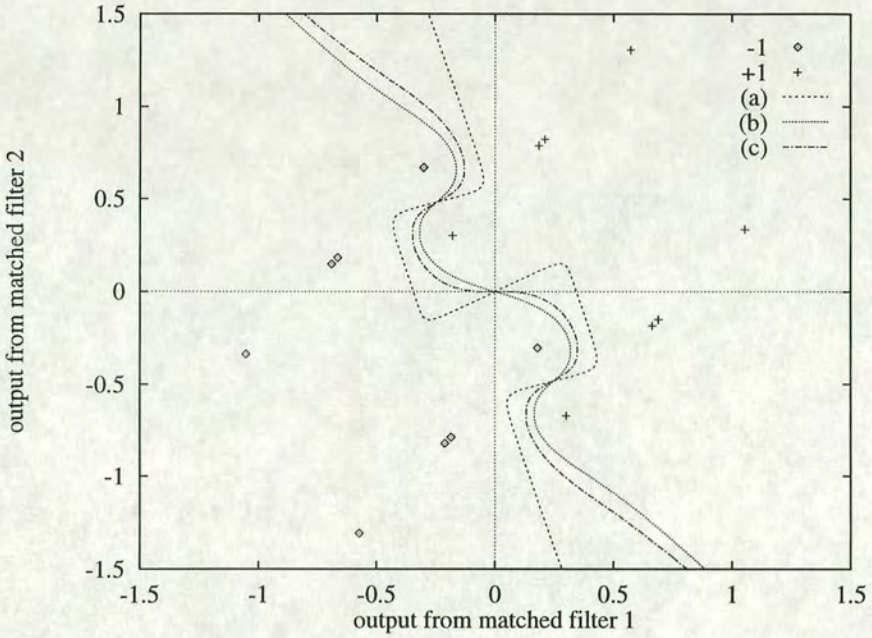

Figure 6.15: *Location of centres and decision boundary of various RBF network receivers for $E_b/N_0 = 15$ dB: (-1) centres produced from a -1; (+1) centres produced from a $+1$; (a) Gaussian kernel decision boundary; (b) decision boundary for ψ_{a_1}; (c) decision boundary for ψ_{a_2} for $v = 1$*

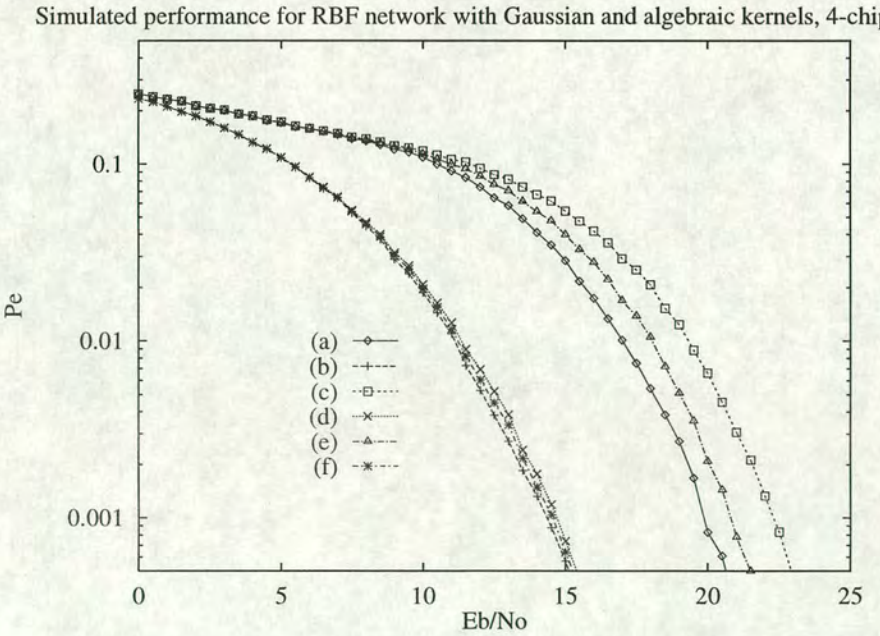

Figure 6.16: *Performance of RBF network receivers with various kernels: (a) Gaussian, user 1; (b) Gaussian, user 2; (c) inverse multi-quadratic ψ_{a_1}, user 1; (d) inverse multi-quadratic, ψ_{a_1} user 2; (e) modified inverse multi-quadratic ψ_{a_2} with $v = 1$, user 1; (f) modified inverse multi-quadratic ψ_{a_2} with $v = 1$, user 2*

The additional parameter v in ψ_{a_2} also permits an investigation of this parameter's influence on the decision boundary and error performance of a network employing this kernel. Concentrating on user 1, the decision boundaries for various values of v for $E_b/N_0 = 10$ dB are shown in Figure 6.17, whilst the corresponding error performance is shown in Figure 6.18.

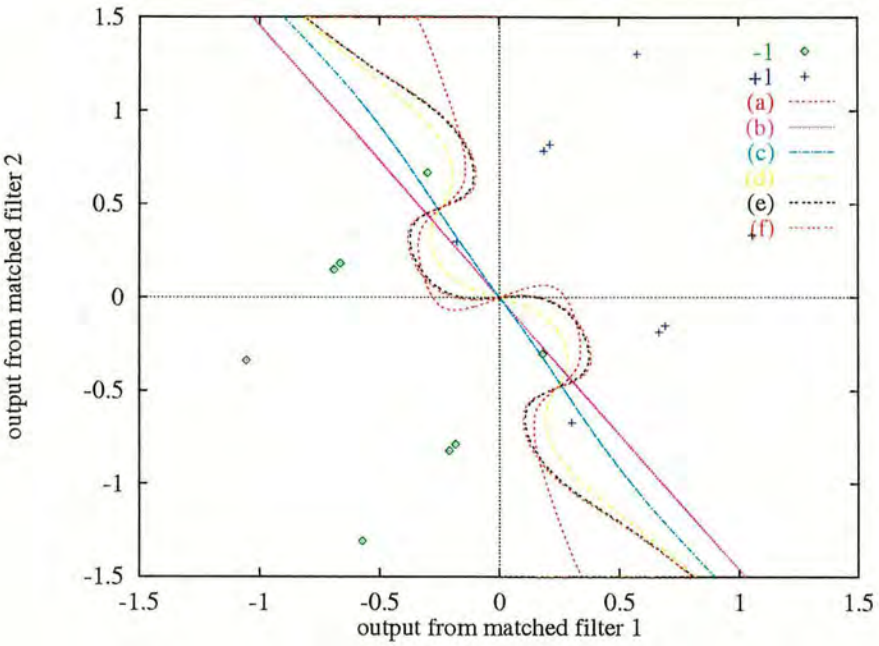

Figure 6.17: *Location of centres and decision boundary of RBF network using ψ_{a_2} kernel function for $E_b/N_0 = 10$ dB: (-1) centres produced from a -1; (+1) centres produced from a $+1$; (a) Gaussian kernel; (b) $v = 0.01$; (c) $v = 0.08$; (d) $v = 1.0$; (e) $v = 10.24$; (f) $v = 81.92$*

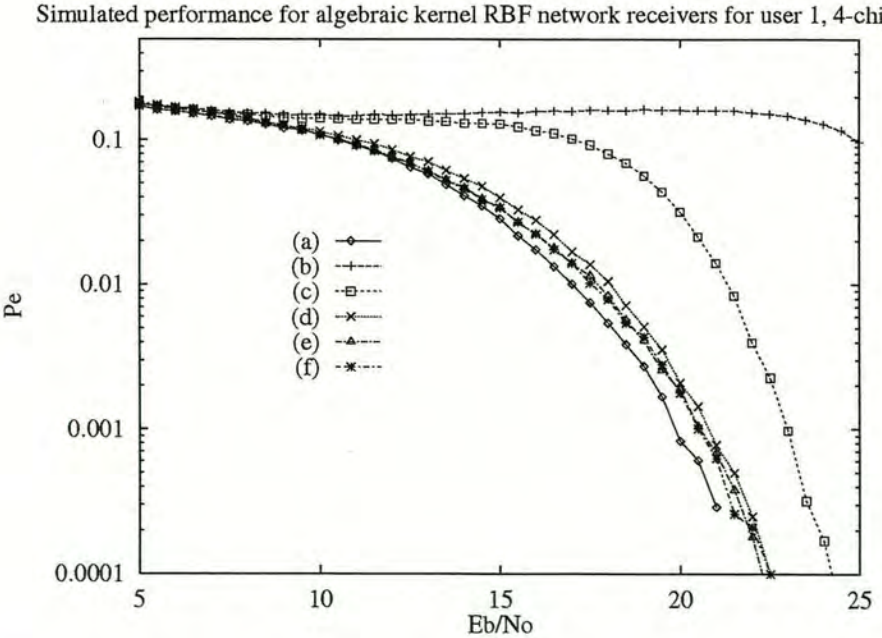

Figure 6.18: *Performance of RBF based receivers with ψ_{a_2} kernel function: (a) Gaussian kernel; (b) $v = 0.01$; (c) $v = 0.08$; (d) $v = 1.0$; (e) $v = 10.24$; (f) $v = 81.92$*

It may be seen that the algebraic kernels for the first two values of v fail to separate the centres correctly for $E_b/N_0 = 10$ dB, and this is reflected in the relatively poor performance of these two receivers. Broadly, there is little advantage in increasing the value of v beyond 1.0, since the performance of the other kernels is so similar. Interestingly, the $v = 0.08$ kernel, although obviously inferior for values of E_b/N_0 below around 15 dB, approaches the performance of the other kernels as E_b/N_0 increases, so that it may be concluded that the influence of the parameter v is only weak as the noise is reduced. Future work may investigate whether this situation may be generalised.

6.4.4 The nearest neighbour receiver

As is apparent from Figure 6.14, when the signal to Gaussian noise ratio, E_b/N_0, is sufficiently large, the Gaussian kernel RBF surface consists of individual peaks and troughs (according as the relevant centre $p \in \mathcal{P}^+$ or $\mathcal{P}^-$ respectively), located at the centres of the network. In this way, this receiver structure is able to compare the input statistic against all the centres and hence obtain an accurate estimate of the original data bit. In addition, the previous section showed that alternative kernels, while offering slightly reduced complexity, are broadly equivalent in terms of error performance, at high values of E_b/N_0. It would appear natural, then, to investigate the performance of a receiver which is based on the centres as calculated previously, but rather than forming the sum in equation 6.1 using the metric to all possible centres, estimates the original data bit by simply considering the nearest[6] centre to the input vector, so that the data estimate for user u is given by

$$\hat{x}_u = w_j : d(\underline{\tilde{x}}, \underline{p}_j) < d(\underline{\tilde{x}}, \underline{p}_i), 1 \leq i \leq N_c, i \neq j \tag{6.7}$$

This nearest neighbour (NN) approach is a commonly occurring problem in many fields in computational geometry [102], and as may be seen in Figure 6.19, the NN decision boundary represents the asymptotic limit of the Gaussian kernel based RBF network as $E_b/N_0 \rightarrow \infty$.

Thus it may be expected that these two approaches will perform similarly as the noise decreases. The error performance against E_b/N_0 of the NN-based receiver, compared to the Gaussian kernel RBF network receiver is shown in Figure 6.20 for both users.

[6] where we again use the Euclidean metric here

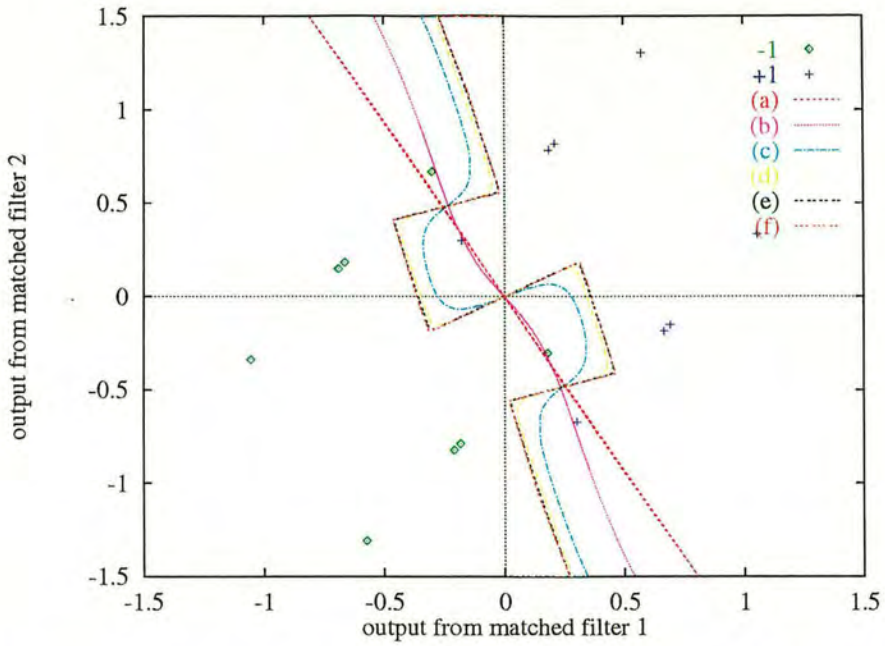

Figure 6.19: *Location of centres and decision boundaries of Gaussian kernel RBF network for various values of E_b/N_0: (-1) centres produced from a -1; (+1) centres produced from a $+1$; (a) 0 dB; (b) 5 dB; (c) 10 dB; (d) 15 dB; (e) 20 dB; (f) NN receiver decision boundary*

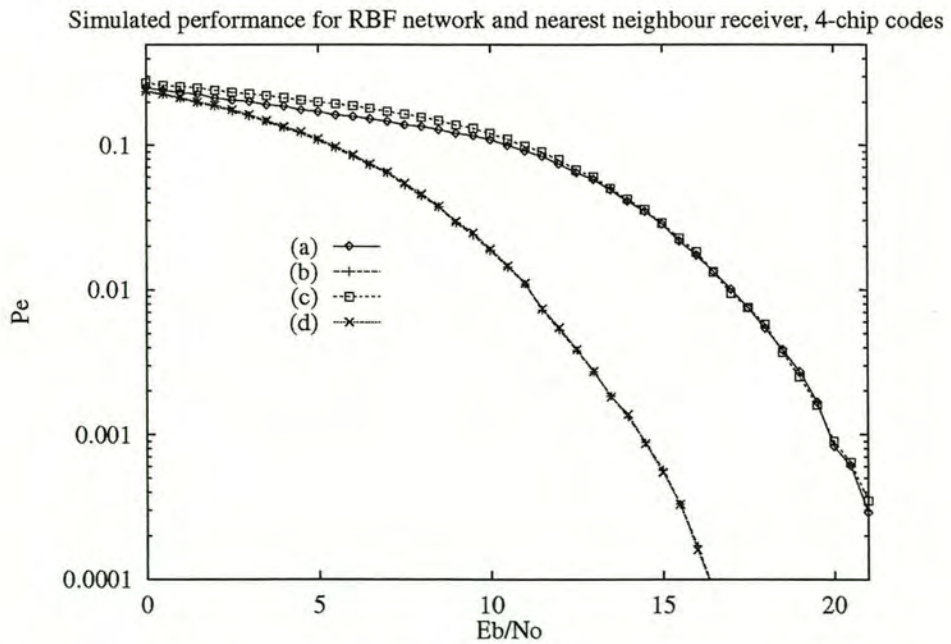

Figure 6.20: *Performance of NN-based receiver compared to Gaussian kernel RBF receiver: (a) RBF, user 1; (b) RBF, user 2; (c) NN, user 1; (d) NN, user 2*

For user 1, the NN receiver has only slightly worse performance than the RBF network for low E_b/N_0, and is almost identical for $E_b/N_0 > 10$ dB as predicted. For user 2, the decision boundaries are very similar, as are the performance curves, as expected, since that user is linearly separable.

Returning to the original 7-chip spreading sequences in AWGN only, the performance of the proposed NN receiver is shown in Figure 6.21, again for the same two values of E_b/N_0 as in the previous case.

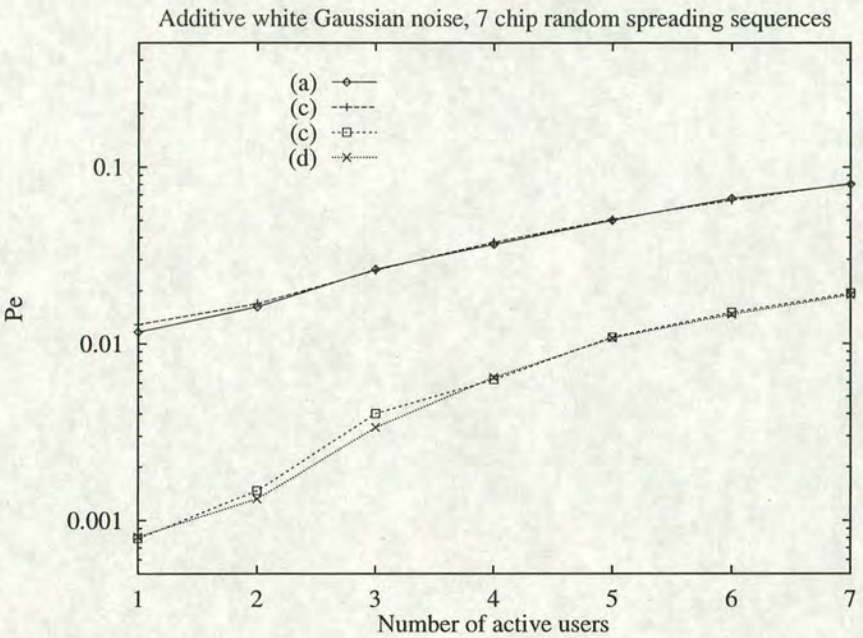

Figure 6.21: *Performance of non-linear receivers in additive white Gaussian noise: (a) RBF, 4 dB; (b) NN, 4 dB; (c) RBF, 7 dB; (d) NN, 7 dB*

As may be seen, the performance of the proposed receiver is very close to that of the Gaussian kernel RBF network receiver for all loading values. Thus, the proposed receiver attains very similar performance characteristics to the standard RBF network receiver, but avoids the associated restrictively high computational complexity.

6.4.4.1 A geometrical interpretation of the nearest neighbour receiver

Efficient algorithms for the NN approach generally consist of two parts; the construction of a tree structure, containing all the centres as nodes, and the traversal of this tree, until the nearest match is found. In 2 dimensions, the construction may be accomplished optimally using $O(N_c)$ storage whilst the search requires $O(\log_2 N_c)$ time [109]. This strategy produces a Voronoi diagram, $\mathcal{V}(\mathcal{P})$ from the set $\mathcal{P}$ of centres, which for the 2-user 4-chip spreading sequence

situation considered here, is shown in Figure 6.22.

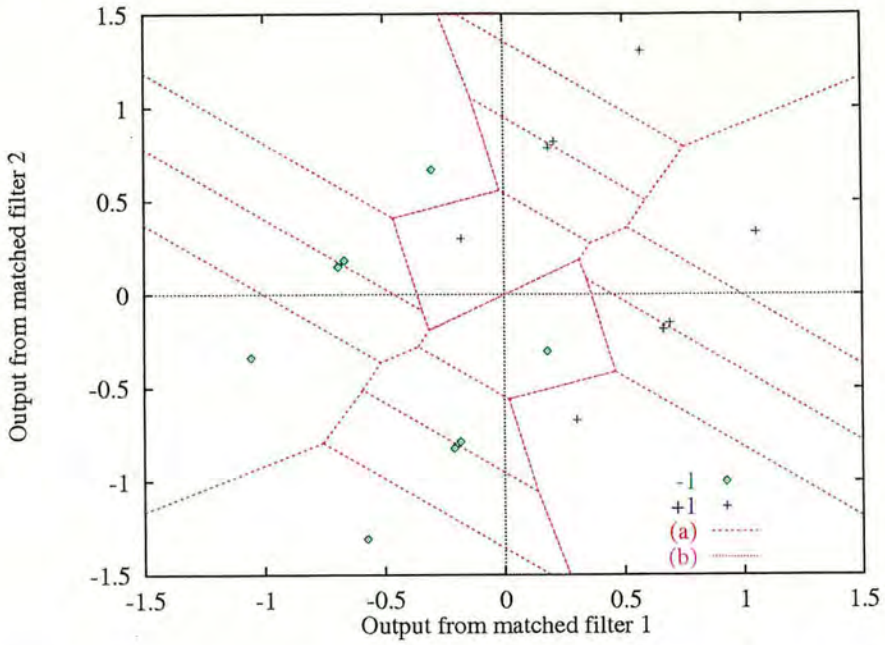

Figure 6.22: *Location of centres and Voronoi diagram: (-1) centres produced from a -1 from user 1; (+1) centres produced from a $+1$ from user 1; (a) Voronoi diagram; (b) NN decision boundary for user 1*

It may be seen that the NN decision boundary for each user is simply a subset of the complete Voronoi diagram, and that a modification of this technique could be used to remove centres whose associated Voronoi polygons $\mathcal{V}(p_i)$ do not border the NN decision boundary, thus increasing the speed of this algorithm. This technique produces a reduced set of centres $\mathcal{P}' \subseteq \mathcal{P}$ for each user. With the scenario considered here, there are 4 centres for each user which may be removed, so that this modified NN algorithm would make 25 % fewer comparisons per data bit, and thus would be correspondingly quicker than the conventional NN algorithm.

This may be seen in Figure 6.23 which shows the performance of the Gaussian kernel RBF network and the NN receiver when the four centres whose polygons are not part of the decision boundary for user 1 are removed from the network.

Clearly, in this case, the performance of the receivers using the reduced set of centres $\mathcal{P}'$ is virtually identical to that of the receivers which use the complete set of centres, $\mathcal{P}$. Future work will consider the development of this approach, with the intention of characterising the ratio of the number of discarded centres to the number of centres in the original network.

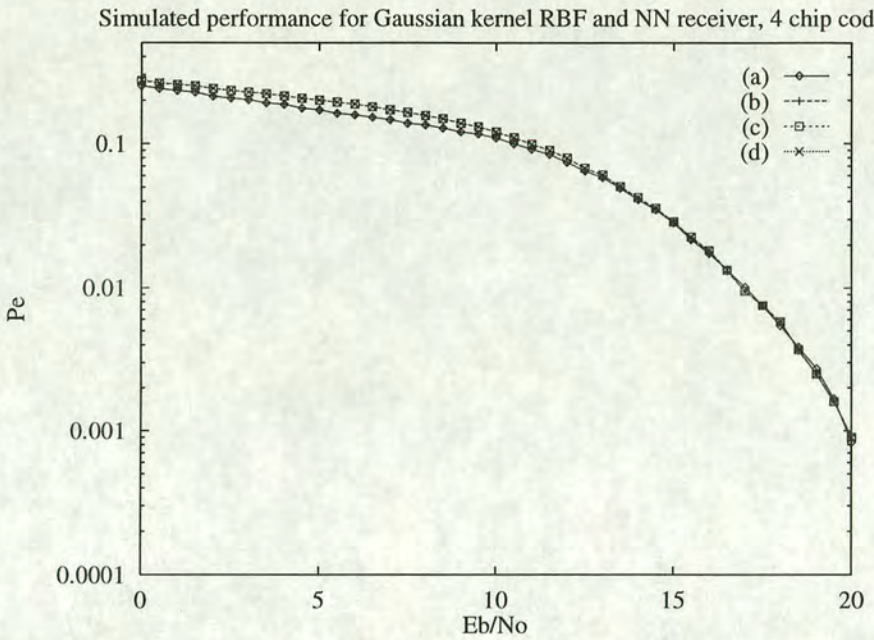

Figure 6.23: *Simulated performance of Gaussian kernel RBF network and NN receiver based on the reduced set of centres, obtained from the Voronoi diagram: (a) Gaussian kernel RBF, complete set; (b) Gaussian kernel RBF, reduced set; (c) NN receiver, complete set; (d) NN receiver, reduced set*

6.4.4.2 Future developments

Since the dimension of the decision space to be partitioned increases linearly with the number of users, the presence of more users means that the NN decision boundary is a $U-1$-dimensional hyperplane. The construction of the Voronoi diagram in higher dimensions is an area of current research [110], but it is shown in [111] that the nearest neighbour may be found in $O((\log_2 N_c)^{U-1}\log_2(\log_2 N_c))$ time; this structure requiring $O(N_c(\log_2 N_c)^{U-1})$ storage. For time-varying channels, the dynamic insertion and deletion of centres could be employed to update the network, or approximate $(1+\epsilon)$ [111] methods could be used if the channel characteristics evolve only slowly.

A possible drawback to the nearest neighbour approach is that this method produces a hard decision, with no indication of the reliability of the estimate, as is required for instance for a soft-decision Viterbi decoder for an FEC encoded DS-CDMA system, as considered in Chapters 4 and 5. As a development, it may be possible to construct a soft decision based on the distance to the nearest centre, or to extend this approach to also consider the next-nearest neighbour, although the excellent performance achieved by the NN algorithm as implemented, may mean that such an approach would be an unnecessary complication.

6.5 Summary

In this chapter, non-linear structures, using radial basis functions have been considered as receivers for the DS-CDMA environment. Various methods of constructing the network have been considered, and the performance of these structures has been simulated and shown to outperform linear structures when the interference is predominantly non-linear in character. The direct implementation, whose input is formed from the received chip-level signal, was shown to have superior performance to a network whose input is obtained by correlating the received signal against either the matched filter, or the matched filter convolved with the channel impulse response.

The chip level DRBF receiver, when employing decision direction was shown to have similar performance to the standard network, so that this method could be investigated to reduce the computational complexity. However, care would be needed to avoid the propagation of errors if this approach is adopted for time-varying channels.

To illustrate the problem more clearly, a sample spreading sequence set and channel impulse response was then considered, which was shown to generate a system with non-linear behaviour. This system was used to investigate methods for reducing the complexity of RBF network receiver structures, firstly by the use of alternative kernels. The asymptotic behaviour of these receivers for high signal to Gaussian noise ratios then prompted an investigation of a receiver based on the nearest neighbour centre to the input. This strategy was shown to provide comparable performance to the standard Gaussian kernel RBF network receiver, and at much reduced computational effort. A graphical interpretation of this receiver was then proposed, and used to provide a scheme for reducing the number of centres in the network. The performance of a receiver based on this reduced set of centres was shown to have virtually identical performance to the original set, regardless of whether the receiver consisted of the Gaussian kernel RBF network, or the proposed nearest neighbour receiver. Finally, suggestions for possible developments of this receiver for a time-varying channel were indicated.

Chapter 7

Conclusions

The main contributions of the work presented will now be indicated. Firstly, a summary of the results obtained is given, with the specific novel contributions arising detailed in section 7.2. Possible future developments of the work are then outlined in section 7.3, with the final conclusions of the thesis presented in section 7.4.

7.1 Summary

An outline was presented of various aspects of the system design of the downlink of a DS-CDMA communications system. A number of alternative receiver structures have been considered, and an idea of the complexity of each of these is summarised in Table 7.1, in which there are U active users, the FEC coding (if present) has rate $R = 1/C$, constraint length K and memory L, and the spreading sequences are of length M chips.

Receiver structure	Storage required	Number of operations
Matched filter	$O(M)$	$O(M)$
Adaptive LMS filter	$O(M)$	$O(M)$
Adaptive RLS filter	$O(M)$	$O(M^2)$
Direct matrix inversion	$O(M^2)$	$O(M^3)$
Viterbi algorithm	$O(2^{K-1})$	$O(L2^{K-1})$
Interference canceller	$O(UM)$	$O(UM)$
Viterbi interference canceller	$O(UM2^{K-1})$	$O(ULM2^{K-1})$
PMF Radial basis function network	$O(2^{2U})$	$O(U2^{2U})$
Nearest neighbour network	$O(2^{2U})$	$O(2U^{U-1}\log_2(2U))$

Table 7.1: The complexity of the receiver structures considered

In the AWGN channel, the convergence and performance of two adaptive receiver structures based on the square error penalty function were compared. The RLS algorithm was shown to be superior to the LMS algorithm, whose properties were shown to be dependent on the number of active users and the background noise level. In a typical urban time varying channel, the RLS algorithm was shown to converge within the same time as for the AWGN channel, although to a greater misadjustment $\mathcal{M}$. The performance of the RLS algorithm in multipath was shown to degrade gracefully with loading and background noise, as in the AWGN only case.

Convolutional coding was considered both as a replacement for and a supplement to direct sequence spreading, and a number of systems, combining FEC coding and direct sequence spreading, for a fixed overall processing gain, were considered. Simulations of these systems demonstrated the ill-effects of simply increasing the convolutional coder constraint length, without a corresponding adjustment in coding rate. MAI was shown to be a significant impairment to the operation of the Viterbi decoder in the receiver, and so a number of parallel interference cancellation schemes were considered. To reduce MAI, the principle of parallel interference cancellation was investigated in the context of signals consisting of both FEC coding and direct sequence spreading. Structures using either the matched filter or the Wiener filter, together with a data decision from a simple hard limiter or a Viterbi decoder were analysed and simulated. The combination of a matched filter receiver with the intermediate Viterbi decoder was shown to provide reasonable performance, without the requirement for the evaluation of the Wiener filter.

Non-linear receivers were shown to provide excellent performance, whether implemented at the chip rate, or at the symbol rate, compared to the equivalent Wiener filter. The inherent complexity of these RBF-based receivers, as the number of active users increases was indicated and a number of methods for reducing this complexity were investigated. Decision direction was shown to provide a possible mechanism for reducing the number of centres which must be considered, at little detriment to the performance. Simpler kernel functions, enabling the more rapid evaluation of the decision function, were shown to provide a mechanism for reducing the complexity of the calculation for each centre. Finally a new receiver structure was proposed, and demonstrated to have comparable performance to the RBF receiver, but at much reduced complexity. The efficient calculation and traversal of structures representing this receiver was indicated, with emphasis on the application of this technique as the number of users increases, and to time-varying multipath channels.

7.2 Contributions

The principal novel contributions to knowledge described in this thesis are as follows :-

- The performance of the RLS algorithm in a time-varying multipath channel was shown to depend on the system chip rate and the choice of resetting strategy. The influence of the forgetting factor λ on the convergence and performance of the receiver was shown to be significant if the tap weights are not reset after each data cycle.

- Orthogonal convolutional coding was shown to be impractical for multiple access systems, unless augmented by a randomising sequence to avoid the same encoded sequence being output for different input conditions. Even when additional randomising stages were included, the orthogonal coding system was shown to have inferior performance compared to the MMSE (Wiener) receiver as the loading was increased for systems with constraint lengths of 3 and 6 (equivalent to linear processing gains of 8 and 64 respectively).

- For systems devoting resources to both FEC coding and direct sequence spreading for a fixed overall processing gain, both Gold and random spreading sequences were considered. With 20 users and a bandwidth expansion factor of around 500, the combination which offered the best performance, using either spreading sequence set, was the rate $1/8$, constraint length 6 convolutional coder, with 63-chip spreading sequences. Increasing the loading caused the rate $1/4$, constraint length 6 system, with 127 chip spreading sequences to offer the best performance, for a number of background noise levels.

- Simulations of the combined Viterbi decoder and MAI canceller confirmed predictions that, for a linear processing gain of 126, significant capacity improvements over the conventional sign decision cancellation receiver were achieved, with the combination of the Wiener filter to despread the signal together with an intermediate Viterbi decoder able to support 50 % capacity at the same probability of error as the single user matched filter receiver.

- The nearest neighbour receiver was shown to have comparable performance to the Gaussian kernel RBF receiver. Interpreting this proposed receiver in terms of a Voronoi diagram provided a mechanism for reducing the number of centres in the network, by discarding those centres which do not contribute to the nearest neighbour decision boundary.

7.3 Future developments

In the simulations described, inter-cell interference from other base stations in the network and interference from other external commmunication systems is simply incorporated into the overall background noise. A possible development, therefore, would be to simulate the effects of realistic structured co-channel interference from neighbouring cells more accurately, or to model more closely the effects of other competing systems.

Effects caused by step-changes in the transmitted signal, due to the abrupt cessation or initiation of a particular user's transmission have not been modelled in this investigation. While these effects may be reduced by limiting the exact times at which such events may occur, it would be interesting to investigate the impact of this on the convergence and error performance of the adaptive algorithms considered. Other adaptive algorithms based either on the mean square error as considered here, or other penalty functions, such as the least mean fourth (LMF) algorithm [112] may prove useful at combatting the effects of MAI, although these may impose additional computational requirements. Decision direction could be employed in conjunction with an adaptive algorithm to avoid the need for training data, although some means must be considered to prevent error propagation caused by incorrect decisions. A wider range of Doppler spreads, corresponding to different vehicle speeds, and a wider range of transmission data rates could also be considered, to investigate the effects of these parameters on the convergence and error performance characteristics of the RLS, and other adaptive algorithms. Other models for the channel may also be considered. The separation of the receiver tasks into channel equalisation, via a pilot signal to estimate the instantaneous channel impulse response and MAI rejection, via an adaptive algorithm, may be worthy of further investigation.

Greater delays may be tolerated in the FEC-decoder portion of the receivers considered in Chapter 4, allowing the use of longer constraint length convolutional coders. While the performance advantages of these FEC coders are clear in the single user environment, the influence of MAI on systems using larger constraint lengths is unclear. In addition, the larger delays may adversely affect the ability of the system to perform in realistic time-scales. The performance of sub-optimal FEC-decoding algorithms, such as the stack or Fano algorithm may also be of interest. The allocation of resources to coding and spreading has been investigated for a relatively large linear processing gain of around 500. It would clearly be useful to also consider the optimal balance of FEC-coding and direct sequence spreading in systems with shorter processing gains, such as may be used in extensions of the GSM system. In addition, the inclusion of a multipath channel may cause a different combination of coding rate and spreading

sequence length to afford better performance. The additional use of an interleaver would be required in this case, to avoid the same part of each user's signal suffering the same attenuation. The use of more powerful FEC structures, such as turbo codes, have been shown to greatly improve single user communications, and whether similar improvements would be possible with multiple access schemes, set against the impact of the extra computational demand, and variable processing delay which these coding structures require, may also be of interest for further work.

The receivers discussed in Chapter 5 are all limited to a single stage of MAI cancellation. An obvious development therefore, would be to investigate the performance of the receivers considered when further cancellation stages are included, although any improvements gained must be taken in the context of the increased complexity and additinal delay thus imposed on the system. The effect of assigning different convolutional coding structures to different users on the efficiency and memory requirement of the Viterbi cancellation receivers may also be of interest. Care would also need to be exercised if such structures were to be considered for the uplink, since the delay on each signal would have to be accurately estimated to properly align the re-spread signals, prior to cancellation. Use of soft decisions in the production of the intermediate signals is likely to lead to a significant performance advantage. In addition, thresholding the soft decisions to only make use of those results which are deemed sufficiently reliable may be a promising strategy, since it may prevent borderline decisions catastrophically affecting the final performance. Alternative despreading filters, which do not require the same level of accuracy in the estimation of the signal to noise ratio, may also prove worthy of future investigation.

In the context of the non-linear receivers described in Chapter 6, the most fruitful improvements are likely to be those which lead to a reduction in complexity of the receiver, without significantly compromising performance. The approximation of the exponential by an algebraic function may prove of merit for any possible application in hardware, while other kernel functions could be investigated to more accurately approximate the Gaussian kernel. Decision direction has been shown to be a valuable method of reducing the number of centres, at little cost to the performance. The number and frequency of control, or training bits, used in this technique, to limit error propagation could be of interest. Focussing on the nearest neighbour receiver, the limiting factor is the efficient construction and rapid traversal of a suitably ordered representation of the centres. The complexity of this problem increases non-linearly with increasing numbers of users, whilst the presence of a time-varying channel will require the dynamic update of the location of the centres. Characterising the number of centres which may be discarded without

serious detriment to the performance, by employing a Voronoi-diagram based approach has been shown to be effective, and the application of this technique for more users, and in a time-varying channel is an obvious extension of the work presented here. Finally, as in the previous chapter, incorporation of soft decisions, possibly suitably thresholded to avoid borderline decisions, may further improve the performance of the nearest neighbour receiver, although, as has been demonstrated, the deviation in performance from the complete Gaussian kernel RBF network is only minimal, so that the increased complexity of this approach may be needless.

7.4 Conclusion

In this thesis, various signal processing techniques have been investigated to attempt to improve the downlink capacity and performance of a cellular DS-CDMA communications system. The principles of this spread spectrum technique were first outlined, including a description of a number of aspects of system design. Adaptive algorithms, which iteratively approximate the Wiener (MMSE) filter have been shown to be useful in countering the effects of a time-varying typical urban multipath channel. The use of forward error correction has been investigated, both as a substitute for and as a supplement to direct sequence spreading. Parallel interference cancellation methods have been combined with FEC decoding, and shown to provide significant increases in capacity, at tolerably moderate increases in overall complexity and processing delay. Finally, non-linear receivers, using radial basis functions, have been shown to provide excellent performance, but at the expense of significant complexity requirements. Methods to reduce the complexity of such receivers have been proposed, and shown to incur little degradation in performance. Thus, several signal processing methods to improve the performance of DS-CDMA systems have been proposed, investigated and evaluated.

References

[1] R. Prasad, "Overview of Wireless Personal Communications: Microwave Perspectives," *IEEE Communications Magazine*, vol. 35, no. 4, pp. 104–108, 1997.

[2] J. Padgett, C. Gunther, and T. Hattori, "Overview of Wireless Personal Communications," *IEEE Communications Magazine*, pp. 28–41, Jan 1995.

[3] A. J. Viterbi, "The Evolution of Digital Wireless Technology from Space Exploration to Personal Communication Services," *IEEE Transactions on Vehicular Technology*, vol. 43, pp. 638–643, Aug 1994.

[4] C. E. Shannon, "Communication in the Presence of Noise," *Proceedings of the IRE*, vol. 37, pp. 10–21, Jan 1949.

[5] W. C. Y. Lee, *Mobile Cellular Telecommunication Systems - International Edition.* McGraw Hill Book Company, 1st ed., 1990.

[6] T. S. Rappaport, *Wireless Communications: Principles and Practice.* London: Prentice-Hall International (UK) Limited, 1st ed., 1996.

[7] D. T. Magill, F. D. Nagali, and G. P. Edwards, "Spread Spectrum Technology for Commercial Applications," *Proceedings of the IEEE*, vol. 82, pp. 572–584, April 1994.

[8] M. Madfors, K. Wallstedt, S. Magnusson, H. Olofsson, P.-A. Backman, and S. Engström, "High Capacity with Limited Spectrum in Cellular Systems," *IEEE Communications Magazine*, vol. 35, pp. 572–584, August 1997.

[9] J. Rapeli, "UMTS: Targets, System Concept and Standardization in a Global Framework," *IEEE Personal Communications*, pp. 20–28, Feb 1995.

[10] W. C. Y. Lee, "Overview of Cellular CDMA," *IEEE Transactions on Vehicular Technology*, vol. VT-40, pp. 291–302, May 1991.

[11] A. P. Hulbert and R. S. Swain, "The Radio Channel," in *Cordless Telecommunications Worldwide* (W. H. Tuttlebee, ed.), ch. 12, pp. 210–251, London: Springer-Verlag, 1997.

[12] K. S. Gilhausen, I. M. Jacobs, R. Padovani, and L. A. Weaver, Jr., "Increased Capacity using CDMA for Mobile Satellite Communication," *IEEE Journal on Selected Areas in Communications*, vol. 8, pp. 503–514, May 1990.

[13] R. A. Scholtz, "The Evolution of SS-MA Communications," *Proceedings of the 3rd IEEE International Symposium on Spread Spectrum Techniques and Applications (ISSSTA), Oulu, Finland*, vol. 1, pp. 4–13, July 1994.

[14] P. G. Flikkema, "Spread Spectrum Techniques for Wireless Communication," *IEEE Signal Processing Magazine*, vol. 14, pp. 26–36, May 1997.

[15] TIA/EIA/IS-95, *Mobile Station-Base Station Compatibility Standard for Dual Mode Wide-Band Spread Spectrum Cellular Systems*. Telecommunication Industry Association, 1993.

[16] R. Padovani, "Reverse Link Performance of IS-95 Based Cellular Systems," *IEEE Personal Communications*, pp. 28–34, April 1994.

[17] S. J. Lipoff, "Personal Communications Networks Bridging the Gap between Cellular and Cordless Phones," *Proceedings of the IEEE*, vol. 82, pp. 564–571, April 1994.

[18] J. J. Blanz, A. Klein, M. Nashan, and A. Steil, "Performance of a Cellular Hybrid C/TDMA Mobile Radio System Applying Joint Detection and Coherent Receiver Antenna Diversity," *IEEE Journal on Selected Areas in Communications*, vol. 12, pp. 568–579, May 1994.

[19] T. Ojanperä, P. A. Ranta, S. Hämäläinen, and A. Lappeteläinen, "Analysis of CDMA and TDMA for 3rd Generation Mobile Radio Systems," *Procedings of the 47th IEEE Vehicular Technology Conference (VTC), Phoenix, Arizona, USA*, vol. 1, pp. 840–844, May 1997.

[20] Bingham, "Multicarrier Modulation for Data Transmission: An Idea Whose Time Has Come," *IEEE Communications Magazine*, pp. 5–14, May 1990.

[21] P. Hoher, P. Hagenauer, E. Offer, and C. Rapp, "Performance of an RCPC-Coded OFDM Based Digital Audio Broadcasting (DAB) Standard," *IEEE Global Telecommunications Conference (Globecom)*, pp. 40–44, December 1991.

[22] K.Fazel, "Performance of CDMA/OFDM for Mobile Communications," *IEEE International Conference on Universal Personal Communications (ICUPC)*, pp. 975–979, October 1993.

[23] G. J. R. P. R. A. Stirling-Gallacher, "Different Channel Coding Strategies for OFDM-CDMA," *Procedings of the 47th IEEE Vehicular Technology Conference (VTC), Phoenix, Arizona, USA*, vol. 2, pp. 845–849, May 1997.

[24] S.Pike, "The Radio Interface for UMTS," *IEE Colloquium on Personal Communications in the 21st Century, London, UK*, pp. 7/1–7/20, February 1998.

[25] R. Pickholtz, D. Schilling, and L. Millstein, "Theory of Spread Spectrum Communications: A Tutorial," *IEEE Transactions on Communications*, vol. COM-30, pp. 855–884, May 1982.

[26] P. M. Schumacher, "Understand the Basics of Spread Spectrum Communications," *Microwaves and RF*, pp. 149–159, May 1993.

[27] G. J. Sauliner, "Supression of Narrowband Jammers in a Spread Spectrum Receiver using Transform Domain Adaptive Filtering," *IEEE Journal on Selected Areas in Communications*, vol. 10, pp. 59–68, May 1992.

[28] L.-M. Li and L. B. Milstein, "Rejection of Narrow-band Interference in PN Spread Spectrum Systems using Transversal Filters," *IEEE Transactions on Communications*, vol. COM-30, pp. 925–928, May 1982.

[29] J. W. Ketchum and J. G. Proakis, "Adaptive Algorithms for Estimating and Suppressing Narrow-band Interference in PN Spread Spectrum Systems," *IEEE Transactions on Communications*, vol. COM-30, pp. 913–924, May 1982.

[30] H. V. Poor and L. A. Rusch, "Narrow-band Interference Suppression in Spread Spectrum CDMA," *IEEE Personal Communications*, vol. 3, pp. 14–27, 1994.

[31] J. Proakis, *Digital Communications*. New York: McGraw-Hill, 2nd ed., 1983.

[32] B. Sklar, "Rayleigh Fading Channels in Mobile Digital Communication Systems Part I: Characterization," *IEEE Communications Magazine*, pp. 90–100, July 1997.

[33] D. I. Laurenson, D. G. M. Cruickshank, and G. J. R. Povey, "A Computationally Efficient Multipath Channel Simulator for the COST 207 Models," *IEE Colloquium on Computer Modelling of Communication Systems*, May 1994.

[34] W. H. Press, S. A. Teukolsky, W. T. Vetterling, and B. P. Flannery, *Numerical Recipies in C: The Art of Scientific Computing*. Trumpington St., Cambridge CB2 1RP: Press Syndicate, University of Cambridge, 2nd ed., 1992.

[35] M. Failli, ed., *Digital Land Mobile Radio Communications - COST 207 : Final Report*. Luxembourg: Commision of the European Communities, 1989.

[36] E. P. Cunningham, *Digital Filtering: An Introduction*. New York, NY, USA: John Wiley & sons, Inc., 1995.

[37] D. Cruickshank, "Suppression of Multiple Access Interference in a DS-CDMA System using Wiener Filtering and Parallel Cancellation," *Proceedings of the IEE: Communications*, vol. 143, pp. 226–230, August 1996.

[38] M. Abramowitz and I. A. Stegun, *Handbook of Mathematical Functions*. New York, USA: Dover Publications Inc, 1972.

[39] R. Kohno, R. Meidan, and L. Milstein, "Spread Spectrum Access Methods for Wireless Communications," *IEEE Communications Magazine*, vol. 23, pp. 58–67, January 1995.

[40] S. B. Maurer and A. Ralston, *Discrete Algorithmic Mathematics*. Reading, Mass., USA: Addison-Wesley, 1991.

[41] P. J. Smith, M. Shaft, and H. Gao, "Quick Simulation: A Review of Importance Sampling Techniques in Communications Systems," *IEEE Journal on Selected Areas in Communications*, vol. 15, pp. 597–613, May 1997.

[42] K. Ben Lataief, K. Muhammad, and J. S. Sadowsky, "Fast Simulation of DS-CDMA with and without coding in Multipath Fading Channels," *IEEE Journal on Selected Areas in Communications*, vol. 15, pp. 626–639, May 1997.

[43] R. S. Mowbray, R. D. Pringle, and P. M. Grant, "Increased CDMA Capacity through Adaptive Co-channel Interference Regeneration and Cancellation," *Proceedings of the IEE*, vol. 139, pp. 515–524, Oct 1992.

[44] D. Kahn, "Cryptology and the Origin of Spread Spectrum," *IEEE Spectrum*, vol. 24, pp. 70–80, Sept 1984.

[45] S. Golomb, *Sequences with Randomness Properties*. Baltimore, MD, USA, Terminal Progress Rep., Contract Req. No. 639498: Glenn L. Martin Co., 1955.

[46] N. Zierler, "Linear Recurring Sequences," *J. SIAM*, vol. 7, Mar 1959.

[47] R. Gold, "Optimal Binary Sequences for Spread Spectrum Multiplexing," *IEEE Transactions on Information Theory*, vol. IT-13, pp. 619–621, Oct 1967.

[48] D. V. Sarwate and M. B. Pursley, "Cross-correlation Properties of Pseudorandom and Related Sequences," *Proceedings of the IEEE*, vol. 68, pp. 593–619, May 1980.

[49] S. W. Golomb, "Shift Register Sequences and Spread Spectrum Communications," *Proceedings of the 3rd IEEE International Symposium on Spread Spectrum Techniques and Applications (ISSSTA), Oulu, Finland*, vol. 1, pp. 14–15, July 1994.

[50] R. Dixon, *Spread Spectrum Systems with Commercial Applications*. Wiley Interscience, 3rd ed., 1994.

[51] R. Gold, "Maximal Recursive Sequences with 3-valued Recursive Cross-correlation Functions," *IEEE Transactions on Information Theory*, vol. IT-14, no. 1, pp. 154–156, 1968.

[52] R. de Gaudenzi, C. Elia, and R. Viola, "Band-Limited QS-CDMA : A Novel Satellite Access Technique for Mobile and Personal Communications Systems," *IEEE Journal on Selected Areas in Communications*, vol. 10, pp. 328–343, Feb 1992.

[53] K. G. Beauchamp, *Walsh Functions and their Applications*. London: Academic Press, 1975.

[54] A. Klein, G. K. Kaleh, and P. W. Baier, "Zero Forcing and Minimum Mean Square Error Equalization for Multiuser Detection in Code Division Multiple-Access Channels," *IEEE Transactions on Vehicular Technology*, vol. 45, pp. 276–287, May 1996.

[55] N. Wiener, *Extrapolation, Interpolation and Smoothing of Stationary Time Series*. New York: Wiley, 1949.

[56] U. Madhow and M. Honig, "MMSE Interference Supression for Direct-Sequence Spread Spectrum CDMA," *IEEE Transactions on Communications*, vol. 42, pp. 3178–3188, December 1994.

[57] D. G. M. Cruickshank, "Optimal and Adaptive FIR Filter Receivers for DS-CDMA," *Proceedings of the IEEE 5th International Symposium on Personal, Indoor and Mobile Radio Communications (PIMRC), The Hague, The Netherlands*, pp. 1339–1345, 1994.

[58] N. Zečević and J. H. Reed, "Blind Adaptation Algorithms for Direct Sequence Spread Spectrum CDMA Single User Detection," *Procedings of the 47th IEEE Vehicular Technology Conference (VTC), Phoenix, Arizona, USA*, vol. 3, pp. 2133–2137, May 1997.

[59] R. W. Lucky, "Techniques for Adaptive Equalisation of Digital Communication Systems," *Bell System Tech. Journal*, vol. 45, pp. 255–286, 1966.

[60] P. M. Grant, C. F. N. Cowan, B. Mulgrew, and J. H. Dripps, *Analogue and Digital Signal Processing and Coding*. Bromley, UK: Chartwell-Bratt, 1989.

[61] B. Widrow, "Adaptive Noise Cancelling: Principles and Applications," *Proceedings of the IEEE*, vol. 63, pp. 1692–1716, Dec 1975.

[62] S. Haykin, *Adaptive Filter Theory*. Englewood Cliffs, New Jersey, USA: Prentice Hall International, 2nd ed., 1991.

[63] J. Yuen, M. Simon, W. Miller, F. Pollara, C. Ryan, D. Divsalar, and J. Morakis, "Modulation and Coding for Satellite and Space Communications," *Proceedings of the IEEE*, vol. 78, pp. 1250–1266, July 1990.

[64] K. Larsen, "Short Convolutional Codes with Maximal Free Distance for Rates 1/2,1/3, and 1/4," *IEEE Transactions on Information Theory*, vol. IT-18, pp. 371–372, 1973.

[65] D. Haccoun, "Decoding Techniques for Convolutional Codes," *Proceedings of the International Symposium on Coding Theory and Applications, Udine, Italy, 1990*, pp. 242–258, 1990.

[66] A. Viterbi, "Error Bounds for Convolutional Codes and an Asymptotically Optimum Decoding Algorithm," *IEEE Transactions on Information Theory*, vol. IT-13, pp. 260–269, April 1967.

[67] Y. Lin and S. Tu, "Modified Multiple Stack Algorithm for Decoding Convolutional Codes," *Proceedings of the IEE: Communications*, vol. 144, no. 4, pp. 3221–228, 1997.

[68] G. Forney, "The Viterbi Algorithm," *Proceedings of the IEEE*, vol. 61, no. 3, pp. 268–277, 1973.

[69] H.-L. Lou, "Implementing the Viterbi Algorithm," *IEEE Signal Processing Magazine*, pp. 42–52, September 1995.

[70] J. Heller and I. Jacobs, "Viterbi Decoding for Satellite and Space Communication," *IEEE Transactions on Communications*, vol. COM-19, no. 5, pp. 835–848, 1971.

[71] J. Laster and J. Reed, "Interference Rejection in Digital Wireless Communications," *IEEE Signal Processing Magazine*, vol. 14, pp. 37–62, May 1997.

[72] Y. Yoon, R. Kohno, and H. Imai, "A Spread Spectrum Multi-Access System with Co-Channel Interference Cancellation for Multipath Fading Channels," *IEEE Journal on Selected Areas in Communications*, vol. SAC-11, no. 7, pp. 1067–1075, 1993.

[73] M. Gastpar and D. Cruickshank, "Two-Stage Wiener Filter Based Cancellation Receivers for DS-CDMA," *IEE Electronic Letters*, vol. 32, pp. 805–806, April 1996.

[74] J. M. Holtzman, "DS-CDMA Successive Interference Cancellation," *Proceedings of the 3rd IEEE International Symposium on Spread Spectrum Techniques and Applications (ISSSTA), Oulu, Finland*, vol. 1, pp. 69–78, July 1994.

[75] Y. Li and R. Steele, "Serial Interference Cancellation Method for CDMA," *IEE Electronic Letters*, vol. 30, pp. 1581–1582, September 1994.

[76] R. Lupas, "Minimum Probability of Error for Asynchronous Gaussian Multiple Access Channels," *IEEE Transactions on Information Theory*, vol. 32, pp. 85–96, January 1986.

[77] S. Moshavi, "Multi-User Detection for DS-CDMA Communications," *IEEE Communications Magazine*, pp. 124–136, Oct 1996.

[78] R. Lupas and S. Verdu, "Near-Far Resistance of Multiuser Detectors in Asynchronous Channels," *IEEE Transactions on Communications*, vol. 38, pp. 496–508, April 1990.

[79] R. Lupas and S. Verdu, "Linear Multiuser Detectors for Synchronous Code Division Multiple-Access Channels," *IEEE Transactions on Information Theory*, vol. 35, pp. 123–136, January 1989.

[80] A. Duel-Hallen, J. Holtzman, and Z. Zvonar, "Multi-user Detection for CDMA Systems," *IEEE Personal Communications*, pp. 46–58, April 1995.

[81] G. J. Gibson, S. Siu, and C. F. N. Cowan, "The Application of Nonlinear Structures to the Reconstruction of Binary Signals," *IEEE Transactions on Signal Processing*, vol. 39, pp. 1877–1884, August 1991.

[82] R. Tanner and D. G. M. Cruickshank, "Volterra Based Receivers for DS-CDMA," *Proceedings of the IEEE 8th International Symposium on Personal, Indoor and Mobile Radio Communications (PIMRC), Oulu, Finland*, vol. 3, pp. 1166–1170, September 1997.

[83] S. Chen, B. Mulgrew, and P. M. Grant, "A Clustering Technique for Digital Communications Channel Equalisation Using Radial Basis Function Networks," *IEEE Transactions on Neural Networks*, vol. 4, pp. 570–579, July 1993.

[84] S. Chen, S. McLaughlin, and B. Mulgrew, "Complex-Valued Radial Basis Function Networks: Application to Digital Communications Channel Equalisation (part II)," *EURASIP Signal Processing Journal*, vol. 36, pp. 175–188, March 1994.

[85] L. Kuncheva and S. Hadjitodorov, "An RBF Network with Tunable Function Shape," *Proceedings of the IEEE International Conference on Pattern Recognition (ICPR), Vienna, Austria*, vol. 1, pp. 645–649, August 1996.

[86] B. Mulgrew, "Applying Radial Basis Functions," *IEEE Signal Processing Magazine*, pp. 50–65, March 1996.

[87] D. D. Falconer and L. Ljung, "Application of Fast Kalman Estimation to Adaptive Equalisation," *IEEE Transactions on Communications*, vol. COM-26, pp. 1439–1446, Oct 1978.

[88] J. E. Mazo, "Analysis of Decision-Directed Equaliser Convergence," *Bell System Tech. J.*, vol. 59, pp. 1857–1876, 1980.

[89] H. Elders-Boll, M. Herper, and A. Busboom, "Adaptive Receivers for Mobile DS-CDMA Communication Systems," *Procedings of the 47th IEEE Vehicular Technology Conference (VTC), Phoenix, Arizona, USA*, vol. 3, pp. 2128–2132, May 1997.

[90] E. Eleftheriou and D. D. Falconer, "Tracking Properties and Steady-state Performance of RLS Adaptive Filter Algorithms," *IEEE Transactions on Acoustics, Speech and Signal Processing*, vol. ASSP-34, pp. 1097–1110, Oct 1986.

[91] S. Qureshi, "Adaptive Equalisation," *IEEE Comun. Mag.*, vol. 20, pp. 9–16, 1982.

[92] G. Povey, "A Decision Directed Spread Spectrum RAKE Receiver for Fast Fading Mobile Channels," *IEEE Transactions on Vehicular Technology*, pp. 742–746, June 1994.

[93] M. H. Verhaegen, "Round-off Error Propagation in Four Generally Applicable, Recursive, Least-squares Estimation Schemes," *Automatica*, vol. 25, pp. 437–444, 1989.

[94] A. Viterbi, "Very Low Rate Convolutional Codes for Maximum Theoretical Performance of Spread Spectrum Multiple Access Channels," *IEEE Journal on Selected Areas in Communications*, vol. 8, pp. 641–649, May 1990.

[95] R. F. Ormondroyd and J. J. Maxey, "Performance of Low-Rate Orthogonal Convolutional Codes in DS-CDMA Applications," *IEEE Transactions on Vehicular Technology*, pp. 320–328, May 1997.

[96] R. Ormondroyd and J. Maxey, "A High Performance CDMA Cellular Radio System Based on Low-Rate Convolutional Coding," *Proceedings of the IEE Conference on Radio Receivers and Associated Systems, Bath, UK*, pp. 17–21, Sep 1995.

[97] G. Boudreau, D. Falconer, and S. Mahmoud, "A Comparison of Trellis Coded Versus Convolutionally Coded Spread Spectrum Multiple Access Systems," *IEEE Journal on Selected Areas in Communications*, vol. 8, pp. 628–640, May 1990.

[98] P. Jung and B. Steiner, "A Joint Detection Mobile Radio System Concept Developed Within COST 231," *Procedings of the 45th IEEE Vehicular Technology Conference (VTC)*, vol. 1, pp. 469–473, July 1995.

[99] J. Conan, "The Weight Spectra of Some Short Low-Rate Convolutional Codes," *IEEE Transactions on Communications*, vol. COM-32, pp. 1050–1053, Sep 1984.

[100] J. Hagenauer, "Forward Error Correcting for CDMA Systems," *Proceedings of the 4th IEEE International Symposium on Spread Spectrum Techniques and Applications (ISSSTA), Mainz, Germany*, vol. 2, pp. 566–569, Sep 1996.

[101] S. Kaiser, "On the Performance of Different Detection Techniques for OFDM-CDMA in Fading Channels," *IEEE Global Telecommunications Conference (Globecom)*, pp. 2059–2063, November 1995.

[102] J. O'Rourke, *Computational Geometry in C.* Trumpington St., Cambridge, UK: Cambridge University Press, 1994.

[103] D. S. Broomhead and D. Lowe, "Multivariable Function Interpolation and Adaptive Networks," *Complex Systems*, vol. 2, pp. 321–355, 1988.

[104] M. J. D. Powell, "Radial Basis Functions for Multivariable Interpolation: A Review," in *Algorithms for Approximation* (J. Mason and M. Cox, eds.), pp. 143–167, Oxford: Clarendon Press, 1987.

[105] D. G. M. Cruickshank, "Radial Basis Function Receivers for DS-CDMA," *IEE Electronic Letters*, vol. 32, pp. 188–190, February 1996.

[106] U. Mitra and H. V. Poor, "Neural Network Techniques for Adaptive Multiuser Demodulation," *IEEE Journal on Selected Areas in Communications*, vol. 12, pp. 1460–1470, December 1994.

[107] R. Arnott, "Adaptive Radial Basis Function Diversity Combiner for Multipath Channels," *IEE Electronic Letters*, vol. 29, pp. 1092–1094, June 1993.

[108] S. Theodoris, C. F. N. Cowan, C. P. Callender, and C. M. S. See, "Schemes for Equalisation of Communication Channels with Nonlinear Impairments," *Proceedings of the IEE: Communications*, vol. 142, pp. 165–171, June 1995.

[109] R. Sproull, "Refinements to Nearest Neighbour Searching in k-Dimensional Trees," *Algorithmica*, vol. 6, pp. 579–589, 1991.

[110] J.-D. Boissonnat, M. Sharir, B. Tagansky, and M. Yvinec, "Voronoi Diagrams in Higher Dimensions under Certain Polyhedral Distance Functions," *Proceedings of the 11th Annual Symposium on Computational Geometry, Vancouver, Canada*, pp. 79–88, 1995.

[111] S. Kapoor and M. Smid, "New Techniques for Exact and Approximate Dynamic Closest-Point Problems," *Proceedings of the 10th Annual Symposium on Computational Geometry, Stony Brook, New York, USA*, pp. 165–174, 1994.

[112] E. Walach and B. Widrow, "The Least Mean Fourth (LMF) Adaptive Algorithm and its Family," *IEEE Transactions on Information Theory*, vol. IT-30, pp. 275–283, 1984.

Appendix A

List of original publications

The original publications arising from this work are as follows:-

- "Convolutional Coding Strategies for DS-CDMA Cellular Communications", by I.W. Band & D.G.M. Cruickshank, published in Proceedings of the 4th IEEE ISSSTA, Mainz, Germany, 1996
- "Efficient Bandwidth Utilisation for CDMA Systems Using Convolutional Codes", by I.W. Band & D.G.M. Cruickshank, published in Proceedings of the IEEE Globecom, London, 1996
- A paper based on the work presented in Chapter 5, entitled "Improving the Capacity of CDMA systems using Convolutional Coding and Interference Cancellation" was submitted in November 1996, and re-submitted in revised form in October 1997 for publication in the *IEE Proceedings:Communications*
- A paper based on the work presented in Chapter 6 and entitled "Complexity Reduction of RBF Network Receiver Structures for DS-CDMA via Kernel Modification and Nearest Neighbour Selection" was submitted in August 1997 to the *IEEE Journal on Selected Areas in Communications*

The above papers are reproduced here.

In addition, part of the work presented in Chapter 4 has been accepted for publication as a chapter of the book "Communications and Coding" (Honary & Darnell, eds) to be published by Research Studies Press Ltd. in 1998.

Convolutional Coding Strategies for Code Division Multiple Access Cellular Communications

I.W. Band* Dr. D.G.M. Cruickshank†

Signals & Systems Group,
Electrical Engineering Department,
Kings Buildings,
University of Edinburgh,
Edinburgh, EH9 3JL, UK
Tel : +44 (0) 131 650 5659
Fax : +44 (0) 131 650 6554

Abstract This paper investigates the use of non-linear convolutional coding techniques for use in a DS-CDMA cellular communication system. Comparisons are made between various error-correction strategies and the Wiener minimum mean square error receiver filter, implemented with the same bandwidth expansion. The use of Gold codes in conjunction with an orthogonal convolutional encoder is shown to produce comparable performance to conventional convolutional coding for single user environments, and to yield reasonable capacity potential for low numbers of users. Future developments are indicated, including the possible application of this system to multipath channels.

I. Introduction

The demand for increased capacity of cellular mobile phone systems is projected [1] to reach some 40 million users in Europe alone by the end of the century. Current digital systems such as the European Global System for Mobiles (GSM), which use time as the discriminant between users to provide multiple access (TDMA), are in competition with potentially higher capacity [2, 3] code division multiple access (CDMA) systems, such as that detailed in the IS-95 Interim Standard for mobile communications [4]. CDMA systems gain a multi-user capability from the shared use of the expansion of signal bandwidth afforded from [5]

$$C = W Log_2(1 + \frac{P}{N}) \qquad (1)$$

where C is the capacity, W the bandwidth and $\frac{P}{N}$ the signal to noise power ratio.

Specific problems are associated with the signal paths from the base station to the mobile receiver (downlink) and the reverse path (uplink). On the downlink, the signal may be subject to the effects of multipath and fading, whilst synchronisation and power control (the near-far problem) are additionally important in the uplink.

In this paper, we restrict attention to the downlink of a synchronous Direct Sequence Code Division Multiple Access (DS-CDMA) cellular communication system employing BPSK symbol modulation, and consider methods of combatting errors through the use of non-linear convolutional codes. The noisy environment considered here is due only to Multiple Access Interference (MAI) from competing users and Additive White Gaussian Noise (AWGN) which may be taken to represent either system or thermal noise.

The performance in AWGN (in terms of the average number of errors over a suitably large number of Monte Carlo simulations) may be considered as a function of the quantity $\frac{E_b}{N_0}$, given by

$$\frac{E_b}{N_0} = \left(\frac{M}{2\sigma^2}\right) \qquad (2)$$

where σ^2 is the signal to noise power variance and M is the bandwidth expansion or processing gain used. The decibel form of $\frac{E_b}{N_0}$ is used in the calculations.

It is envisaged that this work will eventually be incorporated into an environment with fast Rayleigh fading, such as those defined *e.g.* in [6], where preliminary analyses have shown low processing gain values are more suitable, especially with adaptive algorithms. To satisfy this criteria, and also so that the processing gain is a power of 2, for reasons which will become apparent later, we have chosen $M = 8$ for all the simulations reported here.

The focus of the work presented here is on comparing the relative performance of the various techniques, implemented with equal overall processing gain, with that of the Wiener

*Ian.Band@ee.ed.ac.uk
†David.Cruickshank@ee.ed.ac.uk

receiver filter, previously detailed in [7].

Breifly, the Wiener filter gives the weights for the taps of the receiver filter as

$$\underline{h}_{Wiener} = \Phi_{yy}^{-1}\underline{\phi}_{yx} \quad (3)$$

where Φ_{yy} is the autocorrelation matrix of the signal vector $\underline{y}$ input to the receiver, and $\underline{\phi}_{yx}$ is the cross-correlation vector between $\underline{y}$ and the original data symbol x.

This technique requires *a priori* information of all the users' spreading codes and an estimate of $\frac{E_b}{N_0}$, but is the minimum mean square error linear receiver and so is of use as a benchmark against which any proposed strategy must be compared.

The next section describes the various techniques to be studied, while section III presents some results. Finally, section IV discusses the implications of these results with emphasis on future developments.

II. Coding Strategies

In this section, we describe a number of techniques involving the use of non-linear convolutional coding of data to increase the probability of decoding the received data stream with as few errors as possible. This may be viewed as an alternative form of spreading the spectrum of a signal, in which the convolutional code provides the encoded signal, rather than conventional DS-CDMA, in which the chips are simply modulations of pseudo-noise sequences.

Convolutional Encoding

Convolutional encoding [8] is a popular form of forward error correction (FEC), where the output n data chips are a function of the incoming b data bits and the connections of a set of serial shift registers to a set of modulo-2 adders. The number of shift registers is termed the constraint length, K, and the rate of the code is defined as the ratio of input to output digits ($\frac{b}{n}$). Conventionally, the particular configuration is denoted by the octal form of the connections to the mod-2 adder. As an example, the rate $\frac{1}{2}$ constraint length 3 convolutional encoder denoted by $(7,5)$ is shown in figure 1.

Decoding of the convolutionally-encoded data is here performed using the Viterbi Algorithm [9]. Since many subtle variants of this algorithm are frequently employed, it is useful to state explicitly the assumptions made and procedures carried out in this implementation.

The Viterbi Algorithm The Viterbi Algorithm is a maximum likelihood (ML) decoding algorithm [10], which proceeds by constructing a trellis; the surviving branches of which are determined by a comparison between the actual received and possible received signals. If the incoming data samples are first quantised to binary data the process is termed hard decision, while if a higher degree of quantisation is employed and retained for the comparisons, the decoder is said to be using soft decision. The latter improves performance by around $2dB$ for most values of $\frac{E_b}{N_0}$ [11], and is the scheme adopted here.

After an appropriate amount (corresponding to the survivor path length, L) of data has been received and analysed, the algorithm makes a decision on the optimal path back through the trellis and hence deduces the initial data bit. Thus, a decision is only made on a particular data bit after code sequences from the next L data bits have been received. In this implementation, the trellis is re-calculated for each new bit entering the receiver, so that the system approximates to periodically sampling an infinitely long trellis. It has been shown [11] that, provided the survivor path length is chosen greater than 4-5 times the constraint length, this does not adversely affect the performance of the Viterbi algorithm. In the investigations here, L is set to 32.

Multiple Access Convolutional Codes In order to accommodate more users, different convolutional codes (and therefore different trellis structures) are assigned to each user. Due to the short constraint length codes used here, the number of adequate (in terms of mean free distance) connections are limited. Since the optimal connections for a rate $\frac{1}{4}$ code are $(5,7,7,7)$ [12], the connections used here are chosen as follows :-

User	Connection
1	(5,7,7,7,5,7,7,7)
2	(7,5,7,7,7,5,7,7)
3	(7,7,5,7,7,7,5,7)
4	(7,7,7,5,7,7,7,5)
....	.....

The use of longer constraint length codes, and hence a greater choice of connections may be expected to give better performance, nonetheless the shorter codes are retained here for comparison.

The Orthogonal Convolutional Encoder

The orthogonal (or Hadamard) convolutional encoder [13] incorporates a second set of shift registers connected in parallel with the conventional convolutional encoding set. An example of this arrangement is shown in figure 2, which demonstrates the case for a rate $\frac{1}{8}$ constraint length 3 system. The switches at the output of this secondary set are toggled at rates 1, 2, 4, *etc* so that for each data bit input to the top register-set, a unique 2^K-length Walsh code [14] is output. This is the prime motivation for choosing 8 as the processing gain of the previous convolutional coding systems, to enable a direct comparison between the systems.

Multiple access is acheived by assigning each user a unique

1-1 mapping between the two sets of shift registers[15]. The particular Walsh code output thus depends on three quantities; the incoming data bit, the present state of the upper register system, and the arrangement of connections between the two set of registers. Note that this now reduces the effective number of degrees of freedom of the code, since the output code rate is now determined completely by the constraint length, rather than in the conventional case, where these two parameters are independent.

Orthogonal Codes with Random codes

The use of additional Pseudo-Noise (PN) codes has been proposed by Ormondroyd and Maxey [16] to improve the spectral characteristics of the Walsh codes, thus increasing the ability of the scheme to separate users. No additional spectrum spreading is produced by this stage, in which competing users are assigned different random codes, and the output from each orthogonal convolutional encoder is simply multiplied chip-by-chip by the appropriate random code. These random codes have been selected to be the same 8-chip codes used in the Wiener filter calculations, so that no artificial bias is introduced.

Orthogonal codes with Gold codes Finally, we consider the use of Gold codes [17, 18] to modulate the encoded data, rather than using random codes. The motivation for this comes from the conventional synchronous DS-CDMA system in AWGN, where the use of Gold codes to spread the data is more beneficial than random codes, due to the improved cross-correlation qualities of the Gold codes. For this reason, the use of Gold codes is anticipated to give increased separation between users, and that the subsequent performance increase will continue with increasing processing gain. It must be acknowledged that these benefits will be nullified if a multipath channel is considered. Due to the chosen processing gain of 8, we have selected 7-chip Gold codes for this application, augmenting them by a single digit to give a set of extended Gold codes.

III. Results

In this section, we present the results of the various techniques described previously. Without loss of generality, we may concentrate attention on user 1 in the calculation of the performance curves. The basic system diagram is shown in figure 3 in which the encoder element is either a conventional convolutional encoder, or an orthogonal convolutional encoder, and the switches may be set to modulate the output from the encoder by either a random code or a Gold code or not at all. In this way, the effects of the various stages may be considered separately. The output from each user, however coded and/or modulated, is then added coherently to that from the other users to form the transmitted signal vector $\underline{s}$. Additive White Gaussian Noise is then added to form the input to the receiver, $\underline{y}$, where the signal is de-modulated if necessary and then passed on to the Viterbi Decoder, the output from which forms the estimate of the data, $\hat{x}_1$. The ratio of the number of errors to the total number of transmitted data values (typically 1 million trials are performed) forms the main output statistic (Pe), which may be calculated as a function either of number of users for a fixed background noise level, as in the first case, or of background noise level for a fixed number of users, considered in cases 2 and 3.

Case 1: Performance with Number of Users

Figure 4 shows the performance of the various techniques with increasing numbers of users for $\frac{E_b}{N_0} = 5dB$. As may be seen, none of the proposed schemes approach the performance of the Wiener filter for 2 or more users, although they all have lower average error probability when only 1 user is present, as expected.

The performance of the conventional convolutional coding system rapidly deteriorates with increasing users. This result is probably due to the inadequacies of the short constraint length connections used, since the error-correcting capabilities of the codes are being compromised by the contribution from the additional users. The unmodulated orthogonal code system performs better, while the addition of random spreading codes produces a further improvement in performance. Incorporation of Gold codes appears to increase the capacity yet further, at least for low numbers of users, although with such short codes, it would be difficult to claim any significant improvement.

Case 2: Performance against $\frac{E_b}{N_0}$ for 2 users

A more detailed analysis of the 2-user case is shown in figure 5, which shows the performance for a range of noise values. It may be seen that the random codes performance is similar to that when using Gold codes, both systems approaching the minimum mean square error curves. The use of orthogonal or conventional convolutional coding schemes leads to much poorer results. This is probably due to clashes where the same output sequence is generated simultaneously by different users, causing the Viterbi Algorithm to lock on to the wrong path. This situation cannot be resolved by any receiving methodology, but it may be expected that fewer such instances would occur for longer constraint-length codes.

Case 3: Performance against $\frac{E_b}{N_0}$ for 3 users

The 3-user performance curves in Gaussian noise are shown in figure 6. While, as expected, the performance of both the conventional and pure orthogonal systems is now becoming unreliable, the performance of the orthogonal with Gold codes system is now better than that of the orthogonal with random codes. This is probably due to the better cross-correlation values of the Gold codes, enabling the system to cope with more users. The use of longer constraint length code sets with *e.g.* 31-chip Gold codes as modulators may be expected to give even better performance.

IV. Discussion & Future Work

This paper has compared the performance of a number of strategies based on error-correcting codes for use in a DS-CDMA system. The use of orthogonal convolutional codes, together with Gold codes to improve the spectral characteristics of the output Walsh codes, rather than produce any further spreading of the signal spectrum, has been shown to produce performance characteristics comparable to those of conventional convolutional coding for single user scenarios, while permitting reasonable performance for low numbers of competing users.

An obvious development of the work would be to investigate this promising behaviour for longer constraint-length spreading codes, and larger capacity modulating codes such as 31-chip Gold codes.

Another development would be to investigate the suitability of this technique to multipath environments such as those defined in the COST 207 study. A possible difficulty with multipath environments is that the improved performance of the orthogonal Gold code system may be adversely affected, since the advantages of better cross-correlation values with Gold codes may be outweighed by intersymbol interference (ISI). It is anticipated that this will form the next development of this work.

V. Acknowledgement

The authors gratefully acknowledge the support of this work by the UK Engineering and Physical Sciences Research Council, through Grant GR/J46401.

References

[1] I. Groves, "Advances in Personal Communication Services", Proceedings of the IEEE 5th International Symposium on Personal, Indoor and Mobile Radio Communications (PIMRC), The Hague, The Netherlands, vol. 1, pp. 11–14, 1994.

[2] K. Gilhausen, I. Jacobs, R. Padovani & L. Weaver, Jr., "Increased Capacity using CDMA for Mobile Satellite Communication", IEEE Journal Sel. Areas Commun., vol. 8, pp. 503–514, 1990.

[3] R. Kohno, P. Rapajic & B. Vuctetic, "An Overview of Adaptive Techniques for Interference Minimization in CDMA Systems", Wireless Personal Communications, vol. 1, pp. 3–20, 1994.

[4] TIA/EIA/IS-95, Mobile Station-Base Station Compatibility Standard for Dual Mode Wide-Band Spread Spectrum Cellular Systems. Telecommunication Industry Association, 1993.

[5] C. Shannon, "Communication in the Presence of Noise", Proc. IRE, vol. 37, pp. 10–21, 1949.

[6] M. Failli (ed.), Digital Land Mobile Radio Communications - COST 207 : Final Report. Commision of the European Communities, Luxembourg, 1989.

[7] D. Cruickshank, "Optimal and Adaptive FIR Filter Receivers for DS-CDMA", Proceedings of the IEEE 5th International Symposium on Personal, Indoor and Mobile Radio Communications (PIMRC), The Hague, The Netherlands, pp. 1339–1345, 1994.

[8] P. Grant, C. Cowan, B. Mulgrew & J. Dripps, Analogue and Digital Signal Processing and Coding. Chartwell-Bratt, Bromley, UK, 1989.

[9] A. Viterbi, "Error Bounds for Convolutional Codes and an Asymptotically Optimum Decoding Algorithm", IEEE Trans. Inf. Theory, vol. IT-13, pp. 260–269, 1967.

[10] H.-L. Lou, "Implementing the Viterbi Algorithm", IEEE Signal Processing Magazine, pp. 42–52, 1995.

[11] J. Heller & I. Jacobs, "Viterbi Decoding for Satellite and Space Communication", IEEE Trans. Commun., vol. COM-19, pp. 835–848, 1971.

[12] K. Larsen, "Short Convolutional Codes with Maximal Free Distance for Rates $\frac{1}{2}$, $\frac{1}{3}$, and $\frac{1}{4}$", IEEE Trans. Inf. Theory, vol. IT-18, pp. 371–372, 1973.

[13] A. Viterbi, "Very Low Rate Convolutional Codes for Maximum Theoretical Performance of Spread Spectrum Multiple Access Channels", IEEE Journal Sel. Areas Commun., vol. 8, pp. 641–649, 1990.

[14] K. Beauchamp, Walsh Functions and their Applications. Academic Press, London, 1975.

[15] J. Maxey, Private Communication.

[16] R. Ormondroyd & J. Maxey, "A High Performance CDMA Cellular Radio System Based on Low-Rate Convolutional Coding", IEE Conference on Radio Receivers and Associated Systems, Bath, UK, pp. 17–21, 1995.

[17] R. Gold, "Maximal Recursive Sequences with 3-valued Recursive Cross-correlation Functions", IEEE Trans. Inf. Theory, vol. IT-14, pp. 154–156, 1968.

[18] D. Sarwate & M. Pursley, "Cross-correlation Properties of Pseudorandom and Related Sequences", Proceedings of the IEEE, vol. 68, pp. 593–619, 1980.

Figures

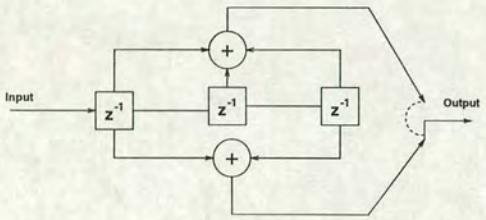

Figure 1: *Rate $\frac{1}{2}$, Constraint Length 3 (7,5) Convolutional Encoder*

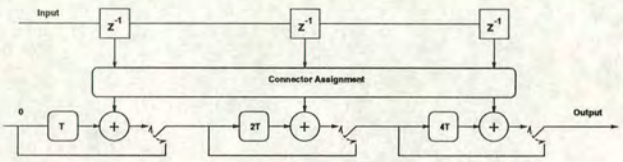

Figure 2: *Rate $\frac{1}{8}$ Orthogonal Convolutional encoder*

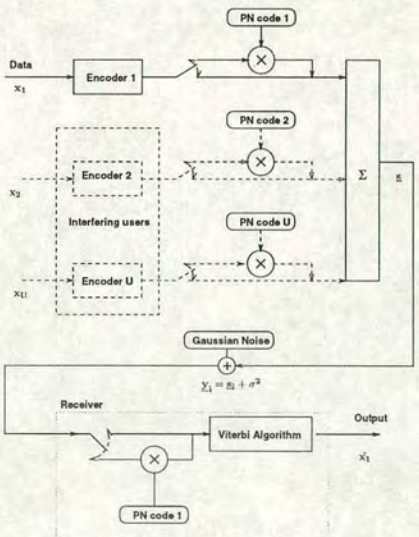

Figure 3: *Flow of data*

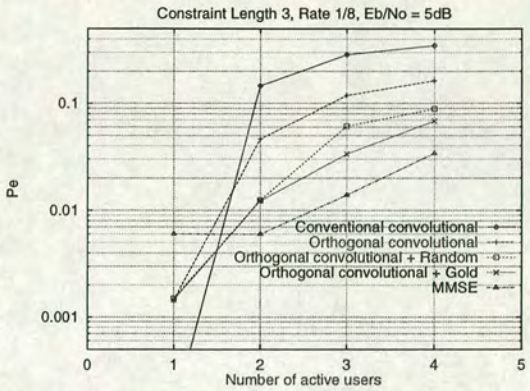

Figure 4: *Probability of error vs Number of active users for the various schemes*

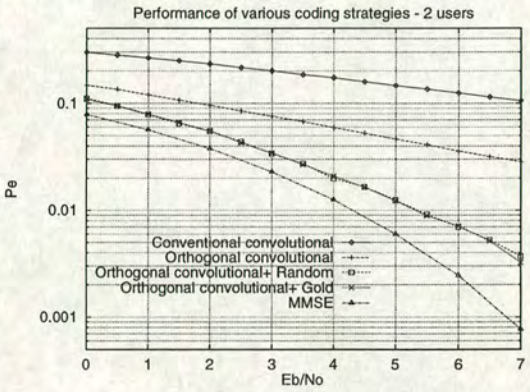

Figure 5: *Performance of various techniques for 2 users*

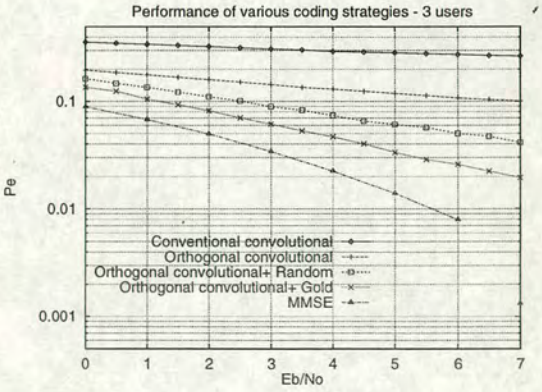

Figure 6: *Performance of various techniques for 3 users*

Efficient Bandwidth Utilisation for CDMA Using Convolutional Codes

I.W. Band* D.G.M. Cruickshank†

Department of Electrical Engineering, University of Edinburgh, EH9 3JL, UK
+44 131 650 5659

ABSTRACT This paper investigates the use of non-linear convolutional coding techniques for use in a DS-CDMA cellular communication system. Particular attention is paid to the relative proportions of convolutional coding and direct sequence spreading which offer the most efficient use of the available processing gain. The dependency of the optimal strategy on various factors, including background noise level, number of active users and coding power is discussed. Future developments are indicated including the possible application of this system to multipath channels, and the use of other coding structures.

1 Introduction

The demand for increased capacity of cellular mobile phone systems is projected [1] to reach some 40 million users in Europe alone by the end of the century. Current digital systems such as the European Global System for Mobiles (GSM), which use time as the discriminant between users to provide multiple access (TDMA), are in competition with potentially higher capacity [2, 3] code division multiple access (CDMA) systems, such as that detailed in the IS-95 Interim Standard for mobile communications [4].

In this paper, we study the downlink (Base station to Mobile) of a bit and chip-synchronous Direct Sequence Code Division Multiple Access (DS-CDMA) cellular communication system, and consider methods of combatting errors by introducing non-linear convolutional codes. The efficient use of signal bandwidth is of primary concern in practical cellular communications applications, so we consider the performance of various systems comprising different proportions of convolutional encoding and direct sequence spreading, whilst maintaining a given overall bandwidth expansion.

Boudreau [5] has calculated the theoretical performance (in terms of Chernoff upper bounds) of systems employing convolutional coding (and trellis coding) as a natural extension of the conventional CDMA principle. The performance of actual systems, however, may be significantly superior (as much as $1.5dB$ in some cases); this improvement being a non-linear function of $\frac{E_b}{N_o}$. The limited amount of simulations in [5] means that it is instructive to consider the simulated performance of such systems.

*Ian.Band@ee.ed.ac.uk
†David.Cruickshank@ee.ed.ac.uk

The noisy environment considered here is due only to Multiple Access Interference (MAI) from competing users and Additive White Gaussian Noise (AWGN) which may be taken to represent either system or thermal noise. The performance in AWGN (in terms of the average number of errors over a large number of Monte Carlo simulations) may be expressed in terms of the decibel form of the quantity $\frac{E_b}{N_0}$, given by

$$\frac{E_b}{N_0} = \left(\frac{M}{2\sigma^2}\right) \quad (1)$$

where σ^2 is the signal to noise power variance and M is the bandwidth expansion or processing gain used.

The next section describes convolutional encoding and decoding in more detail, while section 3 presents some results. Finally, section 4 discusses the implications of these results with emphasis on future developments.

2 Coding Strategies

In this section, we briefly describe the use of non-linear convolutional codes to decrease the probability of error, discuss the decoding algorithm employed and give details of the particular configurations used in this study.

Convolutional Encoding [6] is a popular form of forward error correction (FEC), in which the output C data chips are a function of the incoming b data bits and the connections of a set of serial shift registers to a set of modulo-2 adders. The number of shift registers is termed the constraint length, K, and the rate R of the code is defined as the ratio of input to output digits ($\frac{b}{C}$). In this study, we confine simulations to convolutional codes with $b = 1$ and values of C of 2,4,8 and 16.

The Viterbi Algorithm [7] is a maximum likelihood (ML) decoding algorithm [8], which proceeds by constructing a trellis; the surviving branches of which are determined by a comparison between the actual received and possible received signals. If the incoming data samples are first quantised to binary data the process is termed hard decision, while if the floating point values are retained for the comparison, the decoder is said to be employing soft decision. The latter improves performance by around $2dB$ for most values of $\frac{E_b}{N_0}$ [9], and is the scheme adopted here.

After an appropriate amount (corresponding to the survivor path length, L) of data has been received and ana-

lysed, the algorithm makes a decision on the optimal path back through the trellis and hence deduces the initial data bit. Thus, a decision is only made on a particular data bit after code sequences from L data bits have been received.

Convolutional Code Configurations: It has been shown [9] that, provided the survivor path length is chosen greater than 4-5 times the constraint length, the performance of the Viterbi algorithm is not adversely affected. In the investigations here, L is set to 32, and the values for R and M are shown in table 1, which provides the octal format of the tap connections used for the convolutional codes. It may be seen that the rates of the codes and the lengths of the corresponding PN-sequences have been selected to maintain an overall processing gain (denoted PG in the table) of around 500. The choice of tap connections for rates $\frac{1}{2}$ ($M = 255$ [1]) and $\frac{1}{8}$ ($M = 63$) mirror those in [5] for constraint lengths 3,4 and 5 whilst those for $R = \frac{1}{4}$ are motivated by the results of Larsen [11]. While it is acknowledged that the repetition of the rate $\frac{1}{8}$ code to form the rate $\frac{1}{16}$ code may be sub-optimal, especially for the larger constraint-length systems, this configuration is liable to have similar properties to any optimal arrangement, and is thus employed here.

Table 1: Convolutional codes used in the simulations

K	$R = \frac{1}{2}$ $M = 255$, $PG = 510$	$R = \frac{1}{4}$ $M = 127$, $PG = 508$	$R = \frac{1}{8}$ $M = 63$, $PG = 504$	$R = \frac{1}{16}$ $M = 31$, $PG = 496$
3	(5,7)	(5,7,7,7)	(7,7,7,5,5,5,7,7)	(7,7,7,5,5,5,7,7, 7,7,7,5,5,7,7)
4	(17,15)	(13,15,15,17)	(17,17,13,13,13,15,15,17)	(17,17,13,13,13,15,15,17, 17,17,13,13,13,15,15,17)
5	(23,35)	(25,27,33,37)	(37,33,25,25,35,33,27,37)	(37,33,25,25,35,33,27,37, 37,33,25,25,35,33,27,37)
6	(53,75)	(53,67,71,75)	(53,67,71,75,53,67,71,75)	(53,67,71,75,53,67,71,75, 53,67,71,75,53,67,71,75)

3 Results

In this section, we describe the simulations carried out and present the results of the various scenarios outlined previously. The basic system diagram is shown in figure 1, which also indicates the length of the signal at each of the relevant points.

Referring in more detail to figure 1, the data vector $\underline{x}_1$ of L bits is input to the convolutional encoder, and the resulting LC chips of data are then further spread by the user's pseudo-noise (PN) code to produce a signal of LCM chips. This process is repeated over all active users (with the same convolutional code configuration for each user [2]) and the final transmitted signal vector $\underline{s}$ is then constructed by coherently summing the spread signals over all the users. Additive White Gaussian Noise, represented by the vector $\underline{n}$ is then added chip by chip to this signal to form the input to the receiver, $\underline{y}$. This noise-corrupted signal is then de-modulated by first correlating with the first user's spreading code, and then passing on the resulting LC encoded data bits to the Viterbi Decoder; the output from which forms the estimate, $\underline{\hat{x}}_1$, of the original data vector.

The ratio of the number of errors to the total number of transmitted data values forms the main output statistic (Pe), which may be evaluated as a function either of background noise level, considered in the first four case-studies, or of number of active users for a fixed value of $\frac{E_b}{N_0}$, considered in the last two.

In the first four cases, Gold codes are used as the PN sequences and there are 20 active users present, while in cases 5 and 6, random codes have been chosen to spread the convolutionally-encoded data, and the values of $\frac{E_b}{N_0}$ are held fixed at $2.0dB$ and $4.0dB$ respectively. The choice of random codes is motivated by the fact that in a multipath environment such as those defined in the COST 207 study [12], the presence of intersymbol interference will corrupt the near-orthogonal qualities of Gold codes. Note that in this case, the percentage loading is calculated from the number of active users and the overall processing gain (PG), rather than the length of the appropriate PN code.

Case 1: $K = 3$ The first case considered here is for constraint length 3 and is shown in figure 2. Note that, in the figures, the performance of each system is compared with Binary Phase Shift Keying (BPSK) and conventional DS-CDMA with 511-chip Gold codes. R refers to the convolutional code rate, M to the length of the Gold code used in the direct sequence spreading, and PG to the combined processing gain, via $PG = \frac{M}{R}$.

It is apparent that in this case, the rate $\frac{1}{2}$ system performs better than the other configurations, with the rate $\frac{1}{8}$ system also performing well. The relatively poor performance of the rate $\frac{1}{16}$ system is probably due to the increased cross-correlation of these Gold codes (20 users with 31-chip spreading means that the multiple access interference is more significant than the longer PN-code sys-

[1] Strictly, Gold codes of length 255 do not exist[10], however "Gold-like" sequences may be constructed with the required cross-correlation of -1 at the synchronous point. Those used here are obtained from the m-sequences $[8,2,3,4]_s$ and $[8,3,5,6]_s$

[2] This means that the separation of users is achieved solely by the spread spectrum module. A possible development of this which may be considered in the future would be to assign different tap connections for each user

tems), combined with the possible sub-optimality of the convolutional codes. The reason for the anomalously poor performance of the rate $\frac{1}{4}$ system is less clear, although this may simply be an unfortunate combination of rate and constraint length. Further investigations may provide some insight about this behaviour.

Notwithstanding these comments, even the poorest performing convolutional code is still significantly better than the 20-user conventional CDMA system for values of $\frac{E_b}{N_0}$ greater than about $1dB$.

Case 2: $K = 4$ The results for constraint length 4 systems are presented in figure 3, from which it may be seen that the rate $\frac{1}{4}$ and $\frac{1}{8}$ systems, which are now very similar, are slightly better than the rate $\frac{1}{2}$ system, while the rate $\frac{1}{16}$ codes are still suffering from the increased MAI of the 31-chip Gold codes in a similar way to the K=3 case. The improved performance of the rate $\frac{1}{4}$ system is probably due to the more diverse use of tap connections here than in the previous case. Where a greater variety of tap connections is available, it is prudent to make as full use of them as possible, thus increasing the power of the code and permitting more resources (bandwidth) to be invested in the direct spreading part, to allow greater capacity.

Thus, while the choice of rate and constraint length are notionally independent, the use of appropriate rate codes, which make use of the full range of available connections for a given constraint length can lead to marked improvements in performance.

Case 3: $K = 5$ Figure 4 shows the results obtained using systems with constraint length 5. This appears to confirm the trend noted in case 2, namely that the systems with rates $\frac{1}{2}$ and $\frac{1}{16}$ are inferior to those with rates $\frac{1}{4}$ and $\frac{1}{8}$, which make more efficient use of the increased performance, by virtue of their larger constraint lengths, of the convolutional codes. A point of interest is that now the rate $\frac{1}{16}$ codes are better than the rate $\frac{1}{2}$ system. This is again due to more efficient use of available connections, which is beginning to compensate for the greater MAI of the 31-chip spreading module, in contrast with the first two cases with their shorter constraint lengths.

The performance of the rate $\frac{1}{2}$ system at $\frac{E_b}{N_0}$ values lower than around $1dB$ is also worthy of note, since it is now inferior to conventional CDMA. This is probably also due to the increased power of the convolutional codes, since more errors are introduced from the Viterbi algorithm losing track of the correct path through the trellis. Thus it is not always beneficial simply to increase the constraint length independently, since more errors may be introduced under increased-noise environments. This effect will be examined in more detail in case 5, in which the additional noise will be due to increasing numbers of users.

Case 4: $K = 6$ For constraint length 6, shown in figure 5, the trend outlined previously is reinforced, with the rate $\frac{1}{8}$ and rate $\frac{1}{4}$ systems better than the rate $\frac{1}{16}$ and $\frac{1}{2}$ systems, respectively. The rate $\frac{1}{16}$ system has better performance than before, since again, more efficient use is made of the available tap connections.

As in case 3, the rate $\frac{1}{2}$ system performs significantly poorer than the conventional case for $\frac{E_b}{N_0}$ values below around $1dB$. This is again due to the Viterbi algorithm producing a higher number of errors when an incorrect path through the trellis is selected. Thus, care needs to be exercised when employing a long constraint length, high rate convolutional code under conditions of high noise.

Case 5: $\frac{E_b}{N_0} = 2.0dB$ The performance of these systems with varying numbers of active users may be judged from figure 6, for which the background noise level is set at $2.0dB$ (equivalent to $5.0dB$ signal-to-noise ratio). In this case, at least 1000 errors have been detected for each point on the curves and constraint lengths of 3 and 6 are employed. Random codes are used as the PN sequences to more closely model practical situations, and this means that the trends seen through the previous cases will be accentuated.

For very low loading (around 2 %), the systems behave much as would be expected, although the $K = 3$, rate $\frac{1}{16}$ system performs even worse than conventional CDMA, and the $K = 3$ rate $\frac{1}{4}$ system is only marginally better. In general, the $K = 6$ systems have better performance, due to the increased power of the codes, however it is interesting that even for very low numbers of users, the rate $\frac{1}{2}$ $K = 3$ and $K = 6$ systems are very similar.

As the loading is increased, various effects may be seen. In particular, the only systems which continue to outperform conventional CDMA are the $K = 6$ rate $\frac{1}{4}$ and $K = 3$ rate $\frac{1}{2}$ configurations. These systems represent the most efficient use of the combination of rate, constraint length (and hence code performance) and spreading capacity, and thus have superior performance.

Significantly, the $K = 6$ rate $\frac{1}{8}$ combination, which appeared to be the best for the previous cases with 20 users using Gold codes, does not have such good performance using random codes as the number of users is increased. In addition, the $K = 6$ rate $\frac{1}{2}$ combination has poorer performance than the equivalent $K = 3$ system. Although this may at first appear counter-intuitive, the reason is due to the increased overall noise causing the Viterbi algorithm to lock on to the wrong path through the trellis, and hence produce more errors, analogous to the noisy situations in cases 3 and 4.

Case 6: $\frac{E_b}{N_0} = 4.0dB$ The equivalent results for $\frac{E_b}{N_0} = 4.0dB$ are shown in figure 7. This confirms some of the results in the previous case; specifically, that although the $K = 6$ rate $\frac{1}{2}$ system is better for low loading, as the loading is increased its performance becomes worse than the same rate $K = 3$ system, and that the beneficial effects of most convolutional coding systems are lost as the loading increases. As in the previous case, the optimal system as the number of users is increased is that using $K = 6$ rate $\frac{1}{4}$ convolutional codes, with 127-chip spreading codes.

4 Discussion & Future Work

This paper has compared the simulated performance of a number of strategies utilising non-linear convolutional codes combined with pseudo-noise spreading codes for use in a processing-gain limited DS-CDMA cellular communication system. Convolutional codes with constraint lengths up to $K = 6$ have been considered, with rates of $\frac{1}{2}$, $\frac{1}{4}$, $\frac{1}{8}$ and $\frac{1}{16}$, together with appropriate length spreading sequences.

With an overall processing gain of approximately $27dB$ and 20 active users, the optimal strategy seems to be the combination of a constraint length 6, rate $\frac{1}{8}$ convolutional code and 63-chip Gold spreading codes, although increasing the constraint length may cause a different rate to be optimal. Increasing the number of users and employing random spreading sequences means that this arrangement is no longer optimal, and that convolutional codes of the same constraint length but rate $\frac{1}{4}$ should be used instead. The ill-effects of simply increasing the constraint length without a corresponding adjustment of the code rate are also demonstrated.

These observations serve to exhibit the fine balance that exists between the power of the convolutional code (obtained from its rate and constraint length), the capacity of the spreading sequences and the noise level, whether from the background or from other subscribers on the system.

A development of the work would be to investigate the performance of these techniques in multipath environments such as those defined in the COST 207 study. Alternative methods of convolutional encoding [13, 14] may also prove useful in future studies.

Acknowledgement The authors would like to acknowledge the financial support of this project by the Engineering and Physical Sciences Research Council, through Grant GR/J46401.

References

[1] I. Groves, "Advances in Personal Communication Services," *Proceedings of the IEEE 5th International Symposium on Personal, Indoor and Mobile Radio Communications (PIMRC), The Hague, The Netherlands*, vol. 1, pp. 11–14, Sep 1994.

[2] K. Gilhausen, I. Jacobs, R. Padovani, and L. Weaver, Jr., "Increased Capacity using CDMA for Mobile Satellite Communication," *IEEE Journal Sel. Areas Commun.*, vol. 8, pp. 503–514, May 1990.

[3] R. Kohno, P. Rapajic, and B. Vuctetic, "An Overview of Adaptive Techniques for Interference Minimization in CDMA Systems," *Wireless Personal Communications*, vol. 1, no. 1, pp. 3–20, 1994.

[4] TIA/EIA/IS-95, *Mobile Station-Base Station Compatibility Standard for Dual Mode Wide-Band Spread Spectrum Cellular Systems.* Telecommunication Industry Association, 1993.

[5] G. Boudreau, D. Falconer, and S. Mahmoud, "A Comparison of Trellis Coded Versus Convolutionally Coded Spread Spectrum Multiple Access Systems," *IEEE Journal Sel. Areas Commun.*, vol. 8, pp. 628–640, May 1990.

[6] P. Grant, C. Cowan, B. Mulgrew, and J. Dripps, *Analogue and Digital Signal Processing and Coding.* Bromley, UK: Chartwell-Bratt, 1989.

[7] A. Viterbi, "Error Bounds for Convolutional Codes and an Asymptotically Optimum Decoding Algorithm," *IEEE Trans. Inf. Theory*, vol. IT-13, pp. 260–269, April 1967.

[8] H.-L. Lou, "Implementing the Viterbi Algorithm," *IEEE Signal Processing Magazine*, pp. 42–52, September 1995.

[9] J. Heller and I. Jacobs, "Viterbi Decoding for Satellite and Space Communication," *IEEE Trans. Commun.*, vol. COM-19, no. 5, pp. 835–848, 1971.

[10] D. Sarwate and M. Pursley, "Cross-correlation Properties of Pseudorandom and Related Sequences," *Proceedings of the IEEE*, vol. 68, pp. 593–619, May 1980.

[11] K. Larsen, "Short Convolutional Codes with Maximal Free Distance for Rates $\frac{1}{2}, \frac{1}{3}$, and $\frac{1}{4}$," *IEEE Trans. Inf. Theory*, vol. IT-18, pp. 371–372, 1973.

[12] M. Failli, ed., *Digital Land Mobile Radio Communications - COST 207 : Final Report.* Luxembourg: Commision of the European Communities, 1989.

[13] A. Viterbi, "Orthogonal Tree Codes for Communication in the Presence of White Gaussian Noise," *IEEE Trans. Commun.*, vol. COM-15, pp. 238–242, April 1967.

[14] R. Ormondroyd and J. Maxey, "A High Performance CDMA Cellular Radio System Based on Low-Rate Convolutional Coding," *IEE Conference on Radio Receivers and Associated Systems, Bath, UK*, pp. 17–21, Sep 1995.

1 Figures

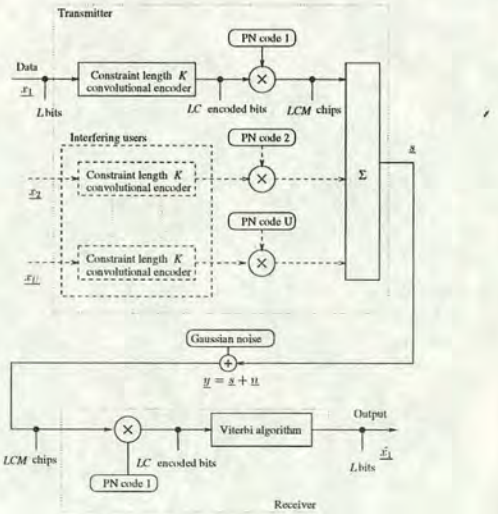

Figure 1: *Flow of data*

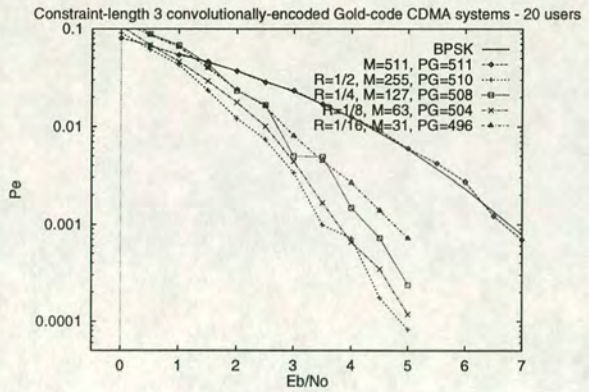

Figure 2: *Performance of K=3 convolutional codes*

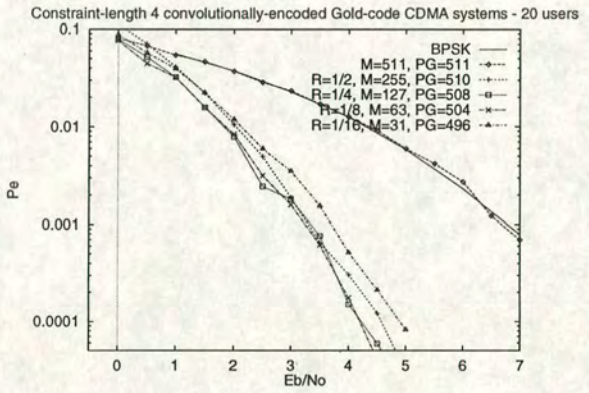

Figure 3: *Performance of K=4 convolutional codes*

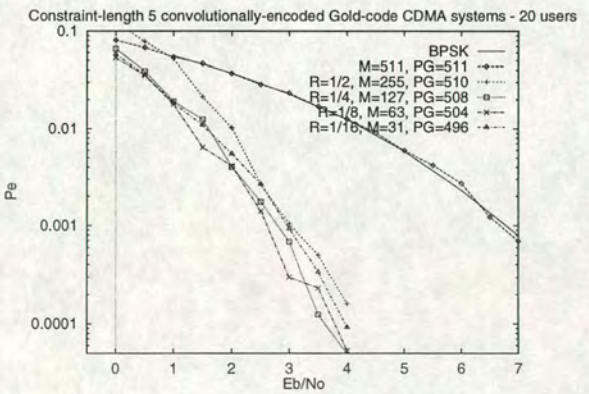

Figure 4: *Performance of K=5 convolutional codes*

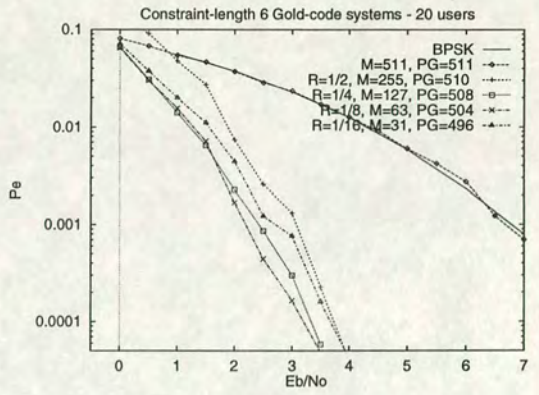

Figure 5: *Performance of K=6 convolutional codes*

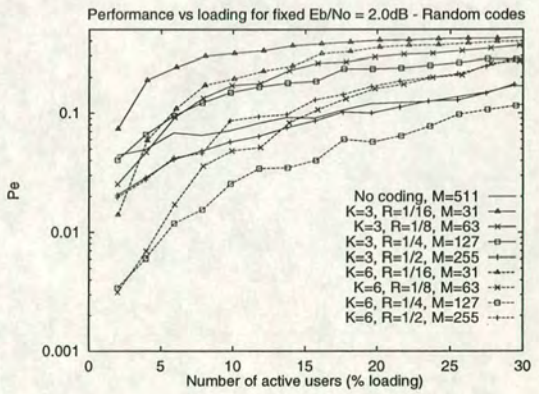

Figure 6: *Performance of K=3 and K=6 convolutional codes for* $\frac{E_b}{N_0} = 2.0dB$

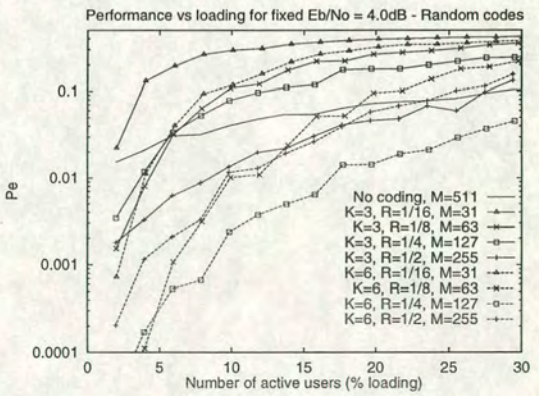

Figure 7: *Performance of K=3 and K=6 convolutional codes for* $\frac{E_b}{N_0} = 4.0dB$

Improving the Capacity of CDMA Systems using Convolutional Coding and Interference Cancellation

I.W. Band* D.G.M. Cruickshank †

Signals & Systems Group,
Electrical Engineering Department,
Kings Buildings,
University of Edinburgh,
Edinburgh, EH9 3JL, UK
Tel : +44 (0) 131 650 5659
Fax : +44 (0) 131 650 6554

Short title: FEC coding and Interference Cancellation Applied to CDMA

Abstract

This paper compares methods of reducing the co-channel interference on a DS-CDMA downlink signal by employing convolutional coding at the base station and a Viterbi decoder as the initial estimator for a parallel cancellation scheme. The combination of a matched filter and the Viterbi algorithm is shown to afford increased performance compared to equivalent bandwidth systems which do not use forward error correction. The use of a Wiener filter to collapse the spectrum of the spread signal leads to even greater capacity improvements. The systems discussed may be implemented with an affordable increase in receiver complexity and processing delay.

1 Introduction

Current predictions [1] for general usage of mobile telecommunications in Europe are beyond that supportable by present systems. One possible contender for efficient use of the limited available bandwidth is direct sequence code division multiple access (DS-CDMA), employing spread spectrum technology. The IS-95 interim standard for CDMA [2], allowing for frequency re-use in neighbouring cells, the even distribution of workload amongst cells, and user-transparent soft hand-off as the call is re-routed from one cell to another, is likely to evolve to be in competition with any schemes chosen for the proposed European Universal Mobile Telecommunication System (UMTS) [3]. Specific characteristics are inherent in CDMA systems however, both in the down-link (Base Station to mobile) and on the reverse path, or up-link.

Those specific to the downlink include the property that all the signals emanate from a common source, so that system resources must be expended on acquiring and maintaining synchronisation with the relevant base station to enable the mobiles to decode the data as reliably as possible.

*e-mail: Ian.Band@ee.ed.ac.uk
†e-mail: David.Cruickshank@ee.ed.ac.uk

The effects of multipath propagation are not considered in this study, although the extension of the systems considered to such realistic environments is an obvious future development.

In this paper, we concentrate on the downlink of a DS-CDMA system, assuming perfect acquisition and synchronisation of the signal, and propose the use of interference cancellation to reduce the multiple access interference (MAI) from competing users, combined with the error-correcting capabilities of convolutional encoding at the transmitter and the Viterbi algorithm (VA) at the receiver to improve the initial estimate inside the canceller. The next section outlines recent related work and section 3 analyses the various systems considered, following which we present some simulation results. Finally, some conclusions are drawn and ideas for future work indicated in section 5.

2 Background

A typical DS-CDMA transmitter is shown in figure 1, in which it may be seen that a sample of the transmitted signal vector $\mathbf{s}$, is generated by the coherent addition of the required user's spreading code (of length N chips) modulated by the required data bit x, to similarly modulated spreading codes for the other users, so that, for a total of U active users, the N-dimensional data vector $\mathbf{y}$ received at the mobile is given by

$$\mathbf{y} = \mathbf{s} + \mathbf{n} = \sum_{j=1}^{U} d_j \mathbf{c}_j + \mathbf{n}, \tag{1}$$

where the data bit $d(j) \in \{-1, +1\}$, the spreading code for user j is $\{\mathbf{c}_{ji}\}_{i=1}^{N}$, and $\mathbf{n}$ is an N dimensional vector of additive white Gaussian noise (AWGN) of variance σ^2. The simplest receiver structure, a matched filter (MF), with tap weights set to the original spreading code, was shown [4] to have relatively poor capacity compared to the minimum mean square error (MMSE), or Wiener filter, which may be successfully approximated via an adaptive algorithm. Convolutional coding [5, 6, 7] is a popular form of error-correction, in which the data bits are converted into a code sequence, which depends not only on the data, but also on the current status of the encoder. DS-CDMA systems are interference limited, predominantly due to MAI from the other active users. The most efficient receivers, therefore, will utilise this knowledge by estimating and subtracting the interfering users' contributions from the suitably delayed received signal, thus increasing the potential of being able to correctly de-correlate this new signal and infer the desired user's data. This is in contrast to joint detection (JD) techniques, which are typically employed on the uplink and have recently received attention as contenders for UMTS through an evolution of the GSM system to include a short-spreading code CDMA portion within an existing GSM timeslot [8]. These multi-user techniques succeed since the interference on all competing users' signals is a sufficient statistic for each data estimate, even though individual soft decisions may not be.

Interference cancellation (IC) was successfully deployed in [9], using a matched filter for the initial estimate, in an asynchronous system using Gold spreading codes. The theoretical analysis of the synchronous system with random spreading codes has been developed in [10], in which a Wiener filter was used for the initial estimate. In [11], a Wiener filter was employed both for the initial estimate and for the final data extraction, and it was there demonstrated that the performance afforded by this arrangement surpassed any other two-stage system.

3 Systems Considered

We take as our common transmitter the system shown in figure 1, whose inputs come from a convolutional coder of rate R, and consider the relative benefits of the four receiver structures shown in figure 2, as compared to a standard matched filter (MF), or matched filter canceller (MFC) receiver, with equivalent processing gain N. The receivers share a common structure; the incoming signal is split into as many parallel paths as required and each replica is correlated with an appropriate de-spreading code. An estimate is then made of the original data bit and the interference is reconstructed and cancelled from a delayed copy of the received signal. This

signal is then despread, before the Viterbi algorithm is applied for the second time to obtain the final data estimate. Although this introduces an extra processing delay since two passes of the decoder are required, the extra delay is linear in the memory of the Viterbi decoder, which is only determined by the constraint length. The complexity and delay associated with two passes of a short constraint length decoder is not exhorbitant when compared to a single pass of a high constraint length decoder, as is currently implemented in the IS-95 system.

3.1 Analysis

Before proceeding to the results from the Monte Carlo simulations, it is instructive to consider an analysis of the expected perfomance of these receivers. It may be shown [10] that the probability of a bit error (p_e) for a single-stage canceller employing matched filters throughout (MFC), without convolutional coding is given by

$$p_e^{MFC}(N, U, E_b/N_0) = Q\left[\sqrt{\frac{N}{\sigma^2 + 4(U-1)p_e^{MF}(N, U, E_b/N_0)}}\right] \tag{2}$$

where

$$p_e^{MF}(N, U, E_b/N_0) = Q\left(\sqrt{\frac{N}{\sigma^2 + (U-1)}}\right) \tag{3}$$

is the error performance of a standard matched filter when U users are operating simultaneously, the signal to Gaussian noise density $E_b/N_0 = N/2\sigma^2$ and $Q(\zeta)$ is the standard Gaussian upper cumulative distribution function. The theoretical analysis [12] of Viterbi decoding of convolutional codes with no MAI leads to the following corresponding expression for $p_e^V(E_b/N_0)$,

$$p_e^V(E_b/N_0) \leq \sum_{d=d_{free}}^{\infty} a_d \phi(d, E_b/N_0) \tag{4}$$

where $\phi(d, E_b/N_0) = Q\left(\sqrt{dRE_b/N_0}\right)$. Regarding the MAI simply as additional noise means that we can combine equations 2 and 4 to give the expected probability of error for receiver structure A, which uses matched filter cancelling with a Viterbi algorithm, or MFC+V, as

$$p_e^{MFC+V}(N, U, E_b/N_0) \leq p_e^V\left(\sqrt{\frac{N}{\sigma^2 + 4(U-1)p_e^{MF}(N, U, E_b/N_0)}}\right) \tag{5}$$

Receiver B is similar to A, except that the intermediate and final de-spreading is achieved by a Wiener filter, as defined in [4]. By analogy with the analysis for receiver A, the expected performance for this receiver may be estimated as

$$p_e^{WFC+V}(N, U, E_b/N_0) \leq p_e^V\left(\sqrt{\frac{N}{\sigma^2 + 4(U-1)p_e^{WF}(N, U, E_b/N_0)}}\right) \tag{6}$$

where $p_e^{WF}(N, U, E_b/N_0)$ is derived in [10]. The intermediate data estimate in the proposed new receiver C is obtained from the use of a Viterbi decoder, so that this is denoted matched Viterbi cancelling with Viterbi, or MVC+V. By a similar argument to the above, the expected performance for this arrangement is given by

$$p_e^{MVC+V}(N, U, E_b/N_0) \leq p_e^V\left(\sqrt{\frac{N}{\sigma^2 + 4(U-1)p_e^{V}(N, U, E_b/N_0)}}\right) \tag{7}$$

Finally, receiver D also has a Viterbi decoder as the initial estimator, but uses a Wiener filter for the de-spreading processes, so will again form a lower bound on the results from an adaptive algorithm.

4 Results

The results presented compare firstly the theoretical performance of the various receiver structures discussed above against the results of Monte Carlo simulations for a fixed background noise level. Then simulations will be considered for a fixed loading. The Viterbi algorithm employed by all the systems uses soft decision decoding and a survivor path length (memory) of 32 data bits. Rate 1/2, constraint length 3 convolutional coding is used for illustrative purposes; the use of more powerful coding may be expected to give suitably enhanced results, at the expense of increased receiver complexity. With the systems using convolutional coding, random codes of length 63 chips are used as the spreading codes, since any multipath channel will likely reduce any special correlation properties of other spreading code sets. For comparison, a standard matched filter (MF) and matched filter canceller (MFC) receiver, without convolutional coding will also be considered, using 126-chip spreading codes, to maintain the same processing gain. To aid comparison, the capacity is expressed as a percentage of the appropriate overall processing gain for the relevant system.

4.1 Theoretical and simulated performance vs capacity for $E_b/N_0 = 5$ dB

Figure 3 shows the predicted theoretical and simulated performances of the various systems for $E_b/N_0 = 5$ dB. As may be seen, the results show reasonable agreement for the matched filter structures, but the simulated performance of the canceller incorporating the Wiener filter is less close to prediction. This is probably due to the accumulation of many assumptions about the Gaussian nature of the multiple access interference, which means that the actual performance is somewhat worse than that predicted. In spite of this, the capacity achieved is significantly improved over the MFC alone. It may be seen that the inclusion of the Viterbi decoder prior to cancellation affords a predicted increase in capacity of approximately 15 %, or 19 users, as compared to the sign-decision approach at a probability of error of around 10^{-3}. This is most likely due to the fact that decisions leading to the wrong code word, or even an impossible code word (since the corresponding transition in the state diagram is impossible), are avoided when the interference is manageable. If the interference becomes too great however, the Viterbi canceller is more likely to be forced into the wrong state, and thus complete code words are in error. This is analogous to the conventional performance of Viterbi decoding of convolutional codes (*e.g.* [7]), where the performance degrades rapidly under high noise conditions. The approximations used for the Viterbi decoder become increasingly less applicable at high interference levels, and this is the reason why the graphs suggest probabilities of error in excess of 0.5.

For low numbers of users, the convolutional coding systems have much better performance than those without, with receiver A supporting 25 users at the same probability of error (10^{-2}) as the single user scenario with the conventional canceller. Use of the Wiener filter (receiver B) as the internal and external de-spreading filter increases this figure to around 38 users. The Viterbi Cancellers (C and D) show very good performance, with the matched filter Viterbi canceller (C) approaching the performance of the sig-decision Wiener canceller (B) around the 10^{-2} performance level. At this level, the Wiener Viterbi Canceller (D) is able to support 60 users, showing that the combination of this structure with an adaptive algorithm could give promising results.

4.2 Simulated performance vs capacity for $E_b/N_0 = 7$dB

The situation for $E_b/N_0 = 7$ dB, shown in figure 4 is similar, with again very good performance achieved by the use of the Wiener filter with the Viterbi canceller. Receiver D is again capable of supporting 60 users at a probability of error of around 10^{-3}, which is the same as for the single user with conventional cancelling structures without forward error correction. It must also be acknowledged that the new structures do suffer from poorer performance as the loading is increased beyond a certain level, but this is in the area where very little can be done to alleviate the effects of large multiple access interference, so that no communication is possible anyway.

4.3 Performance vs E_b/N_0 for fixed capacity

The performance of the various systems for 31 and 50 active users (25% and 40% of the overall processing gain respectively) is shown in figures 5 and 6 respectively. For 31 users, receiver C is approaching the performance of receiver D, indicating that for reasonably low numbers of users, a matched filter could be employed successfully, without recourse to using an adaptive algorithm to approximate the Wiener filter.

For the higher levels of MAI experienced with the system at 40 % capacity, it may be seen that the systems employing Wiener filters have better performance, as may be expected, but that the inclusion of the proposed new structure still leads to increased performance. Indeed, even at this loading, receiver D is still able to achieve an estimated p_e of around 10^{-3} at $E_b/N_0 = 6$ dB, an improvement of 1 dB over even the conventional single user system.

5 Conclusions

We have proposed a new receiver structure for DS-CDMA, employing parallel multiple access interference cancellation, which obtains its initial estimate using a Viterbi decoder. The performance of this receiver has been estimated analytically and simulated using matched filters and Wiener filters to provide the direct sequence spreading. These structures have also been compared to conventional cancellation techniques, and equivalent processing-gain matched filters and matched filter cancellers. Significant performance improvements have been achieved, with the new system, employing a Wiener filter, able to support 60 users (50% of the processing gain) at the same probability of error as the single user conventional case for a range of background noise values. In moderate capacity regimes, the use of a matched filter in our proposed system approaches the performance of a Wiener filter combined with conventional cancellation.

A drawback of the new system is the increased processing delay, however it may be expected that this will be offset by the performance gains achieved.

The extension of this work to multipath environments is an obvious development, which needs to be investigated in the future. The use of soft-output devices prior to cancellation [13] may also improve performance by weighting less heavily those decisions which have been judged less reliable, and thus reducing error-propagation. Additionally, the use of non-linear filters, perhaps employing radial basis function (RBF) networks instead of the matched filter or Wiener Filter may prove useful in those cases where the multiple access interference is too great for our proposed system. A hybrid approach invoving combinations of the above proposals may also prove useful.

In conclusion, we have presented a promising technique for the reduction of multiple access interference in a DS-CDMA system which is practically feasible.

6 Acknowledgement

The authors gratefully acknowledge the financial support of this work by the UK Engineering and Physical Sciences Research Council, through Grant GR/J46401.

References

[1] J. Padgett, C. Gunther, and T. Hattori, "Overview of Wireless Personal Communications," *IEEE Communications Magazine*, pp. 28–41, Jan 1995.

[2] TIA/EIA/IS-95, *Mobile Station-Base Station Compatibility Standard for Dual Mode Wide-Band Spread Spectrum Cellular Systems.* Telecommunication Industry Association, 1993.

[3] J. Rapeli, "UMTS: Targets, System Concept and Standardization in a Global Framework," *IEEE Personal Communications*, pp. 20–28, Feb 1995.

[4] D. G. M. Cruickshank, "Optimal and Adaptive FIR Filter Receivers for DS-CDMA," *Proceedings of the IEEE 5th International Symposium on Personal, Indoor and Mobile Radio Communications (PIMRC), The Hague, The Netherlands*, pp. 1339–1345, 1994.

[5] P. M. Grant, C. F. N. Cowan, B. Mulgrew, and J. H. Dripps, *Analogue and Digital Signal Processing and Coding*. Bromley, UK: Chartwell-Bratt, 1989.

[6] J. Heller and I. Jacobs, "Viterbi Decoding for Satellite and Space Communication," *IEEE Transactions on Communications*, vol. COM-19, no. 5, pp. 835–848, 1971.

[7] I. Band and D. Cruickshank, "Efficient Bandwidth Utilisation for CDMA Using Convolutional Codes," *Proceedings of the IEEE Global Telecommunications Conference (Globecom), London, UK*, vol. 2, pp. 1306–1310, November 1996.

[8] P. Jung and B. Steiner, "A Joint Detection Mobile Radio System Concept Developed Within COST 231," *Procedings of the 45th IEEE Vehicular Technology Conference (VTC)*, vol. 1, pp. 469–473, July 1995.

[9] R. S. Mowbray, R. D. Pringle, and P. M. Grant, "Increased CDMA Capacity through Adaptive Co-channel Interference Regeneration and Cancellation," *Proceedings of the IEE*, vol. 139, pp. 515–524, Oct 1992.

[10] D. Cruickshank, "Suppression of Multiple Access Interference in a DS-CDMA System using Wiener Filtering and Parallel Cancellation," *Proceedings of the IEE: Communications*, 1996.

[11] M. Gastpar and D. Cruickshank, "Two-Stage Wiener Filter Based Cancellation Receivers for DS-CDMA," *IEE Electronic Letters*, vol. 32, pp. 805–806, April 1996.

[12] J. Conan, "The Weight Spectra of Some Short Low-Rate Convolutional Codes," *IEEE Transactions on Communications*, vol. COM-32, pp. 1050–1053, Sep 1984.

[13] J. Hagenauer, "Forward Error Correcting for CDMA Systems," *Proceedings of the 4th IEEE International Symposium on Spread Spectrum Techniques and Applications (ISSSTA), Mainz, Germany*, vol. 2, pp. 566–569, Sep 1996.

7 Figures

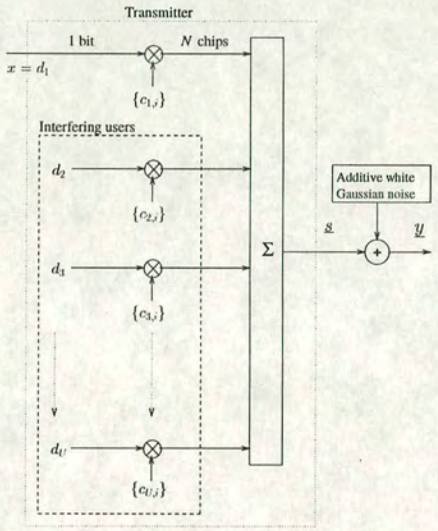

Figure 1: *Conventional DS-CDMA Transmitter*

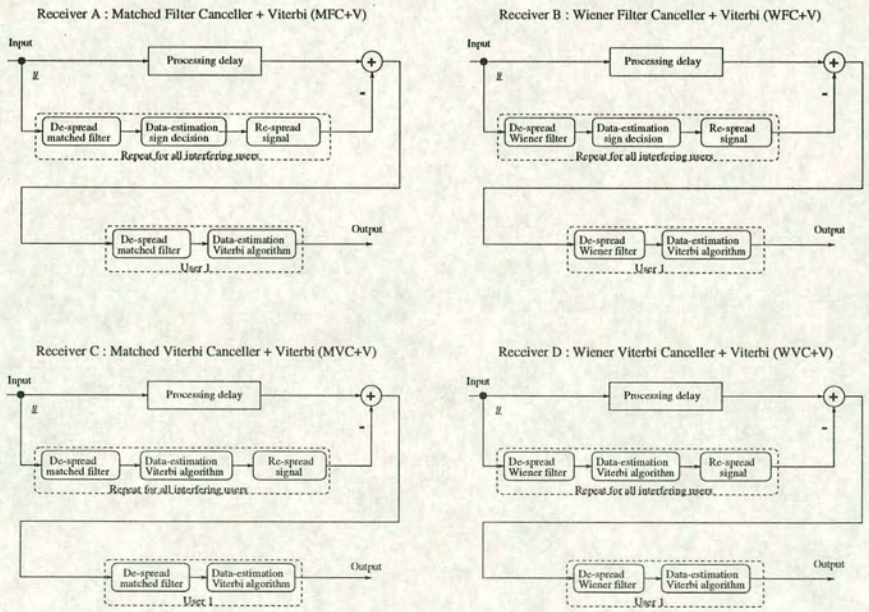

Figure 2: *The various receiver structures considered*

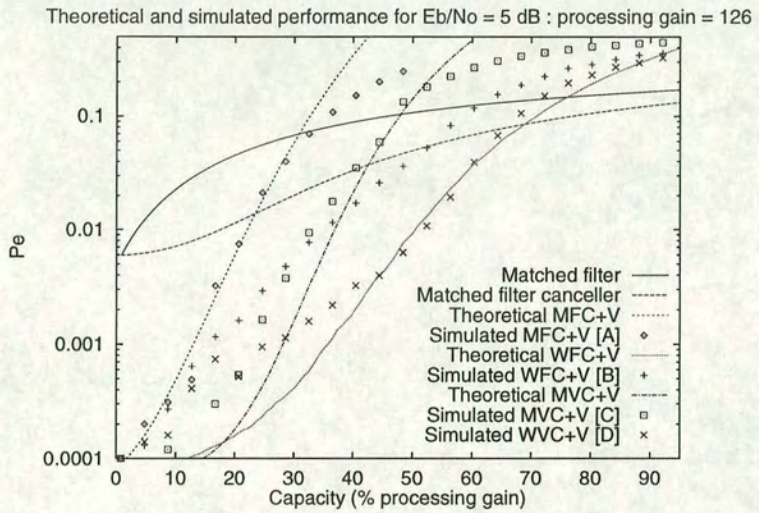

Figure 3: *Theoretical and simulated probability of error vs percentage capacity for the various schemes for* $E_b/N_0 = 5$ *dB*

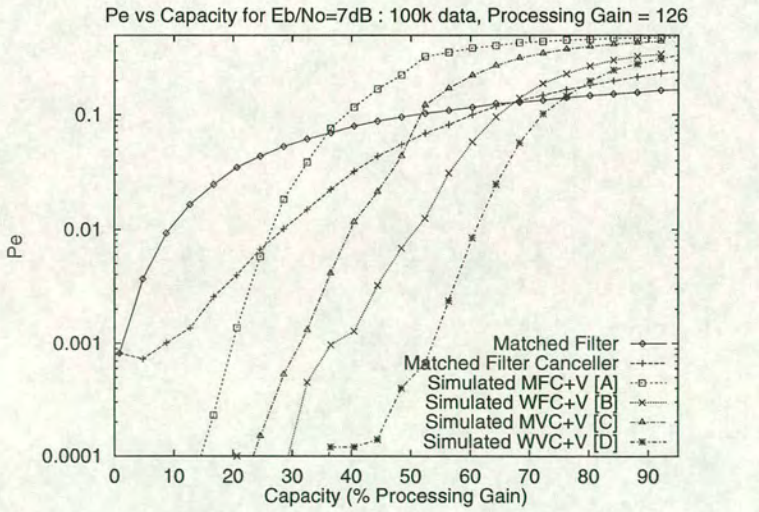

Figure 4: *Probability of error vs percentage capacity for the various schemes for* $E_b/N_0 = 7dB$

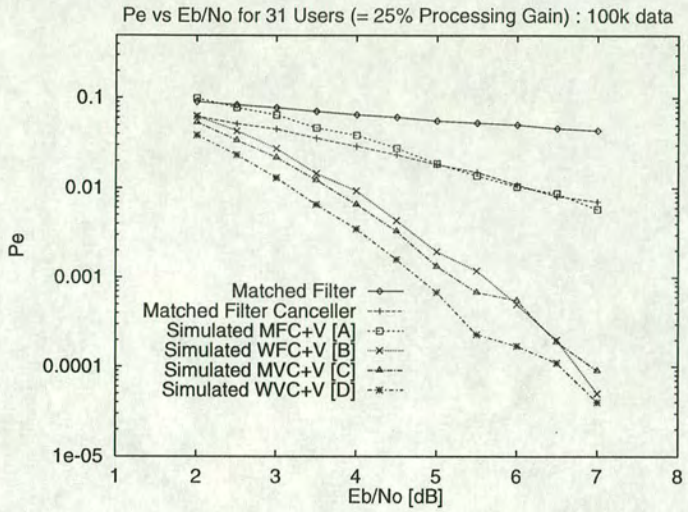

Figure 5: *Probability of error vs E_b/N_0 for 31 active users*

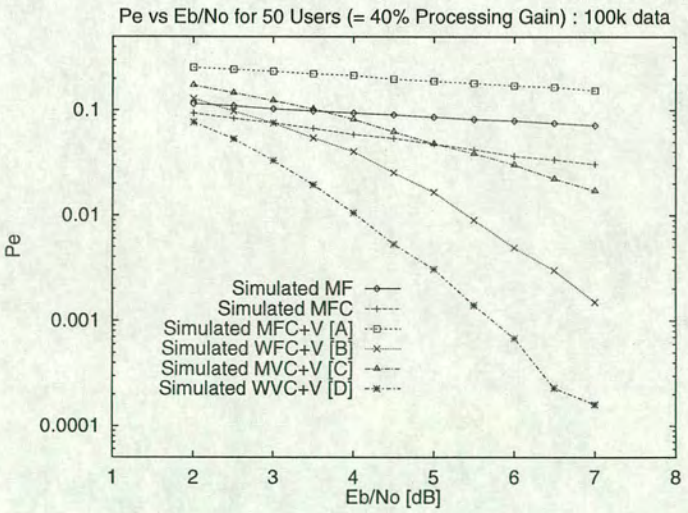

Figure 6: *Probability of error vs E_b/N_0 for 50 active users*

Complexity reduction of RBF network receivers for DS-CDMA via kernel modification and nearest neighbour selection

I.W. Band* D.G.M. Cruickshank † B. Mulgrew ‡

Signals & Systems Group,
Electrical Engineering Department,
The Kings Buildings,
University of Edinburgh,
Edinburgh, EH9 3JL, UK
Tel : +44 (0) 131 650 5659
Fax : +44 (0) 131 650 6554

Abstract

This paper investigates complexity reduction techniques for radial basis function (RBF) network based DS-CDMA receivers. The performance advantage obtained from adopting this non-linear receiver structure must be weighed against the corresponding increase in system complexity, and so there exists a need to reduce this complexity. Alternative kernels are first investigated, showing that the Gaussian kernel may be replaced by an algebraic kernel, at little detriment to the performance. Then a nearest neighbour approach is outlined, and its implementation analysed in terms of the Voronoi diagram. Finally, conclusions are drawn and suggestions for future development are outlined.

1 Introduction

Direct sequence code division multiple access (DS-CDMA) technology is a strong contender for the proposed European third generation universal mobile telecommunications system (UMTS) and the worldwide future public land mobile telecommunications system (FPLMTS) [1]. An implementation of this spread spectrum approach has been adopted as the North American personal communications system (PCS) interim standard IS-95 [2], and is rapidly gaining commercial success.

This work is concerned with the downlink (the path from the base station to the mobile) of such a DS-CDMA system, on which there are three main sources of interference; multiple access interference which occurs from cross-correlations if non-orthogonal sequences are used to spread the data, corruption of the transmitted signal by the communication channel, and background noise. The important aspects of the downlink are that the individual user's spread signals are bit and chip-synchronous, and that the combined signal passes through a common multipath channel.

*Ian.Band@ee.ed.ac.uk
†David.Cruickshank@ee.ed.ac.uk
‡Bernie.Mulgrew@ee.ed.ac.uk

The traditional method of collapsing the spectrum is for the mobile to use a RAKE receiver, with a bank of correlators, whose weights are either matched to the original spreading codes, or obtained via convolution with the impulse response of the channel. The soft decisions thus obtained may optionally be further processed (e.g. by a minimum mean square error filter) before being thresholded to provide the final estimate of the data. However, the presence of a multipath channel can cause the space spanned by these intermediate soft decisions to no longer be linearly separable, so that the estimated signal may contain a significant number of errors.

This situation is analogous to the exclusive OR problem, which was demonstrated to be solved by the use of a non-linear radial basis function (RBF) network in [3], or the problem of equalisation of an unknown channel, for which RBF functions have also been shown to provide good performance [4]. A review of the theoretical basis of functional approximation via RBF networks is given in [5]. Although this approach has been applied to many problems for which linear techniques are unsuitable [6], only a relatively small number of authors (*e.g.* [7], [8]) have considered RBF network based receiver structures for DS-CDMA, since the excellent performance obtained is only achieved at the expense of increased computational complexity.

In this paper, we investigate the use of an RBF network to attempt to combat the effects of the channel and thus recover the intended data. The RBF will be implemented at the output of a bank of matched filters, in contrast to [7] and [8], in which the network is constructed from the chip-level signal. If the number of users is less than the spreading sequence length, then the approach adopted here reduces the dimension of each centre in the network, as will be shown later. In particular, the contribution of this paper is the proposition of methods of reducing the complexity of the traditional RBF structure, whilst minimising the resultant reduction in system performance.

The scenario to be considered will first be outlined in section 2, which also demonstrates the simulated performance of an RBF network receiver filter in Gaussian noise. To illustrate the situation more clearly, attention is then fixed on a specific set of spreading sequences in a particular channel. This combination is then shown to exhibit the property of non-linear separability discussed above, which limits the performance of the minimum mean square error (Wiener) linear filter. The increased complexity of the RBF network receiver, compared to this Wiener filter, is also indicated.

Section 3 then describes the use of alternative kernel functions of lower complexity than the Gaussian kernel, and presents some results obtained from Monte Carlo simulations. The application of the nearest neighbour (NN) approach is then considered in section 4, which also investigates the performance of this new structure. Finally some conclusions are drawn and possible future developments of this new approach to contend with time-varying channels are outlined in section 5.

2 The scenario considered

2.1 The downlink of a DS-CDMA system

The baseband downlink of a chip and bit-synchronous DS-CDMA communication system is shown schematically in Figure 1, which demonstrates the implementation of the RBF network as a post matched filter (PMF) signal processing block.

The data bits $\{x_u, 1 \leq u \leq U\}$ are first used to modulate the user-specific spreading sequences $\{\underline{c}_u, 1 \leq u \leq U\}$. These pseudo-noise (PN) codes are of length M chips, and the resultant signals are then synchronously combined to form the transmitted signal vector $\underline{s}$, given by

$$\underline{s} = \sum_{u=1}^{u=U} \underline{c}_u x_u \tag{1}$$

The modulation scheme chosen is BPSK, and only real-valued signals are considered here. This signal then passes through a multipath channel, which is here modelled by a linear transversal filter with impulse response $H(z) = \sum_{j=0}^{j=n_h} h_j z^{-j}$, where z^{-1} represents a delay of one chip and

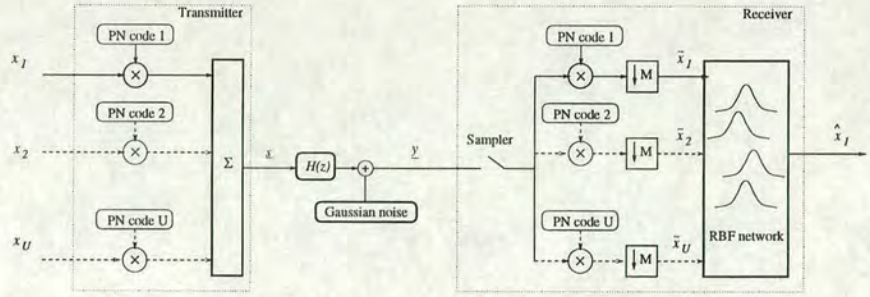

Figure 1: *DS-CDMA system with an RBF network processing block after the matched filter bank*

n_h is the number of chips spanned by the impulse response of the channel. The subsequent vector components are then added to iid samples of additive white Gaussian noise (AWGN) of zero mean and variance σ^2, where the signal to Gaussian noise ratio, E_b/N_0, is given by

$$\frac{E_b}{N_0} = \frac{M}{2\sigma^2} \tag{2}$$

to give the signal, $\underline{y}$, received by the mobile.

2.2 Construction of the network

The inputs to the RBF network, $\{\tilde{x}_u, 1 \leq u \leq U\}$, are obtained from the output of the bank of matched filters, sampled at the symbol rate. Perfect synchronisation will be assumed in the following.

An alternative to this arrangement is to dispense with the matched filters and construct the RBF network based on the chip-level signal as is considered in [7]. This method will not be considered here, but the application of the techniques described in this paper to this structure may be considered in future.

Given suitable estimates for the parameters of the channel, the centres for the RBF network may be calculated by forming all possible combinations of spreading sequences and taking the noise-free signal as the input to the matched filter bank. For this scenario, the number of centres N_c is given by 2^{U+2n_h-2}, where U is the number of active users, and n_h is the number of chips spanned by the impulse response of the multipath channel.

The set of centres of the network may be represented by $\mathcal{P} = \{\underline{p}_i : p_i = \underline{c}_i.(\underline{h}(z) * \underline{s}), 1 \leq i \leq N_c\}$, and, concentrating on the required user, it will be useful to define $\mathcal{P}^+$ as the set $\{\underline{p}_i \in \mathcal{P} :$ Original data bit was a $+1\}$, and $\mathcal{P}^-$ as the set $\{\underline{p}_i \in \mathcal{P} :$ Original data bit was a $-1\}$. Clearly, for this approach to be successful, it is required that $\mathcal{P} = \mathcal{P}^+ \cup \mathcal{P}^-$ and $\mathcal{P}^+ \cap \mathcal{P}^- = \emptyset$. With these conditions met, the dimension of $\mathcal{P}$ is simply the number of inputs to the network, which in this scenario equals the number of active users. The weights of the network, denoted $\{w_i : 1 \leq i \leq N_c\}$ are taken to be the sign of the data bit which produced that centre.

The estimate of the original data bit is then given by a sign decision on

$$f(\underline{y}) = \sum_{i=1}^{N_c} w_i \psi(d(\underline{y}, \underline{p}_i)) \tag{3}$$

where we have taken $d(\cdot,\cdot)$ to be the usual l_2 Euclidean metric, and $\psi(\cdot)$ is the kernel function, which controls the shape of each basis function, and must be monotonic in its argument. There are various choices for kernel functions, which will be investigated further in section 3, but for the initial investigations, the Gaussian kernel, defined by

$$\psi(\zeta) = \psi_G(\zeta) = \exp\left(-\frac{\zeta^2}{2\sigma^2}\right) \tag{4}$$

where σ is as in equation 2, will be used.

2.3 The Gaussian noise channel

To demonstrate the effectiveness of employing an RBF network based receiver structure for DS-CDMA, we shall consider the case for 7-chip random spreading sequences when no multipath channel is present. The performance, in terms of the probability of error (P_e) over a statistically significant number of trials, of the RBF receiver is shown in Figure 2, for E_b/N_0 values of $4dB$ and $7dB$. The performance is compared with the minimum mean square error (MMSE, or Wiener) filter, also implemented at the outputs of the matched filter bank. This structure is often referred to as the MMSE multi-user detector (MUD) [9].

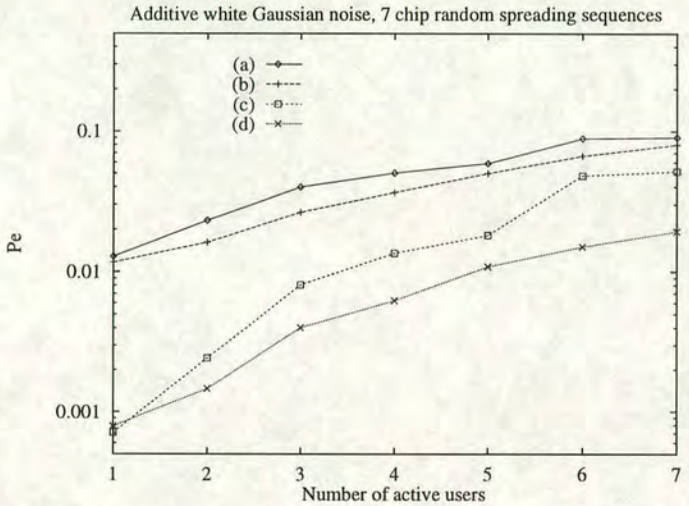

Figure 2: *Performance in additive white Gaussian noise: (a) Wiener, 4dB; (b) RBF, 4dB; (c) Wiener, 7dB; (d) RBF, 7dB*

Because non-orthogonal spreading sequences are used, the noise at the output from each matched filter in Figure 1 is correlated, so that strictly, the Mahalanobis metric [6] should be used in equation 3, however, even with the Euclidean metric, the performance of the RBF receiver is clearly superior to that using the Wiener filter as the loading is increased. To reduce the computational overhead therefore, we shall retain the Euclidean metric in the subsequent calculations.

To illustrate more clearly the effects of non-linearity on the RBF and MMSE based receivers, we shall now consider a specific spreading sequence set and multipath channel in some detail.

2.4 Example situation

The spreading sequence set on which we now concentrate consists of a two-user "broken" 4-chip code set, given by $c_1 = (+1, +1, -1, -0.7)^T$, $c_2 = (+1, -1, +1, -1)^T$, and the multipath channel is defined at the chip rate by $H(z) = 0.25 + z^{-1}$. Note that the power of the noise has not been adjusted to compensate for the inefficient code employed by user 1, which has been artificially created to make a simple nonlinearly separable problem.

The number of centres in the RBF network is thus $2^{2+2(2)-2} = 16$, and the location of these centres from user 1's point of view is shown in Figure 3. From the diagram, it is apparent that the output space spanned by the centres from user 1 is non-linearly separable, *i.e.* it is not possible to draw a straight line which correctly partitions the output space to separate centres produced from opposite data bits. Although the locations are the same as for user 1, the centres from user 2's point of view are linearly separable, since the associated weights are different. This may be seen in the figure which also shows the decision boundaries[1] for both users for the bit-level Wiener filter and the Gaussian kernel RBF network for $E_b/N_0 = 15dB$.

[1] where the value of the RBF function in equation 3 is identically zero

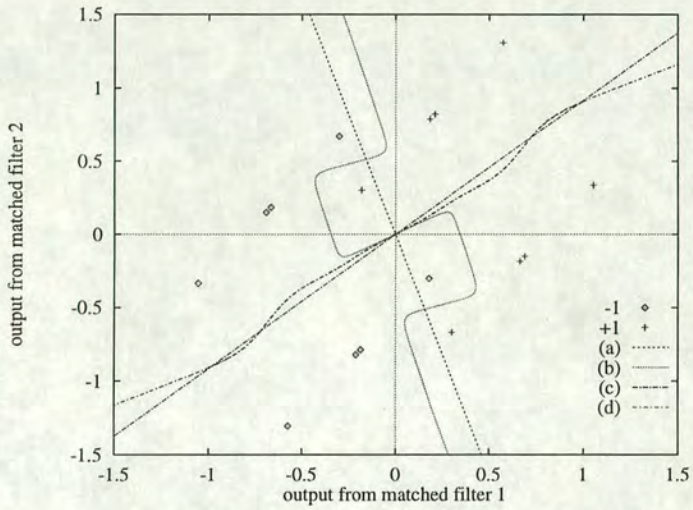

Figure 3: *Location of centres and decision boundaries of receivers for $E_b/N_0 = 15dB$: (-1) centres produced from a -1 from user 1; (+1) centres produced from a $+1$ from user 1; (a) Bit level Wiener filter decision boundary (user 1); (b) Bit level Wiener filter decision boundary (user 2); (c) RBF network decision boundary (user 1); (d) RBF network decision boundary (user 2)*

At this noise level, the Gaussian kernel RBF network correctly partitions the output space, and thus a reasonable error perfomance may be expected. However, the linear decision boundary obtained using the bit-level Wiener filter for user 1 is not able to correctly separate the centres as required for the reasons outlined above. Indeed, it may be expected that this filter will cause 2 out of every 16 data points to be in error for user 1, leading to a predicted $P_e \simeq 0.125$. These predictions may be verified by considering Figure 4, which shows the error performance of the RBF and bit-level Wiener filters for a range of noise values.

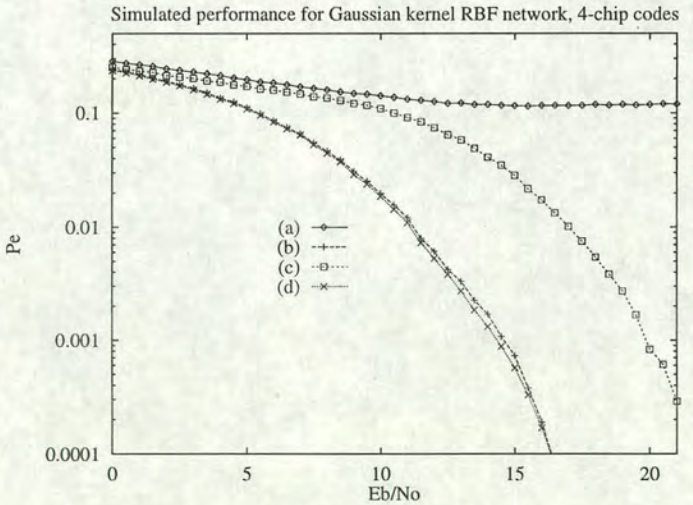

Figure 4: *Performance of RBF and Wiener based receivers : (a) Wiener, user 1; (b) Wiener, user 2; (c) RBF, user 1; (d) RBF, user 2*

As predicted, the Wiener filter for user 1 reaches an irreducible P_e of around 0.125 for high values of E_b/N_0, while the performance of the bit-level RBF processor increases with the signal to Gaussian noise ratio. Since user 2 is linearly separable, the performance of the linear Wiener and non-linear RBF network receivers are very similar.

The variation of the performance of the RBF network receiver with E_b/N_0 for user 1 may be

predicted from Figure 5 , which shows the surface generated by the RBF network from equation 3 for three values of E_b/N_0.

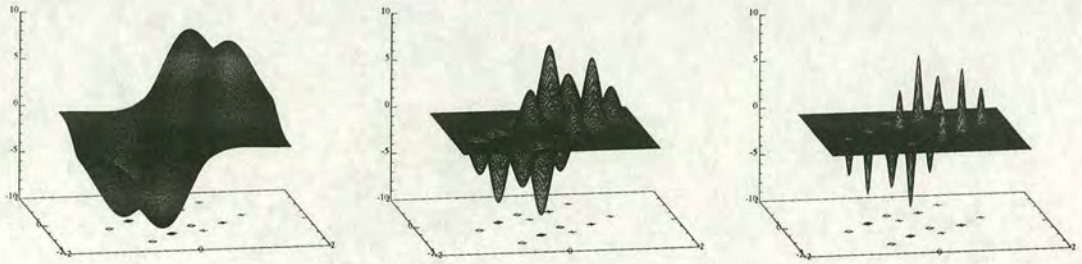

5dB *15dB* *25dB*

Figure 5: *Centres and generated surfaces for the Gaussian kernel RBF for* $E_b/N_0 = 5, 15$ *and* $15dB$

Clearly, for low values of E_b/N_0, the spread of the basis functions leads to a loss in distinction, so that individual centres are aggregated together, and thus the performance is relatively poor. As the signal to Gaussian noise ratio increases, more definition is achieved, so that individual centres now contribute separately, leading to increased performance.

2.5 Discussion

The increased performance of the RBF networks must be set against the corresponding increase in computational complexity required, so that adoption of this non-linear strategy can only be considered feasible in conjunction with some methods for reducing the inherent complexity of RBF based receivers. This complexity arises from two sources; the first is the number of calculations required per centre, while the second is the number of centres which must be stored. In this paper, we shall investigate methods of reducing the number of calculations required per centre, although in section 4.1, we shall demonstrate that some centres are effectively redundant.

3 Complexity reduction through different kernel functions

The first method of complexity reduction is to employ alternative kernels in equation 3. The Gaussian kernel defined in equation 4 requires a series of exponential calculations, which may impose too great a computational load on the receiver, so we first consider the inverse multi-quadratic kernel [6], defined by

$$\psi(\zeta) = \psi_{a_1}(\zeta) = \frac{1}{\sqrt{\zeta^2 + \sigma^2}} \tag{5}$$

and the modified inverse multi-quadratic, defined by

$$\psi(\zeta) = \psi_{a_2}(\zeta) = \frac{1}{1 + v\frac{\zeta^2}{2\sigma^2}} \tag{6}$$

both of which are simpler functions of the metric than the exponential used in equation 3.

The decision boundaries for these algebraic kernels, again for user 1, compared to that for the Gaussian kernel of the previous section, are shown in Figure 6 for $E_b/N_0 = 15dB$.

The algebraic kernels are clearly able to separate the centres arising from different data bits, although the reduced decay rate of the algebraic kernels causes their decision boundaries to always be interior to the Gaussian kernel decision boundary, so that their performance may be expected to be slightly worse.

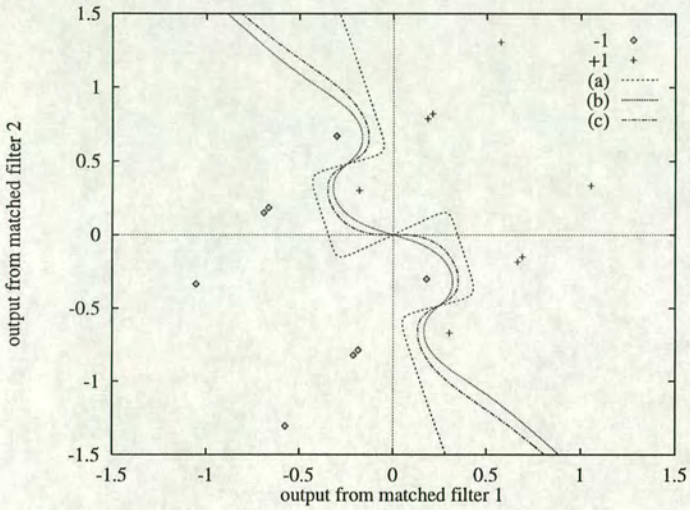

Figure 6: *Location of centres and decision boundary of various RBF network receivers for* $E_b/N_0 = 15dB$*: (-1) centres produced from a* -1*; (+1) centres produced from a* $+1$*; (a) Gaussian kernel decision boundary; (b) decision boundary for* ψ_{a_1}*; (c) decision boundary for* ψ_{a_2} *for* $v = 1$

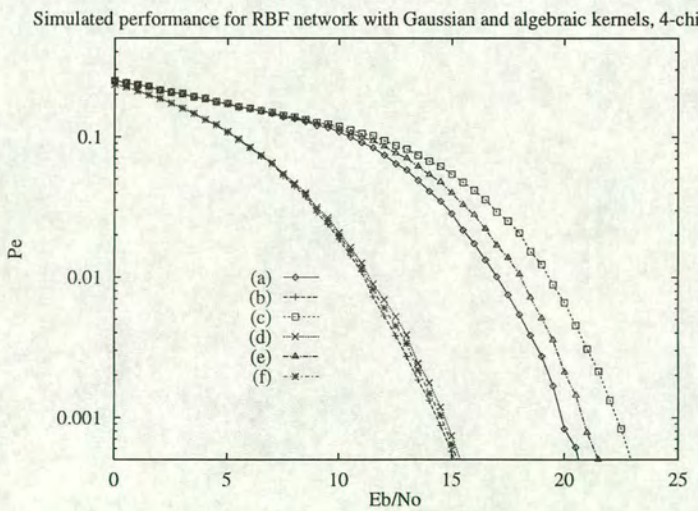

Figure 7: *Performance of RBF based receivers with various kernels: (a) Gaussian, user 1; (b) Gaussian, user 2; (c) inverse multi-quadratic* ψ_{a_1}*, user 1; (d) inverse multi-quadratic,* ψ_{a_1} *user 2; (e) modified inverse multi-quadratic* ψ_{a_2} *with* $v = 1$*, user 1; (f) modified inverse multi-quadratic* ψ_{a_2} *with* $v = 1$*, user 2*

The error performance of these algebraic kernels is shown in Figure 7.

As may be seen, the modified kernel has slightly better performance than the traditional inverse multi-quadratic kernel, and both algebraic kernels have only slightly poorer performance than the full Gaussian kernel.

The additional parameter v in ψ_{a_2} also permits an investigation of this parameter's influence on the decision boundary and error performance of a network employing this kernel. Concentrating on user 1, the decision boundaries for various values of v for $E_b/N_0 = 10dB$ are shown in Figure 8, whilst the corresponding error performance is shown in Figure 9.

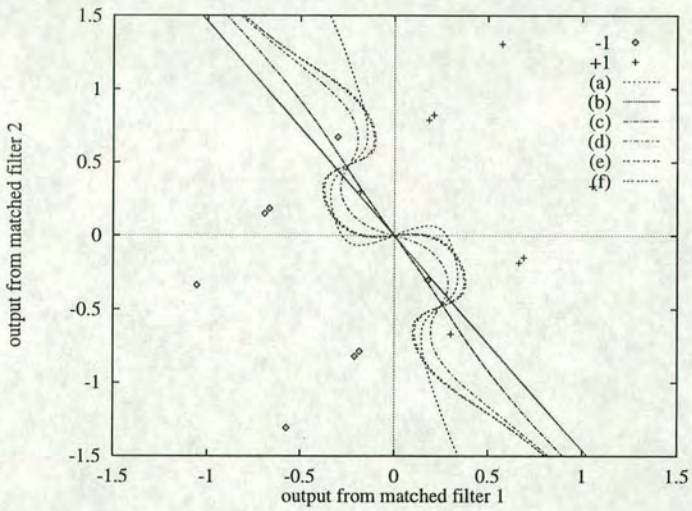

Figure 8: *Location of centres and decision boundary of RBF network using ψ_{a_2} kernel function for $E_b/N_0 = 10dB$: (-1) centres produced from a -1; (+1) centres produced from a $+1$; (a) Gaussian kernel; (b) $v = 0.01$; (c) $v = 0.08$; (d) $v = 1.0$; (e) $v = 10.24$; (f) $v = 81.92$*

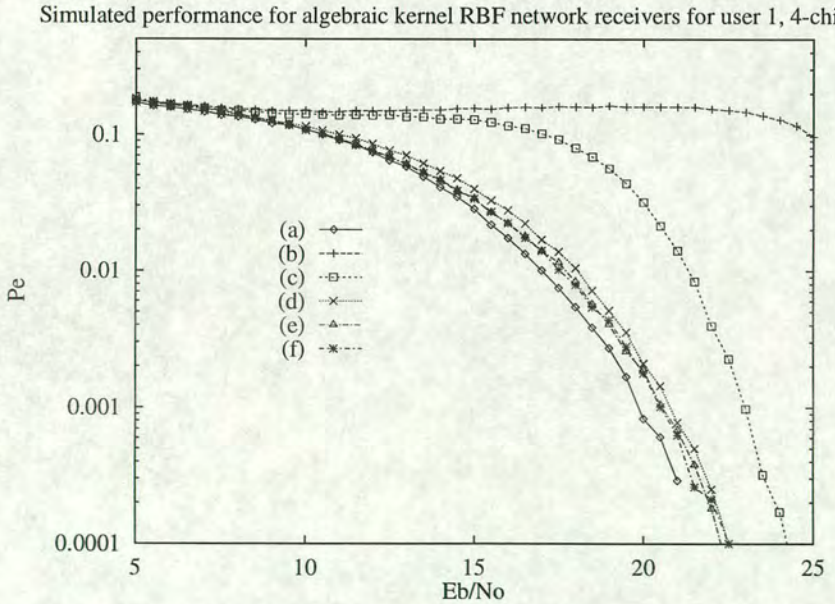

Figure 9: *Performance of RBF based receivers with ψ_{a_2} kernel function: (a) Gaussian kernel; (b) $v = 0.01$; (c) $v = 0.08$; (d) $v = 1.0$; (e) $v = 10.24$; (f) $v = 81.92$*

It may be seen that the algebraic kernels for the first two values of v fail to separate the centres correctly for $E_b/N_0 = 10dB$, and this is reflected in the relatively poor performance of these

two receivers. Broadly, there is little advantage in increasing the value of v beyond 1.0, since the performance of the other kernels is so similar. Interestingly, the $v = 0.08$ kernel, although obviously inferior for values of E_b/N_0 below around $15dB$, approaches the performance of the other kernels as E_b/N_0 increases, so that it may be concluded that the influence of the parameter v is only weak as the noise is reduced. Future work may investigate whether this situation may be generalised.

4 The nearest neighbour approach

As is apparent from Figure 5, when the signal to Gaussian noise ratio, E_b/N_0, is sufficiently large, the Gaussian kernel RBF surface consists of individual peaks and troughs (according as the relevant centre $p \in \mathcal{P}^+$ or $\mathcal{P}^-$ respectively), located at the centres of the network. In this way, this receiver structure is able to compare the input statistic against all the centres and hence obtain an accurate estimate of the original data bit. In addition, the previous section showed that alternative kernels, while offering slightly reduced complexity, are broadly equivalent in terms of error performance, at high values of E_b/N_0. It would appear natural, then, to investigate the performance of a receiver which is based on the centres as calculated previously, but rather than forming the sum in equation 3 using the metric to all possible centres, estimates the original data bit by simply considering the nearest[2] centre to the input vector, so that the data estimate for user u is given by

$$\hat{x}_u = w_j : d(\underline{\tilde{x}}, \underline{p}_j) < d(\underline{\tilde{x}}, \underline{p}_i), 1 \leq i \leq N_c, i \neq j \tag{7}$$

This nearest neighbour (NN) approach is a commonly occuring problem in many fields in computational geometry [10], and as may be seen in Figure 10, the NN decision boundary represents the asymptotic limit of the Gaussian kernel based RBF network as $E_b/N_0 \rightarrow \infty$.

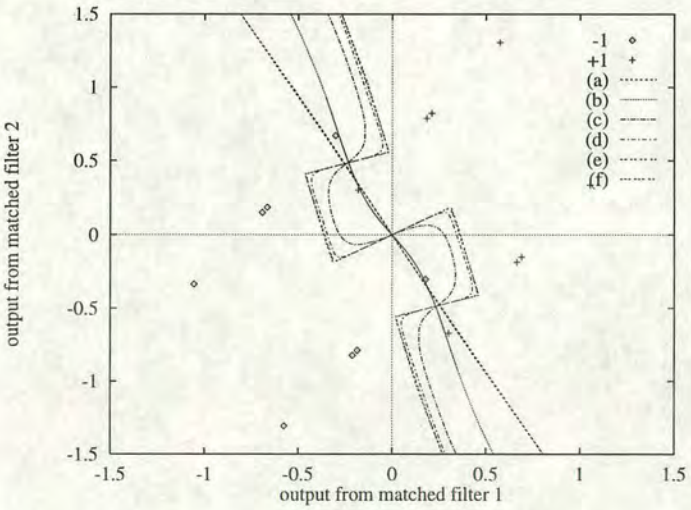

Figure 10: *Location of centres and decision boundaries of Gaussian kernel RBF network for various values of E_b/N_0: (-1) centres produced from a -1; (+1) centres produced from a $+1$; (a) $0dB$; (b) $5dB$; (c) $10dB$; (d) $15dB$; (e) $20dB$; (f) NN receiver decision boundary*

Thus it may be expected that these two approaches will perform similarly as the noise decreases. The error performance against E_b/N_0 of the NN-based receiver, compared to the Gaussian kernel RBF network receiver is shown in Figure 11 for both users.

For user 1, the NN receiver has only slightly worse performance than the RBF network for low E_b/N_0, and is almost identical for $E_b/N_0 > 10dB$ as predicted. For user 2, the decision boundaries

[2] where we again use the Euclidean metric here

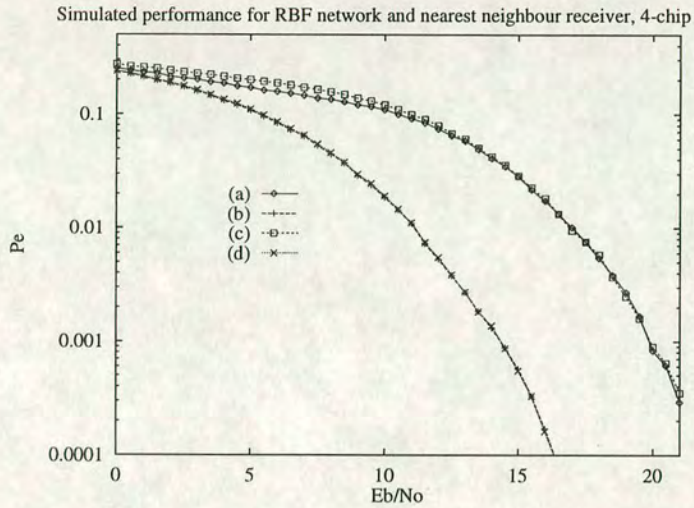

Figure 11: *Performance of NN-based receiver compared to Gaussian kernel RBF receiver: (a) RBF, user 1; (b) RBF, user 2; (c) NN, user 1; (d) NN, user 2*

are very similar, as are the performance curves, as expected, since that user is linearly separable.

Returning to the original 7-chip spreading sequences in AWGN only, the performance of the proposed NN receiver is shown in Figure 12, again for the same two values of E_b/N_0 as in the previous case.

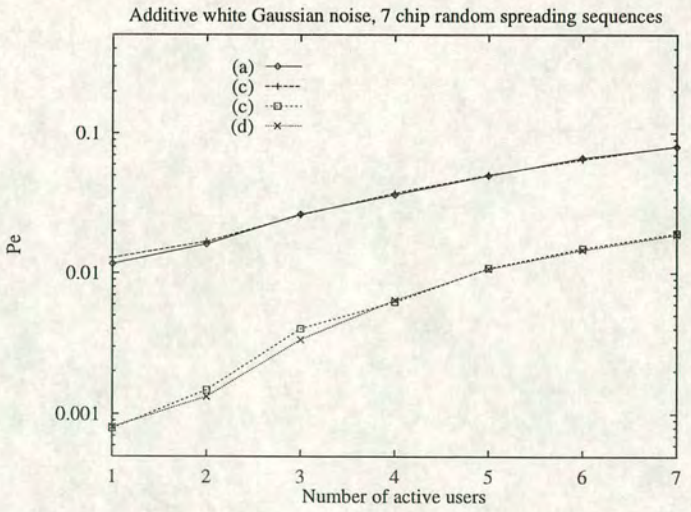

Figure 12: *Performance in additive white Gaussian noise: (a) RBF, 4dB; (b) NN, 4dB; (c) RBF, 7dB; (d) NN, 7dB*

As may be seen, the performance of the proposed receiver is very close to that of the Gaussian kernel RBF network receiver for all loading values. Thus, the proposed receiver attains very similar performance characteristics to the standard RBF network receiver, but avoids the associated restrictively high computational complexity.

4.1 Graphical interpretation of the nearest neighbour approach

Efficient algorithms for the NN approach generally consist of two parts; the construction of a tree structure, containing all the centres as nodes, and the traversal of this tree, until the nearest match

is found. In 2 dimensions, the construction may be accomplished optimally using $O(N_c)$ storage whilst the search requires $O(\log_2 N_c)$ time [11]. This strategy produces a Voronoi diagram, $\mathcal{V}(\mathcal{P})$ from the set $\mathcal{P}$ of centres, which for the 2-user 4-chip spreading sequence situation considered here, is shown in Figure 13.

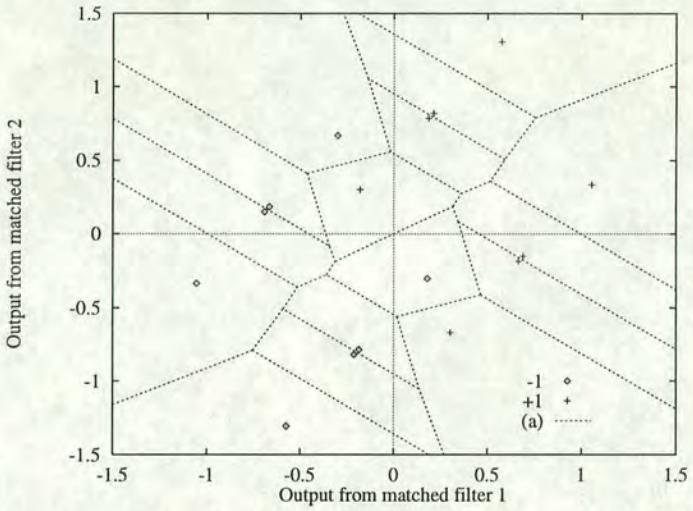

Figure 13: *Location of centres and Voronoi diagram: (-1) centres produced from a -1 from user 1; (+1) centres produced from a $+1$ from user 1; (a) Voronoi diagram*

It may be seen that the NN decision boundary for each user is simply a subset of the complete Voronoi diagram, and that a modification of this technique could be used to remove centres whose associated Voronoi polygons $\mathcal{V}(p_i)$ do not border the NN decision boundary. This technique produces a reduced set of centres $\mathcal{P}' \subseteq \mathcal{P}$ for each user. With the scenario considered here, there are 4 centres for each user which may be removed, so that this modified NN algorithm would make 25 % fewer comparisons per data bit, and thus would be correspondingly quicker than the conventional NN algorithm.

This may be seen in Figure 14 which shows the performance of the Gaussian kernel RBF network and the NN receiver when the four centres whose polygons are not part of the decision boundary for user 1 are removed from the network.

Clearly, in this case, the performance of the receivers using the reduced set of centres $\mathcal{P}'$ is virtually identical to that of the receivers which use the complete set of centres, $\mathcal{P}$. Future work will consider the development of this approach, with the intention of characterising the ratio of the number of discarded centres to the number of centres in the original network.

Since the dimension of the decision space to be partitioned increases linearly with the number of users, the presence of more users means that the NN decision boundary is a $U-1$-dimensional hyperplane. The construction of the Voronoi diagram in higher dimensions is an area of current research [12], but it is shown in [13] that the nearest neighbour may be found in $O((\log_2 N_c)^{U-1}\log_2(\log_2 N_c))$ time; this structure requiring $O(N_c(\log_2 N_c)^{U-1})$ storage. For time-varying channels, the dynamic insertion and deletion of centres could be employed to update the network, or approximate $(1+\epsilon)$ [13] methods could be used if the channel characteristics evolve only slowly.

A possible drawback to the nearest neighbour approach is that this method produces a hard decsion, with no indication of the reliability of the estimate, as is required for instance for a soft-decision Viterbi decoder for a DS-CDMA system. As a development, it may be possible to construct a soft decision based on the distance to the nearest centre, although the excellent performance achieved by the NN algorithm as implemented, may mean that such an approach would be an unnecessary complication.

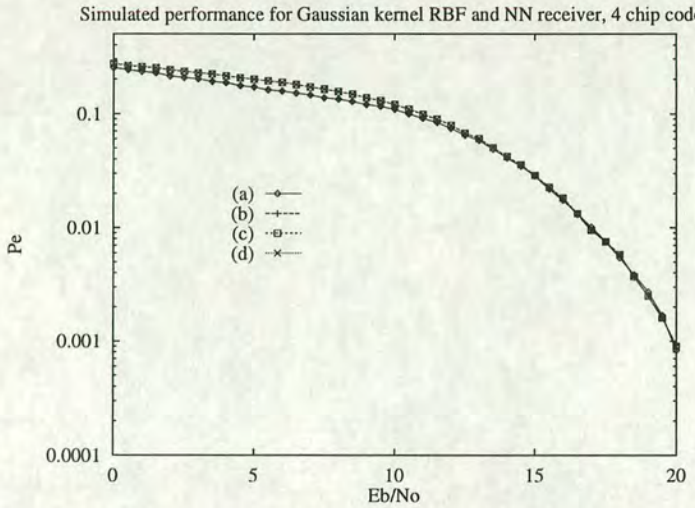

Figure 14: *Simulated performance of Gaussian kernel RBF network and NN receiver based on the reduced set of centres, obtained from the Voronoi diagram: (a) Gaussian kernel RBF, complete set; (b) Gaussian kernel RBF, reduced set; (c) NN receiver, complete set; (d) NN receiver, reduced set*

5 Conclusions

In this paper, we have considered the reduction in computational complexity of the non-linear RBF network receiver for the downlink of a DS-CDMA system. The RBF receiver was first demonstrated to have excellent performance, and be able to correctly estimate the data even when the decision space is non-linearly separable. The use of alternative kernels in the evaluation of the RBF soft decision was shown to be of value in reducing the computational complexity with little performance loss at usable signal to noise ratios. It was also shown that at higher signal to noise ratios, the output from the RBF network is dominated by a subset of the total number of centres. This prompted the proposal to use simply the nearest centre of the network to provide the decision, and a receiver based on this approach was shown to have comparable performance to the complete network with Gaussian kernels, and at much reduced complexity. An interpretation of this algorithm, in terms of the Voronoi diagram was outlined, and a possible technique to reduce the number of centres which must be considered was outlined. Suggestions for the use of this non-linear receiver in a system serving more subscribers, and in a time-varying channel, were also given.

References

[1] T. Ojanperä, P. A. Ranta, S. Hämäläinen, and A. Lappeteläinen, "Analysis of CDMA and TDMA for 3rd Generation Mobile Radio Systems," *Procedings of the 47th IEEE Vehicular Technology Conference (VTC), Phoenix, Arizona, USA*, vol. 1, pp. 840–844, May 1997.

[2] TIA/EIA/IS-95, *Mobile Station-Base Station Compatibility Standard for Dual Mode Wide-Band Spread Spectrum Cellular Systems.* Telecommunication Industry Association, 1993.

[3] D. S. Broomhead and D. Lowe, "Multivariable Function Interpolation and Adaptive Networks," *Complex Systems*, vol. 2, pp. 321–355, 1988.

[4] S. Chen, S. McLaughlin, and B. Mulgrew, "Complex-Valued Radial Basis Function Networks: Application to Digital Communications Channel Equalisation (part II)," *EURASIP Signal Processing Journal*, vol. 36, pp. 175–188, March 1994.

[5] M. J. D. Powell, "Radial Basis Functions for Multivariable Interpolation: A Review," in *Algorithms for Approximation* (J. Mason and M. Cox, eds.), pp. 143–167, Oxford: Clarendon Press, 1987.

[6] B. Mulgrew, "Applying Radial Basis Functions," *IEEE Signal Processing Magazine*, pp. 50–65, March 1996.

[7] D. G. M. Cruickshank, "Radial Basis Function Receivers for DS-CDMA," *IEE Electronic Letters*, vol. 32, pp. 188–190, February 1996.

[8] U. Mitra and H. V. Poor, "Neural Network Techniques for Adaptive Multiuser Demodulation," *IEEE Journal on Selected Areas in Communications*, vol. 12, pp. 1460–1470, December 1994.

[9] A. Klein, G. K. Kaleh, and P. W. Baier, "Zero Forcing and Minimum Mean Square Error Equalization for Multiuser Detection in Code Division Multiple-Access Channels," *IEEE Transactions on Vehicular Technology*, vol. 45, pp. 276–287, May 1996.

[10] J. O'Rourke, *Computational Geometry in C.* Trumpington St., Cambridge, UK: Cambridge University Press, 1994.

[11] R. Sproull, "Refinements to Nearest Neighbour Searching in k-Dimensional Trees," *Algorithmica*, vol. 6, pp. 579–589, 1991.

[12] J.-D. Boissonnat, M. Sharir, B. Tagansky, and M. Yvinec, "Voronoi Diagrams in Higher Dimensions under Certain Polyhedral Distance Functions," *Proceedings of the 11th Annual Symposium on Computational Geometry, Vancouver, Canada*, pp. 79–88, 1995.

[13] S. Kapoor and M. Smid, "New Techniques for Exact and Approximate Dynamic Closest-Point Problems," *Proceedings of the 10th Annual Symposium on Computational Geometry, Stony Brook, New York, USA*, pp. 165–174, 1994.

Appendix B

Additive white Gaussian noise channel calculations

Many of the simulations discussed in the thesis are conducted with respect to the additive white Gaussian noise channel, and all are performed using binary phase shift keying (BPSK) modulation. This Appendix develops the expressions for the signal to Gaussian noise ratio and the theoretical prediction for the probability of error for BPSK in the Gaussian channel, as described in [31].

B.1 Signal to Gaussian noise ratio

The background noise level in a communications system may be characterised by the single sided-noise density, N_0. The relationship between this quantity and the linear processing gain, g_P, may be determined by the following.

Let z represent Gaussian-distributed random deviate with zero mean and variance σ^2, *i.e.*

$$z \sim \mathcal{N}\left(0, \sigma^2\right) \tag{B.1}$$

where

$$\sigma^2 = \frac{N_0}{2} \tag{B.2}$$

The signal to Gaussian noise ratio, denoted E_b/N_0 is an adjusted form of the conventional signal to noise ratio (SNR), taking into account the processing gain afforded by the spreading and despreading process.

If the processing gain consists of a mixture of signature sequences of length M, and forward error

correcting coding of rate $1/C$, the overall processing gain will be given by $g_P = MC = N_s$. Thus, for each data bit to be transferred to the mobile, the output baseband signal from the base station transmitter consists of N_s chips. If the amplitude of each chip in this signal is denoted A_c, then the energy transmitted *per data bit* will be given by

$$E_b = N_s A_c \tag{B.3}$$

Here, $A_c = 1$ so that the decibel form of the signal to Gaussian noise ratio is thus given by

$$\frac{E_b}{N_0} = 10 \log_{10} \frac{N_s}{2\sigma^2} \tag{B.4}$$

This is the fundamental measure of background noise throughout the simulations presented.

B.2 Probability of error using BPSK in the AWGN channel

The theoretical probability of error, P_e, of an unspread signal in the additive white Gaussian noise (AWGN) channel may be derived via the following argument.

Let x_1 be the transmitted data bit. Then, since the modulation scheme is BPSK, a data bit error will occur if the decision is made that the original transmitted data bit was the complementary symbol $-x_1$.

Assume, without loss of generality, that $x_1 = 1$. Then it is evident that a data bit error will occur if the decision statistic

$$r = \sqrt{E_b} + z < 0 \tag{B.5}$$

where E_b is the total energy per bit, and z is a Gaussian random variable whose statistics are as described in Equation B.1.

Let the probability of this error event be denoted P_1, then

$$P_1 = P(-x_1 \text{ estimated } | x_1 \text{ transmitted }) = \int_{-\infty}^{0} p(r|x_1) dr \tag{B.6}$$

where $p(r|x_1)$ is the conditional probability density function of r, given that x_1 was transmitted. For the AWGN channel, this probability density is given by

$$p(r|x_1) = \frac{1}{\sqrt{\pi N_0}} \exp - \left[\frac{(r - \sqrt{E_b})^2}{N_0} \right] \tag{B.7}$$

where the noise variance is given by $N_0/2$.

Substituting B.7 in B.6 yields

$$P_1 = \frac{1}{\sqrt{\pi N_0}} \int_{-\infty}^{0} \exp - \left[\frac{(r - \sqrt{E_b})^2}{N_0} \right] dr \tag{B.8}$$

By making the change of variable

$$t = \sqrt{\frac{2}{N_0}}(r - \sqrt{E_b}) \tag{B.9}$$

Equation B.8 may be re-written as

$$P_1 = \frac{1}{\sqrt{2\pi}} \int_{-\infty}^{-\sqrt{2E_b/N_0}} \exp(-t^2/2) dt \tag{B.10}$$

Reversing the limits of integration, and since the above expression also holds when $x_1 = -1$, the final error probability may be written as

$$P_e = Q\left(\sqrt{\frac{2E_b}{N_0}}\right) \tag{B.11}$$

where $Q(\cdot)$ is defined [38] by

$$Q(x) = \frac{1}{\sqrt{2\pi}} \int_{x}^{\infty} \exp(-t^2/2) dt \tag{B.12}$$

Equivalently, B.11 may be expressed as

$$P_e = \frac{1}{2} \operatorname{erfc}\left(\sqrt{\frac{E_b}{N_0}}\right) \tag{B.13}$$

which is the form used to generate the results shown in Figure B.1.

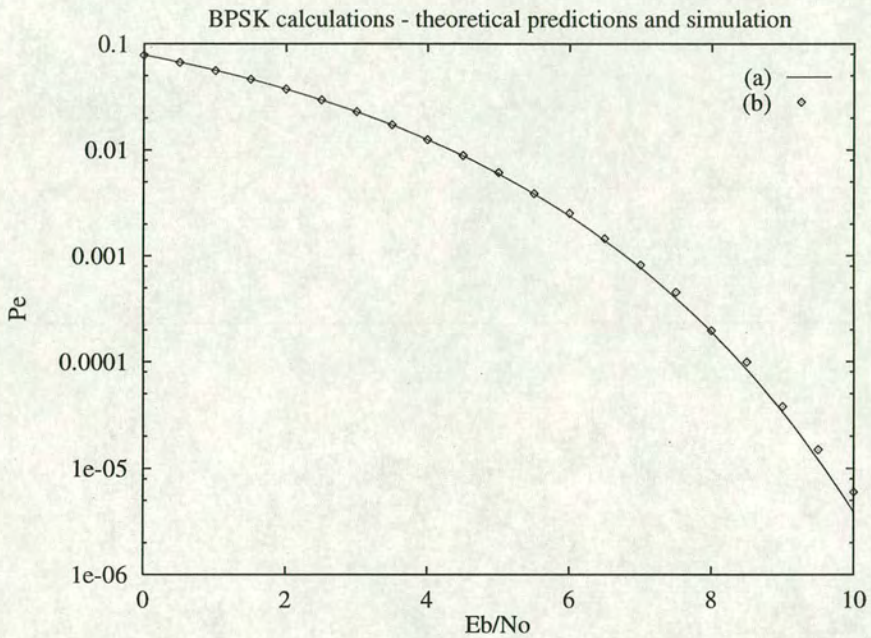

Figure B.1: *Theoretical and simulated probability of error for BPSK modulation in the AWGN channel: (a) theoretical predictions; (b) Monte Carlo simulation results*

Appendix C

Software

The routines supplied by Dr. D. Laurenson to allocate and de-allocate memory dynamically are detailed below.

```
/* gen_array provides functions to create and destroy arrays of */
/* arbitrary size and dimension, with an arbitrary size of element */
/* The result should be type cast to the desired pointer type at */
/* the calling level.  Note that compilation of this code will */
/* result in a warning if -Wmissing_prototypes is used in the */
/* compile options */
/* Usage: */
/*   a = (double ***)gen_array(sizeof(double), 3, 10, 7, 4);  */
/* */
/* generates a 10 by 7 by 4 array of doubles, and */
/* del_array(a, 3, 10, 7, 4); */
/* destroys it. */


#include<stdio.h>
#include<malloc.h>
#include<varargs.h>

#ifdef __STDC__
void *_gen_array(unsigned, int, va_list);
#else
void *_gen_array();
#endif

void *_gen_array(sze, dims, ap)
      unsigned sze;
      int dims;
```

```
      va_list ap;
{
  void *tmp;
  int i, j, lngth;


  lngth = va_arg(ap, int);
  if (dims==1) {
    if ((tmp = malloc(sze * lngth)) == NULL) {
      printf("\n *** Warning : Failed to allocate enough memory *** \n");
      return(NULL);
    }
  } else {
    if ((tmp = malloc(sizeof(void *) * lngth)) == NULL) {
      printf("\n *** Warning : Failed to allocate enough memory *** \n");
      return(NULL);
    }
    for (i=0; i<lngth; i++) {
      if ((((void **)tmp)[i] = _gen_array(sze, dims-1, ap)) == NULL) {
        printf("\n *** Warning : Failed to allocate enough memory *** \n");
        for (j=0; j<i; j++) {
          free((char *) ((void **)tmp)[i]);
          return(NULL);
        }
      }
    }
  }
  return(tmp);
}

void *gen_array(sze, dims, va_alist)
      unsigned sze;
      int dims;
      va_dcl
{
  void *tmp;
  va_list ap;

  va_start(ap);
  tmp = _gen_array(sze, dims, ap);
  va_end(ap);
```

```
  return(tmp);
}

#ifdef __STDC__
void _del_array(void *, int, va_list);
#else
void _del_array();
#endif

void _del_array(tmp, dims, ap)
      void *tmp;
      int dims;
      va_list ap;
{
  int i, lngth;

  if (dims==1) {
    free((char *) tmp);
  } else {
    lngth = va_arg(ap, int);
    for (i=0; i<lngth; i++) {
      _del_array(((void **)tmp)[i], dims-1, ap);
    }
    free((char *) tmp);
  }
}

void del_array(tmp, dims, va_alist)
      void *tmp;
      int dims;
      va_dcl
{
  va_list ap;

  va_start(ap);
  _del_array(tmp, dims, ap);
  va_end(ap);
}
```